ֆ&G 3609 (Project 00/53)

Probabilistic Seismic Hazard Assessment of New Zealand:

M Stirling, G McVerry, K Berryman, P McGinty, P Villamor, R Van Dissen, D Dowrick, J Cousins, R Sutherland

Client Report 2000/53

Probabilistic Seismic Hazard Assessment of New Zealand:

New Active Fault Data Seismicity Data Attenuation Relationships and Methods

Authors

Mark Stirling
Graeme McVerry
Kelvin Berryman
Peter McGinty
Pilar Villamor
Russ Van Dissen
David Dowrick
Jim Cousins
Rupert Sutherland

May 2000

Institute of
GEOLOGICAL
& NUCLEAR
SCIENCES
Limited

RESEARCH FOUNDATION

Probabilistic Seismic Hazard Assessment of New Zealand: New Active Fault Data, Seismicity Data, Attenuation Relationships and Methods
- Institute of Geological & Nuclear Sciences Ltd

Foreword

The report on the above project presents a major advance in the assessment of seismic hazards throughout New Zealand. For the first time comprehensive use of active fault data complements and, for some aspects, dominates the use of historical and instrumental records for the assessment of the seismic hazards.

For reliable probabilistic estimates, the duration covered by the data base should be long when compared with the recurrence intervals between significant events arising from a given source. The active fault record satisfies this criterion, but the historical and instrumental records fall far short of it. However, the fault record may be seriously incomplete in some regions of the country.

Estimation of the extent to which the fault record is incomplete is assisted by an understanding of the faulting and associated tectonic mechanisms and by increasing information on the resulting surface movements and deformations. Some allowance for the extent of fault record incompleteness can be made when interpreting seismic hazard assessments.

National and international reviewers agree that the researchers have made very effective use of international best practice, and their own research on local conditions, when deriving New Zealand seismic hazards from the available data. The reviewers also generally endorse the researchers' proposals to extend and strengthen the present seismic hazard assessments.

This project demonstrates that recent assessments of New Zealand seismic hazards have substantial deficiencies. However, care should be exercised in deciding the extent and timing of the utilisation of the project's outcomes for various aspects of seismic impact reduction. Consideration should include the limitations of the data sets available, and the advances which may be achieved during the next few years.

R Ivan Skinner
Director
EQC Research Foundation

Earthquake Commission Research Foundation
Level 10, Castrol House, 36 Customhouse Quay, P O Box 311, Wellington, New Zealand
Telephone (04) 499-0045   Fax (04) 499 0046

Institute of
GEOLOGICAL
& NUCLEAR
SCIENCES
Limited

Probabilistic Seismic Hazard Assessment of New Zealand:

New Active Fault Data, Seismicity Data, Attenuation Relationships and Methods

Mark Stirling, Graeme McVerry, Kelvin Berryman, Peter McGinty, Pilar Villamor, Russ Van Dissen, David Dowrick, Jim Cousins and Rupert Sutherland

Prepared for

EARTHQUAKE COMMISSION RESEARCH FOUNDATION

Institute of Geological & Nuclear Sciences client report 2000/53
Project Number 41984B.10

May 2000

Gracefield Research Centre, 69 Gracefield Road, PO Box 30368, Lower Hutt, New Zealand, Telephone: +64-4-570 1444, Facsimile: +64-4-570 4600

A Crown Research Institute

EXECUTIVE SUMMARY

We present the results of a new probabilistic seismic hazard analysis (PSHA) for New Zealand. The PSHA incorporates geological data describing the location and earthquake recurrence behaviour of 305 active faults, a seismicity catalogue with greatly improved locations for many events, new attenuation relationships for peak ground acceleration and spectral acceleration developed specifically for New Zealand, and state-of-the-art PSH methodology developed in New Zealand and the USA. The methodology and data used in the PSHA builds on the data and methods used in an experimental PSHA of New Zealand by Stirling et al. (1998), and supersedes the PSHAs of Matuschka et al. (1985) and Smith and Berryman (1983, 1986), which were largely based on the historical record of earthquakes (historical recording began with European settlement in 1840). These models served as the basis for the current New Zealand Loadings Standard NZS4203:1992 (Standards New Zealand, 1992). PSH maps produced from our new model show the highest hazard to occur in Fiordland (vicinity of the Fiordland subduction zone and the offshore extent of the Alpine Fault), along the axial tectonic belt (Westland, Marlborough, north Canterbury, Wellington, Wairarapa, western Hawkes Bay and eastern Bay of Plenty), the Taupo Volcanic Zone (TVZ, a zone of active crustal extension and volcanism running from the central North Island volcanoes to the Bay of Plenty), and in the seismically active area of north Westland/southwest Nelson (area of the Buller and Inangahua earthquakes). The maps show generally similar patterns of hazard to the maps of Stirling et al (1998), but very different patterns to those shown on the maps of Smith and Berryman (1983, 1986) and Matuschka et al. (1985). The largest differences exist in the vicinity of the major active faults, which generally have not produced large earthquakes in historic time, but have produced them abundantly in prehistoric time.

Examination of the PSHA at the major population centres reveals that they have the following rank in decreasing order of hazard; Wellington, Christchurch, Dunedin and Auckland. The hazard is highest in Wellington, since it is close to a number of major active faults, and within an area of high seismicity in historical time. In comparison, the other centres are generally located in areas away from the major active faults, and in areas of relatively low seismicity rates.

CONTENTS

FIGURE CAPTIONS

Figure 1: The plate tectonic setting of New Zealand. The country is divided into the neotectonic provinces identified by Berryman and Beanland (1988).

Figure 2: The 305 active fault sources used as input for the PSHA. The numbers beside each fault correspond to the index numbers given in the fault table (Appendix 1).

Figure 3: The distribution of shallow crustal seismicity in New Zealand (a), and the deeper seismicity of the Fiordland and Hikurangi subduction zones (b). The seismotectonic zones we have defined to sort the catalogue, assign initial regional maximum cutoff magnitudes (M_{cutoff}), and calculate parameter b of the Gutenberg-Richter relationship for seismicity are shown in (a). In the case of (b), many of the deep zones overlap in plan view, so we show the seismicity of each zone as a particular colour, rather than trying to colour-code the actual zones. The vertical extents of the seismotectonic zones have been defined from the spatial and depth distribution of seismicity, and are shown on each plot as a depth range beside the zone number (e.g. "z20 10-45 km" indicates that zone 20 has a depth range of 10 to 45 km). Since the crustal and deep sources have been defined at different scales, the lower-depth-limit of a crustal zone sometimes overlaps with the upper-depth-limit of a deep zone. In these cases the seismicity parameters calculated for the crustal zones are assumed to represent the seismicity of the overlapping areas. In (c) we show the seismicity for the three different time periods of completeness for events of all depths from 1900 to 1997, and cross sections of seismicity across and beneath the country. See the locations of the cross sections on the "Magnitude 6.5" map. Cross sections are oriented with the northwest end to the left of the page. Maps and cross sections in (c) are taken from McGinty (1999).

Figure 4: Contours of (a)-(e) the maximum-likelihood cumulative number of events per year for $M \geq 4$, calculated from three catalogue completeness levels and magnitudes ($M \geq 4$ since 1964, $M \geq 5$ since 1940, and $M \geq 6.5$ since 1840); (f)-(j) parameter b of the Gutenberg-Richter relationship LogN=A-bM, and; (k) the maximum "cutoff" magnitude (M_{cutoff}) assumed for distributed earthquakes, for various depth layers beneath the country. The contours have been made over a gridwork of N, b and M_{cutoff} that have been smoothed with a Gaussian smoothing function, in which the correlation distance (standard deviation) is set to 50 km. Since M_{cutoff} for all of the deep seismotectonic zones is set to 7, we only show a contour plot of M_{cutoff} for the crustal (20 km) depth layer. Note that white areas on the bvalue plots are where no seismicity exists in the depth range shown.

Figure 5: (a)-(f). Probabilistic seismic hazard maps for New Zealand for site class B (intermediate soil). The maps show the levels of pga and 5% damped response spectral acceleration (0.2 and 1s period) with return periods of 475 years (i.e. 10% probability in 50 years) and 1000 years (10% probability in 105 years).

Figure 6: Seismic hazard curves for site class B of the annual rate of exceedance for various levels of pga (a), and 5% damped response spectral acceleration (1s period; b) at the centres of Auckland, Wellington, Christchurch, Dunedin and Otira. Otira is included in the plots as a useful comparison to the main centres, since it is located in the area of highest hazard in the country (Fig. 5).

Figure 7: Response spectra for Auckland, Wellington, Christchurch, Dunedin and Otira, for 475 and 1000 year return periods for site class B.

Figure 8: Disaggregation plots for Auckland, Wellington, Christchurch, Dunedin and Otira. The plots show the percentage contribution to the 475 and 1000 year levels of hazard (Fig. 7) of the various magnitudes and source-to-site distances of earthquake sources in the model. The plots are produced for pgas and 1s spectral accelerations for site class B.

Figure 9: Comparison of the 475 year return period spectra for the five centres obtained in this study (NHM), and the Matuschka et al. (1985) study, and by using the modified Katayama attenuation model of the 1985 study with our NHM seismicity model.

1.0 INTRODUCTION

1.1 General

In this report we present the results of a probabilistic seismic hazard analysis (PSHA) for New Zealand that represents a significant improvement on earlier national PSHAs. In our analysis, we combine geologic data describing the geometry and activity of 305 major active earthquake faults (locations, fault lengths, fault type, slip rates, single event displacements, estimated magnitudes, and average recurrence intervals), and combine these data with historical seismicity data to develop PSH maps for the country. Our approach is to use the geologic data and historical observations of large earthquakes to estimate the locations, magnitudes, and recurrence rates of future large earthquakes. We then use historical seismicity data (earthquake data recorded instrumentally since 1940, and earthquake data derived largely from interpretation of felt intensity data over the period 1840-1940; magnitude scales used are a mixture of moment magnitude, M_W, local magnitude, M_L and surface wave magnitudes M_S) to estimate the locations, magnitudes, and recurrence rates of moderate-to-large "distributed" earthquakes in and around the mapped faults. Our PSH maps show the peak ground accelerations (pga) and 5% damped response spectral accelerations (SA) for 0.2s and 1s periods, (often referred to as "SA(0.2s)" and "SA(1s)") expected for return periods of 475 years (i.e. 10% probability in 50 years) and 1000 years (i.e. 10% probability in 105 years) at average soil sites (Class B site conditions of Standards New Zealand, 1992).

The prime motivation for our study is that the existing national PSH maps are now out of date in terms of the methodology and data used to estimate hazard. The widely used national seismic hazard maps of Matuschka et al. (1985) and Smith and Berryman (1983, 1986) were largely based on the historical record of earthquakes, and did not explicitly incorporate geological data. More recently, national PSH maps have been published that incorporate both geological and historical seismicity data, and new methods for the treatment of historical seismicity (Stirling et al., 1998), but these maps used an unpublished interim version of the current attenuation model, and preliminary versions of the fault database and historical earthquake catalogue. Our PSHA is developed from the Stirling et al. PSHA, with improvements to the treatment of historical seismicity, the introduction of new ground motion attenuation relationships for New Zealand to the model, and use of a much enlarged and revised active fault database. These are new data describing the earthquake recurrence behaviour of active faults in New Zealand, largely collected by GNS, and the Natural Hazards Research Centre of the University of Canterbury (Pettinga et al., 1998). Furthermore, the locations and magnitudes of many earthquakes in the historical catalogue have been refined for use in this study (McGinty 1999).

1.2 Review of the 1985 hazard model

The Matuschka et al. (1985) seismic hazard study served as the basis for the current New Zealand Loadings Standard NZS4203:1992 (Standards New Zealand, 1992). It made use of a seismicity model developed by Smith and Berryman (1983, 1986) and a Japanese response spectrum attenuation model developed by Katayama (1982) and modified for New Zealand conditions. When the hazard analysis was published in 1985, it was one of the earliest applications of uniform hazard spectra as the basis for developing code loadings. The Matuschka et al. model grew out of earlier work at the University of Canterbury (Peek et al., 1980; Mulholland, 1982).

The seismicity model divided New Zealand into a number of regional source zones of uniformly distributed seismicity, each characterised by a rate parameter a_4 (the annual number of earthquakes per 1000 km^2 exceeding magnitude 4), a b-value, and a maximum magnitude M_{max}. These parameters were derived primarily from an analysis of historical seismicity, with some ad hoc adjustment on the basis of geological input. There was no explicit modelling of faults in the model. However, the maximum magnitudes were usually assigned from geological input on the magnitudes estimated for active faults in each region.

The response spectrum attenuation model specified the spectral values for each period as a product of a magnitude term, a distance term and a site class term. The magnitude and distance terms were defined for five magnitude classes (4.5-5.3, 5.4-6.0, 6.1-6.7, 6.8-7.4 and 7.5-7.9), and five distance classes (0-19 km, 20-59 km, 60-119 km, 120-199 km and 200-405 km). The distance factors were modified in such a way that effectively no site was closer than 20 km to an earthquake source. These modifications to the attenuation relation, and the lack of active fault sources in the model, meant that there was no increase in the estimated hazard within the immediate vicinity of major active faults. This process led to a significant underestimation of the hazard adjacent to the most active fault systems.

The Katayama model used four site classes, although two of these were usually combined in Japanese practice. These three remaining site classes were interpreted for New Zealand conditions as the three site subsoil categories adopted in NZS42032:1992, namely: (a) rock or very stiff soil sites; (b) intermediate soil sites; and (c) flexible or deep soil sites.

The hazard results were presented in terms of contour maps of the 5% damped response spectrum acceleration at 0.2s, SA(0.2s), for Katayama's ground class III, corresponding to the intermediate soil category of NZS4203:1992. The contour maps were formed from estimates obtained for a 0.5° by 0.5° grid spacing throughout the country. The value at 0.2s usually corresponded to the peak of the uniform hazard spectrum for a given return period. The 450 year return period map was adopted for the zone factor Z in the code, apart from limitation of the range to 0.6g to 1.2g rather than the calculated range of 0.3g to 1.3g. The adoption of a Z value of 0.6g for the lower seismicity region of the country around Auckland and in Northland imposed considerable conservatism in this region on the estimates derived directly from the hazard analysis.

2.0 NEOTECTONICS AND HISTORICAL SEISMICITY

New Zealand straddles the boundary of the Australian and Pacific plates, where relative plate motion is obliquely convergent across the plate boundary at about 50 mm/yr at the latitude of East Cape, 40 mm/yr at the latitude of central New Zealand, and 35 mm/yr in the Fiordland area (De Mets et al. 1994; Fig. 1). The relative plate motion is expressed in New Zealand by the presence of numerous active faults (Fig. 2), and a high rate of small-to-moderate (M<7) earthquakes (Fig. 3), including the occurrence of many large earthquakes (M7-7.9) and one great earthquake (M>8) in historic time. The historic record of M≥6.5 earthquakes dates from 1840, which was the time that European settlement began in New Zealand. A southeast-dipping subduction zone lies at the far southwestern end of the country ("Fiordland subduction zone" in Fig. 1), and this is linked to a major northwest-dipping subduction zone in the eastern North Island ("Hikurangi subduction zone" in Fig. 1) by a 1000 km long zone of dextral oblique slip faults ("Axial tectonic belt" in Fig. 1). The majority of the relative plate motion is accommodated by the faults of the axial tectonic belt in the area between the Fiordland and Hikurangi subduction zones.

The Hikurangi subduction interface dips beneath the eastern North Island, and abrupt changes in the spatial and depth distribution of seismicity along the subduction interface (Fig. 3) have been suggested as marking "tears" or segment boundaries in the subduction zone (Reyners, 1983, 1998). However, only one large earthquake, and no great earthquakes are known to have been produced by the Hikurangi subduction interface in historic time (since 1840), so that little is known about the earthquake potential of this feature. The Fiordland subduction zone dips southeast offshore from Fiordland, and is steeply dipping beneath Fiordland. The Fiordland subduction interface also shows abrupt changes in seismicity patterns along strike, and the lateral extent of the aftershock zone of a recent large earthquake (the M7, 1993 August 10 Fiordland earthquake; Van Dissen et al. 1994) shows that rupture lengths less than the length of the entire subduction zone do occur. Some of the highest rates of seismicity in the country occur within the subducted plates of the subduction zones. High rates of moderate earthquakes also occur above the Fiordland subduction zone, and to a lesser extent above the Hikurangi subduction zone.

The axial tectonic belt is a zone of dextral transpression, most dramatically illustrated by the southern section of the Alpine Fault (Fig. 1), where dextral slip rates of 26±7 mm/yr are observed (Berryman & Beanland, 1988; Berryman et al. 1992; Sutherland & Norris, 1995). The Alpine Fault accommodates a large portion of the relative plate motion in the central South Island, but the fault has not produced any large or great earthquakes in historic time. It is presently characterised by low rates of seismicity. Geologic data provide evidence for the occurrence of great earthquakes on the Alpine Fault with return times of hundreds of years.

Plate motion is distributed across a number of parallel faults with slip rates > 1 mm/yr in the axial tectonic belt of the northern South Island (the Marlborough faults), and across faults and the Hikurangi subduction zone in the southern and eastern North Island (Fig. 1). Faults in the axial tectonic belt show strike-slip, dip-slip and oblique-slip motion. Many moderate or larger earthquakes have occurred within the axial tectonic belt in historic time, including the two largest historical earthquakes (the M_w 8.1-8.2, 1855 Wairarapa earthquake, and M_w 7.8 Napier earthquake).

The Taupo Volcanic Zone (Fig. 1) is a zone of active crustal extension that has developed in response to the southward migration of back arc spreading from the Havre Trough (Fig. 1) into the continental margin of New Zealand in the last two million years (Cole & Lewis, 1981). The crustal extension is occurring across the zone at a rate of about 10mm/yr (e.g. Berryman & Beanland, 1988, Villamor and Berryman, in press), and normal faults typically have slip rates of 0.2-1 mm/yr in the zone. Several moderate-sized earthquakes have produced surface ruptures in the Taupo Volcanic Zone (TVZ) in historic time, the most recent being the M_w 6.5, 1987 March 2 Edgecumbe earthquake produced by a normal slip rupture of the Edgecumbe Fault. High rates of small earthquakes also characterise the TVZ.

Faults located away from the axial tectonic belt and TVZ tend to have slip rates that are about an order of magnitude less than the faults in those areas. Reverse faults with slip rates of 0.1 - 1 mm/yr characterise the style of faulting in central Otago and south Canterbury (Fig. 1), and similar slip rates characterise the reverse faults in north Westland and Nelson (Fig. 1). The reverse faults have developed in response to the oblique compression across the plate boundary. The M_w7.6, 1929 Buller, and M_w7.2, 1968 Inangahua earthquakes occurred on reverse faults in the Nelson - north Westland area, and high seismicity rates are observed near the epicenters of these earthquakes. The western North Island is a broad zone of relatively stable crust, disrupted only by normal faults in the northeast and southwest (Fig. 1). Several $M \geq 6.5$ earthquakes have occurred within the western North Island in historic time, all in the southwest. Finally, the Canterbury-Chathams platform is an area of stable continental crust that stretches well east of the map boundary in Fig. 1. Very few earthquakes have occurred on the Canterbury-Chathams platform in historic time.

3.0 PROBABILISTIC SEISMIC HAZARD ANALYSIS

3.1 Method and Analysis

The PSHA methodology of Cornell (1968) forms the basis for our analysis. The steps taken to undertake our PSHA are: (1) to use geologic data and the historical earthquake record to define the locations of earthquake sources across and beneath the country, and the likely magnitudes, tectonic type or mechanism, and frequencies of earthquakes that may be produced by each source; and (2) to estimate the ground motions that the sources will produce at a gridwork of sites that cover the entire country. The computation of ground motions in (2) is achieved with a seismic hazard code that is an improved version of the code developed by Stirling et al. (1998). Improvements to the code are in the treatment of "distributed" seismicity for input to the PSHA, and the new ground motion attenuation relationships for New Zealand (McVerry et al., 2000) that are incorporated into the code.

3.2 Earthquake Sources

3.2.1 Faults

We show the 305 fault sources used in our PSHA in Figure 2, and list them in Appendix 1 (note that there is no fault number 220). The values listed are the parameters for each fault that are input to the hazard analysis, together with values given in brackets for the magnitudes M_{max} and average recurrence intervals that are calculated within the computer code. The fault data are obtained largely from Stirling et al. (1998), from unpublished GNS data held in consulting reports, computer databases, and in recent field notes. The starting point for developing the fault database was a review of the fault database of Stirling et al. (1998) by one of the authors (Van Dissen). The Stirling et al. database was largely developed from published sources, and so did not incorporate most of the unpublished data held at GNS. Van Dissen's review provided new data and references for many faults, particularly faults in the Wellington region (e.g. the Northern Ohariu and Whitemans Valley Faults) and Marlborough (e.g. Clarence and Awatere Faults). Large amounts of unpublished fault data were then extracted from GNS client reports on geologic investigations in the Marlborough, Canterbury, Westland, Otago, Bay of Plenty-Taupo and East Cape regions (Mazengarb et al. 1997; Pettinga et al., 1998; Stirling et al., 1999; Van Dissen et al. 1993; Woodward Clyde & GNS 1999). Finally, numerous unpublished fault data were extracted from computer files, field notes and plate tectonic reconstructions, which improved the coverage of fault sources in the East Cape region (unpublished data of C. Mazengarb), Westland-northwest Canterbury and Taupo-Taihape areas (unpublished data of K. Berryman and P. Villamor) and western Southland (plate boundary model of R. Sutherland).

The fault traces shown on Figure 2 are generalisations of the mapped fault traces. These generalised faults are appropriate for regional scale PSHA. Using the methodology of Stirling et al. (1998) we divide a given fault into more than one source if: (1) geological data and/or the rupture length of a historic earthquake provide evidence for a fault having separate rupture segments (e.g., the Awatere Fault is divided into two sources); or, (2) a fault has wide (>5km) steps in the fault trace. Data bearing on the geometry (e.g., fault dip) and activity (slip rates, single event displacements, and recurrence intervals) of the fault sources are also listed in Appendix 1. Our method of estimating the likely maximum magnitude ("M_{max}" in Appendix 1) and recurrence interval of M_{max} earthquakes produced by each fault source in Figure 2 varies according to the quantity and quality of available data for each fault. Where possible, the magnitudes of large historical earthquakes (usually well constrained from instrumental records or from MM intensity data) and lengths of the associated surface ruptures are used to define the M_{max} and length of particular fault sources. If historical observations are unavailable for a fault source, then the next most preferable method of defining M_{max} is to use published estimates of single-event displacements and fault area, and the equations for seismic moment and moment magnitude:

$$M_o = \mu AD \qquad (1)$$

and,

$$\log M_o = 16.1 + 1.5 M_{max} \qquad (2)$$

in which M_o is the seismic moment (in dyne-cm) corresponding to M_{max}, μ is the rigidity modulus of the crust of the Earth, A is the fault area, and D is the single event displacement (equation 1 is from Aki & Richards, 1980, and equation 2 is from Hanks & Kanamori, 1979). To calculate fault area we use the depth to the base of the seismogenic layer (the depth to the base of seismicity recorded in the region surrounding the fault in GNS's earthquake catalogue) and dip of the fault to estimate the fault width, and estimates of the fault length from the length of surface traces. Lastly, if single-event displacement data are unavailable, then an empirical regression of Wells & Coppersmith (1994) is used to estimate M_{max} from fault rupture area. The average recurrence interval (T) assigned to M_{max} is either: the published estimate from geological investigations; the recurrence interval calculated with the equation

$$T = D/S \qquad (3)$$

if a published recurrence interval estimate is unavailable (D is average single-event displacement and S is the fault slip rate); or the recurrence interval calculated with the equation of Wesnousky (1986).

$T = M_o/M_{orate}$ (4)

if single event displacement data are unavailable (M_{orate} is the rate of seismic moment release on the fault, equal to μAS, in which μ = the rigidity modulus, 3 x 10^{11} dyne/cm^2, A=fault area, and S=fault slip rate in cm/yr). Where possible, we use the preferred values of D, S and T in equations 1 - 4, and otherwise use values that are the means of the minimum and maximum values. We also use the mean or preferred values of M_{max} (Appendix 1) in the equations.

Recent field studies and interpretations have resulted in major changes to estimated parameters of some of the fault sources since the Stirling et al. (1998) PSHA, and these require special explanation. These changes have occurred either for faults that have had alternative rupture segmentation models developed for them, or for faults or fault zones that have been mapped in more detail than before. Significant new field investigations have carried out for the Alpine Fault (Berryman et al. 1998; Yetton et al., 1998), the Hope, Kakapo and Kelly Faults (Berryman & Villamor, unpublished field data), the Porters Pass Fault Zone and neighbouring faults (Pettinga et al. 1998; Stirling et al., 1999), and faults in the TVZ (Villamor & Berryman, unpublished field data). These new data have been incorporated into the PSH model. In the case of the Alpine Fault we develop southern (fault segment 5, in Fig. 2c) and two alternative northern (segment 6, Kaniere-Tophouse, and segment 8, Haupiri-Tophouse) rupture segments, and allow segments 5 and 6 to overlap in central Westland. This is in keeping with Yetton et al.'s (1998) explanation for the relatively short (c. 100-200 year) recurrence intervals for Alpine Fault earthquakes in central Westland. However, we also incorporate an alternative explanation for the short recurrence intervals, which is that the structural complexity of the central Westland area (i.e. where the Hope, Kelly and Kakapo Faults intersect the Alpine Fault) also allows shorter segments of the fault to rupture this section of the fault (Berryman pers. comm.). Specifically, we develop a 60km rupture segment (segment 7, Kaniere-Haupiri) that coincides with the overlap zone of the southern and northern segments. Recurrence intervals for all of the segments are then calculated with the constraint that they sum to the recurrence intervals derived from the field data. Over the 60 km long overlap zone, the combined recurrence interval is 200 years. For the Hope, Kelly and Kakapo Faults, the main difference in the treatment of these faults from Stirling et al. (1998) is that the southwestern extent of the Hope Fault (i.e. southwest of the Hanmer Basin) has a considerably slower slip rate than previously assumed, and the slip rate surplus is instead taken up on the Kelly and Kakapo Faults (Berryman and Villamor pers. comm.).

For the Porters Pass Fault zone (Porters Pass, Coopers, Glentui, Lees Valley, Mt Thomas, and Mt Grey faults; Pettinga et al. 1998), we accommodate two equally plausible models for earthquake occurrence into the PSHA. These are a segmented model, in which all six faults rupture as separate earthquake sources, and an unsegmented model, in which the whole fault zone ruptures in a single earthquake. Using eqs (1) to (4), the recurrence intervals of earthquakes for the two segmentation models are calculated by assuming that each model contributes to 50% of the slip rate along the fault zone.

Major improvements have been made to the fault database in the TVZ over that of Stirling et al. (1998). While the literature available to Stirling et al. (1998) only allowed them to incorporate 15 TVZ faults into the model, we now have a total of 54 TVZ faults in our model. The biggest improvement to the TVZ is the removal of the simplistic "Taupo Fault Belt North" and "South" sources (Stirling et al. 1998) and replacement with faults sources defined for that area in recent studies (Villamor pers comm).

We characterise the earthquake potential of the Hikurangi and Fiordland subduction zones in the virtual absence of any large-to-great earthquakes having occurred on the subduction interfaces in historic time, and a lack of paleoseismic data that can be attributed to subduction zone earthquakes. Our approach for the Hikurangi subduction zone is to combine the results of several alternative subduction earthquake models (Appendix 1). Two of these models (models 1 and 2) use empirical regressions developed from global subduction zone earthquakes (Abe, 1975; Somerville et al., 1999) to estimate the M_{max} for earthquakes on the Hikurangi subduction interface from estimates of the area of subduction interface segments. The segments are defined from the results of Reyners (1998, 1999), and from changes in the cumulative slip rate of dip slip faults along the upper plate of the subduction zone in central Hawkes Bay (Beanland et al., 1998). The recurrence intervals for the subduction interface earthquakes are then estimated by taking account of the relative plate motion rates orthogonal to the subduction zone at the latitude of each segment, the amount of the plate motion taken up by dip-slip faults in the upper plate, and estimates of the degree of coupling (ratio of seismic slip to total slip) on the plate interface. The global average for the "coupling coefficient" is about 0.5 (Hyndman et al. 1997). Typical M_{max} values of 7.5 to 7.9, (associated with single event displacements of about 3m) and recurrence intervals of between 140 and 400 years are estimated by way of models 1 and 2 if it is assumed that these earthquakes accommodate all of the coseismic slip on the interface. A third model (model 3) allows for the possibility that subduction zone earthquakes are great (M>8), and therefore have much longer recurrence intervals (600 to 1200 years) if these earthquakes are assumed to accommodate all of the coseismic slip on the interface. The justification for model 3 is that earthquakes in the upper plate have produced large (~8m) displacements (e.g. 1931 M_w 7.8 Hawkes Bay earthquake), and these would be consistent with the stress regime of a strongly coupled subduction interface that slips with large single-event displacements (Haines & Darby, 1987). Furthermore, the short recurrence intervals calculated for models 1 and 2 are in conflict with the absence of large subduction interface earthquakes in the historical record. If models 1 and 2 are entirely viable then we would expect there to have been at least one of these earthquakes on the five Hikurangi subduction interface segments in the last 150 years. In Appendix 1 we combine the three models to develop a subduction interface earthquake model with a weighting scheme that gives model 3 a weight equal to the combined weights of models 1 and 2. The resulting recurrence intervals range from 600 to 2400 years for large to great Hikurangi subduction interface earthquakes.

For the Fiordland subduction zone, we use a relatively simple kinematic model that is based upon field observations, and is partially constrained by the relative plate motion. The Alpine Fault intersects the coast at Milford Sound, where it is known to have a displacement rate of 26±6 mm/yr and is thought to fail in great earthquakes about every 300 years (Cooper & Norris, 1990; Sutherland & Norris 1995). The offshore geometry of faults, including the extension of the Alpine Fault, is known from detailed swath mapping and seismic reflection data, but little is known about fault slip-rates or earthquake potential (e.g. Delteil et al., 1996; Melhuish et al. 1999; Barnes et al. 1999; Wood et al. 2000; and references therein). The onshore region has been geologically mapped (e.g. Bishop, 1986; Bishop et al., 1990; Turnbull & Uruksi, 1993; Turnbull & Uruski, 1995; and references therein), but there is no relevant paleoseismic data, and only preliminary data concerning the location of active fault traces (Van Dissen, 1993; Turnbull & Uruski, 1995; GNS, unpublished data; Otago University, unpublished data). The existence of known faults with young (<3 Ma), strongly deformed and uplifted marine sediments adjacent to them (e.g. Turnbull & Uruski, 1995), combined with significant topography that is spatially correlated with geological structures, suggests the region currently has a moderate or high tectonic tempo. In addition, the deformation pattern of basement rocks suggests Fiordland has moved >100 km north in the last 30 m.y., suggesting a minimum average strike-slip displacement rate of 3 mm/yr on faults east of Fiordland (Sutherland, 1999). Although there are insufficient data to construct a robust set of fault sources for southwestern South Island, our sources developed for this report are based on a wide range geological data.

We define offshore faults in this study on the basis of detailed bathymetric and seismic data that were collected by GNS, NIWA, and their predecessors during the last 30 years. There has been considerable collaborative GNS-NIWA effort during the last decade, and significant progress has been made towards mapping the location of offshore fault traces, and estimating their slip-rates. The estimation of recurrence intervals and maximum magnitudes is difficult for offshore earthquake sources, but is necessary and will require further collaborative effort.

3.2.2 Distributed Earthquake Sources

In addition to defining the locations, magnitudes and frequencies of large (M7-7.9) to great ($M \geq 8$) earthquakes on the crustal faults and subduction zones, we also allow for the occurrence of moderate-to-large (M~5 up to some maximum cutoff magnitude) "distributed" earthquakes both on and away from the major faults. Our main reason for considering distributed earthquakes in our PSHA is that a large percentage of earthquakes in the historical record have not occurred directly on the mapped faults. Of the 85 largest historical New Zealand earthquakes studied by Dowrick & Rhoades (1999) for modelling attenuation of intensity, only five ruptured the onshore land surface. Presumably the seismogenic width greatly exceeds the width of earthquake rupture in most cases, which allows the earthquakes to occur without rupturing the ground surface, either on mapped faults or on unknown faults. Such is the case for most earthquakes of less than M6.5 in California (Wesnousky 1986). In New Zealand, a good example of a distributed earthquake is the M_w 6.8 1994 Arthur's Pass earthquake, which occurred on a previously unknown fault, and did not rupture to the surface.

We apply a methodology developed from that of Stirling et al. (1998) to characterise the PSH from distributed earthquakes. We use the spatial distribution of seismicity recorded since 1840 to estimate the likely locations and recurrence rates of distributed earthquakes at a gridwork of point sources across and beneath the country. Our minimum magnitude for distributed earthquakes (M5.25) is slightly larger than the M5.0 typically used in PSHA (the lower-bound magnitude for damaging ground motions), and is chosen to eliminate the erroneously high short period accelerations predicted for $M<5.25$ earthquakes with the McVerry attenuation model (Section 3.2). M5.25 was also used as the minimum magnitude by Matuschka et al (1985).

We first divide the country into 37 seismotectonic zones (14 crustal and 23 deep zones enclosing the subsurface seismicity to a depth of 100 km; Fig 3). The zones are assigned depth ranges shown in Figure 3a for the crustal zones and in Figure 3b for the deep zones. For the purposes of this study, the bases of the crustal zones are assumed to correspond to the base of the seismogenic crust. The maximum cutoff magnitude (M_{cutoff}) is separately estimated for the 37 seismotectonic zones, based on criteria such as the approximate magnitude of the largest historical earthquakes that have not been able to be assigned to specific faults (e.g., the M_w 6.8 1994 Arthur's Pass earthquake), how comprehensively the zone has been studied to identify active faults (i.e. the "completeness" of the fault database in that zone), and the particular tectonic regime of the zone (e.g. a zone likely to enclose blind thrusts). All zones are set at M_{cutoff}=7.0, except for zone 5 (M_{cutoff}=7.5; most of the zone is offshore, and few active fault studies have taken place onshore), zone 6 (M_{cutoff}=7.8; the zone has produced earthquakes up to this magnitude on blind thrusts), zone 8 (M_{cutoff}=7.7; the zone has produced earthquakes close to this magnitude on previously unknown faults) and zone 14 (M_{cutoff} = 7.1, a magnitude slightly larger than the 1993 August 10 Fiordland earthquake).

The next step is to decluster the catalogue by the method of Reasenberg (1985), and then use the method of McGinty (1999) to assign new depths to the "restricted depth" earthquakes. "Restricted depth" events are the large number of events in the catalogue that were randomly assigned depths of 5, 12 and 33km because of poor depth control. Our procedure is to then subdivide the catalogue according to the 14 crustal and 23 deep seismotectonic zones, with the seismicity in each zone shown in Figures 3a and 3b. We next define five layers of point sources over the map area (at depths of 10, 30, 50, 70, and 90km) with a spacing of 0.1° in latitude and longitude, and then use a Gutenberg-Richter distribution $\log N = A - bM_w$ (N=number of events ≥ moment magnitude M_w, and A and b are empirical constants; Gutenberg & Richter, 1944) to estimate the recurrence rates of distributed earthquakes at each point source. Gutenberg and Richter found that this type of distribution of seismicity applied to large areas, and it has also been shown to describe the fault zone earthquakes that are less in size than the M_{max} of the fault (e.g., Stirling et al. 1996). The SEISRISK programme CALCRATE (Bender & Perkins, 1987; Hanson et al. 1992) is then used to calculate parameter b of the Gutenberg-Richter relationship for each seismotectonic zone, and that value of b is then assigned to each point source within the zone. CALCRATE allows the use of different magnitude completeness levels for various time periods to calculate parameter b, and is based on the methodology of Weichert (1980). Since the New Zealand historical earthquake catalogue is in general complete for M≥4 since 1964, M≥5 since about 1940, and M≥6.5 since 1840, we use these three completeness levels and time periods to calculate b for the zones. As with the b-values, the M_{cutoff} assigned to each point source is simply the M_{cutoff} of the enclosing seismotectonic zone.

Following calculation of the b-values, the earthquake hypocentres found inside each grid cell (i.e. within ± 10 km depth of the grid layer) are counted to give "N values" for each grid cell. Three N values are calculated for each grid cell based on the three generalised catalogue completeness levels and time periods in the earthquake catalogue; N1=N(M≥4 for 1964-97), N2=N(M≥5 for 1940-97), and N3=N(M≥6.5 for 1840-1997). Within each grid layer, the three sets of gridded N values, b and M_{cutoff} values are then spatially smoothed with a Gaussian smoothing function, following the methodology of Stirling et al. (1998). For each grid cell, the smoothing involves multiplying the N, b and Mcutoff values for the grid cell and all of the neighboring values within the particular grid layer (i.e., the values that are within a specified horizontal distance from the grid cell) by the Gaussian function, summing all of the products, and then dividing by the sum of all of the Gaussian functions. The equation is:

$$N \text{ or } B \text{ or } Mcutoff(smoothed) = \Sigma\, ((N \text{ or } B \text{ or } Mcutoff(each\ site))e^{-d^2/c^2}) \,/\, \Sigma\, (e^{-d^2/c^2})$$

(5)

in which *c* is the correlation distance (50km), and *d* is the distance from the centre of the grid cell to the centre of each neighbouring grid cell (neighbouring grid cells greater than 3x the correlation distance from the grid cell are not used in equation 5). The Gaussian smoothing preserves the total number of earthquakes in the catalogue after every N value in the gridwork has been smoothed with equation 5. The 50km correlation distance is used since it has been found to produce a spatial distribution of N values that correlates well with the general seismicity patterns across the country (Stirling et al. 1998). No smoothing is done in the vertical axis (i.e. between the various grid layers). The recurrence rates of M5.25 - M_{cutoff} events at each point source are then calculated from the three sets of smoothed N values by way of the following maximum likelihood method to give a Gutenberg-Richter A-value based on the entire catalogue:

$$A=log[(N1 + N2 + N3)/(tb1 + tb2 + tb3)] \qquad (6)$$

in which,

$$tb1=ctime1 \times 10^{(-magmin1 \times b)}$$
$$tb2=ctime2 \times 10^{(-magmin2 \times b)}$$
$$tb3=ctime3 \times 10^{(-magmin3 \times b)}$$

and,

ctime1=1997-1964; ctime2=1964-1940; ctime3=1940-1840.

The A value is then used in the Gutenberg-Richter relationship (this time equal to logN/yr=A-bM) to solve for N/yr(M≥4), and then the incremental rates (n/yr=M) are calculated for each 0.1 increment of magnitude from M5.25 to M_{cutoff}. We show plots of the b-value, N/yr(M≥4) for the five depth layers, and M_{cutoff} for the 10km (crustal) layer in Figure 4. Since M_{cutoff} is set to 7 for all of the deeper zones, we do not show the M_{cutoff} for these zones.

Our methodology for the treatment of distributed seismicity is an improvement over the commonly used approach in PSHA of defining large area source zones over a region and uniformly distributing the seismicity recorded inside each source across the source. This is because our methodology preserves the smooth transitions in seismicity rates within and across the boundaries of the seismotectonic zones, and avoids the "edge effects" that often appear on hazard maps when adjacent area sources enclose areas of significantly different seismicity rates. Though Peek's (1980) use of "fuzzy" boundaries between area sources removed these "edge effects" in early New Zealand PSH maps, our methodology also preserves spatial variations of seismicity *within* the sources. Our methodology is also an improvement over that of Stirling et al. (1998), who only considered crustal seismicity, a single completeness level ($M \geq 4$ for the period 1964-96), single M_{cutoff} (7.5), and single b value (1.1) for the entire country. In Figure 4 we show maps of the distribution of $N(M \geq 4)$ per year, the b-value and the M_{cutoff} for the various layers of point sources in our model. Note that M_{cutoff} is set to 7.0 for all except the 0 to 20 km depth layer. It has the disadvantage that for some grid points in low seismicity locations N1, N2 and N3 will be zero, because the seismicity rates are lower than can be detected in the observation periods, while the true seismicity is non-zero. The lowest seismicity rate that can be detected with 90% certainty in the 33 year completeness period for $M \geq 4$ from a 50km radius circle is approximately 8×10^{-4} events per year per $0.1^{\circ} \times 0.1^{\circ}$ grid cell.

3.3 Attenuation Model

3.3.1 Introduction

The attenuation relationships used in this study have been developed recently by McVerry et al. (2000) for 5% damped acceleration response spectra (SA(T)) from a data set of New Zealand earthquake records, supplemented by pga values from overseas records in the near-source range (less than 10km source-to-site distance) that is lacking in the New Zealand data. The attenuation model takes account of the different tectonic types of earthquakes in New Zealand (i.e. crustal, subduction interface and dipping slab) and their range of centroid depths. The attenuation expressions for crustal earthquakes have further subdivisions, through mechanism terms, for different types of fault rupture (strike-slip, normal, oblique/reverse and reverse). The model was developed for site classifications which were based on those of the current New Zealand Loadings Standard NZS4203:1992, with one modification of the site classifications to give better matching of the New Zealand spectra, and a subdivision of the rock classification for specialist applications. A term was also included in the attenuation expression to model the rapid attenuation of high-frequency motions through the Taupo Volcanic Zone.

The McVerry et al. attenuation model is used in this study because it has specific relevance to New Zealand conditions, in contrast to most other available attenuation relationships, which were developed from either global strong motion data or data from other regions of the world. The McVerry et al. model is presented below, including discussion of features that affect the hazard estimates calculated in this study. Graphs of the pgas estimated from the attenuation model as a function of magnitude, distance, tectonic type and focal mechanism, are shown in Appendix 2, along with spectra for a selection of magnitudes, source-to-site distances and tectonic types. All plots are for site class B, the class assumed for all results presented in this report.

3.3.2 Site Classification

The development of the response spectrum attenuation model began using the site class categories (a), (b) and (c) of the current New Zealand Loadings Standard NZS4203:1992 (Standards New Zealand, 1992). In NZS4203:1992, category (a) nominally corresponds to rock or very stiff soil sites with natural periods less than 0.25s, category (b) corresponds to intermediate soil sites and category (c) to flexible or deep soil sites with natural periods estimated as greater than 0.6s. The Standard gives thicknesses of various types of soil that conform to categories (a) and (c).

It was found that stiff soil sites included in the NZS4203 site category (a) "rock or very stiff soil" exhibited pgas and spectra similar to the category (b) "intermediate soil sites" rather than to rock sites. Accordingly, category (a) sites with more than 3m of soil were combined with category (b) sites to form the new class B. This separation of the stiff soil sites of category (a) from rock sites was also found necessary in the development of the Zhao et al. (1997) pga attenuation model. NZS4203:1992 category (c) "flexible or deep soil sites" carried over directly to Class C. Classes B and C were combined into a single "soil" class for the Zhao et al. pga study, but the differences in the site terms were statistically significant at longer periods in the response spectrum study, and were retained for all periods.

Class B is defined as soil sites with periods less than 0.6s. If the shear-wave velocity profile is known for a site, NZS4203:1992 allows the period to be estimated from four times the shear-wave travel-time from rock to the surface. Measured velocities or travel-times are usually not available for New Zealand sites, so most site classifications are made from the descriptions of the materials at the sites and their thicknesses. Table 1 lists the depths of different types of materials given in the code as corresponding to the changeover between classes B and C, with lesser depths taken as class B.

The New Zealand site classifications are based on estimated or measured travel-times from "rock" to the surface, rather than on the average shear-wave velocity in the top 30m as in recent US building codes. The main differences between the New Zealand and US classifications arise where there are thick deposits of reasonably high-velocity materials, such as gravels, over rock. The New Zealand classification recognises that these sites have the potential of amplification at periods around their site periods, so does not include them in the same class as shallower deposits of the same materials which do not have the potential for substantial amplification at moderate-to-long periods.

The site classifications also differ from those of the Abrahamson & Silva (1997) and Youngs et al. (1997) attenuation models that served as the starting points for developing the New Zealand response spectrum attenuation expressions for crustal and subduction zone earthquakes respectively (see Section 3.3.3). Abrahamson & Silva (1997) combined rock sites and sites with shallow soil up to 20m thick in their "rock" class, which is thus intermediate between the New Zealand classes A and B. Their "soil" class consists of deep soil greater than 20m thick, similar to New Zealand class C but including some class B sites as well. The Youngs et al. (1997) rock class is similar to New Zealand Class A, but their soil class is for soil greater than 20m thickness, with shallow soil not covered by either of their classes. Both studies excluded soft soil with shear wave velocities less than 150m/s, as in the development of the McVerry et al. model.

Also relevant for comparing the results with earlier New Zealand hazard studies are the site classifications used by Katayama (1982). Katayama's four ground types were as used for bridge design in Japan. Type I is Tertiary or older rock (bedrock), or a diluvial layer of less than 10m thickness above bedrock, with natural periods less than 0.2s. Type II is more than 10m of diluvium or less than 10m of alluvium, with site periods between 0.2s and 0.4s. Type III is an alluvial layer less than 25m thick, with less than 5m thickness of liquefiable or low-strength soil, with site periods between 0.4s and 0.6s. Type IV is other than the above, usually soft alluvial layers or reclaimed land, with site periods exceeding 0.6s. In Japanese design practice, Types II and III are usually combined. Categories (a), (b) and (c) of NZS4203:1992 were interpretations for New Zealand condition of Types I, II/III and IV respectively, so can be compared directly to the corresponding Katayama ground types.

TABLE 1: DESCRIPTION OF SITE CLASS B CLASSIFICATION BASED ON NZS4203:1992

Site Class B (Intermediate soil sites)

Sites where the low amplitude natural period is less than 0.6s, or sites with depths of soils less than the following values:

Soil type and description		**Depth of soil (m)**
Cohesive soil	Representative undrained shear strengths (kPa)	
Soft	12.5-25	20
Firm	25-50	25
Stiff	50-100	40
Very stiff	100-200	60
Cohesionless soil	Representative SPT (N) values	
Loose	4-10	40
Medium dense	10-30	45
Dense	30-50	55
Very dense	> 50	60
Gravels	> 30	100

The code commentary notes that the soil descriptions and associated properties correspond to those of the New Zealand Geomechanics Society (1988), "Guidelines for the Field Description of Soils and Rocks in Engineering Use".

It also notes that:

"Where a site consists of layers of several types of material, the contribution of each layer to the natural period may be estimated by multiplying 0.6s by the ratio of its thickness to that listed for its soil type. The total period may then be estimated by summing the contribution for each layer."

3.3.3 Form of the McVerry et al. Model

Limited ranges of magnitude and distance and insufficient records in the response spectrum dataset prevented the development of a robust model purely from the New Zealand data. Instead, overseas attenuation models that provided reasonable matches to the New Zealand data were selected as "base models", and then some of their coefficients were modified to improve the matches. One base model was selected for crustal earthquakes and another for subduction-zone earthquakes Constraints were imposed so that the selected models controlled the behaviour at short distances where New Zealand data were lacking.

As a starting point for the development of the McVerry et al. attenuation model, the New Zealand data were compared with recent overseas attenuation models by calculating residuals between the data for the various tectonic classes of earthquakes and the predictions of appropriate attenuation models. The Abrahamson and Silva (1997), Idriss (1991), Boore et al. (1997) and Sadigh et al. (1997) attenuation models were considered for crustal earthquakes, and the Crouse (1991) and Youngs et al. (1997) models for subduction zone earthquakes. The residuals were examined as a function of magnitude, distance, centroid depth and response spectrum period for each earthquake source and site category. All of the crustal models provided adequate fits to the New Zealand data at most periods. The two subduction zone models provided poor fits to New Zealand data from shallow slab and interface earthquakes, generally over-estimating the data at short spectral periods and under-estimating them at longer periods. As a result of these comparisons, the Abrahamson & Silva (1997) (A&S) model was selected as a suitable base model for crustal earthquakes, and the Youngs et al. (1997) model as the base model for subduction zone earthquakes.

The approach was to perturb the base models, constraining some parameters but modifying others to obtain better matches to the New Zealand data. The regressions for the free coefficients were performed using the Abrahamson and Youngs (1992) random effects methodology, using source code provided by Abrahamson. The random effects model is a maximum likelihood method that accounts for correlations in the data recorded in the same earthquake. This is achieved by modelling two error terms, an intra-event residual and an inter-event residual. The inter-event residual gives the average error for data from the same earthquake event. The intra-event residuals represent the remaining variability in errors between data from the same event. The implementation of the random effects model in the McVerry et al. study allowed magnitude-dependent intra-event standard errors but inter-event standard errors that were independent of magnitude. Both the intra-event and inter-event standard errors were functions of spectral period, with the regressions for each spectral period performed separately.

The form of the model for the median response spectrum values for site class B is given in equation 7 for crustal earthquakes and in equation 8 for subduction zone earthquakes. The coefficient values are listed in Table 2.

For crustal earthquakes:

$\ln SA_B(T) = \mathbf{C_1(T)} + C_{4AS}\,(M-6) + C_{3AS}(T)\,(8.5-M)^2 + \mathbf{C_5(T)}\,r +$

$$(\mathbf{C_8(T)} + C_{6AS}\,(M\text{-}6))\ \ln\,(r^2 + C_{10AS}{}^2(T))^{1/2} + \mathbf{C_{46}(T)}\ r_{VOL} + C_{32}\ CN + C_{33AS}(T)\ CR \quad (7)$$

with CN = -1 for normal mechanism crustal earthquakes, 0 otherwise
CR = 0.5 for reverse/oblique mechanisms, 1.0 for reverse mechanisms, 0 otherwise

For subduction zone earthquakes:

$$\ln SA_B(T) = \mathbf{C_{11}(T)} + (C_{12Y} + (C_{15}(T) - \mathbf{C_{17}(T)})\ C_{19Y})\ (M\text{-}6) + C_{13Y}(T)\ (10\text{-}M)^3 +$$

$$\mathbf{C_{17}(T)}\ \ln\,(r + C_{18Y}\exp(C_{19Y}\,M)) + \mathbf{C_{20}(T)}\ H_C + \mathbf{C_{24}(T)}\ SI + \mathbf{C_{46}(T)}\ r_{VOL}\,(1 - DS) \quad (8)$$

with SI = 1 for subduction interface earthquakes, 0 otherwise
DS = 1 for deep slab earthquakes, 0 otherwise

and $C_{15}(T) = C_{17Y}(T)$, and $C_{12Y}(T)$ the Youngs et al. coefficient of the (M-6) term

M is moment magnitude, r is the shortest distance in km from the site to the fault rupture, and r_{VOL} is the length in km of the part of the source-to-site path that lies in the volcanic zone. Other parameters are the mechanism for crustal earthquakes, indicated by CN and CR; the tectonic type for subduction zone earthquakes, indicated by SI and DS; and the centroid depth H_C for subduction zone earthquakes. Earthquakes within the subducting slab are separated into shallow slab earthquakes at depths less than 50 km, for which the predominant mechanisms are normal or oblique, and deep slab earthquakes which usually have reverse or strike-slip focal mechanisms. The equations apply for moment magnitudes 5 to 7.5, and distances up to 400 km.

Coefficients that were fitted in the regressions are shown in bold. Parameters subscripted $_{AS}$ and $_{Y}$ were held to Abrahamson & Silva or Youngs et al. values, respectively. The model expressions give the median (50-percentile) value of $SA_B(T)$, the 5% damped acceleration response spectrum value (in units of "g") for the stronger of two arbitrarily orientated orthogonal horizontal components for site class B.

$SA_B(T)$ has a log-normal distribution with median values given by equations 7 and 8 and magnitude-dependent standard errors Sigmatotal(M,T) of ln $SA_B(T)$ defined in terms of the parameters SigmaM6(T), Sigslope(T) and Tau(T), as given in equations 9a and 9b. The parameter values are listed in Table 2.

TABLE 2: COEFFICIENTS OF THE ATTENUATION MODEL P2MRF5AC FOR SITE CLASS B

Period	0.000	0.075	0.10	0.20	0.30	0.40	0.50	0.75	1.00	1.50	2.00	3.00	
1	0.59021	1.64284	2.08360	1.63354	0.97823	0.68110	0.74598	0.26915	0.20183	-0.39613	-0.68381	-1.19739	free
3	0.00000	0.03000	0.02800	-0.01380	-0.03600	-0.05180	-0.06350	-0.08620	-0.10200	-0.12000	-0.12000	-0.17260	fixed
4	-0.14400	-0.14400	-0.14400	-0.14400	-0.14400	-0.14400	-0.14400	-0.14400	-0.14400	-0.14400	-0.14400	-0.14400	fixed
5	-0.00967	0.01011	-0.00958	-0.01061	-0.01108	-0.01044	-0.00944	-0.00859	-0.00709	-0.00751	-0.00751	-0.00674	free
6	0.17000	0.17000	0.17000	0.17000	0.17000	0.17000	0.17000	0.17000	0.17000	0.17000	0.17000	0.17000	fixed
8	-0.65469	-0.89543	-0.96827	-0.73174	-0.51073	-0.46256	-0.51891	-0.50359	-0.60867	-0.53197	-0.53197	-0.51984	free
10	5.60000	5.58000	5.50000	5.10000	4.80000	4.52000	4.30000	3.90000	3.70000	3.55000	3.55000	3.50000	fixed
11	8.98560	9.43477	10.15544	11.42270	10.40980	9.63810	9.53207	8.25309	7.85831	7.49288	7.20520	5.63637	free
12	1.41400	1.41400	1.41400	1.41400	1.41400	1.41400	1.41400	1.41400	1.41400	1.41400	1.41400	1.41400	fixed
13	0.00000	0.00000	-0.00110	-0.00270	-0.00360	-0.00430	-0.00480	-0.00570	-0.00640	-0.00730	-0.00730	-0.00890	fixed
15	-2.55200	-2.70700	-2.65500	-2.52800	-2.45400	-2.40100	-2.36000	-2.28600	-2.23400	-2.16000	-2.16000	-2.03300	fixed
17	-2.56727	-2.62147	-2.68877	-2.78783	-2.55600	-2.44827	-2.48662	-2.34444	-2.35600	-2.36279	-2.36279	-2.10982	free
18	1.78180	1.78180	1.78180	1.78180	1.78180	1.78180	1.78180	1.78180	1.78180	1.78180	1.78180	1.78180	fixed
19	0.55400	0.55400	0.55400	0.55400	0.55400	0.55400	0.55400	0.55400	0.55400	0.55400	0.55400	0.55400	fixed
20	0.01550	0.001778	0.01668	0.01470	0.01206	0.01354	0.01215	0.01008	0.00874	0.0071	0.00716	-0.00337	free
24	-0.50962	-0.58245	-0.71566	-0.77265	-0.68932	-0.40172	-0.34432	-0.10891	-0.02921	-0.1188	-0.11882	-0.30130	free
32	0.20000	0.20000	0.20000	0.20000	0.20000	0.20000	0.20000	0.20000	0.20000	0.2000	0.20000	0.20000	fixed
33	0.26000	0.26000	0.26000	0.26000	0.19800	0.15400	0.11900	0.05700	0.01300	-0.0490	-0.04900	-0.15600	fixed
46	-0.03279	-0.03430	-0.03573	-0.03831	-0.03582	-0.03342	-0.03238	-0.02855	-0.02539	-0.0201	-0.02012	-0.01651	free
SigmaM6	0.4865	0.5281	0.5398	0.5703	0.5505	0.5627	0.5680	0.5562	0.5629	0.5394	0.5394	0.5701	
Sigslope	0.1261	0.0970	0.0673	0.0243	0.0861	-0.1405	0.1444	0.0932	-0.0749	-0.0056	-0.0056	0.0934	
Tau	0.2687	0.3217	0.3088	0.2726	0.2112	0.2005	0.1476	0.1794	0.2053	0.2411	0.2411	0.2406	
SigtotM6	0.5558	0.6184	0.6219	0.6321	0.5896	0.5973	0.5869	0.5844	0.5992	0.5909	0.5909	0.6188	

Model P2MRF5AC (T=2s adjusted)
Uses foreign data for PGA, with A and C overseas records repeated 5 times
Volcanic path term, two rock site classes, W and M/S,
Different attenuation coefficients for M/S and other classes, with r=0 constraints
PGA only data from PGA6F5AC.TXT, SA from QKE9_ALL.TXT r=0 crustal & SZ constraint, c28=0, c30=a11
SA'(T) coefficients from S2VPSMR model
Results generated 28/1-1/2/99, edited from *.OUT files 1/2/99 by G. McVerry, re-edited for class B only 29/3/00distance 0-400km, c5*r term for crustal, common atten & depth term for SZ

Sigma (M,T)	=	SigmaM6(T) + Sigslope (T) * (M-6)	$5 < M < 7$	
	=	SigmaM6(T) – Sigslope(T)	$M < 5$	(9a)
	=	SigmaM6(T) + Sigslope(T)	$M > 7$	

Sigmatotal (M,T)	=	sqrt ($Sigma(M,T)^2 + Tau(T)^2$)	for all M	(9b)

The McVerry attenuation model was derived from all the available New Zealand strong-motion data that satisfied various selection criteria, and also from some digital seismograph records converted to accelerograms to increase the number of rock records available. The New Zealand dataset lacks records in the near-source region, at distances of less than 11km from the source, and at magnitudes of M_w 7.3 and greater. Accordingly, some constraints have been applied to the attenuation models for the near-source regions, and for large magnitudes. In addition, for pgas (i.e. SA(0s), the New Zealand records were supplemented with 66 overseas records at distances of 10 km or less from the source, which were included directly in the regression analysis for determining the model. The selection of near-source records included some from the Northridge and Kobe earthquakes. The near-source selection is representative rather than comprehensive. Some records were excluded because we had insufficient information about the source regions to define the shortest source-to-site distance or about site conditions to assign the appropriate New Zealand classification.

The near-source constraint used in the McVerry et al. study was to require that the crustal and subduction zone expressions for rock sites matched the magnitude-dependence of the base models at zero distance (r=0). The values of two of the coefficients, $C_4(T)$ and $C_6(T)$, of the crustal model governed by the near-source constraint differed insignificantly from their A&S values, so they were left unchanged. The constraint required that the quadratic magnitude term be as for A&S, i.e. $C_3(T)=C_{3AS}(T)$. For subduction zone earthquakes, the r=0 constraint led to a relationship shown in equation 8 for the coefficient of the (M-6) linking the coefficients of the linear magnitude and ln(distance) terms, and the cubic magnitude term had to be the same as in the Youngs et al. model. Also, coefficients that occurred nonlinearly in the attenuation equations were constrained to their values in the base models.

In common with many but not all modern attenuation relations, the attenuation expressions of equations 7 and 8 exhibit partial magnitude saturation at short distances, that is, there is less dependence on magnitude at short distances than at large distances. In the crustal earthquake expression, this is achieved through the M ln(distance) term, as in the A&S model. For the subduction zone expression, it is achieved by adding the Youngs et al. magnitude-dependent expression to the distance in the ln(distance) term.

A departure from the A&S model is that A&S had different values for the magnitude coefficient C_4 for the magnitude ranges less than and greater than magnitude 6.4. The coefficient was larger for the small magnitude range, leading to lesser magnitude saturation at magnitudes less than 6.4. In the regression against New Zealand data, it was found that using the large magnitude coefficient for all magnitudes gave a better fit. A consequence of this is that small magnitudes may have relatively stronger effects at short distances for the McVerry et al. model than for the A&S model. This modification to the model was introduced before the overseas near-source pga was introduced to the dataset used in the regressions, so that there were no data from distances less than 11km when this modification was introduced. This change is likely to be a factor in the observation that uniform hazard spectra estimated with the McVerry et al. model appear very sensitive to the lower cutoff magnitude, showing very strong shorter period components when magnitudes less than 5.25 are retained.

Another change from the A&S model was the introduction of the anelastic attenuation term $C_5(T)r$. This term was found necessary when the maximum distance range of the data was extended to 400 km, compared to less than 250 km in the A&S dataset. The increased distance range was used to obtain sufficient rock records and volcanic path records. In earlier forms of the model where the maximum distance for crustal data was restricted to 200 km, this term was statistically insignificant. The numerical value of this term is small for distances of a few tens of kilometres or less that govern hazard estimates for all but possibly the largest spectral periods considered in the model, but its inclusion affects the values of the coefficients C8(T) of the ln(distance) terms.

High attenuation of earthquake waves in part of the volcanic region of the North Island has been recognised for many years (e.g. Haines, 1981). The increased attenuation in the volcanic region has been modelled by the term $C_{46}(T)\ r_{VOL}$ applied for crustal, shallow-slab and interface earthquakes, where the source-to-site path includes a distance r_{VOL} (km) through the whole TVZ. The determination of the whole TVZ as the highly attenuating region is described by Cousins et al. (1999). While the geometric attenuation term dominates for nonvolcanic paths at distances less than 100-200 km, the anelastic attenuation is of similar importance for volcanic paths for short spectral periods. For example, the total anelastic term halves pga values over only 16 km in the volcanic region, while requiring more than 70 km to have the same effect on its own (i.e. neglecting the geometric attenuation) outside the volcanic zone. The volcanic path effect is less severe for periods exceeding 0.5s.

For the purposes of this study, the whole TVZ was approximated by source zone 3 (Fig. 3a). As further approximations, the volcanic region attenuation term was applied to the whole path for sources (both distributed point sources and fault sources) within zone 3, but ignored for the part of the travel path through zone 3 of earthquake waves propagating from sources outside it.

Similar effects to the volcanic region attenuation occur at depth (e.g. Mooney, 1970), but were ignored in the McVerry et al. study for deep-slab earthquakes because of the difficulties of modelling the high attenuation zone in three dimensions. Deep-slab records likely to have been affected by high attenuation in the mantle under the volcanic region were omitted from the analysis.

The model will significantly over-estimate the spectra from deep-slab sources involving propagation through the highly attenuating mantle. Work is in progress identifying the source and site combinations affected by high attenuation in the mantle, and developing a volcanic-path type modification to the attenuation expression of equation 8 for highly-attenuating mantle paths.

For crustal earthquakes, there are mechanism terms, C_{32} CN for normal-mechanism earthquakes and $C_{33AS}(T)$ CR for reverse/oblique or reverse mechanisms. Both of these terms were constrained in the analysis, the reverse/oblique term to period-dependent large-magnitude values from A&S model, and the normal term to a constant value based on analyses by Spudich and Abrahamson (Abrahamson, pers. comm.). The normal mechanism term corresponds to a factor of 0.82 on strike-slip spectra accelerations for all periods, and the reverse mechanism term to factors on the strike-slip accelerations varying from 1.30 in the 0s to 0.2s range, to 1.01 at 1s period, and 0.86 at 3s period. A&S had larger reverse-mechanism factors at magnitudes less than 6.4, with a maximum short-period factor of 1.84 for magnitudes of 5.8 and less, but such strong magnitude-dependence of the reverse-mechanism term was not supported by the New Zealand data.

The subduction zone expression for weak rock is based on the rock expression of Youngs et al. (1997). The coefficient $C_{17}(T)$ of the ln(distance) attenuation term has been fitted from the regression against New Zealand data, but subject to the constraint that the magnitude dependence at zero distance is the same as for the Youngs et al. model. Period-dependent coefficients of the interface and centroid depth terms were fitted from the regression analysis, rather than taken as the constant values of the Youngs et al. model which were fitted from pga data but applied for all spectral periods. In the McVerry et al. model, the period-dependent interface coefficients show much stronger slab motions relative to interface motions than for the Youngs et al. model in the 0.1s to 0.3s range, and lesser slab versus interface effects for periods of 0.4s and greater. The interface coefficients correspond to ratios close to 1.0 for periods of 0.75s and greater. The depth effect is much greater than for the Youngs et al. model, especially for periods up to 1s.

Separate additive terms with respect to shallow-slab earthquakes were considered for interface earthquakes and deep-slab earthquakes, but were statistically significant only for interface earthquakes, as in the Youngs et al. model. Differences in attenuation rates for shallow-slab, deep-slab and interface earthquakes were not statistically significant. Consequently, modelled spectral accelerations for shallow- and deep-slab earthquakes differ only by the effect of the depth term, and by the inclusion of the volcanic path term for shallow-slab earthquakes.

The Youngs et al. model gave nonlinear site effect terms through having different coefficient values in the rock and soil attenuation expressions. In the McVerry et al. model, site effects for soil sites were modelled directly through site response terms, with the same site effect terms imposed for crustal and subduction zone earthquakes. Nonlinear soil response factors that are a function of the estimated median weak-rock pgas, as used by A&S, were allowed to model the ratios of the spectra for soil sites, classes B and C, with respect to those for weak-rock sites. However, a linear site response factor was found to give the best fit for site class B, although this result may reflect the paucity of records of strong near-source motions for which any nonlinear effects would be most apparent. Nonlinear soil response factors were retained for Class C sites (not presented in this report), for which the modelled spectra are amplified with respect to those for weak-rock sites at short periods at low amplitudes of motion, but deamplified for strong motions. The site response factor for Class B has been included in the constant terms $C_1(T)$ for crustal earthquakes and $C_{11}(T)$ for subduction zone earthquakes in equations 7 and 8.

There were fewer response spectra than pga records available for the study, because (a) acceleroscope and undigitized records contribute pgas but no spectra; (b) response spectra data were included only for frequencies where their amplitudes exceeded noise levels; and (c) near-source overseas records have been used only for pgas to date. It was found that the pga estimates $SA'(0)$ from the response spectrum dataset were different from the estimates $SA'(0)$ from the larger pga dataset. The differences were most important for near-source pgas from crustal earthquakes on rock and deep soil sites. The estimates were more in line with overseas models for the pga than for the response spectrum dataset, with the $SA'(0)$ values generally less than those from overseas models. It was decided to scale the response spectrum values for other spectral periods by the pga ratio, thus retaining the spectral shapes from the response spectrum dataset. This modification is incorporated in the coefficients listed in Table 2. This approach has the potential problem of imposing inappropriate spectral shapes near-source if the near-source spectral shapes SA(T)/SA(0) are in fact different from those at greater distances. It is intended to include near-source overseas spectra rather than just pga values in future development of the attenuation model, in that we now have most of the spectra as well as pga values available.

3.4 Computation of Hazard

We use the locations, sizes, tectonic types or crustal mechanisms (slip types), and recurrence rates of earthquakes defined in our source model to estimate the PSH for a gridwork of sites with a grid spacing of 0.1 degrees in latitude and longitude (about 10km spacing). Our measures of PSH are the acceleration levels (pga, 5% damped response spectral acceleration at 0.2 and 1s period) with 475 year and 1000 year return periods at class B (intermediate soil) sites. We use the standard methodology of PSHA (Cornell, 1968) to construct PSH maps. For a given site, we: (1) calculate the annual frequencies of exceedance for a suite of ground motion levels (i.e. develop a "hazard curve") from the magnitude, recurrence rate, earthquake type, and source-to-site distance of earthquakes predicted from the source model; and (2) estimate the maximum acceleration level that is expected with a 10% probability of exceedance in 50 and 105 years. These time periods and probabilities are chosen to show the accelerations that have return periods of 475 and 1000 years, respectively. These are return periods of interest to engineers and planners. For each site, step (1) is repeated for all sources in the source model, and (2) is calculated by summing the results of (1) to give the annual frequencies of exceedance for a suite of acceleration levels at the site due to all sources (i.e. acceleration levels of 0.05g, 0.1 to 2g at increments of 0.1, and 3g), and finding the ground motion levels that correspond to annual frequencies of 1/475 and 1/1000.

In calculating the ground motions expected in a certain time period, we assume a Poisson model of earthquake occurrence, in that we base our estimates of hazard on the average time-independent rate of earthquake occurrence on each fault, and do not calculate time-dependent hazard that would take into account the elapsed time since the last earthquake on the fault. The Poissonian model is also applied to the Alpine Fault, in contrast to the methodology used in our recent PSHA for the Canterbury region (Stirling et al. 1999) which considered time dependent estimates of earthquake probabilities for the Alpine Fault (Yetton et al. 1998). We treat the Alpine fault in this manner since there is currently active debate going on as to the most appropriate conditional probability model for assessing earthquake probabilities (e.g. Ellsworth, 1999). In our calculation of ground motions with the McVerry attenuation model we adopt the standard practice of modern PSHA and take into account the uncertainty in estimates of ground motion from the attenuation model in the calculation of PSH. The general method is to assume that each estimate of ground motion calculated with the attenuation equation at a site is the median of a log-normal distribution, with an associated standard deviation. The standard deviations are usually equal to about 0.5 in natural log units of ground motion. The median and standard deviation are then used to estimate the probability of exceedance for a suite of ground motion levels up to 3 standard deviations below and above the median. Only magnitudes 5.25 and greater are included in the hazard analysis as discussed in Section 3.2.2.

Since the McVerry attenuation model has separate expressions for crustal earthquakes of different slip type or focal mechanism (i.e. strike slip, normal and reverse, and slip types intermediate between these extremes), and separate expressions for subduction interface, shallow slab and deep slab earthquakes, we estimate accelerations with the attenuation expression applicable to the slip type and tectonic environment of each earthquake source. Each fault is assigned a particular slip type, and the attenuation expression for that slip type is used for the fault in the hazard calculations. In the case of the dipping subduction interface sources we use the interface attenuation expression. For the distributed seismicity (point) sources, the slip type assigned to the point source is the slip type of the enclosing seismotectonic zone (Fig. 4). For the deep zones we simply use the shallow and deep slab expressions, based on the observation that essentially all of the deep seismicity in the country is attributed to the dipping Hikurangi and Fiordland slabs. Application of the "volcanic path" attenuation expression for the TVZ, which strongly reduces accelerations with distance, is limited to faults and point sources located in the TVZ, taken as corresponding to seismotectonic zone 3 of Fig. 3a. More sophisticated application of the "volcanic path" term (e.g. attenuation of accelerations passing through the TVZ from outside sources) cannot be performed until the 3-dimensional geometry of the TVZ is better defined. The deep slab expression is valid only for source-to-site paths up the dipping slab. We use it for all sites for deep slab sources, overestimating the motions for those sites involving propagation paths through the highly attenuating mantle.

3.5 Hazard Estimates

3.5.1 Hazard Maps

In Figure 5 we show maps of the levels of pga and 5% damped response spectral acceleration (0.2, and 1s period) with return periods of 475 and 1000 years (10% probability of exceedance in 50 and 105 years, respectively. Incorporation of fault data into the PSH model produces very different patterns of hazard across the region to the earlier maps of Matushka et al. (1985) and Smith and Berryman (1983, 1986), and generally similar patterns of hazard to the maps of Stirling et al. (1998). The highest 475 year accelerations (pgas of over 1g, 0.2s spectral accelerations of over 3g, and 1s accelerations of over 0.6g) occur in the west of the South Island. These areas are in the vicinity of the Alpine, Hope, Kakapo and Kelly Faults (fault segments 5, 7 and 150-152 in Fig. 2). The latter three faults are also in areas of relatively high distributed crustal seismicity. Relatively high 475 year accelerations at short spectral periods (peak accelerations of <0.6g outside the Alpine Fault high hazard zone for 475 years) 0.5g, and 0.2s spectral accelerations of over 1.4g) are also observed in north Westland and western Nelson, and these are attributed to the high distributed seismicity rates in the area of the Buller and Inangahua earthquakes. However, since these distributed seismicity sources produce many more moderate earthquakes than large earthquakes, the long period (1s) accelerations only amount to 0.2 to 0.3g.

The highest accelerations in the North Island occur along the northeast striking faults of the Axial Tectonic Belt and TVZ. Here, pga and 0.2s and 1s spectral accelerations reach maximum values of over 0.6g, 1.8g, and 0.5g, respectively over small areas. The TVZ faults and distributed seismicity source also produce a zone of high hazard to the southwest and northeast of Lake Taupo on the 475 year maps. The contribution to the 475 year hazard from the Hikurangi subduction zone is to produce a broad zone of relatively high hazard from the TVZ to the East Coast. For pga this measures about 0.3 to 0.4g, and the corresponding values of 0.2s spectral acceleration are 1.2 to 1.4g, and 0.2 to 0.4g for 1s acceleration. Hazard progressively decreases to the south and north of all of these areas. The lowest hazard in the country is in Northland, and the lowest in the South Island is in Southland (Fig. 6). The hazard may be underestimated in these regions, in that the seismicity rate has been modelled as zero in places, while the minimum rate of earthquakes that can be detected with 90% reliability from the completeness levels of the historical seismicity catalogue is approximately 8×10^{-4} events per year greater than magnitude 4 per $0.1^\circ \times 0.1^\circ$ grid cell.

The 1000 year PSH maps generally show much higher hazard than the 475 year maps, for the simple reason that the longer timespan allows more earthquakes to contribute to the hazard. All of the areas described above show highest hazard on the 1000 year maps. Differences of 0.1g for pga and 1s spectral acceleration, and 0.2g for 0.2s spectral acceleration are typically observed between the maps. Some of the largest differences in pga (differences of 0.2g) are observed in the foothills of the Southern Alps, northwest of Christchurch.

The PSH maps generally show a smooth distribution of hazard that is highest along the major plate boundary faults of the axial tectonic belt and the subduction zones, and progressively decreases away from these areas. However, this progressive decrease in hazard is locally interrupted by zones of anomalously high or low hazard. A small circular zone of unusually high hazard appears on most of the maps in northern Southland/southern Central Otago. This zone is attributed to the relatively short earthquake recurrence intervals estimated for the Blue Mountain and Spylaw Faults (Appendix 1, faults 162 and 163 on Fig. 2). Since these recurrence intervals are simply based on field reconnaissance of the area, and not detailed field investigations (Stirling et al. 1998), the hazard in this zone may be unrealistically high. Another area of anomalous hazard is in the TVZ, to the south of Lake Taupo. This area does not show as high hazard as the area north of Lake Taupo, yet the extension rate across the TVZ is presumed to be similar in all areas. The discrepancy may be due to incomplete knowledge of the TVZ faults south of Lake Taupo. The small zones of high hazard in the Raukumara Peninsula region (area of Gisborne, East Cape and the northeastern Bay of Plenty) are attributed to faults characterised from field reconnaissance (Mazengarb pers comm.). Since the area has not been the focus of detailed paleoseismic investigations, two possible explanations for the small zones of anomalously high hazard are: (1) that there may be many more, as yet undiscovered active faults in this area that would homogenise the hazard if incorporated into the model, and; (2) that earthquake recurrence intervals for the faults in the area have been underestimated, leading to overestimation of the hazard at sites close to these faults. Lastly, the "corridor" of lower hazard between Rotorua and Mount Maunganui on the 475 year pga map is due two factors. The first is the effect of the Kerepehi Fault (fault segments 94-97 in Fig. 2a) to the northwest of TVZ adding to the hazard from the distributed seismicity. The second is the use of the "volcanic path" attenuation expression for distributed earthquake sources in the TVZ (seismotectonic zone 3 in Fig. 3), which reduces the 475 year pga in the corridor from that to the northwest for this part of the TVZ that has no modelled fault sources (Fig. 2a).

There are some notable differences in the PSH maps produced in this study from those of Stirling et al. (1998), despite the generally similar pattern of hazard across the country as a whole. Some of the largest differences are located in the Raukumara peninsula area, and are attributed to differences in modelling of the Hikurangi subduction interface in the two studies. The Stirling et al. study assumed an uncoupled Hikurangi subduction zone in this area (i.e. nil potential for subduction interface earthquakes), which resulted in much lower hazard than the hazard shown in Figure 5. The other large difference is that the hazard is lower than estimated by Stirling et al. in the TVZ. This is due to the major differences in modelling of the TVZ faults in the two studies, and implementation of the volcanic path attenuation relationship in our study.

3.5.2 Site Specific Hazard

In addition to defining maps of the expected levels of pga and spectral accelerations for New Zealand, we also compare the PSH model at five sites from diverse seismotectonic environments around the country. The sites are the four major populations centres (Auckland, Wellington, Christchurch, and Dunedin), which respectively come from areas of low, high, low and low concentrations of active faults and historical seismicity, and Otira, located in the area of highest hazard in the country (Fig. 5).

In Figure 6 we show hazard curves (graphs of the annual rate of exceedance for a suite of acceleration levels) for the five centres. The annual rate of exceedance is the inverse of the return period. There is considerable spread in the graphs of pga (Fig. 6A) and 1s response spectral acceleration (Fig. 6B) for the five centres. Specifically, the graphs show more than a factor-of-10 to 100 range in annual rate for a given acceleration, and about a factor-of-10 range in acceleration for a given annual rate. Clearly the township of Otira shows the highest hazard, consistent with a location close to major active faults (e.g. Alpine Fault), and within an area of relatively high historical seismicity (Fig. 3). In decreasing order of hazard are the centres of Wellington (close to five major faults, above the Hikurangi subduction interface, and in an area of high historical seismicity), Christchurch (at a distance of about 50km from a number of active faults in the foothills of the Southern Alps), and Dunedin and Auckland (both generally away from areas of active faults, and in areas of relatively low seismicity rates). The slopes of the hazard curves are generally similar, except for the lower-than-average slopes for pga in Dunedin and Otira (Fig. 6A), and the higher-than-average slopes at long return periods (>500 years) for Otira. The increasing influence of the Akatore Fault on the hazard for Dunedin as the return period increases takes Dunedin from hazard levels similar to those of Auckland at return periods of about 100 years and less up to levels similar to those of Christchurch at return periods of several thousand years. For Otira, the short average recurrence intervals of rupture on neighbouring active faults that govern its hazard lead to saturation effects becoming apparent for return periods exceeding about 500 years.

The five centres can also be compared by way of response spectra calculated for given return periods. In Figure 7 we show spectra for return times of 475 years (i.e. 10% probability of exceedance in 50 years; Fig. 7A) and 1000 years (Fig. 7b). The spectra for all five centres show their highest accelerations at the 0.2s spectral level (a typical observation in strong motion seismology), and the pgas are slightly greater than the 1s spectral acceleration for all spectra. The 1000 year spectrum generally shows around a one-third increase in accelerations over the 475 year spectrum for a given centre, except for Otira where the increase is about 25% and Dunedin where it is around 50%.

Next, we show disaggregation plots for the five centres in Figure 8. These plots show the percentage contribution to the hazard for a particular return period from the various earthquake sources in the source model. They demonstrate the different contributions of magnitude and distance that govern the hazard in the five locations, and the different contributors to the hazard for short (e.g. pga) and long (e.g. 1s) spectral periods. In Figure 8 we show disaggregation plots for pga and 1s spectral acceleration, for 475 year and 1000 year return times. Twenty plots are shown in total.

In the case of Auckland, virtually all of the hazard comes from the distributed seismicity sources, which contribute over 97% of the pga hazard and about 85% of the SA(1s) hazard for the 475-year and 1000-year return periods considered. The Kerepehi North Fault (segment 94 in Fig 2a and Appendix I), modelled as producing magnitude 6.7 earthquakes at a distance of 62km from Auckland with an average recurrence interval of 2500 years, makes a small contribution to the hazard in Auckland which is apparent in the SA(1s) disaggregation plots.

In contrast, Wellington's hazard is dominated by fault sources. The strong influence of the Wellington Fault is evident from the peaks on the disaggregation plots (Fig. 8) at Mw 7.3 and a distance of less than 10 km. The Wellington Fault, modelled with magnitude 7.3 earthquakes with an average recurrence interval of 600 years on the Wellington-Hutt Valley segment (Wellington SW, segment number 157) at a distance of 3 km, makes about a 60% contribution to the hazard of Wellington for the four cases considered. The second largest peak in the pga plots corresponds to the contribution (about 15%) from the Wairarapa Fault (segment 58) in magnitude 8.1 earthquakes at 20 km distance. The Wairarapa Fault makes a similar percentage contribution to the SA(1s) hazard, which also includes 10-15% contributions from the Hikurangi subduction interface (segments 63, 68 and 73) in the magnitude 7.8-8.4 range at about 23km distance under the city. Magnitude-distance cells corresponding to distributed seismicity sources rarely contribute more than 2% to the hazard (the small peaks at M_w<6 and distance<50km) for return periods of 475 years and 1000 years.

The pga hazard of Christchurch comes from a combination of distributed seismicity sources at less than 50km (the peaks at Mw<6.5 and distances < 50km), contributing 55-60% of the 475-year and 1000-year hazard, and the faults at the western edge of the Canterbury Plains (e.g. Ashley Fault; the peaks at M>6.5 and distances of 30km to 50km). The Alpine Fault (segment 5, Milford-Haupiri) only contributes a maximum of about 2% to the pga hazard of Christchurch, as seen in Figure 8 as the small peak centred at Mw 8 and a distance of 130km on the pga plots. On the other hand, the Alpine Fault is the single largest contributor to the SA(1s) hazard, at slightly over 20%. The other large peak in the SA(1s) disaggregation plots, centred at magnitude 7.2 and 30km distance, is the combined contribution of the Ashley, Springbank and Pegasus 1 Faults (segments 30, 31 and 32 in Fig. 2). The overall contribution from modelled faults is over 90% of the estimated SA(1s) hazard for Christchurch.

In Dunedin, most of the hazard comes from the distributed seismicity sources (the peaks at Mw<6.9 and distances < 60km) and from the Akatore Fault (fault 280), with magnitude 7.1 earthquakes at 13km distance with an average recurrence interval of 3000 years. The percentage contribution of the Akatore Fault to the 1000 year hazard (about 30% for both pga and SA(1s)) is about double the 475 year contribution of 16%.The distributed seismicity contributes 70-80% of the pga hazard and about 45% of the SA(1s) hazard for these return periods.

Lastly, the hazard at Otira is overwhelmingly dominated by large-magnitude earthquakes on the nearby faults that have short average recurrence intervals, with virtually negligible contribution to the hazard from the distributed seismicity sources. The Kelly Fault (fault 146) producing magnitude 7.2 earthquakes at a distance of about 2km from Otira contributes about 50% of the estimated pga hazard and 60-65% of the SA(1s) hazard for return periods of 475 years and 1000 years. The Milford-Haupiri segment of the Alpine Fault (segment 5) produces magnitude 8.1 earthquakes at a distance of about 10 km with an average recurrence interval of 300 years. The closeness of the fault sources and their associated large-magnitude earthquakes with short average recurrence intervals translate to very high estimates of the 475-year and 1000-year motions.

The last set of results presented (Figures 9a-e) are comparisons of the 475-year return period spectra for site class B at the five locations from this study (labelled 475 years NHM) with those resulting using the seismicity (Smith & Berryman) and attenuation (modified Katayama) models of the Matuschka et al. (1985) study. To separate the effects of changes to the seismicity and attenuation models between the current study and the 1985 study, results are also presented using the new seismicity model with the modified Katayama attenuation model used in 1985.

For Auckland, the new class B spectrum is typically about 80% of the 1985 values, although as low as about 50% at 1s period. At periods up to about 0.35s, the changes can be attributed about equally to the seismicity and attenuation components of the model. For periods of 0.4s and greater, the changes result almost totally from the attenuation model.

For Wellington, the short-period part of the spectrum (up to 0.5s) has increased considerably from that estimated from the 1985 model, especially around the peak of the spectrum at 0.2s period. The SA(0.2s) value has increased from 1.28g to 1.64g. This change appears to result almost entirely from the new attenuation model, in that the new and old (Smith & Berryman) seismicity models give very similar results using the modified Katayama attenuation model (results labelled "475yrs Matuschka" and "475yrs Mod. Katayama" repectively). However, this is misleading, in that the hazard disaggregations discussed previously (Figure 8) show that the 475 year hazard estimated for Wellington in the current study is dominated by contributions from fault sources. In particular, the Wellington-Hutt Valley segment of the Wellington Fault at a distance of 3km contributes about 60% of the estimated hazard. The Smith & Berryman seismicity model that was used in the 1985 study did not include fault sources, so the similarity of the results using the two different seismicity models with the modified Katayama attenuation model does not mean that the seismicity models are essentially the same around Wellington. The important feature is the combination of the new attenuation model with the new seismicity model. The modified Katayama attenuation model is inappropriate for modelling near-fault motions, as it produces no change in estimated spectra for distances between 0km and 20km. The new McVerry et al. attenuation model produces a substantial increase in spectral accelerations as the distance decreases from 20km. It is thus able to produce estimates of the motions resulting from the Wellington Fault source (e.g. median pga of 0.60g and median SA(0.2s) value of 1.82g at 3km from a magnitude 7.3 strike-slip fault) that are much more in line with observed near-fault motions than the values (median pga= 0.26g, median SA(0.2s) = 0.66g) given by the modified Katayama model. At 0.75s and beyond, there is little difference in the results from the three models.

For Christchurch, the 475 year spectra are similar in character between the three models. The new model gives increased 475 year values with respect to the 1985 study up to 0.5s period, and similar values at longer periods. The results from the two seismicity models using the modified Katayama attenuation model are very similar. For Christchurch, estimation of near-source spectra accelerations is not a factor, so it appears that the seismicity distribution around Christchurch is approximately equivalent in the two seismicity models, although in the new model some of it is represented by fault sources at moderate and large distances rather than purely by distributed seismicity. The new attenuation model appears to give greater values than the modified Katayama model in the short-period range from 0.1s to 0.4s, and reduced values in the 0.75s-1.5s period band.

For Dunedin, the short-period spectral values from the new model are similar to those of the 1985 model, but reduced for periods of about 0.3s and greater. The comparisons using the modified Katayama model show a large decrease in spectral values for the new seismicity model. However, the much stronger motions associated with the Akatore Fault for the new attenuation model counteracts much of this difference.

For Otira, the new estimates are considerably increased because of the inclusion of fault sources. In the short-period band, the modified Katayama attenuation model is unable to produce the levels of near-source motion expected from the Kelly and Alpine Faults, so the new attenuation model boosts the estimated spectra considerably.

In summary, the new study produces considerably different results from the 1985 study. At some sites, particularly those near active faults, the estimated spectra have increased by large amounts, while at other locations the estimated spectra are reduced. The combination of a response spectrum attenuation expression that is able to produce realistic levels of near-fault motions with a seismicity model that includes fault sources is an important feature of the new seismic hazard model.

4.0 SUMMARY AND CONCLUSIONS

We have developed a new PSH model for New Zealand that incorporates geological data describing the location and earthquake recurrence behaviour of 305 active faults, a seismicity catalogue with greatly improved locations for many events, new attenuation relationships for pga and spectral acceleration developed specifically for New Zealand, and state-of-the-art PSH methodology developed in New Zealand and the USA. The model replaces the Matuschka et al. (1985) and Smith and Berryman (1986) models, which were largely based on the historical record of earthquakes. PSH maps produced from the new model show the highest hazard to occur in Fiordland (vicinity of the Fiordland subduction zone and the offshore extent of the Alpine Fault), along the axial tectonic belt (Westland, Marlborough, north Canterbury, Wellington, Wairarapa, western Hawkes Bay and eastern Bay of Plenty), the TVZ (from the central North Island volcanoes to the Bay of Plenty), and in the seismically active area of the Buller and Inangahua earthquakes (north Westland/southwest Nelson). As such, the maps show similar patterns of hazard to the experimental maps produced by Stirling et al. (1998), but considerably different patterns to those of Smith and Berryman (1983, 1986). Since the latter maps have long served as the basis for the loadings code, and have been applied to numerous engineering, planning, and insurance applications, our new maps are expected to produce significantly different estimates of hazard for future applications of this nature.

Interrogation of the PSHA at the four major centres reveals that they have the following rank in decreasing order of hazard: Wellington, Christchurch, Dunedin and Auckland. The hazard is highest in Wellington since it is close to a number of major active faults, and in an area of high seismicity in historical time. In comparison, the other centres are generally located in areas away from the major active faults, and in areas of relatively low seismicity rates. For Auckland, virtually all of the hazard comes from distributed seismicity sources. The disaggregation of the hazard shows a more complicated picture for Christchurch and Dunedin. For Christchurch, distributed sources contribute most of the pga hazard, but modelled fault sources contribute nearly all the hazard in terms of response spectral accelerations for 1s period. For Dunedin distributed seismicity sources are the most important at short return periods, but the Akatore Fault becomes increasingly important as the return period increases.

5.0 FUTURE DEVELOPMENTS AND SENSITIVITY STUDIES

We can identify a number of important areas of future research that will improve our estimates of seismic hazard for New Zealand. First, the estimates of PSH (Figs. 5 and 6) are provided for a single site condition (intermediate soils), and do not take into account the variable site conditions that exist across the country. Our attenuation model and computer code allows five site conditions to be modelled, with maps similar to Figure 5 able to be produced for each site condition. Variable site conditions may have a significant influence on ground motions in many areas of the country (e.g. low-lying areas of the Wellington region and areas of Christchurch). We therefore recommend that information on surface geology be factored into our PSHA to produce estimates of PSH that incorporate the actual site conditions at each location. At the simplest level this would involve choosing the site class applicable to the geology of each site (from published geological maps), and using the appropriate attenuation expression to estimate the PSH at that site. To more thoroughly address the issue of site conditions, basin effects should also be considered in future PSHAs. Research on this topic will eventually provide amplification factors due to basin geometry, and these will be readily imported into PSHA.

Another limitation of our study is that all the estimates of seismic hazard are made according to the preferred, or mean values of the various parameters (e.g. magnitude, recurrence rate, M_{cutoff} for distributed seismicity), and do not incorporate the uncertainties in these parameters. While it is standard practice for regional PSHA to use preferred parameters (as we have done), we recommend that the PSHA be extended to quantify the uncertainty in estimates of PSH as a result of our uncertainty in the input parameters. Such information will be most useful for the towns and cities, but could also be provided for the entire region. The most effective way of quantifying the uncertainty in input parameters is by way of a "Monte Carlo" style sampling of a logic tree analysis (Reiter 1991, pp. 220-222). Repeated sampling of a logic tree of parameters according to weights assigned to each choice of parameter (branch of the logic tree), calculation of the hazard with each sample of the logic tree, and comparison of all the hazard estimates will quantify the uncertainty in PSH. This is routinely achieved for site-specific PSHAs, but is uncommon in regional or national PSHAs.

For the distributed seismicity the historical catalogue includes a mix of magnitude scales. Conversion of these magnitudes to moment magnitude (M_W) involves considerable uncertainty, especially for deep earthquakes, that has not been taken into account in the present study. Rhoades (1996) has developed a methodology that accounts for these uncertainties in magnitudes that will be incorporated into the hazard calculations.

We have based our PSH estimates on time-independent (Poissonian) probabilities of earthquake occurrence, and have not taken into account the elapsed time since the last earthquake on any of the faults (conditional probability estimates). Effort should be focused on developing conditional probability estimates for the well studied faults in the country, such as the major strike-slip faults in the axial tectonic belt. One such model has been developed for the Alpine Fault (Yetton et al. 1998), but this model needs to be evaluated against alternative, equally plausible conditional probability models (e.g. Ellsworth, 1999). Also related to "non-poissonian" earthquake occurrence is the issue of fault interaction and earthquake clustering in space and time. Historical observations in areas like northern Turkey and the Central Nevada Seismic Belt (e.g. Caskey et al. 1997) provide evidence for earthquake clustering in space and time. In PSHA this information should be used to show that the probability of an earthquake on one fault is in part conditional on the occurrence of an earthquake on a neighbouring fault, and that the expected hazard of a region in one relatively short time period (e.g. 50 years) could be considerably different to the expected hazard in another such time period.

The parameters assigned to the Hikurangi and Fiordland subduction zones are entirely based on modelling, and are unconstrained by actual data. Increased effort needs to go into undertaking research to constrain the degree of coupling of the subduction interface, and the timing of large-to-great subduction interface earthquakes in the paleoearthquake record.

The attenuation model used in this study has some shortcomings that should be resolved. An example is the unusually high short-period accelerations produced by the model for $M<5.25$ earthquakes. Future improvements to the strong motion database and further modelling of these data will undoubtedly improve the estimates of acceleration from the attenuation model, especially in the near-source zone. In addition, it is intended to incorporate other recent New Zealand attenuation relationship into the model, such as the Dowrick and Rhoades (1999) Modified Mercalli intensity expression, and the Zhao et al. (1997) pga model. For further analysis of the sensitivity of the results to the selection of the attenuation model, calculations will be performed for several overseas models. Currently the Abrahamson and Silva (1997), Sadigh et al. (1997), Katayama (1986) and modified Katayama (Matuschka et al. 1985) models are included in the computer code, to which the Boore et al. (1997) model will be added. Other future developments will be proper implementation of the TVZ attenuation expression, and modelling of the high attenuation in the mantle from deep slab earthquakes, as quantified for intensities by Dowrick and Rhoades (1999).

Finally, efforts should be focused on developing methods to test our estimates of PSH, and those of future PSHAs. Currently, many workers use historical earthquake records to test PSH maps, but the short duration of historical records in most countries make them inadequate for testing PSH estimates that incorporate prehistoric earthquake data. Work on the use of field criteria such as precariously-balanced rocks to test the estimates of PSH is progressing in the western USA, and similar studies should be promoted in New Zealand. Precariously-balanced rocks may provide upper estimates of the ground motions that have occurred at specific sites for time periods of thousands of years (e.g. Stirling et al., 1998).

6.0 ACKNOWLEDGMENTS

The funding of the Earthquake Commission Research Foundation to produce this report is gratefully acknowledged. Numerous people in addition to those included as authors deserve acknowledgement for their assistance in this study. Martin Reyners and Terry Webb provided assistance in developing the earthquake recurrence intervals and magnitudes for the Hikurangi subduction zone. Julian Garcia collected much fault data from recent literature, and Colin Mazengarb provided assistance with developing fault parameters for the Raukumara peninsula. Jarg Pettinga and Mark Yetton provided many new data for this study via the Canterbury Regional Council seismic hazard analysis. Haidee Davidson and David Kennedy are thanked for report preparation. John Zhao, Norm Abrahamson, Paul Somerville and Nancy Smith contributed to the development of the New Zealand response spectrum attenuation relation, in studies partly funded by the former Electricity Corporation of New Zealand. Much of the work that has gone into developing the New Zealand model has been funded by the Public Good Science Fund.

7.0 REFERENCES

Abe, K., 1975. Reliable estimation of the seismic moment of large earthquakes. *Journal of Physics of the Earth, 23:* 381-390.

Abrahamson, N.A. and Youngs, R.R. 1992. A stable algorithm for regressions analysis using the random effects model. *Bulletin of the Seismological Society of America 82:* 505-510.

Abrahamson, N.A. and Silva, W.J. 1997. Empirical response spectral relations for shallow crustal earthquakes. *Seismological Research letters: 68,* 94-127.

Aki, K., and Richards, P.G. 1980. *Quantitative Seismology: Theory and Methods,* W.H. Freeman, San Francisco, California.

Barnes, P., Davy, B., Sutherland, R., Delteil, J. 1999. Structure and kinematics of the offshore Fiordland margin, New Zealand. *Geological Society of New Zealand Miscellaneous Publication 107A*, p. 11.

Beanland, S., Hancox, G. T., Townsend, T., Van Dissen, R. 1997. *Waikaremoana power station earthquake hazard assessment.* GNS client report 33397D.

Beanland, S., Melhuish, A., Nicol, A., and Ravens, J. 1998. Structure and deformational history of the inner forearc region, Hikurangi subduction margin, New Zealand. *New Zealand Journal of Geology and Geophysics 41:* 325-342.

Begg, J.G., and Van Dissen, R.J. 1998. Whitemans Valley Fault: a newly discovered active second order fault near Wellington, New Zealand – implications for regional seismic hazard. *New Zealand Journal of Geology and Geophysics 41*:441-448.

Bender, B. and Perkins, D.M. 1987. *Seisrisk II: A computer program for seismic hazard estimation.* U.S. Geological Survey Bulletin 1772.

Benson, A., Little, T., Van Dissen, R. J., Hill, N., Townsend, D., 1998. Paleoseismicity of the eastern section of the Awatere fault, New Zealand. *Programme & abstracts, Geological Society of New Zealand & New Zealand Geophysical Society Joint Annual Conference. Geological Society of New Zealand miscellaneous publication 101B* : 43.

Berryman, K.R., and Beanland, S. 1988: The rate of tectonic movement in New Zealand from geological evidence.*Transactions of the Institute of Professional Engineers of New Zealand 15*: 25-35.

Berryman, K.R., Beanland, S., Cooper, A.F., Cutten, H.N., Norris, R.J., Wood, P.R. 1992: The Alpine Fault, New Zealand: Variation in Quaternary structural style and geomorphic expression. *Annales Tectonicae Supplement to Volume 6*: 126-163.

Berryman, K.R. , Hull, A.G, Smith, E.G.C. 1995. Deterministic estimates of earthquake hazard in Australasia: a comparison of Wellington, Auckland and Melbourne. *Pacific Conference of Earthquake Engineering. Australian Earthquake Engineering Society 1* : 49-58.

Berryman, K.R., Cooper, R.F., Norris, R.J., Sutherland, R., Villamor, P. 1998: Paleoseismic investigation of the Alpine Fault at Haast and Okuru. Geological Society of New Zealand and New Zealand Geophysical Society Joint Annual Conference. Programme and Abstracts. *Geological Society of New Zealand Miscellaneous Publication 101A:* 44.

Berryman, K.R., Beanland, S., Wesnousky, S.G., 1998. Paleoseismicity of the Rotoitipakau Fault Zone, a complex normal fault in the Taupo Volcanic Zone New Zealand. *New Zealand Journal of Geology and Geophysics* 41 : 449-465.

Bishop, D.G. 1986. *Geological map of New Zealand 1:50 000, Sheet B46-Puysegur, Map (1 sheet) and notes (36 p.),* Dep. of Sci. and Ind. Res., Wellington.

Bishop, D.G.; Blattner, P.; and Landis, C.A., 1990: *Miscellaneous map of New Zealand, Sheet 16 - Hollyford. Map (1:75 000) and notes (40 p.).* Department of Scientific and Industrial Research, Wellington.

Boore, D.M., Joyner, W.B., and Fumal, T. 1997: Equations for estimating horizontal response spectra and peak acceleration in western North American earthquakes. *Seismological Research Letters 68 :* 128-153.

Caskey, S.J., Wesnousky, S.G., Zhang, P., Slemmons, D.B., 1996: Surface faulting of the 1954 Fairview Peak (Ms7.2) and the Dixie Valley (Ms6.8) earthquakes, Central Nevada. *Bulletin of the Seismological Society of America 86*: 761-787.

Cole, J.W. and Lewis, K.B., 1981: Evolution of the Taupo-Hikurangi subduction system. *Tectonophysics 72*: 1-21.

Cooper A.F., and Norris, R.J. 1990. Estimates for the timing of the last coseismic displacement on the Alpine Fault, northern Fiordland, New Zealand. *New Zealand Journal of Geology and Geophysics,* 33 : 303-307.

Cornell, C.A. 1968: Engineering seismic risk analysis. *Bulletin of the Seismological Society of America 58*: 1583-1606.

Cousins, W.J., Zhao, J.X, and Perrin, N.D. 1999. A model for the attenuation of peak ground acceleration in New Zealand based on seismograph and accelerograph data, *Bulletin of the New Zealand Society for Earthquake Engineering. 32:* 193-220.

Crouse, C.B. 1991. Ground-motion attenuation equations for earthquakes on the Cascadia subduction zone, *Earthquake Spectra,* 7 : 201-236.

Delteil, J.; Collot, J-Y.; Wood, R.; Herzer, R.; Calmant, S.; Christoffel, D.; Coffin, M.; Ferriere, J.; Lamarche, G.; Lebrun, J-F.; Mauffret, A.; Pontoise, B.; Popoff, M.; Ruellan, E.; Sosson, M.; Sutherland, R. 1996: From strike-slip faulting to oblique subduction: a survey of the Alpine Fault-Puysegur Trench transition, New Zealand, results of cruise Geodynz-sud leg 2. *Marine geophysical researches 18:* 383-399.

DeMets, C., Gordon, R.G., Argus, D.F., and Stein, S. 1994: Current plate motions. *Geophysical Journal International 101*: 425-478.

Dowrick, D.J., and Rhoades, D.A. 1999: Attenuation of Modified Mercalli intensity for New Zealand earthquakes, *Bulletin of the New Zealand National Society for Earthquake Engineering 21:* 55-89.

Ellsworth, W. Matthews, M.V., Nadeau, R.M., Nishenko. S.P., Reasenberg, P.A., and Simpson, R.W. 1999: A physically-based earthquake recurrence model for estimation of long-term earthquake probabilities (Extended Abstract). *Workshop on Earthquake Recurrence: State of the Art and Directions for the Future.* Instituto Nazionale de Geofisica, Rome, Italy. 22-25 February 1999.

Fellows, D.L. 1996. *Preliminary paleoseismic assessment of the Wairoa North fault.* ARC Environment Technical Publication No. 75.

Grapes, R., Little, T., and Downes, G. 1997. The 1855 Wairarapa, New Zealand, Earthquake - Analysis of Historical Data. *Bulletin of the New Zealand National Society of Earthquake Engineering,* 30: 271-368.

Grapes, R.H., Little, T.A., Browne, Rait, G.J. 1997. *Ngapotiki Thrust, White Rock and Te Kaukau Point, Southeast Wairarapa: Active and inactive structures of the Hikurangi forearc.* Geological Society of New Zealand Annual Conference, November 1997. Field Trip Guide FT2.

Grapes, R., Little, T., and Downes, G. 1998. Rupturing of the Awatere Fault during the 1848 October 16 Marlborough earthquake, New Zealand: historical and present day evidence. *New Zealand Journal of Geology and Geophysics 41*:387-399.

Gutenberg, B. and Richter, C.F. 1944: Frequency of earthquakes in California. *Bulletin of the Seismological Society of America 34*: 185-188.

Haines, A.J. 1981. A local magnitude scale for New Zealand earthquakes, *Bulletin of the Seismological Society of America*, 71 : 275–294.

Haines, A.J., Darby, D.J. 1987. *Preliminary dislocation models for the 1931 Napier & 1932 Wairoa earthquakes.* New Zealand Geological Survey report EDS 114.

Hanks, T.C. and Kanamori, H., 1979: A moment magnitude scale. *Journal of Geophysical Research, 84*: 2348-2350.

Hanson, S.L., Thenhaus, P.C., Chapman-Wilbert, M. and Perkins, D.M., 1992: *Analyst's manual for USGS seismic hazard programs adapted to the Macintosh computer system.* U.S. Geological Survey Open File Report 92-529.

Heron, D., Van Dissen, R.H., and Sawa, M. 1998. Late Quaternary movement on the Ohariu Fault, Tongue Point to McKays Crossing, North Island, New Zealand. *New Zealand Journal of Geology and Geophysics 41 : 419-440.*

Hull, A.G., and Dellow, G.D. 1993 *Earthquake hazards in the Taranaki region.* GNS client report 1993/03.

Hyndman, R.D., Yamano, M., and Oleskevich, D.A. 1997. The seismogenic zone of subduction thrust faults. *The Island Arc 6*, 244-260.

Idriss I. M. 1991. *Selection of earthquake ground motions at rock sites*, Report prepared for the Structures Division, Building and Fire Research Laboratory, National Institute of Standards and Technology, Department of Civil Engineering, University of California, Davis.

Katayama, T. 1982. An engineering prediction model of acceleration response spectra and its application to seismic hazard mapping. *Earthquake Engineering and Structural Dynamics*, 10: 149-163.

Kelsey, H.M., Hull, A.G., Cashman, S.M., Berryman, K.R., Cashman, P.H. Trexler, J.H., Begg, J.G. 1998. Paleoseismicity of an active reverse fault in a forearc setting : The Poukawa fault zone, Hikurangi forearc, New Zealand. *The Geological Society of America Bulletin* 110 : 1123-1148.

Lecointre, J.A. Neal, V.E., Pamer, A.S. 1998. Quaternary lahar stratigraphy of the Western Ruapehu ring plain, *New Zealand Journal of Geology & Geophysics* 41 : 221-245.

Little, T.A., Grapes, R. 1998. Late Quaternary strike-slip on the eastern part of the Awatere fault, South Island, New Zealand. *The Geological Society of America Bulletin* 110 : 127-148.

Matuschka, T., Berryman, K.R., O'Leary, A.J., McVerry, G.H., Mulholland, W.M. and Skinner, R.I. 1985: New Zealand seismic hazard analysis, *Bulletin of the New Zealand National Society for Earthquake Engineering*, 18 : 313-322.

Mazengarb, C., Cousins, J., Dellow, G., Townsend, T. 1997. *Earthquake and related hazards in the Gisborne District.* Institute of Geological and Nuclear Sciences Client Report 1997/44692D.13.

McGinty, P. 1999: Preparation of the New Zealand Seismicity Catalogue for a probabilistic seismic hazard analysis of New Zealand. *Abstracts. New Zealand Geophysical Society and Meterological Society of New Zealand Joint conference,* Victoria University of Wellington 1-3 September 1999.

McVerry, G.H., Zhao, J.X., Abrahamson, N.A., Somerville, P.G. 2000. Crustal and subduction zones attenuation relations for New Zealand earthquakes. *Paper No. 1834, Proceedings of the 12th World Conference of Earthquake Engineering 2000*. Auckland, New Zealand.

Melhuish, A., Sutherland, R., Davey, F.J., Lamarche, G., 1999. Crustal structure and neotectonics of the Puysegur oblique subduction zone, New Zealand. *Tectonophysics 313*: 335-362.

Mooney, H.M. 1970. Upper mantle inhomogeneity beneath New Zealand: seismic evidence, *Journal of Geophysical Research, 75 :* 285-309.

Mulholland, W.M. 1982. *Estimation of design earthquake motions for New Zealand.* Research Report 82-9. Department of Civil Engineering, University of Canterbury.

National Earthquake Hazard Reduction Program (NEHRP) 1994. 1994 *Recommended Provisions for Seismic Regulations of New Buildings: Part 1, Provisions*, issued by Federal Emergency Management Agency, FEMA 222A, 290 pp.

New Zealand Geomechanics Society 1998. *Guidelines for the field descriptions of soils and rocks in engineering use.*

Nicol, A and Van Dissen, R.J. 1997. *Late Miocene to recent fault and fold deformation east of Martinborough, Wairarapa.* Geological Society of New Zealand annual conference, November 1997. Field Trip Guide FT3.

Peek, R. 1980. *Estimation of seismic risk for New Zealand. A seismicity model and preliminary design spectra.* Research report 80-21, Department of Civil Engineering, University of Canterbury.

Peek, R., Berrill, J.B. and Davis, R.O. 1980. A seismicity model for New Zealand. *Bulletin of the New Zealand National Society for Earthquake Engineering, 13:* 355-364.

Pettinga, J.R., Chamberlain, C.G., Yetton, M.D., Van Dissen, R.J., and Downes, G., 1998. *Earthquake Hazard and Risk Assessment Study (Stage 1 – Part A); Earthquake Source Identification and Characterisation.* Canterbury Regional Council Publication U98/10.

Reasenberg, P. 1985. Second-order moment of central California seismicity, 1969-1982. *Journal of Geophysical Research 90*: 5479-5496.

Reiter, L. 1991. *Earthquake hazard analysis. Issues & insights.* Columbia University Press. 253pp.

Reyners, M. 1983: Lateral segmentation of the subducted plate at the Hikurangi margin, New Zealand: seismological evidence. *Tectonophysics 96*: 203-223.

Reyners, M. 1998: Plate coupling and the hazard of large subduction thrust earthquakes at the Hikurangi subduction zone, New Zealand.*New Zealand Journal of Geology and Geophysics 41:* 343-354.

Reyners, M. 1999: Quantifying the hazard of large subduction thrust earthquakes in Hawkes Bay. Abstracts. *New Zealand Geophysical Society and Meterological Society of New Zealand Joint Conference*, Victoria University of Wellington 1-3 September 1999.

Reyners, M., Robinson, R., & McGinty, P. 1997. Plate coupling in the northern South Island and southernmost North Island, New Zealand, as illuminated by earthquake focal mechanisms. *Journal of Geophysical Research 102* : 15197-15210.

Rhoades, D.A. 1996. Estimation of the Gutenberg-Richter relation allowing for individual earthquake magnitude uncertainties. *Tectonophysics, 258* : 71-83.

Sadigh, K., Chang, C.-Y., Egan, J.A., Makidisi, F. and Youngs, R.R. (1997). Attenuation relationships for shallow crustal earthquakes based on Californian strong motion data, *Seismological Research Letters*, 68 : 180-189.

Schermer, E., Van Dissen, R.J., Berryman, K.R., 1999. *In search of the source of the 1934 Pahiatua earthquake.* Final report on EQC Research project 97/320.71 pp.

Smith, W.D. and Berryman, K.R. 1983. Revised estimates of earthquake hazard in New Zealand. *Bulletin of the New Zealand National Society for Earthquake Engineering.* 16 : 259-276.

Smith, W.D. and Berryman, K.R. 1986: Earthquake hazard in New Zealand: inferences from seismology and geology. *Bulletin of the Royal Society of New Zealand 24*: 223-243.

Somerville, P.G., Sato, T., Ishii, T. 1999: Characterising subduction earthquake slip models for the prediction of strong ground motion. *EOS Transactions, American Geophysical Union 1998 Fall Meeting* 79(46), F658.

Standards New Zealand, 1992. *Code for Practice for General Structural Design and Design Loadings for Buildings. Volume 1: Code of practice. NZS 4203:1992.*

Stirling, M.W., Wesnousky, S.G. and Shimazaki, K. 1996. Fault trace complexity, cumulative slip,and the shape of the magnitude-frequency distribution for strike-slip faults: a global survey. *Geophysical Journal International 124:* 833-868.

Stirling, M.W., Wesnousky, S.G. and Berryman, K.R., 1998. Probabilistic seismic hazard analysis of New Zealand. *New Zealand Journal of Geology and Geophysics 41:* 355-375.

Stirling, M.W., Yetton, M., Pettinga, Y., Berryman, K.R., Downes, G. 1999. *Probabilistic seismic hazard assessment and earthquake scenarios for the Canterbury region, and historic earthquakes in Christchurch. Stage 1 (Part B) of Canterbury Regional Council's earthquake hazard and risk assessment study.* Institute of Geological and Nuclear Sciences Client Report 1999/53.

Sutherland, R.; Norris, R. J. 1995: Late Quaternary displacement rate, paleoseismicity and geomorphic evolution of the Alpine Fault: Evidence from near Hokuri Creek, south Westland, New Zealand. *New Zealand journal of Geology and geophysics 38:* 419-430.

Sutherland, R. 1999. Cenozoic bending of New Zealand basement terranes and Alpine Fault displacement: a brief review. *New Zealand Journal of Geology and Geophysics 42* : 295-301.

Turnbull, I.M., Uruski, C.I. and others, 1993. *Cretaceous and Cenozoic sedimentary basins of western Southland, South Island, New Zealand.* Institute of Geological and Nuclear Sciences, Ltd. Monograph 1 (New Zealand Geological Survey basin studies 4), Wellington.

Turnbull, I.M., Uruski, C.I. 1995. *Geology of the Monowai-Waitutu area, scale 1:50,000.* Institute of Geological and Nuclear Sciences geological map 19, Lower Hutt, New Zealand.

Van Dissen, R.J., Begg, J. Palmer, A., Nicol, A., Darby, D., and Reyners, M. 1998. Newly discovered active faults in the Wellington region. *New Zealand National Society for Earthquake Engineering Technical Conference and AGM*, pp. 1-7. Wairakei, Taupo, March 1998.

Van Dissen, R.J. and Palmer, A.S. 1998. Northern Ohariu fault. A newly discovered active strike-slip fault in Horowhenua, New Zealand. Geological Society of New Zealand Miscellaneous Publication 101A. *Geological Society of New Zealand Annual Conference*, Christchurch 1998, p234.

Van Dissen, R, and Nicol, A. 1998 . Paleoseismicity of the middle Clarence Valley section of the Clarence fault, Marlborough, New Zealand. *Programme & abstracts, Geological Society of New Zealand & New Zealand Geophysical Society Joint Annual Conference. Geological Society of New Zealand miscellaneous publication 101B* : 233.

Van Dissen, R.J., Lindqvist, J.K. and Turnbull, I.M. 1993. *Earthquake hazards in the Southland region.* Institute of Geological and Nuclear Sciences Client Report 1993/66.

Villamor, P. and Berryman, K. (in review). A Late Quaternary extension rate in the Taupo Volcanic Zone, New Zealand, derived from fault slip data, to be submitted to *New Zealand Journal of Geology and Geophysics.*

Villamor, P., Van Dissen, R.J., and Downes, G. 1998. *Moawhango dam stability analysis Task 2 Seismic source characterisation.* GNS Client report 43812B.11.

Weichert, D.H. 1980 : Estimation of the earthquake recurrence parameters for unequal observation periods for different magnitudes. *Bulletin of the Seismological Society of America. 70:* 1337-1346.

Wells, D.L., and K.J. Coppersmith 1994. New empirical relationships among magnitude, rupture length, rupture width, rupture area, and surface displacement. *Bulletin of the Seismological Society of America 84*: 974-1002.

Wesnousky, S.G. 1986. Earthquakes, Quaternary faults and seismic hazard in California. *Journal of Geophysical Research 91*: 12587-12631.

Wood, R.A., Herzer, R., Sutherland, R., Melhuish, A. 2000. Cretaceous-Tertiary tectonic history of the Fiordland margin, New Zealand. *New Zealand Journal of Geology and Geophysics*, in press.

Woodward Clyde and Institute of Geological and Nuclear Sciences 1999 : *Waitaki River Power Stations. Seismic Loads Assessment.* Draft Client report for Electricity Corporation of New Zealand.

Yetton, M.D., Wells, A., and Traylen, N.J. 1998. *The probability and consequences of the next Alpine Fault earthquake.* EQC Research Report 95/193.

Youngs, R.R., Chiou, S.-J., Silva, W.J., and Humphrey, J.R. 1997. Strong ground motion attenuation relationships for subduction zone earthquakes, *Seismological Research Letters, 68 : 58-73.*

Zhao, J.X., Dowrick, D.J., and McVerry, G.H. 1997. Attenuation of peak ground accelerations in New Zealand earthquakes. *Bulletin of the New Zealand National Society for Earthquake Engineering. 30* : 133-158.

FIGURE CAPTIONS

Figure 1: The plate tectonic setting of New Zealand. The country is divided into the neotectonic provinces identified by Berryman and Beanland (1988).

Figure 2: The 305 active fault sources used as input for the PSHA. The numbers beside each fault correspond to the index numbers given in the fault table (Appendix 1).

Figure 3: The distribution of shallow crustal seismicity in New Zealand (a), and the deeper seismicity of the Fiordland and Hikurangi subduction zones (b). The seismotectonic zones we have defined to sort the catalogue, assign initial regional maximum cutoff magnitudes (M_{cutoff}), and calculate parameter b of the Gutenberg-Richter relationship for seismicity are shown in (a). In the case of (b), many of the deep zones overlap in plan view, so we show the seismicity of each zone as a particular colour, rather than trying to colour-code the actual zones. The vertical extents of the seismotectonic zones have been defined from the spatial and depth distribution of seismicity, and are shown on each plot as a depth range beside the zone number (e.g. "z20 10-45 km" indicates that zone 20 has a depth range of 10 to 45 km). Since the crustal and deep sources have been defined at different scales, the lower-depth-limit of a crustal zone sometimes overlaps with the upper-depth-limit of a deep zone. In these cases the seismicity parameters calculated for the crustal zones are assumed to represent the seismicity of the overlapping areas. In (c) we show the seismicity for the three different time periods of completeness for events of all depths from 1900 to 1997, and cross sections of seismicity across and beneath the country. See the locations of the cross sections on the "Magnitude 6.5" map. Cross sections are oriented with the northwest end to the left of the page. Maps and cross sections in (c) are taken from McGinty (1999).

Figure 4: Contours of (a)-(e) the maximum-likelihood cumulative number of events per year for $M \geq 4$, calculated from three catalogue completeness levels and magnitudes ($M \geq 4$ since 1964, $M \geq 5$ since 1940, and $M \geq 6.5$ since 1840); (f)-(j) parameter b of the Gutenberg-Richter relationship LogN=A-bM, and; (k) the maximum "cutoff" magnitude (M_{cutoff}) assumed for distributed earthquakes, for various depth layers beneath the country. The contours have been made over a gridwork of N, b and M_{cutoff} that have been smoothed with a Gaussian smoothing function, in which the correlation distance (standard deviation) is set to 50 km. Since M_{cutoff} for all of the deep seismotectonic zones is set to 7, we only show a contour plot of M_{cutoff} for the crustal (20 km) depth layer. Note that white areas on the bvalue plots are where no seismicity exists in the depth range shown.

Figure 5: (a)-(f). Probabilistic seismic hazard maps for New Zealand for site class B (intermediate soil). The maps show the levels of pga and 5% damped response spectral acceleration (0.2 and 1s period) with return periods of 475 years (i.e. 10% probability in 50 years) and 1000 years (10% probability in 105 years).

Figure 6: Seismic hazard curves for site class B of the annual rate of exceedance for various levels of pga (a), and 5% damped response spectral acceleration (1s period; b) at the centres of Auckland, Wellington, Christchurch, Dunedin and Otira. Otira is included in the plots as a useful comparison to the main centres, since it is located in the area of highest hazard in the country (Fig. 5).

Figure 7: Response spectra for Auckland, Wellington, Christchurch, Dunedin and Otira, for 475 and 1000 year return periods for site class B.

Figure 8: Disaggregation plots for Auckland, Wellington, Christchurch, Dunedin and Otira. The plots show the percentage contribution to the 475 and 1000 year levels of hazard (Fig. 7) of the various magnitudes and source-to-site distances of earthquake sources in the model. The plots are produced for pgas and 1s spectral accelerations for site class B.

Figure 9: Comparison of the 475 year return period spectra for the five centres obtained in this study (NHM), and the Matuschka et al. (1985) study, and by using the modified Katayama attenuation model of the 1985 study with our NHM seismicity model.

Figure 1

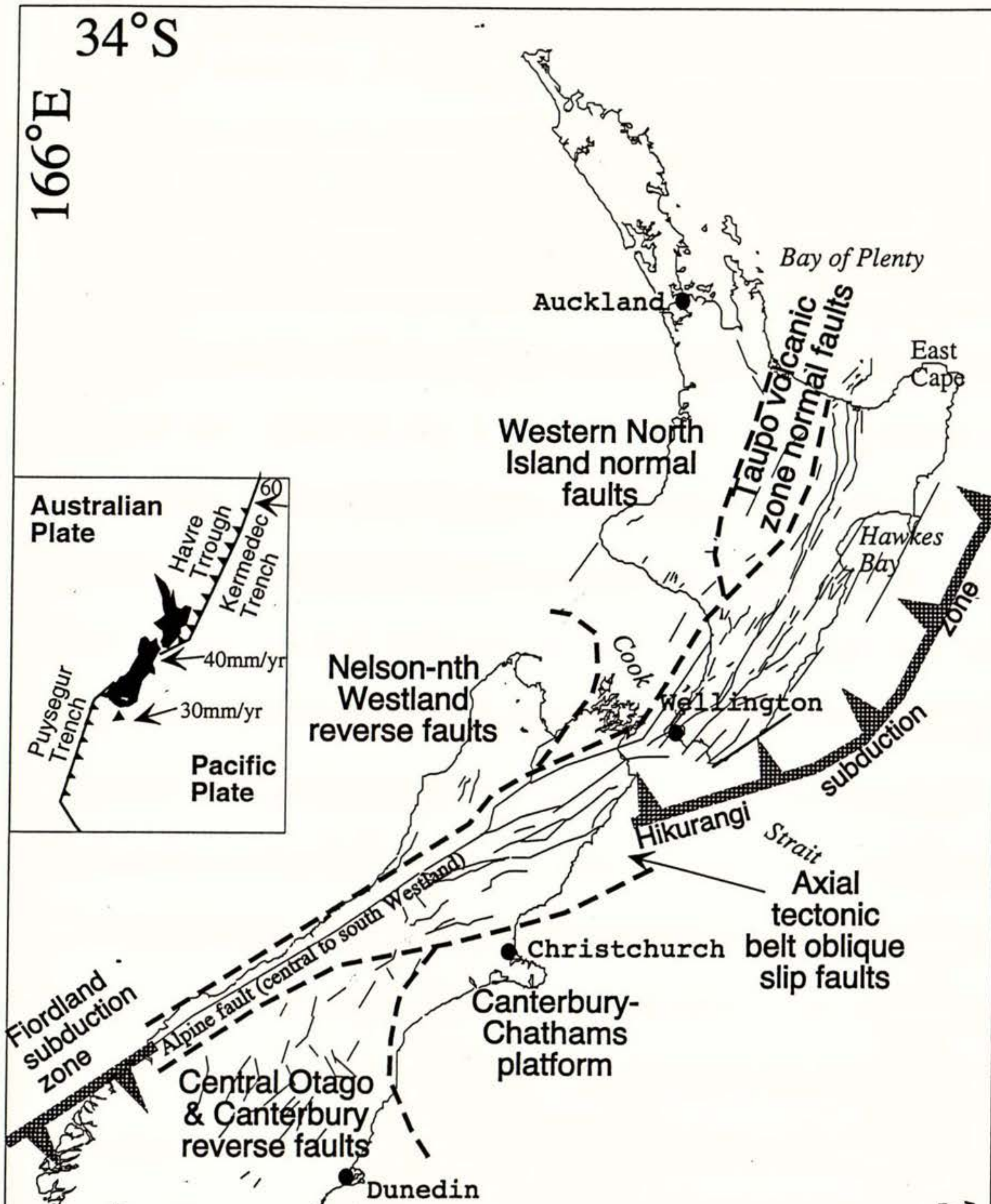
34°S
166°E
Australian Plate
Havre Trrough
Kermedec Trench
60
40mm/yr
30mm/yr
Puysegur Trench
Pacific Plate
Bay of Plenty
Auckland
Taupo volcanic zone normal faults
East Cape
Western North Island normal faults
Hawkes Bay
Cook
Strait
Nelson-nth Westland reverse faults
Wellington
subduction zone
Hikurangi
Axial tectonic belt oblique slip faults
Alpine fault (central to south Westland)
Christchurch
Fiordland subduction zone
Canterbury-Chathams platform
Central Otago & Canterbury reverse faults
Dunedin
100 km
48°S
179°E

Figure 2a

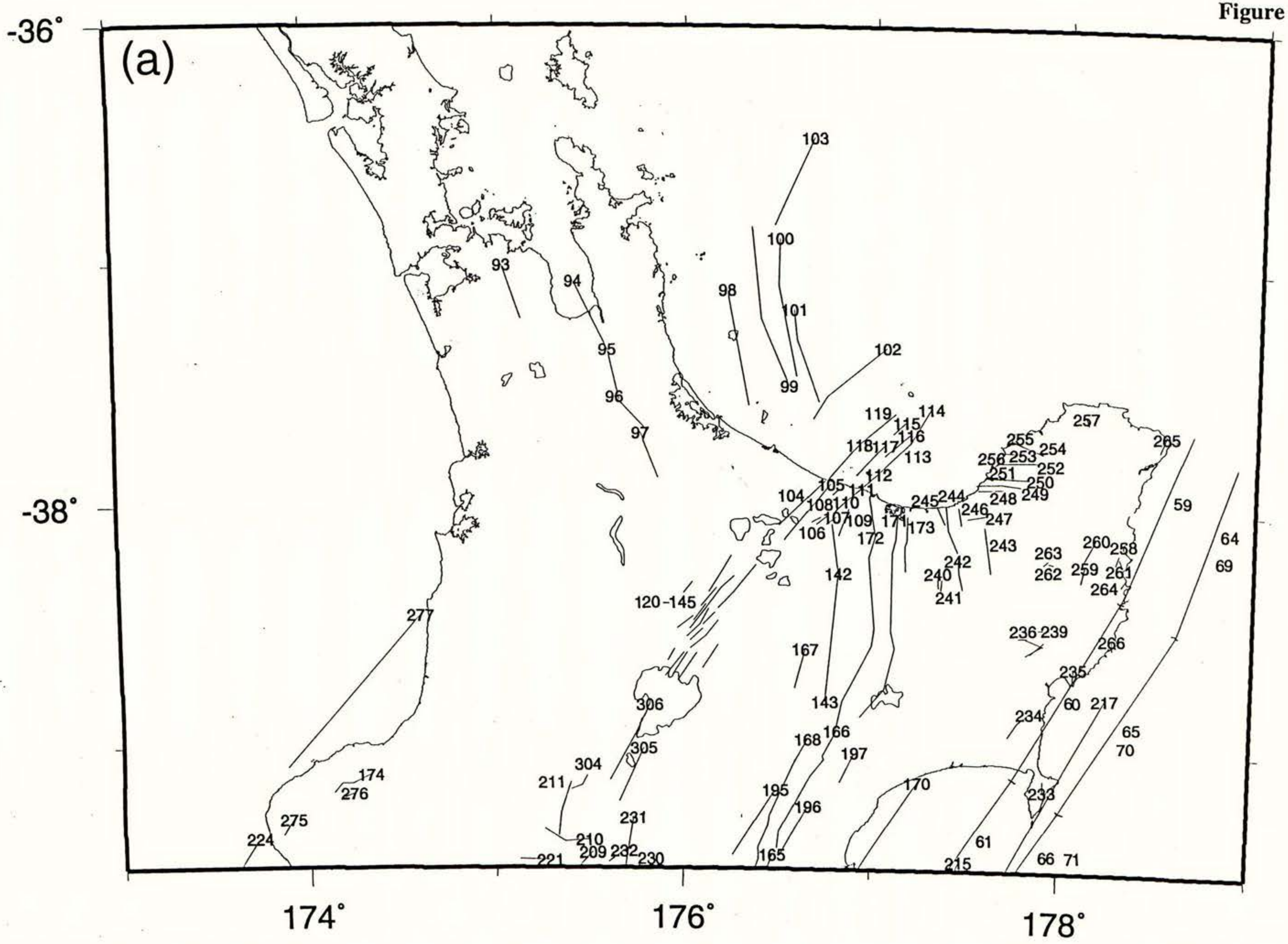
(a)
-36°
-38°
174°
176°
178°
93
94
95
96
97
98
99
100
101
102
103
104
105
106
107
108
109
110
111
112
113
114
115
116
117
118
119
120-145
142
143
165
166
167
168
170
171
172
173
174
195
196
197
209
210
211
215
217
221
224
230
231
232
233
234
235
236-239
240
241
242
243
244
245
246
247
248
249
250
251
252
253
254
255
256
257
258
259
260
261
262
263
264
265
266
275
276
277
304
305
306
59
60
61
64
65
66
69
70
71

Figure 2b

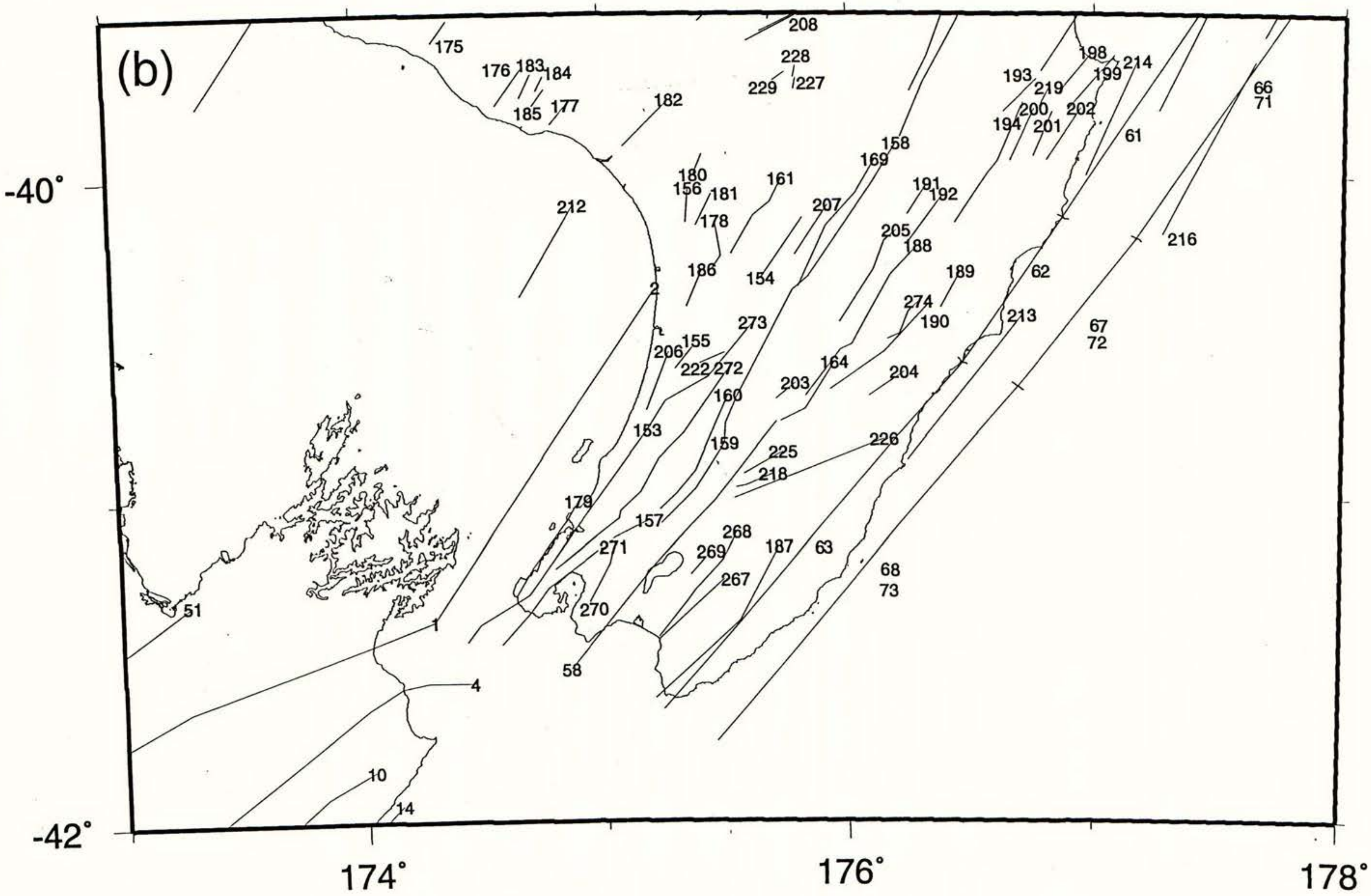
(b)
-40°
-42°
174°
176°
178°
175
176
183
184
185
177
182
208
228
229
227
212
180
156
181
178
161
207
158
169
191
192
193
198
214
219
199
200
202
194
201
61
66
71
216
205
188
186
154
189
62
2
274
190
213
273
155
206
222
272
67
72
164
204
203
160
153
159
225
218
226
179
157
268
271
269
187
63
68
73
267
270
51
1
58
4
10
14

Figure 2c

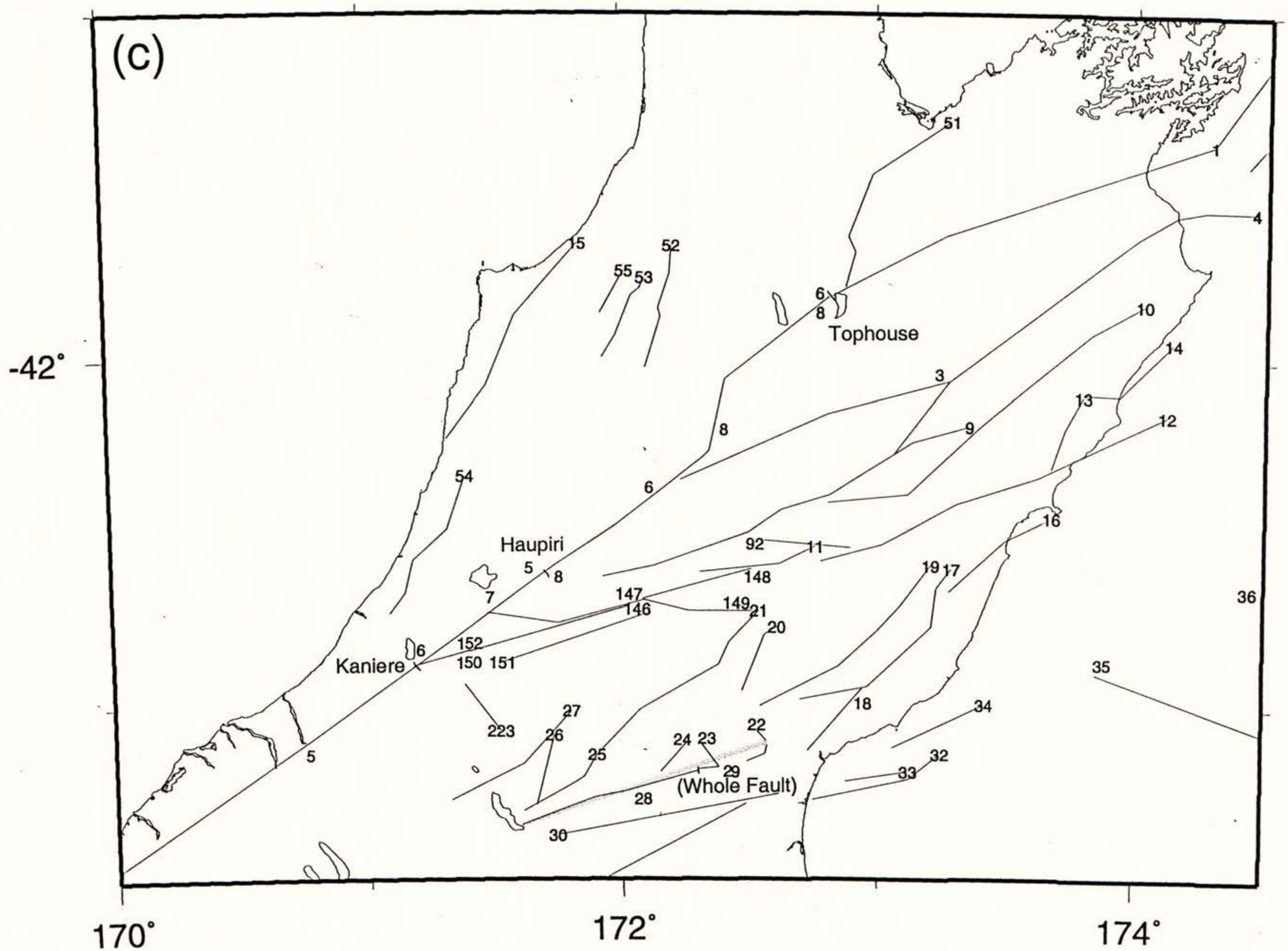
(c)
-42°
170°
172°
174°
Tophouse
Haupiri
Kaniere
(Whole Fault)
1
4
51
15
52
55
53
6
8
10
14
3
13
12
9
8
54
6
16
92
11
5
8
148
19
17
36
7
147
146
149
21
20
152
150
151
6
35
18
34
27
223
26
24
23
22
25
29
32
33
28
30
5

Figure 2d

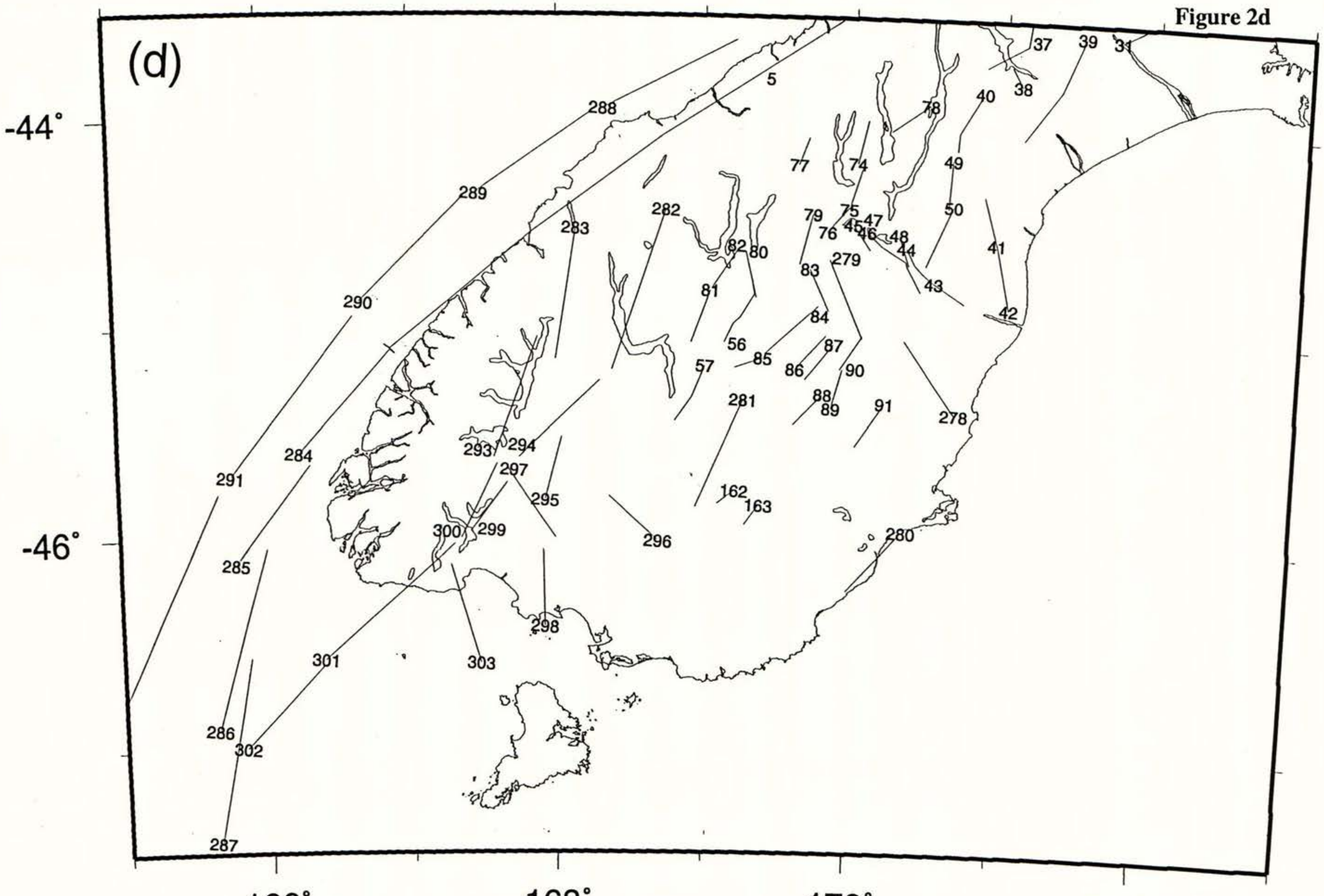
(d)
-44°
-46°
166°
168°
170°
172°
5
31
37
38
39
40
41
42
43
44
45
46
47
48
49
50
56
57
74
75
76
77
78
79
80
81
82
83
84
85
86
87
88
89
90
91
162
163
278
279
280
281
282
283
284
285
286
287
288
289
290
291
293
294
295
296
297
298
299
300
301
302
303

Figure 3a

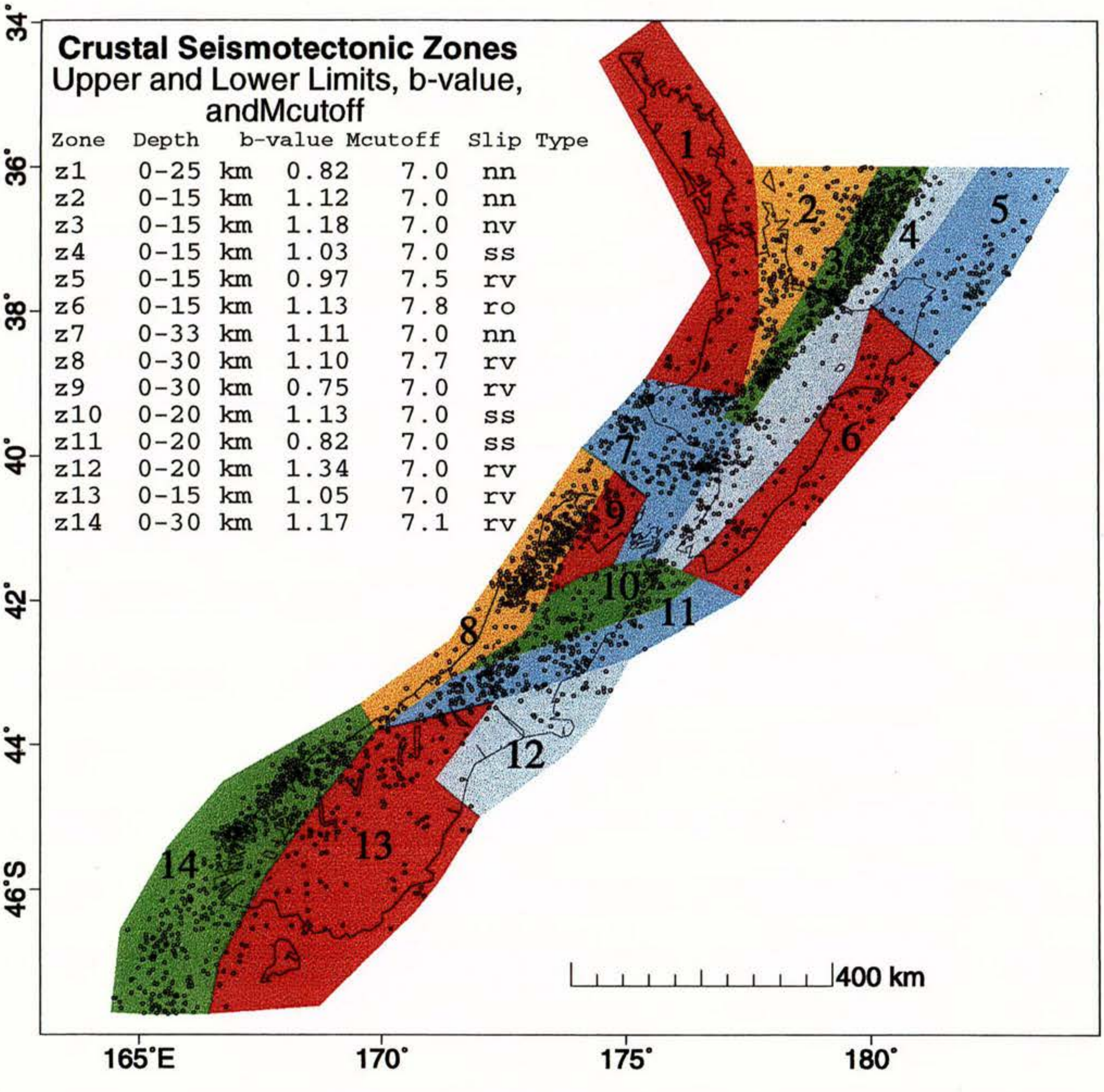

Crustal Seismotectonic Zones
Upper and Lower Limits, b-value, andMcutoff
Zone Depth b-value Mcutoff Slip Type
z1 0-25 km 0.82 7.0 nn
z2 0-15 km 1.12 7.0 nn
z3 0-15 km 1.18 7.0 nv
z4 0-15 km 1.03 7.0 ss
z5 0-15 km 0.97 7.5 rv
z6 0-15 km 1.13 7.8 ro
z7 0-33 km 1.11 7.0 nn
z8 0-30 km 1.10 7.7 rv
z9 0-30 km 0.75 7.0 rv
z10 0-20 km 1.13 7.0 ss
z11 0-20 km 0.82 7.0 ss
z12 0-20 km 1.34 7.0 rv
z13 0-15 km 1.05 7.0 rv
z14 0-30 km 1.17 7.1 rv
1
2
3
4
5
6
7
8
9
10
11
12
13
14
400 km
34°
36°
38°
40°
42°
44°
46°S
165°E
170°
175°
180°

Figure 3b

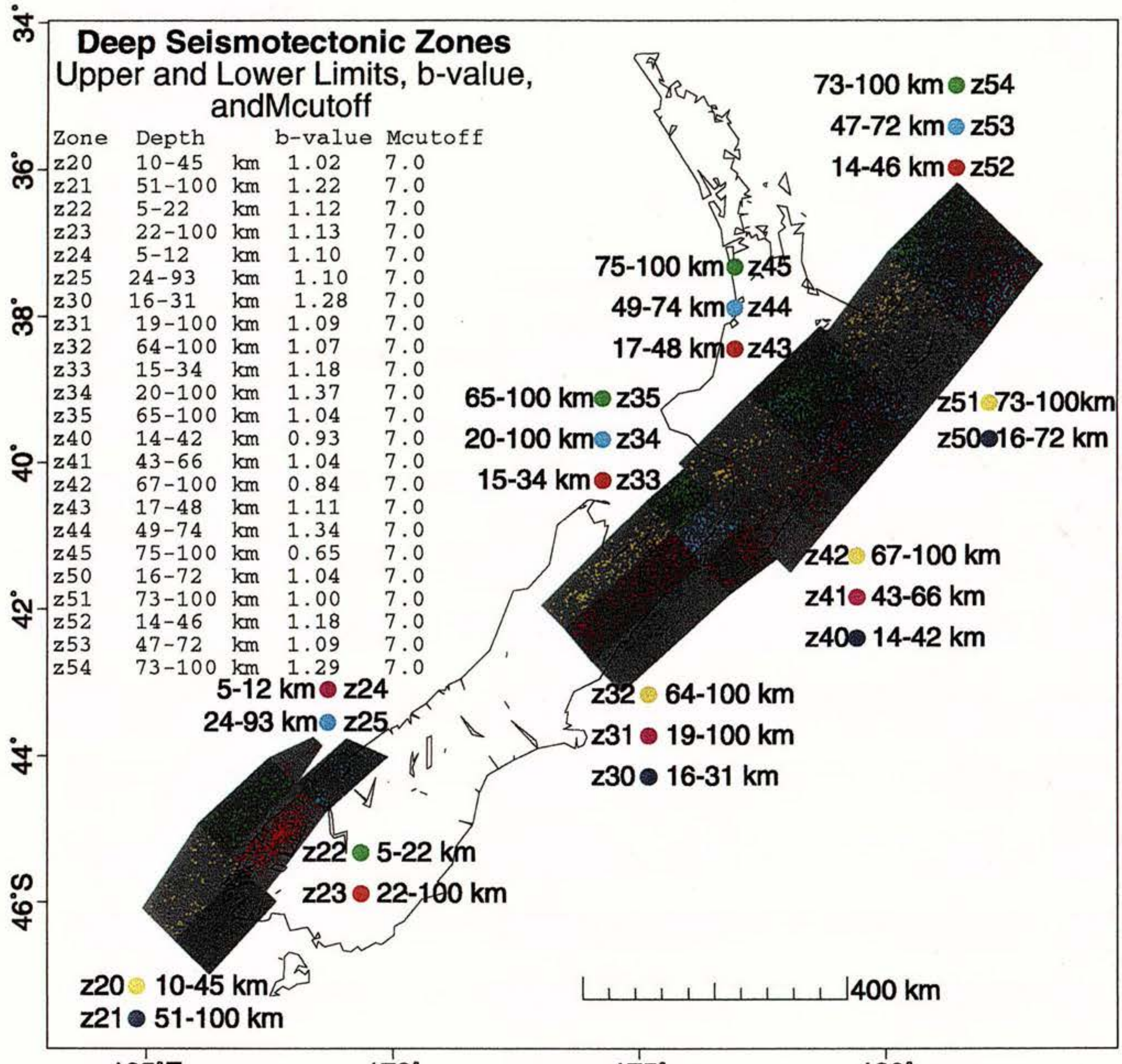
Deep Seismotectonic Zones
Upper and Lower Limits, b-value, andMcutoff
Zone Depth b-value Mcutoff
z20 10-45 km 1.02 7.0
z21 51-100 km 1.22 7.0
z22 5-22 km 1.12 7.0
z23 22-100 km 1.13 7.0
z24 5-12 km 1.10 7.0
z25 24-93 km 1.10 7.0
z30 16-31 km 1.28 7.0
z31 19-100 km 1.09 7.0
z32 64-100 km 1.07 7.0
z33 15-34 km 1.18 7.0
z34 20-100 km 1.37 7.0
z35 65-100 km 1.04 7.0
z40 14-42 km 0.93 7.0
z41 43-66 km 1.04 7.0
z42 67-100 km 0.84 7.0
z43 17-48 km 1.11 7.0
z44 49-74 km 1.34 7.0
z45 75-100 km 0.65 7.0
z50 16-72 km 1.04 7.0
z51 73-100 km 1.00 7.0
z52 14-46 km 1.18 7.0
z53 47-72 km 1.09 7.0
z54 73-100 km 1.29 7.0
73-100 km z54
47-72 km z53
14-46 km z52
75-100 km z45
49-74 km z44
17-48 km z43
65-100 km z35
20-100 km z34
15-34 km z33
z51 73-100km
z50 16-72 km
z42 67-100 km
z41 43-66 km
z40 14-42 km
5-12 km z24
24-93 km z25
z32 64-100 km
z31 19-100 km
z30 16-31 km
z22 5-22 km
z23 22-100 km
z20 10-45 km
z21 51-100 km
400 km
34°
36°
38°
40°
42°
44°
46°S
165°E
170°
175°
180°

Figure 3c

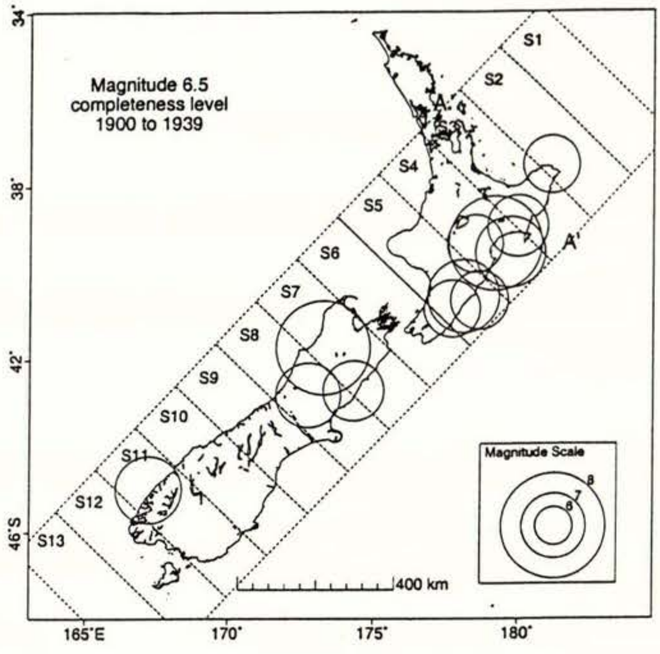

Magnitude 6.5
completeness level
1900 to 1939
S1
S2
S4
S5
S6
S7
S8
S9
S10
S11
S12
S13
A
A'
Magnitude Scale
8
7
6
400 km
34°
38°
42°
46°S
165°E
170°
175°
180°

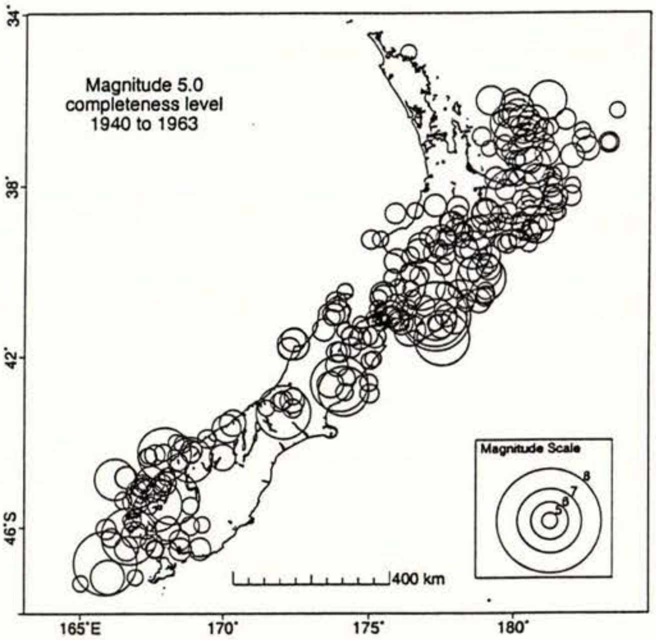

Magnitude 5.0
completeness level
1940 to 1963
Magnitude Scale
8
7
6
5
400 km
34°
38°
42°
46°S
165°E
170°
175°
180°

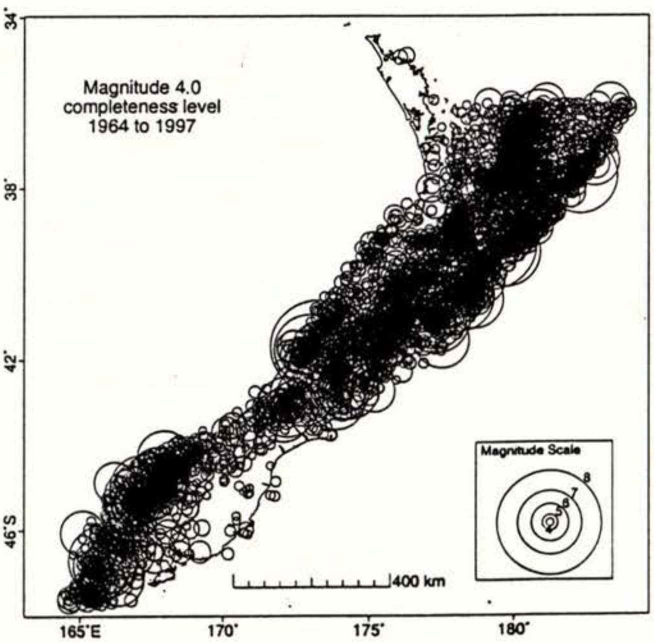

Magnitude 4.0
completeness level
1964 to 1997
Magnitude Scale
8
7
6
5
400 km
34°
38°
42°
46°S
165°E
170°
175°
180°

Figure 3c continued

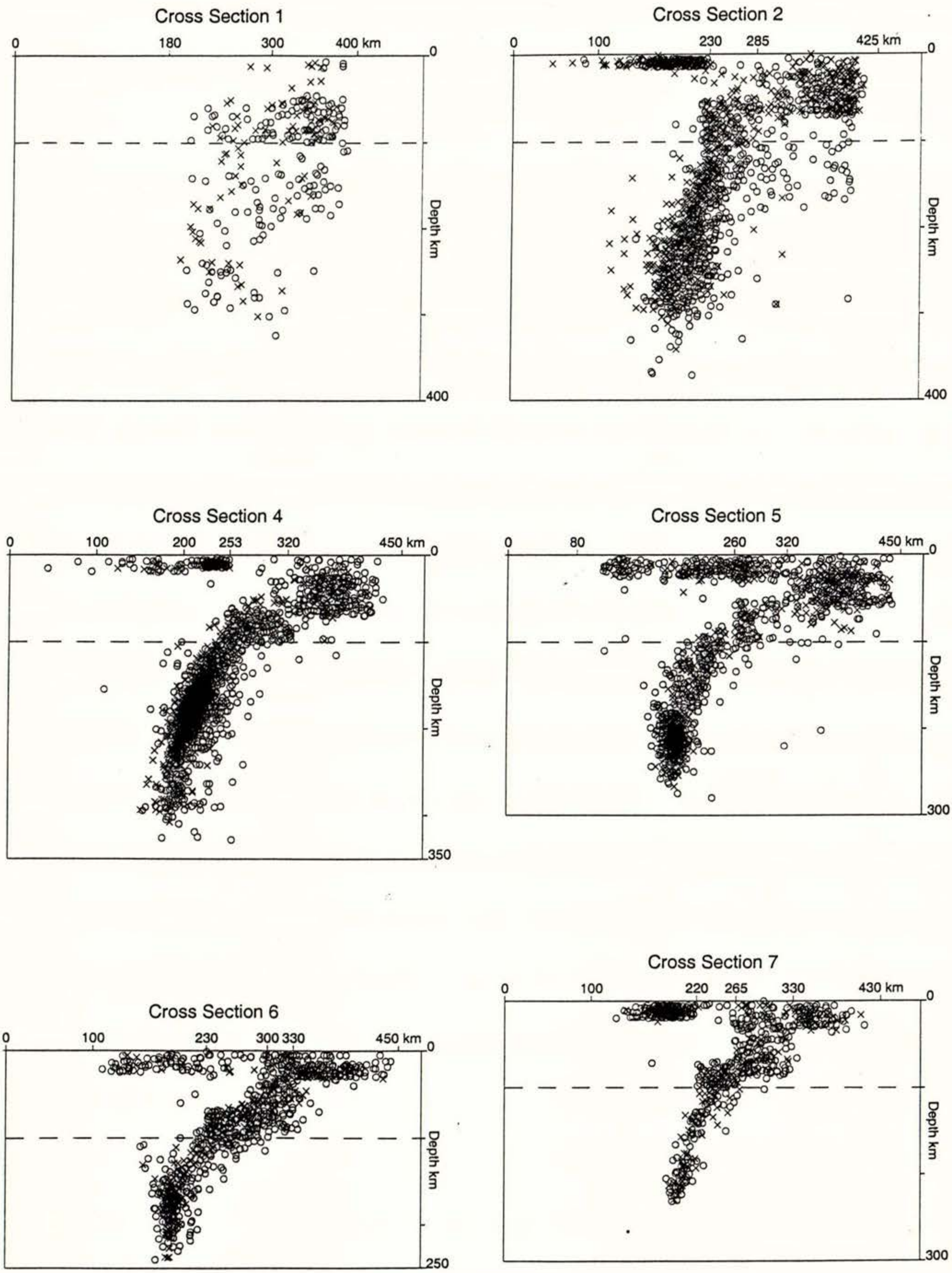

Figure 3c continued

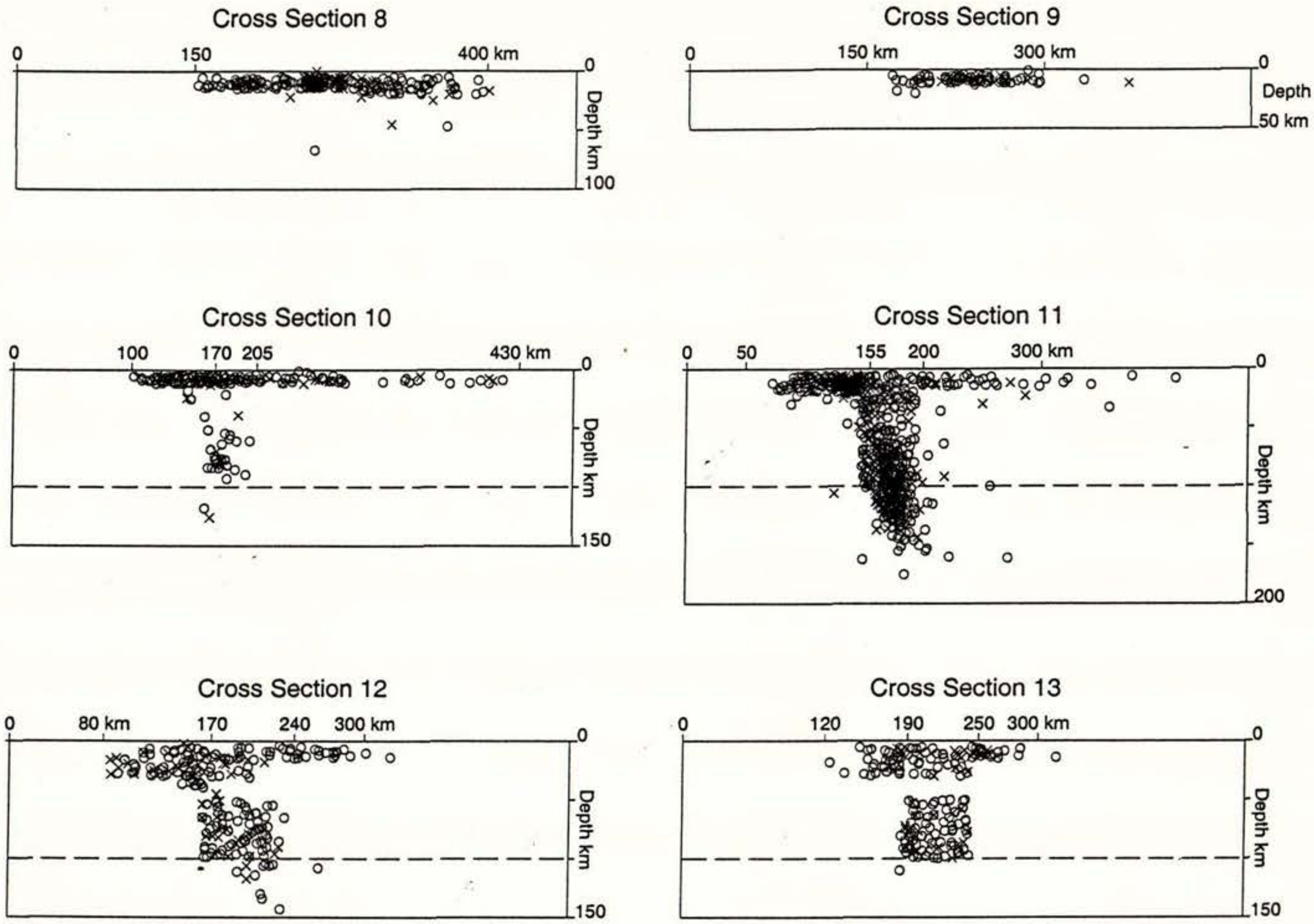

Figure 4a

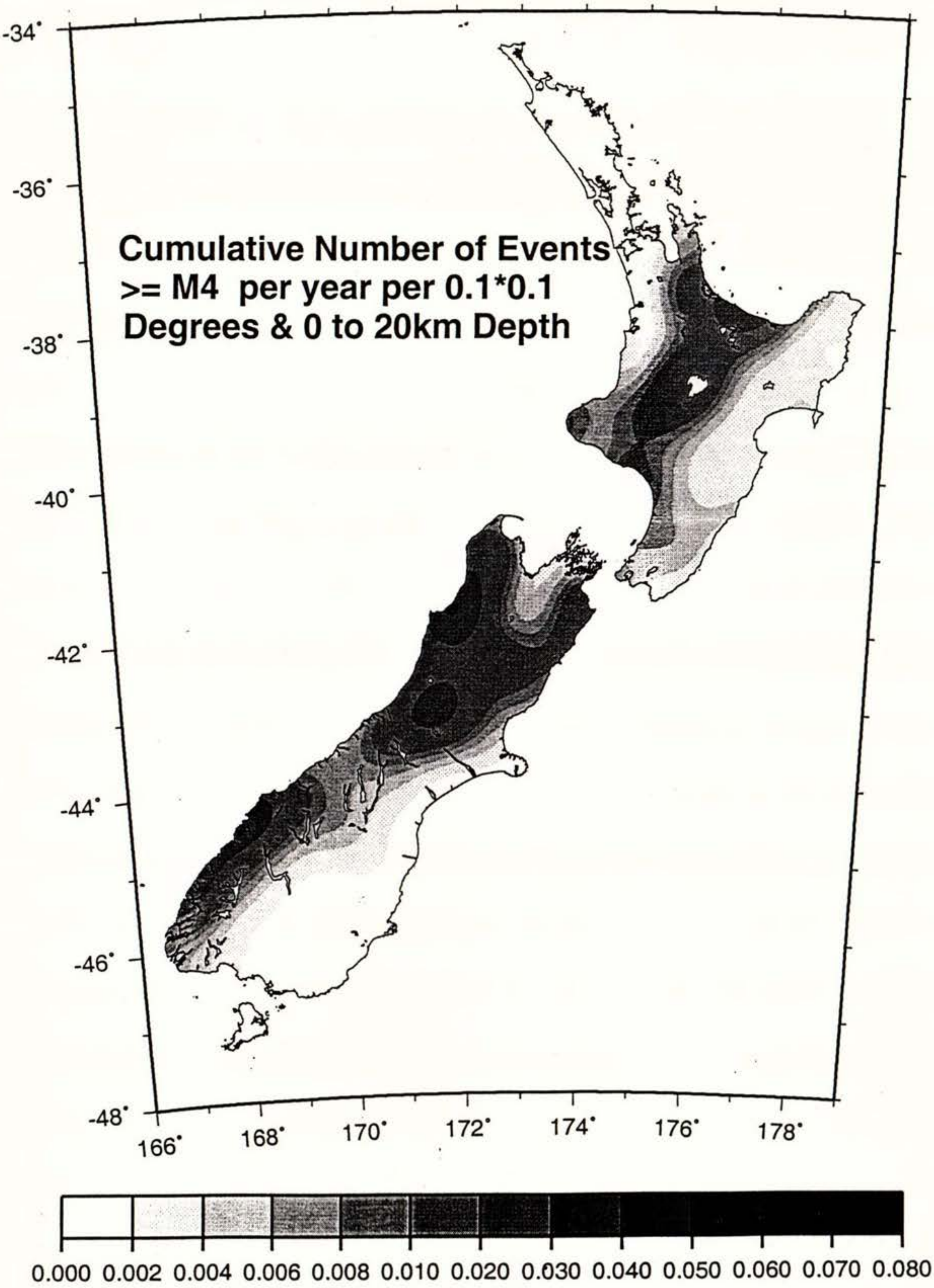

Cumulative Number of Events
>= M4 per year per 0.1*0.1
Degrees & 0 to 20km Depth
-34°
-36°
-38°
-40°
-42°
-44°
-46°
-48°
166°
168°
170°
172°
174°
176°
178°
0.000 0.002 0.004 0.006 0.008 0.010 0.020 0.030 0.040 0.050 0.060 0.070 0.080

Figure 4b

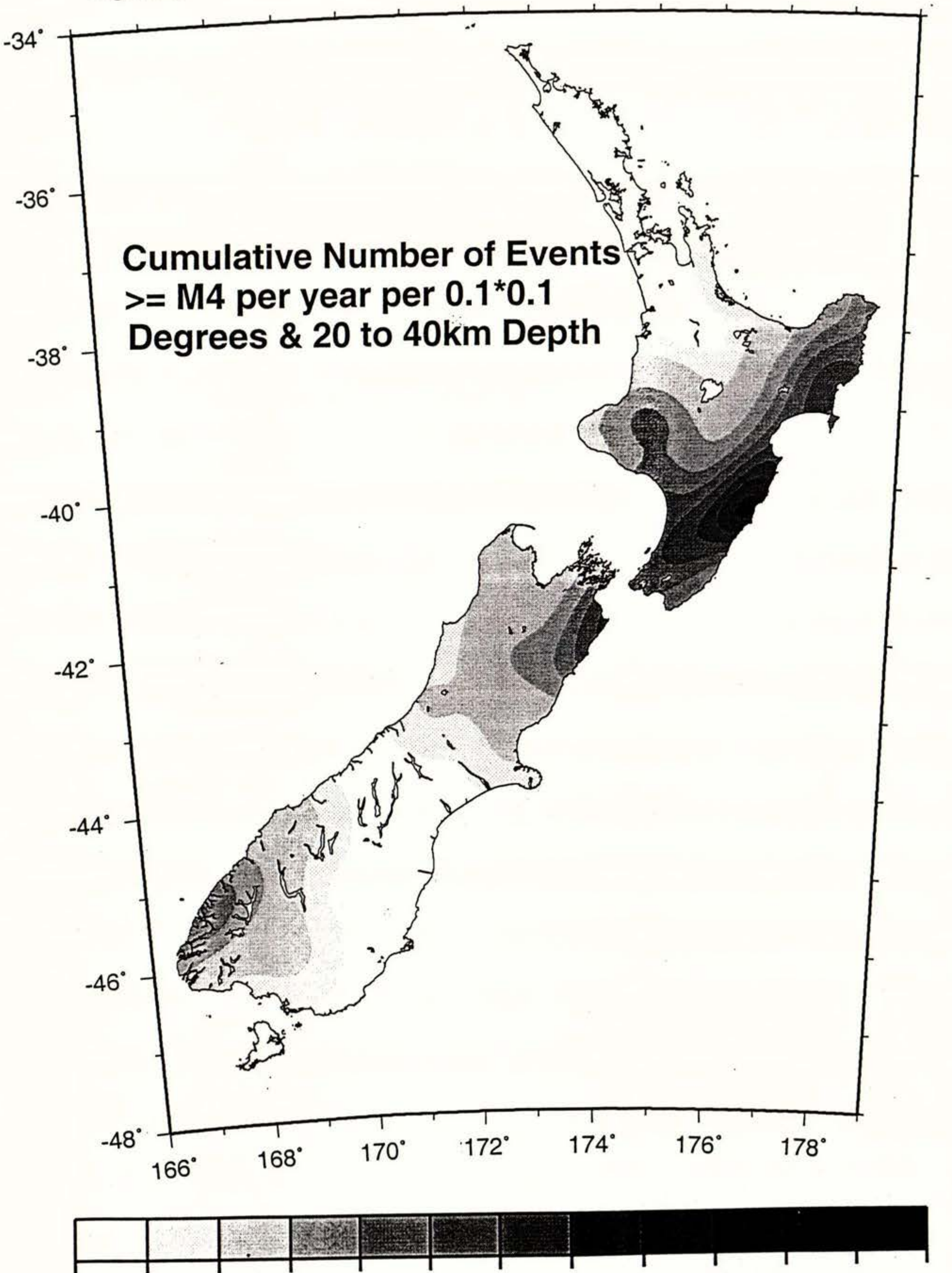
Cumulative Number of Events
>= M4 per year per 0.1*0.1
Degrees & 20 to 40km Depth
-34°
-36°
-38°
-40°
-42°
-44°
-46°
-48°
166°
168°
170°
172°
174°
176°
178°
0.000 0.001 0.010 0.100 0.200 0.300 0.400 0.500 0.600 0.700 0.800 0.900 1.000

Figure 4c

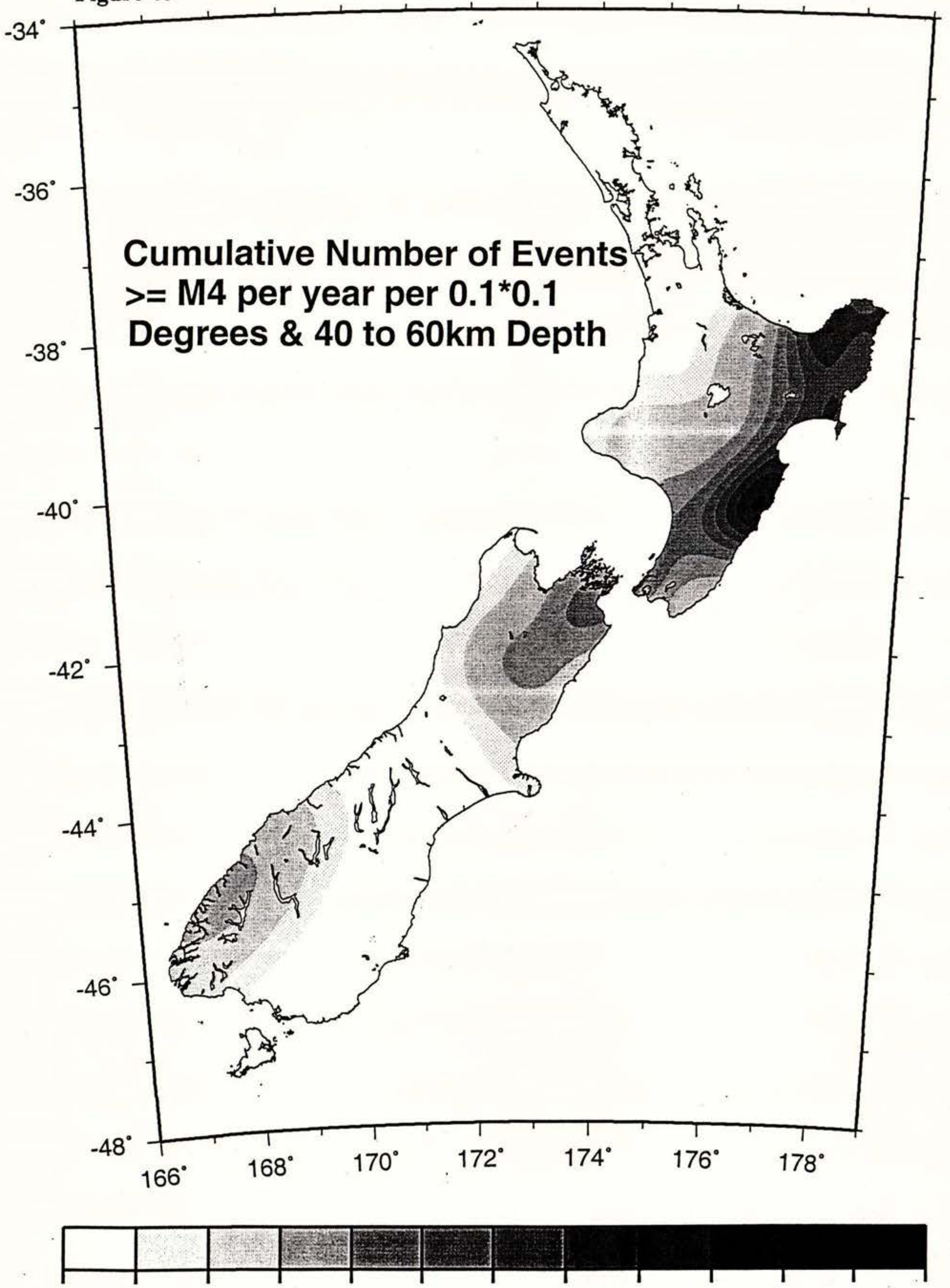

Cumulative Number of Events
>= M4 per year per 0.1*0.1
Degrees & 40 to 60km Depth
-34°
-36°
-38°
-40°
-42°
-44°
-46°
-48°
166°
168°
170°
172°
174°
176°
178°
0.000 0.001 0.010 0.100 0.200 0.300 0.400 0.500 0.600 0.700 0.800 0.900 1.000

Figure 4d

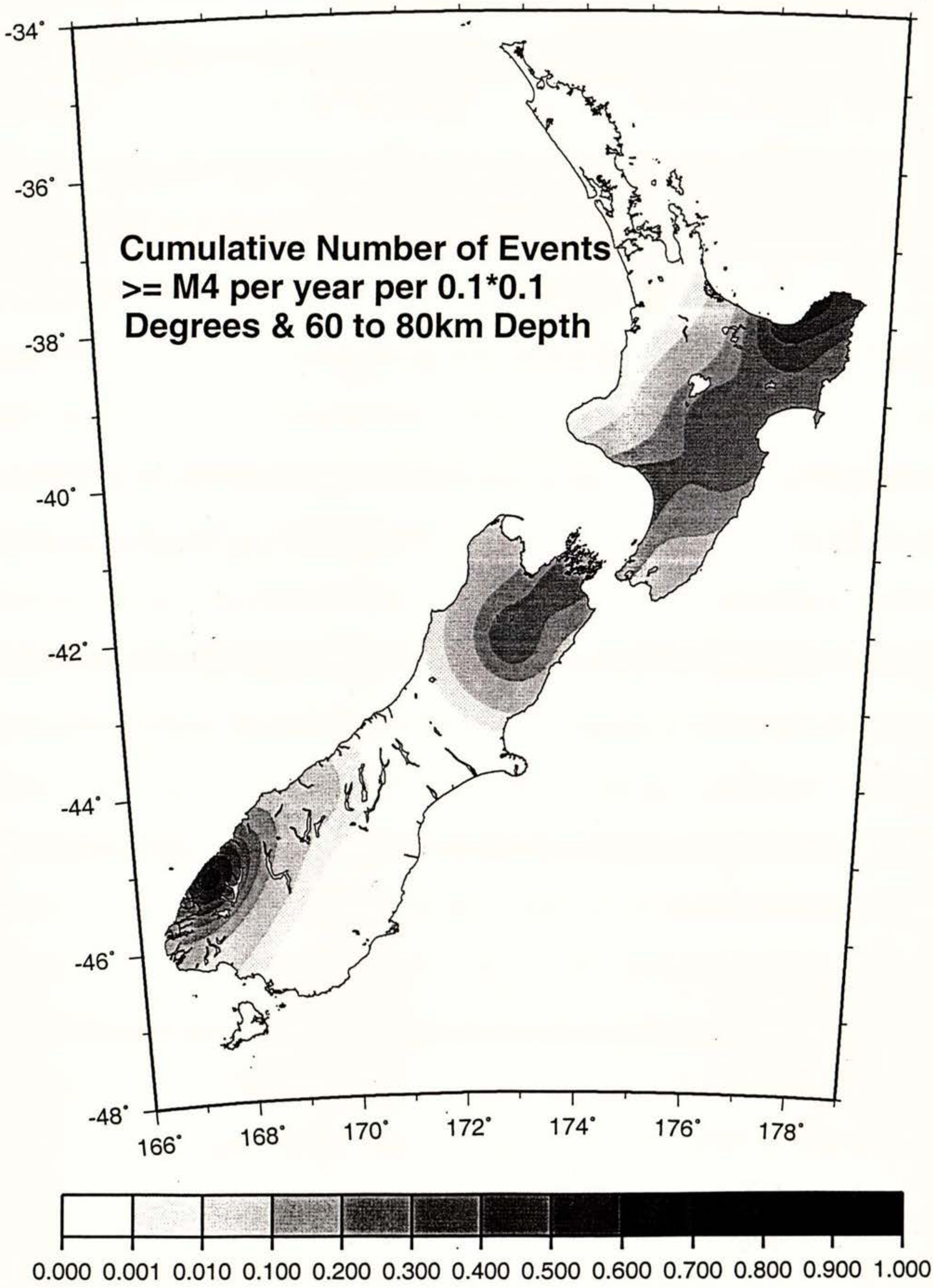

Cumulative Number of Events
>= M4 per year per 0.1*0.1
Degrees & 60 to 80km Depth
-34°
-36°
-38°
-40°
-42°
-44°
-46°
-48°
166°
168°
170°
172°
174°
176°
178°
0.000 0.001 0.010 0.100 0.200 0.300 0.400 0.500 0.600 0.700 0.800 0.900 1.000

Figure 4e

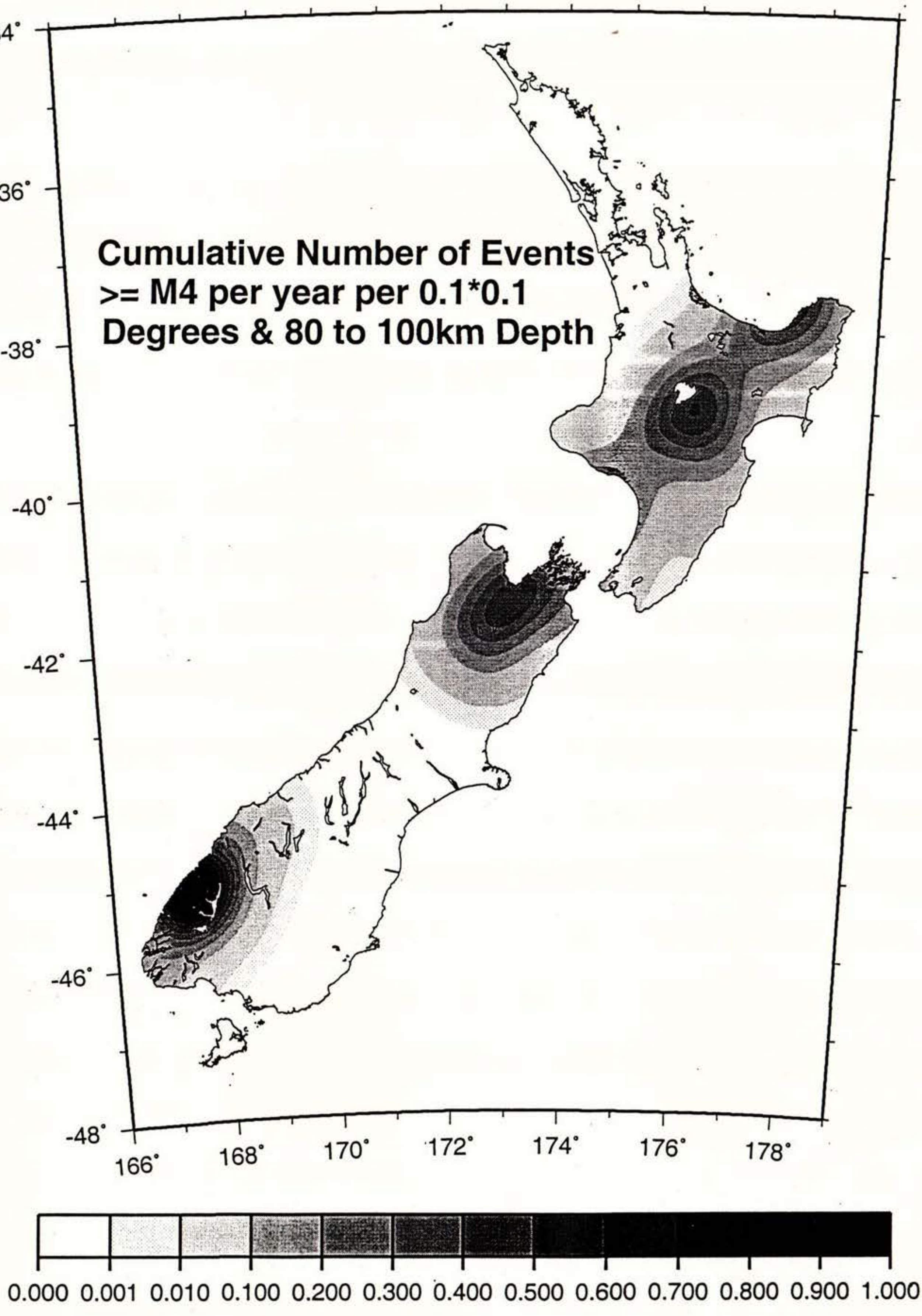
Cumulative Number of Events
>= M4 per year per 0.1*0.1
Degrees & 80 to 100km Depth
-34°
-36°
-38°
-40°
-42°
-44°
-46°
-48°
166°
168°
170°
172°
174°
176°
178°
0.000 0.001 0.010 0.100 0.200 0.300 0.400 0.500 0.600 0.700 0.800 0.900 1.000

Figure 4f

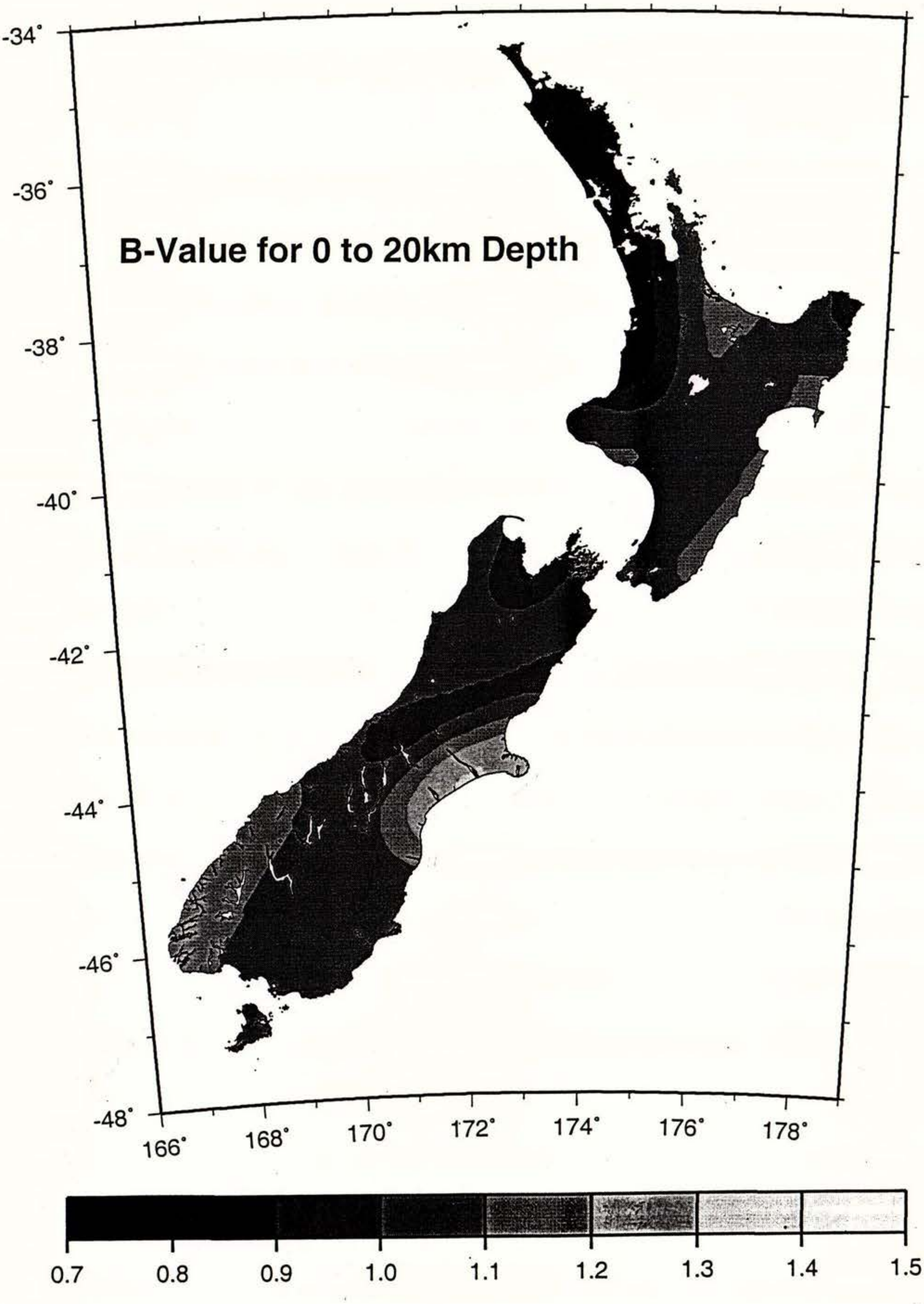
B-Value for 0 to 20km Depth
-34˚
-36˚
-38˚
-40˚
-42˚
-44˚
-46˚
-48˚
166˚
168˚
170˚
172˚
174˚
176˚
178˚
0.7
0.8
0.9
1.0
1.1
1.2
1.3
1.4
1.5

Figure 4g

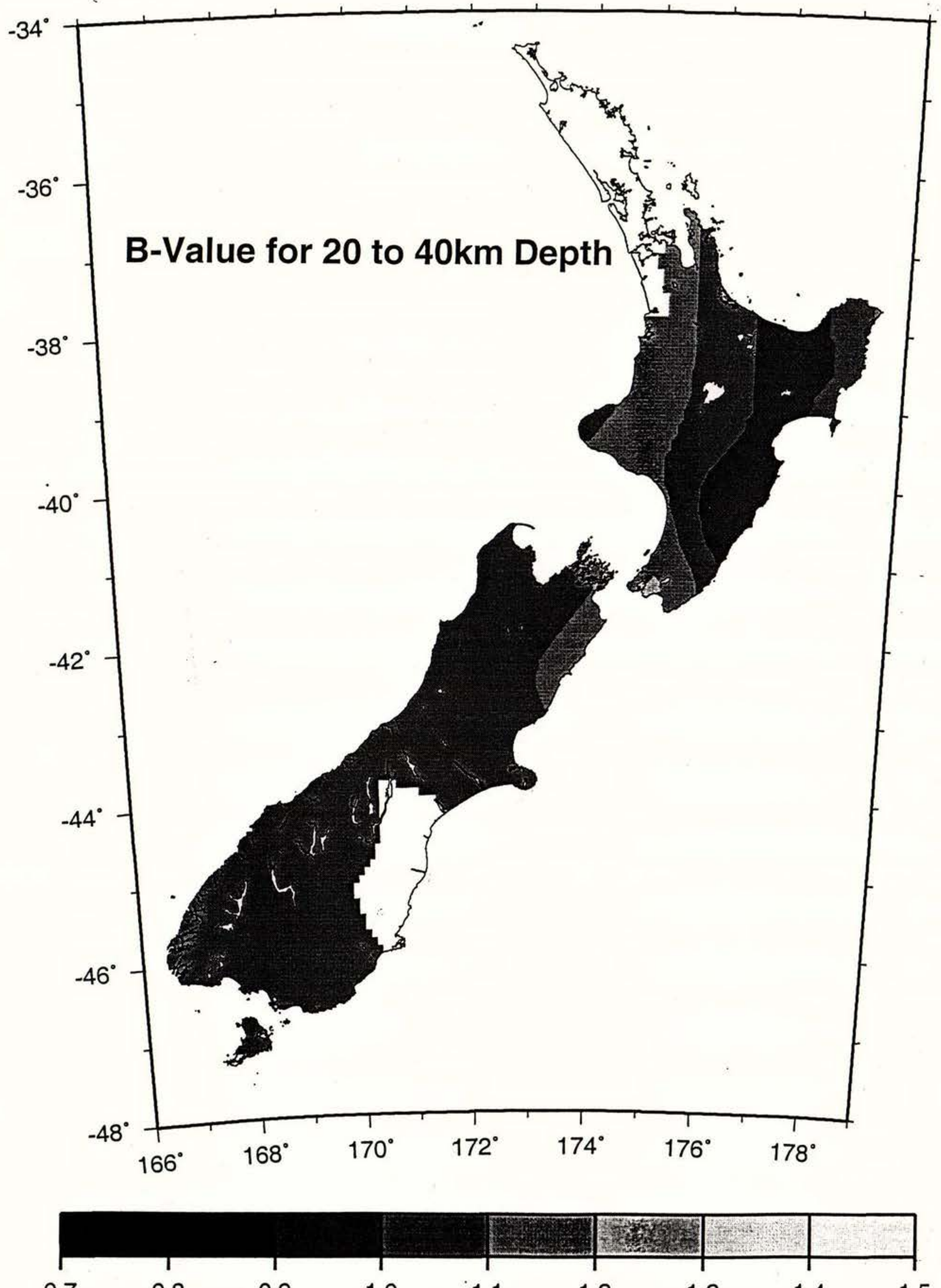

B-Value for 20 to 40km Depth
-34°
-36°
-38°
-40°
-42°
-44°
-46°
-48°
166°
168°
170°
172°
174°
176°
178°
0.7
0.8
0.9
1.0
1.1
1.2
1.3
1.4
1.5

Figure 4h

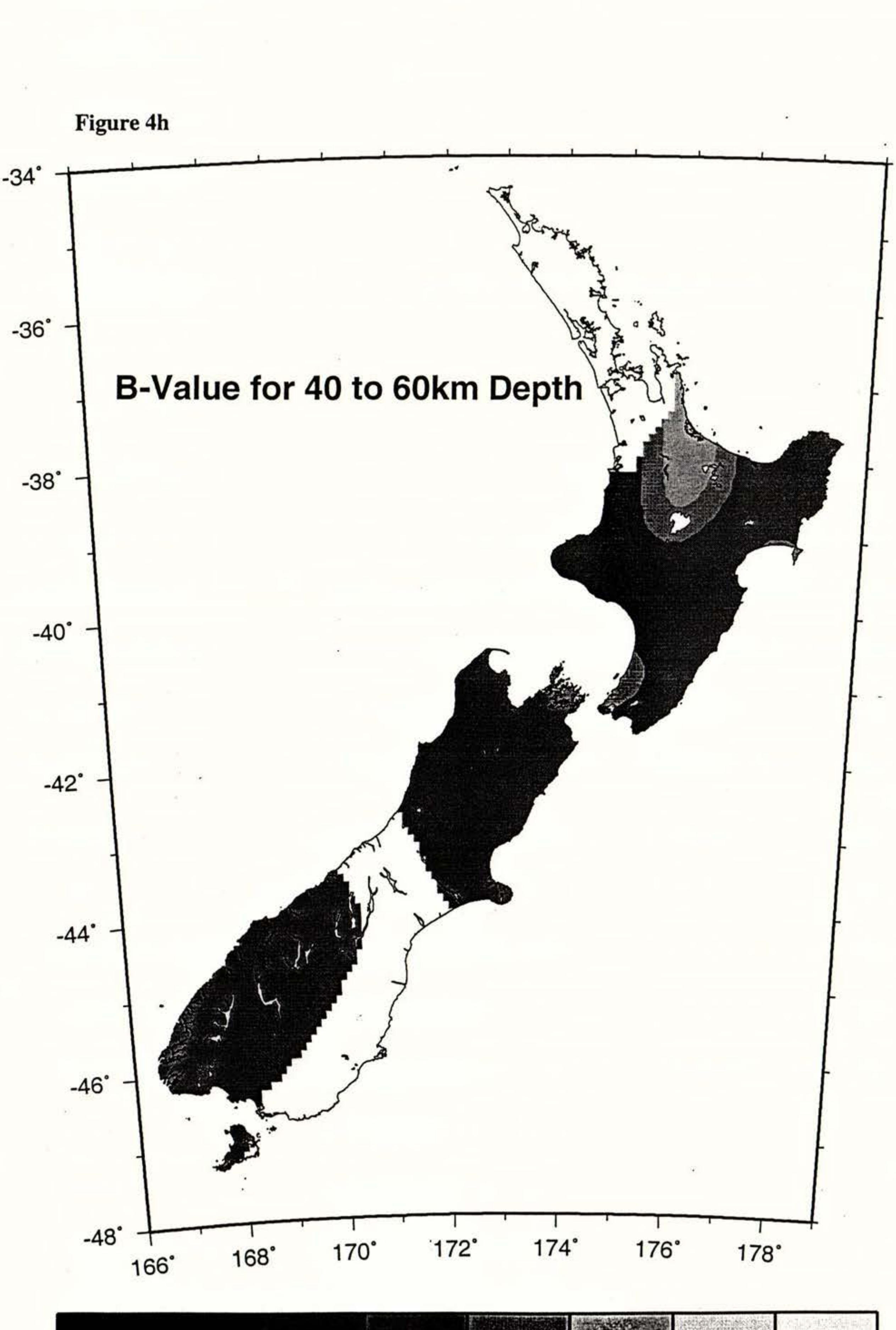
B-Value for 40 to 60km Depth
-34°
-36°
-38°
-40°
-42°
-44°
-46°
-48°
166°
168°
170°
172°
174°
176°
178°
0.7
0.8
0.9
1.0
1.1
1.2
1.3
1.4
1.5

Figure 4i

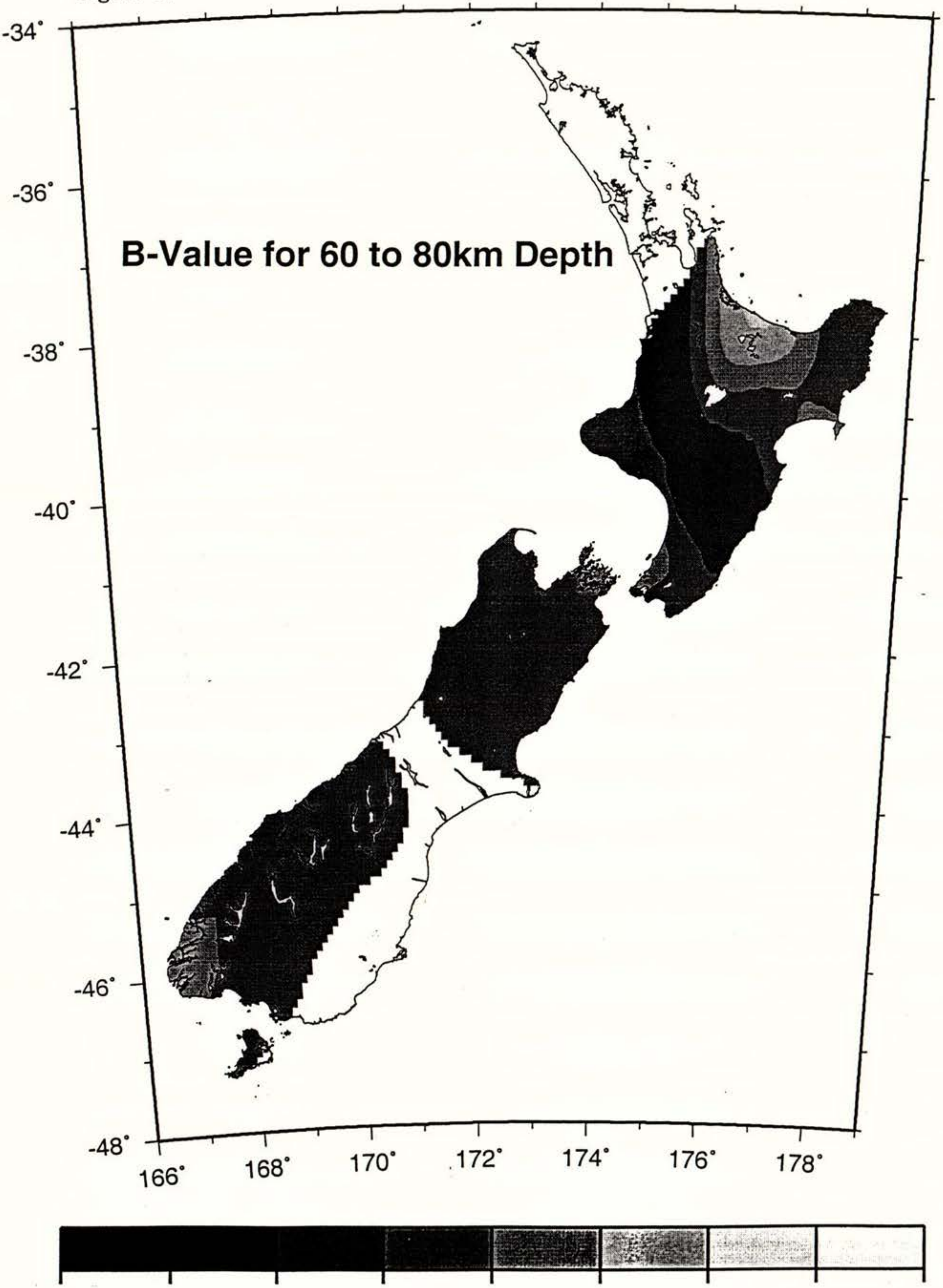
B-Value for 60 to 80km Depth
-34°
-36°
-38°
-40°
-42°
-44°
-46°
-48°
166°
168°
170°
172°
174°
176°
178°
0.7
0.8
0.9
1.0
1.1
1.2
1.3
1.4
1.5

Figure 4j

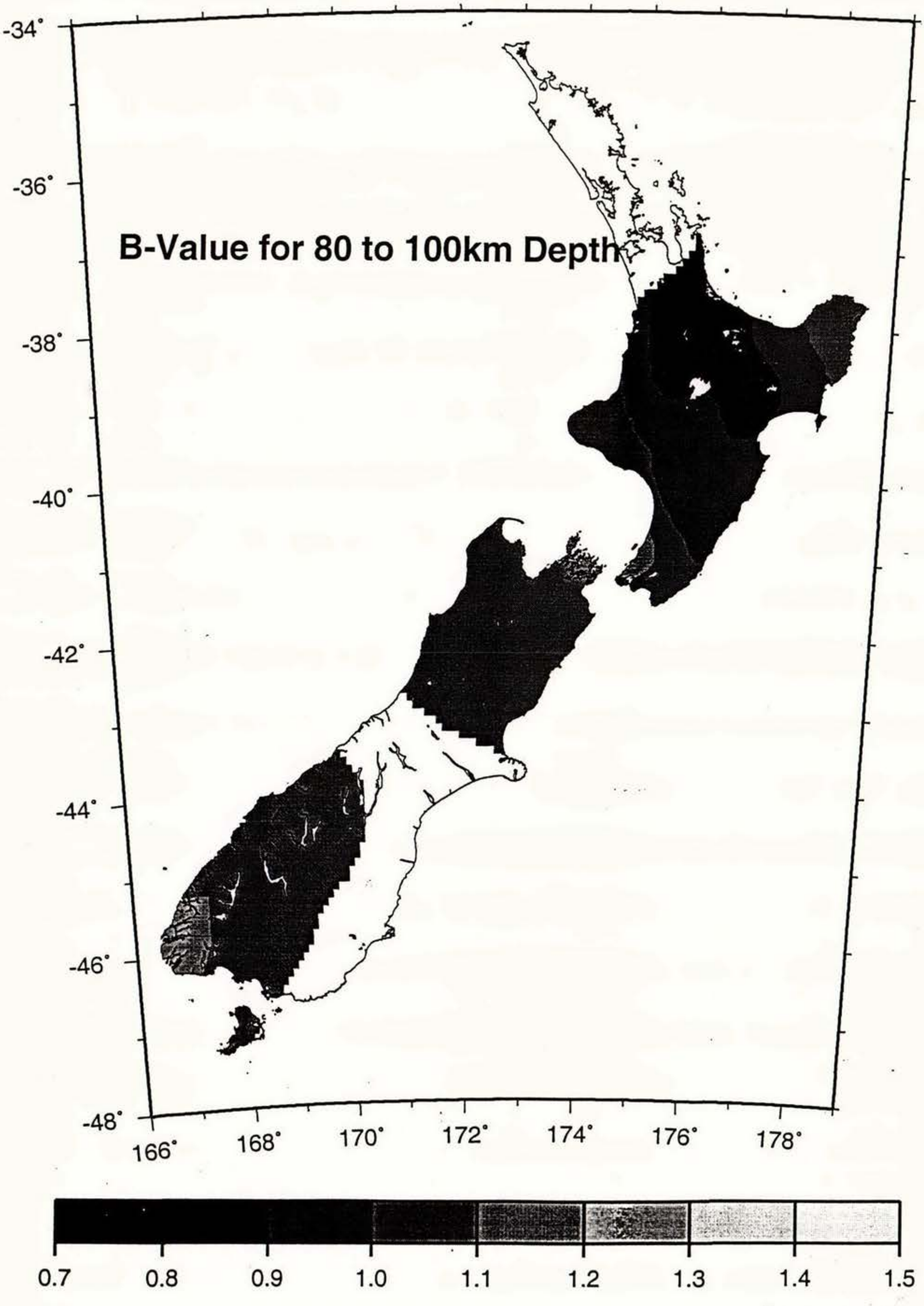

B-Value for 80 to 100km Depth
-34°
-36°
-38°
-40°
-42°
-44°
-46°
-48°
166°
168°
170°
172°
174°
176°
178°
0.7
0.8
0.9
1.0
1.1
1.2
1.3
1.4
1.5

Figure 4k

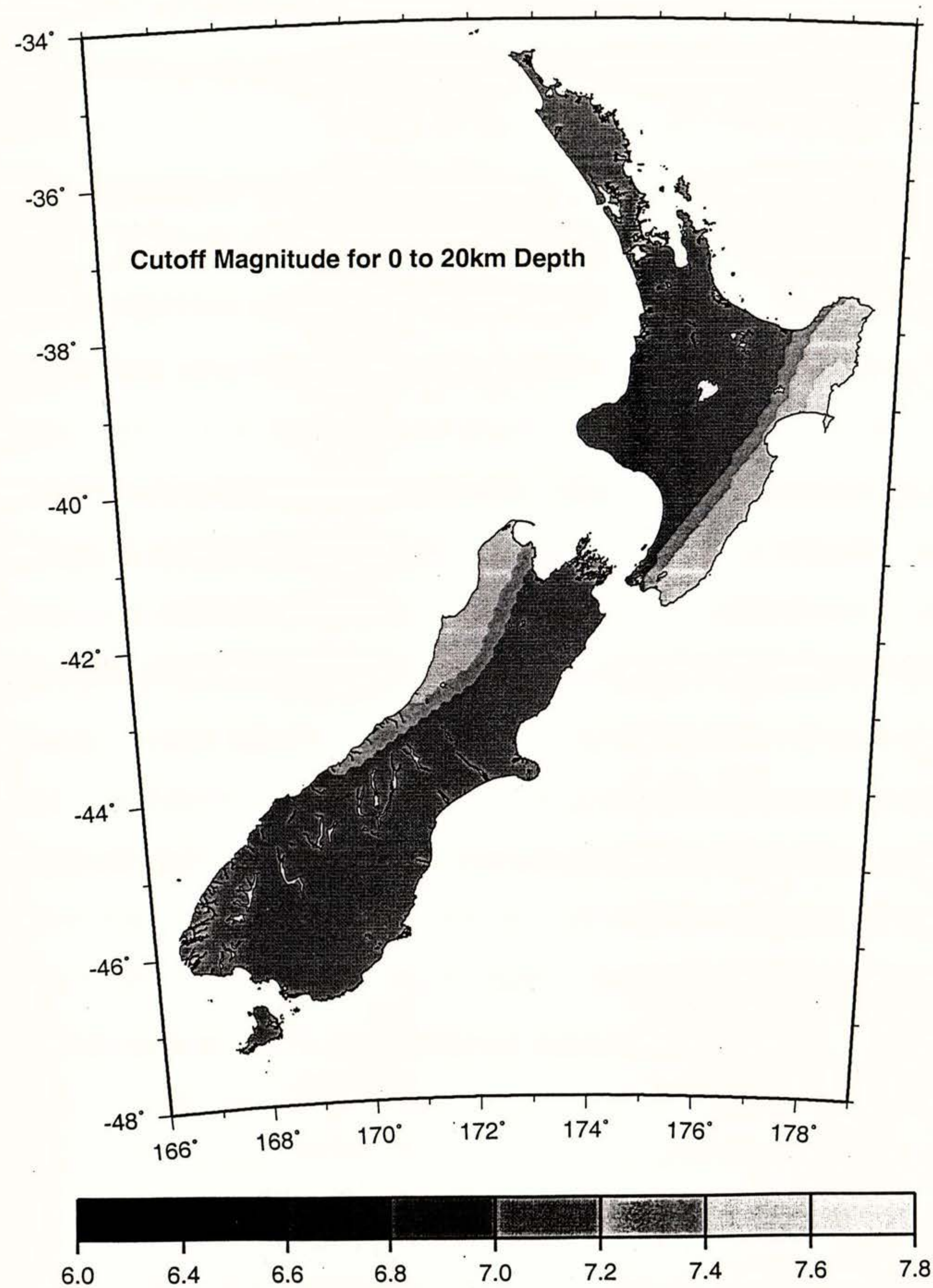
Cutoff Magnitude for 0 to 20km Depth
-34°
-36°
-38°
-40°
-42°
-44°
-46°
-48°
166°
168°
170°
172°
174°
176°
178°
6.0
6.4
6.6
6.8
7.0
7.2
7.4
7.6
7.8

Figure 5a

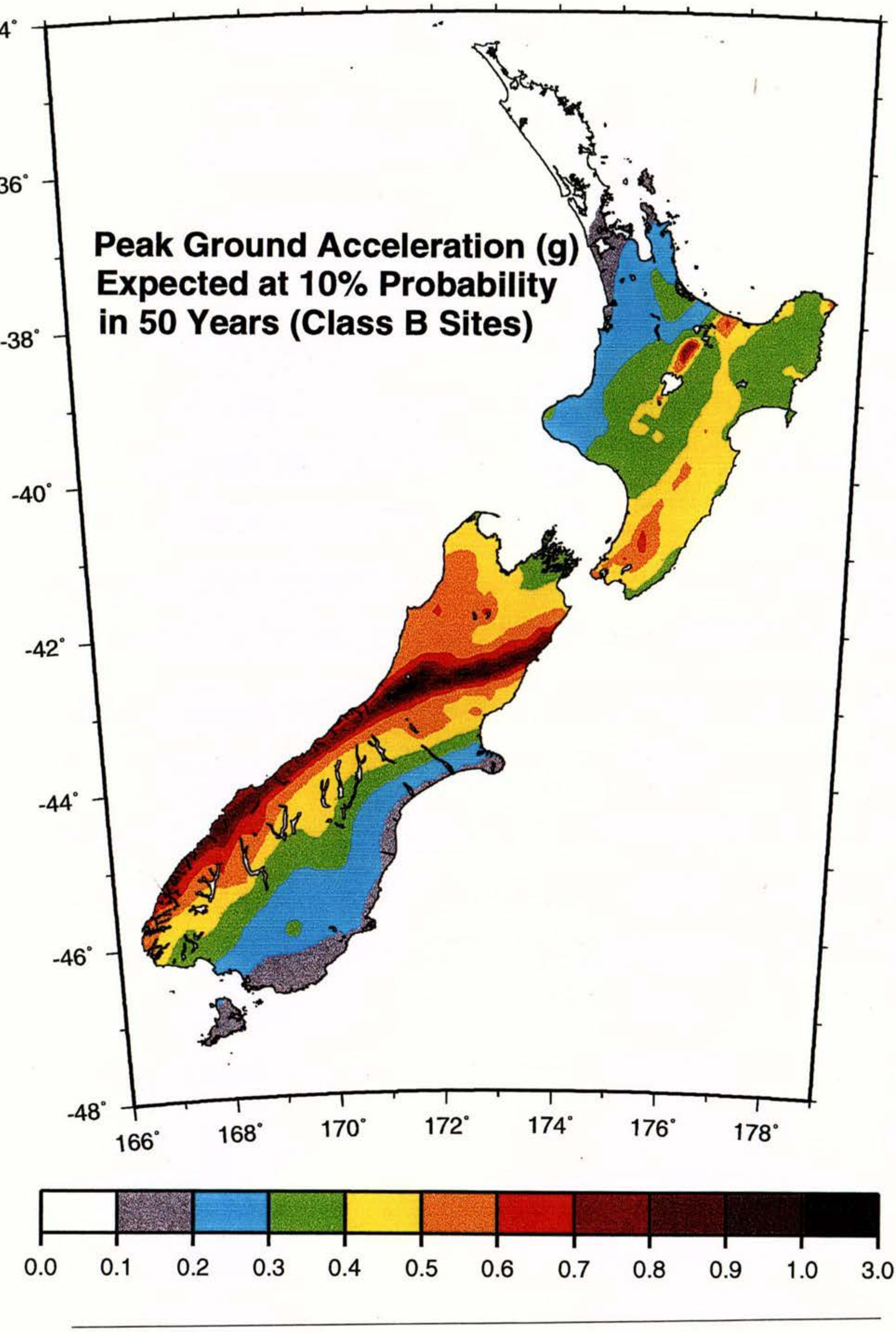
Peak Ground Acceleration (g)
Expected at 10% Probability
in 50 Years (Class B Sites)
-34°
-36°
-38°
-40°
-42°
-44°
-46°
-48°
166°
168°
170°
172°
174°
176°
178°
0.0
0.1
0.2
0.3
0.4
0.5
0.6
0.7
0.8
0.9
1.0
3.0

Figure 5b

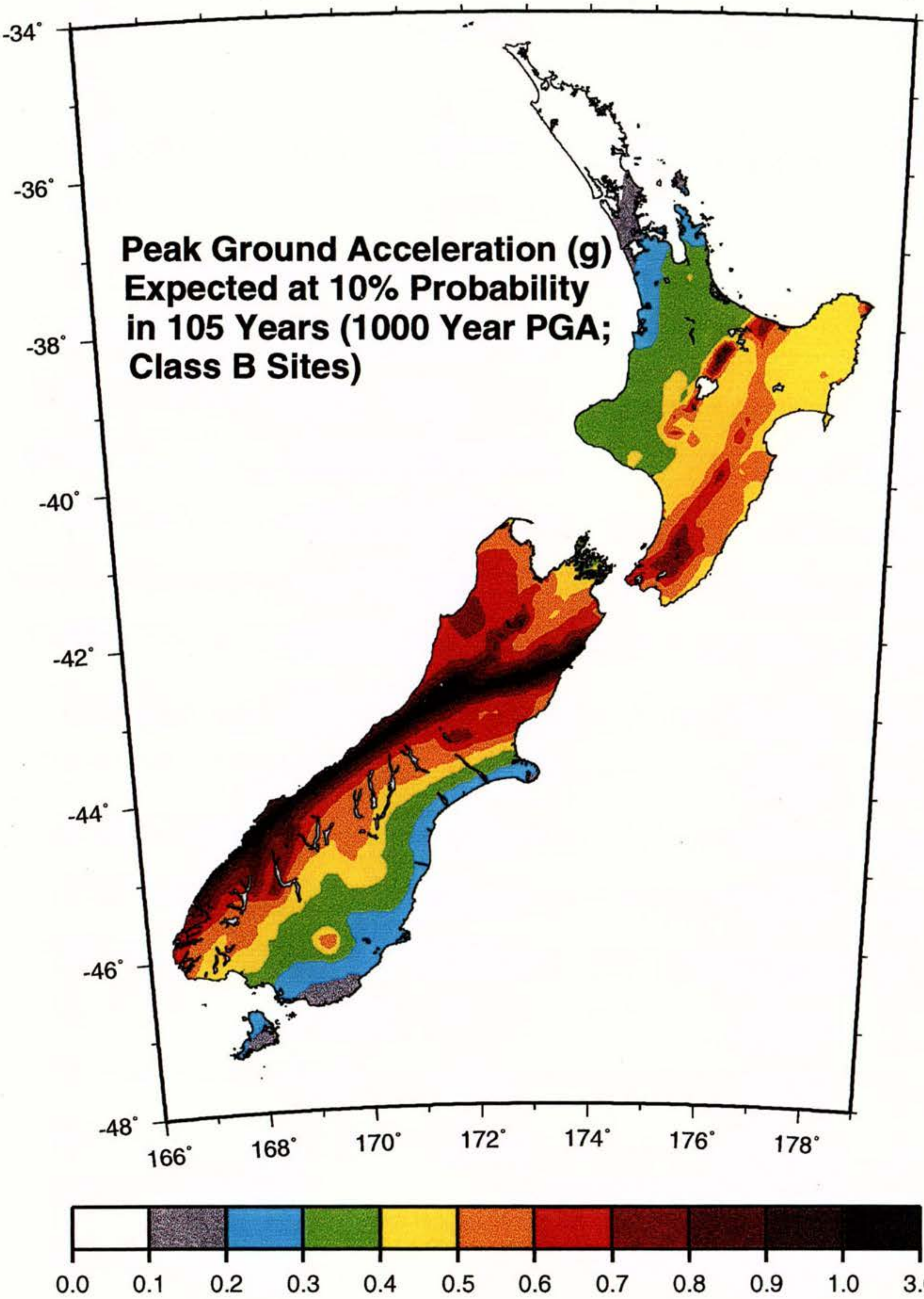
Peak Ground Acceleration (g)
Expected at 10% Probability
in 105 Years (1000 Year PGA;
Class B Sites)
-34°
-36°
-38°
-40°
-42°
-44°
-46°
-48°
166°
168°
170°
172°
174°
176°
178°
0.0
0.1
0.2
0.3
0.4
0.5
0.6
0.7
0.8
0.9
1.0
3.0

Figure 5c

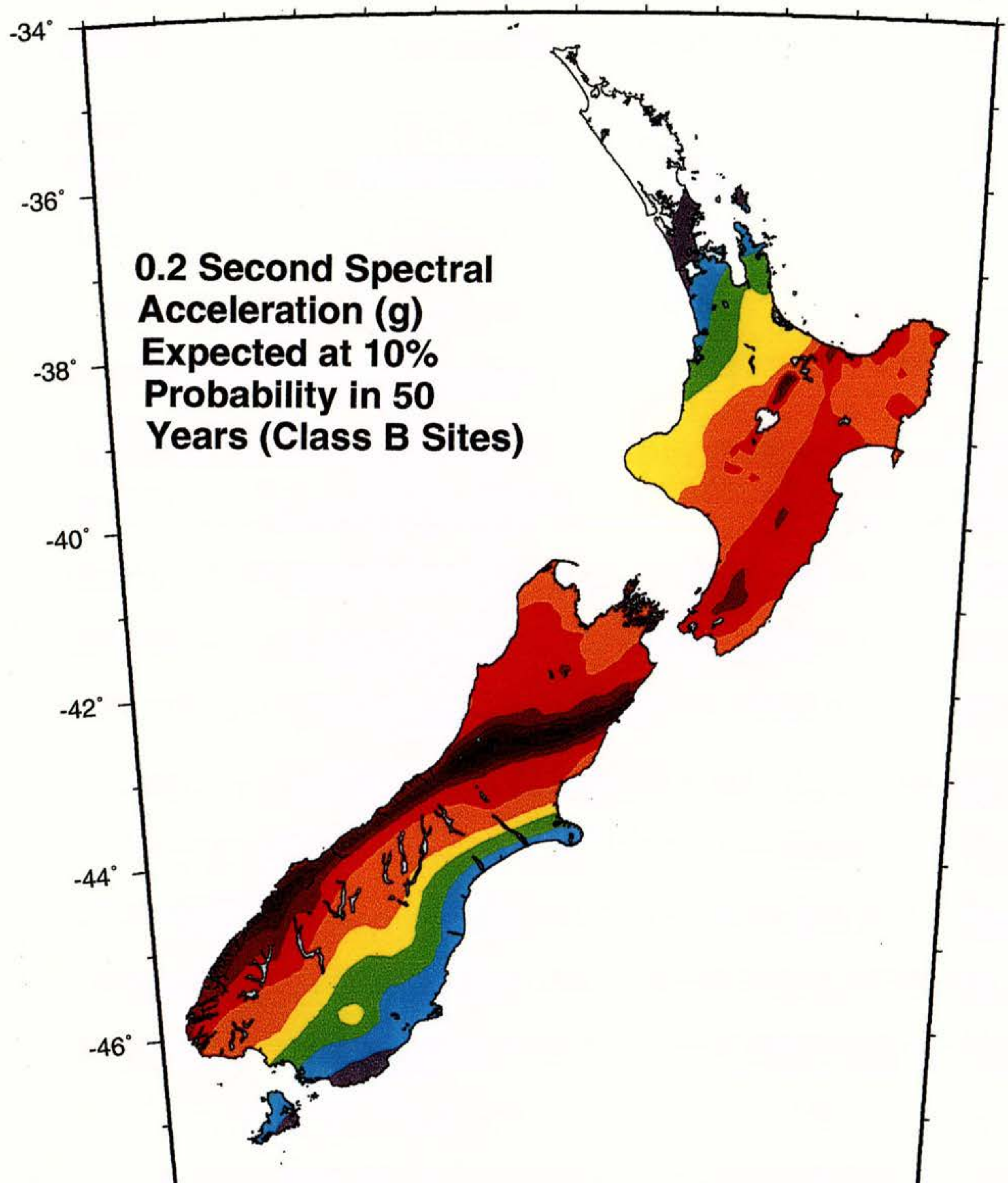

0.2 Second Spectral Acceleration (g) Expected at 10% Probability in 50 Years (Class B Sites)
-34°
-36°
-38°
-40°
-42°
-44°
-46°
-48°
166°
168°
170°
172°
174°
176°
178°
0.0
0.2
0.4
0.6
0.8
1.0
1.4
1.8
2.2
2.6
3.0
5.0

Figure 5d

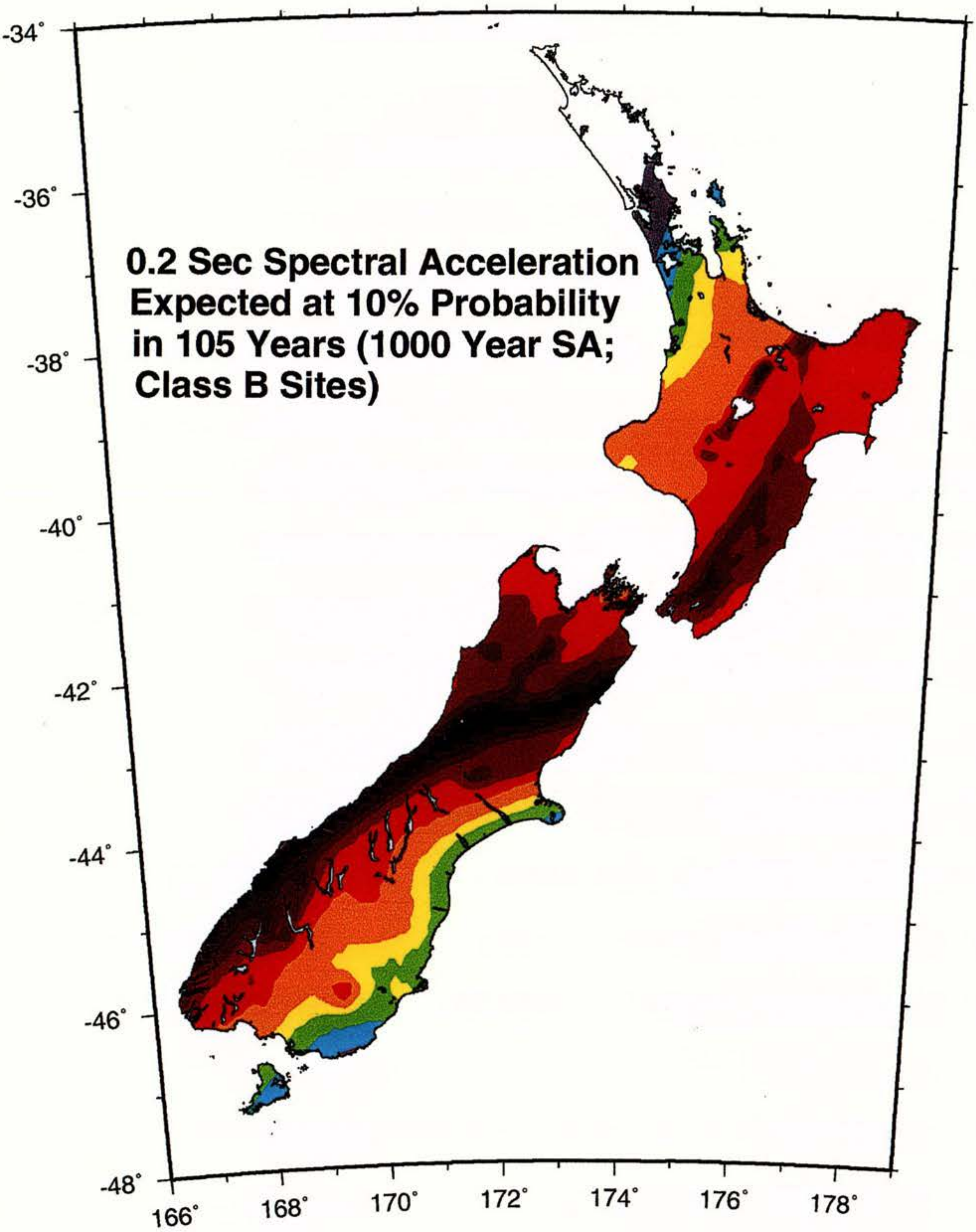
0.2 Sec Spectral Acceleration
Expected at 10% Probability
in 105 Years (1000 Year SA;
Class B Sites)
-34°
-36°
-38°
-40°
-42°
-44°
-46°
-48°
166°
168°
170°
172°
174°
176°
178°
0.0
0.2
0.4
0.6
0.8
1.0
1.4
1.8
2.2
2.6
3.0
5.0

Figure 5e

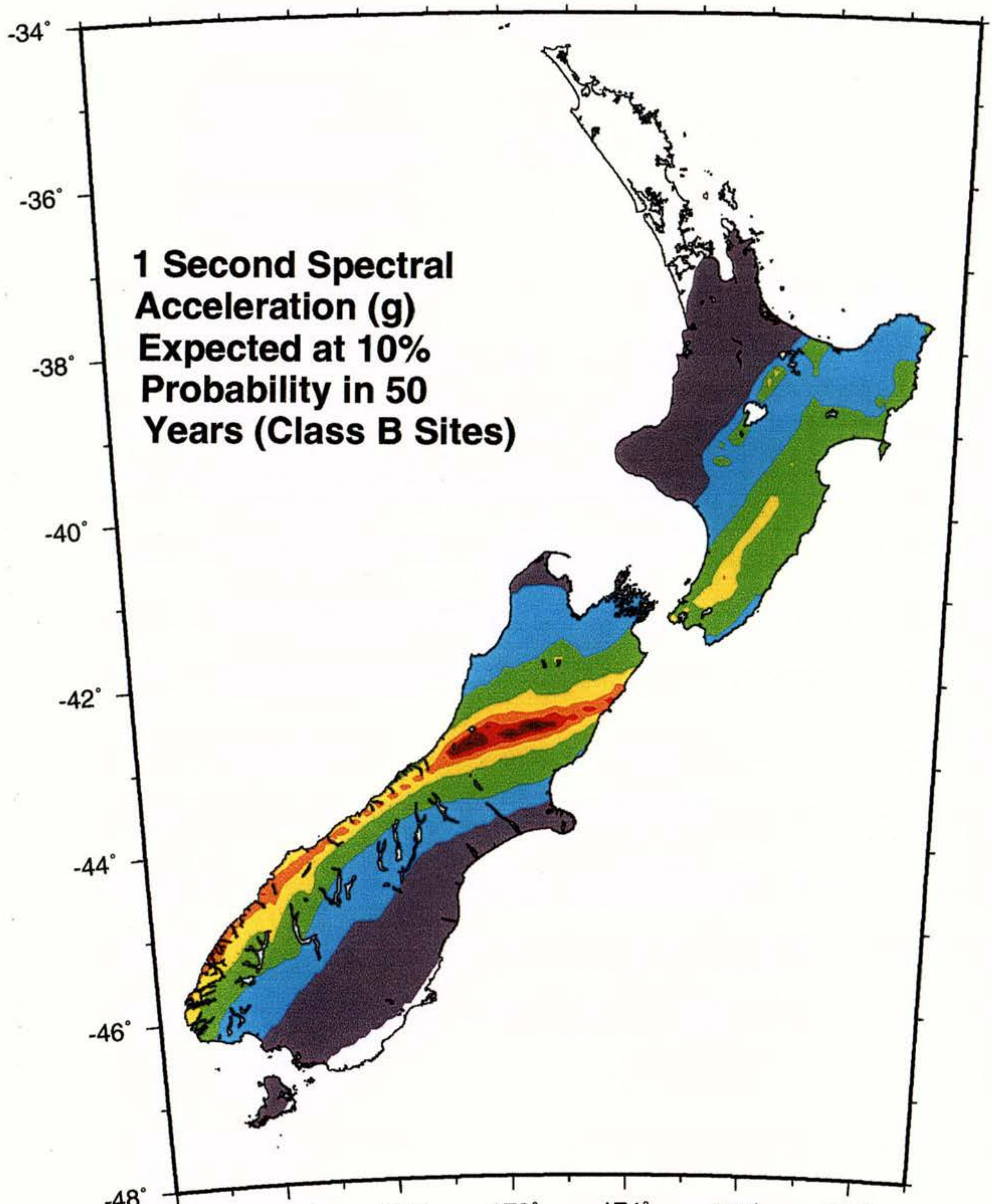

1 Second Spectral Acceleration (g) Expected at 10% Probability in 50 Years (Class B Sites)
-34°
-36°
-38°
-40°
-42°
-44°
-46°
-48°
166°
168°
170°
172°
174°
176°
178°
0.0
0.1
0.2
0.3
0.4
0.5
0.6
0.7
0.8
0.9
1.0
3.0

Figure 5f

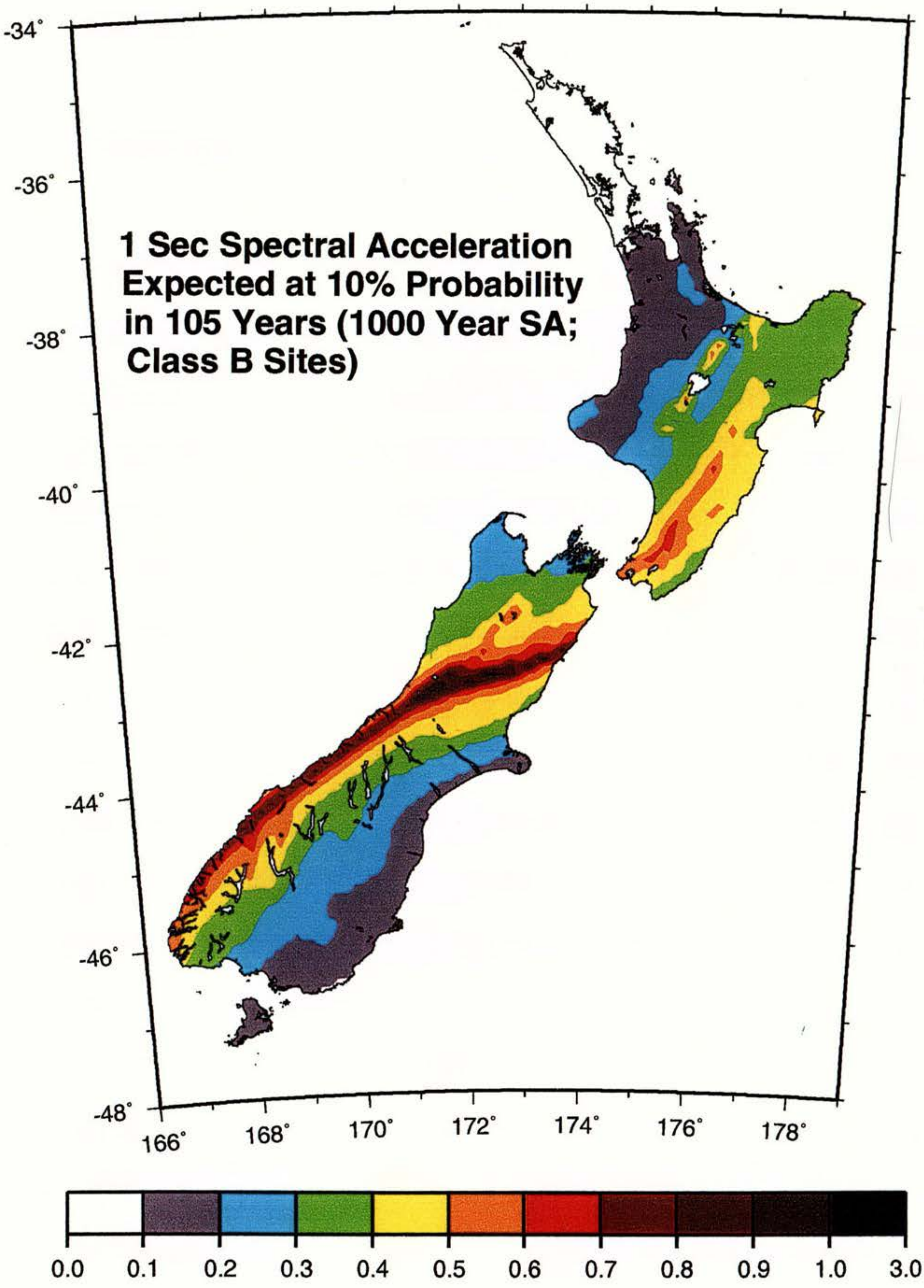

1 Sec Spectral Acceleration
Expected at 10% Probability
in 105 Years (1000 Year SA;
Class B Sites)
-34°
-36°
-38°
-40°
-42°
-44°
-46°
-48°
166°
168°
170°
172°
174°
176°
178°
0.0
0.1
0.2
0.3
0.4
0.5
0.6
0.7
0.8
0.9
1.0
3.0

Figure 6a

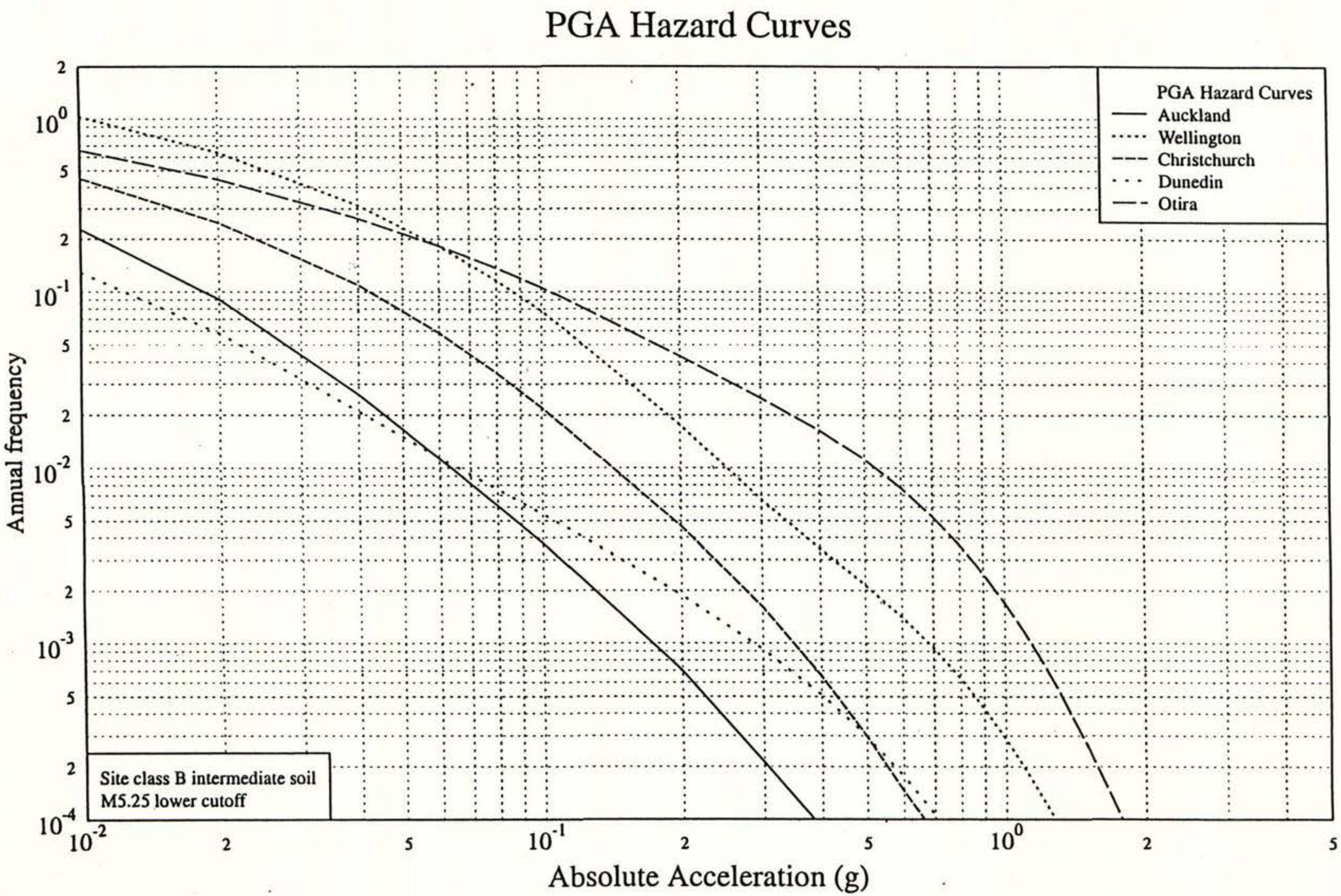
PGA Hazard Curves
PGA Hazard Curves
Auckland
Wellington
Christchurch
Dunedin
Otira
Site class B intermediate soil
M5.25 lower cutoff
Annual frequency
Absolute Acceleration (g)

Figure 6b

SA(1s) Hazard Curves

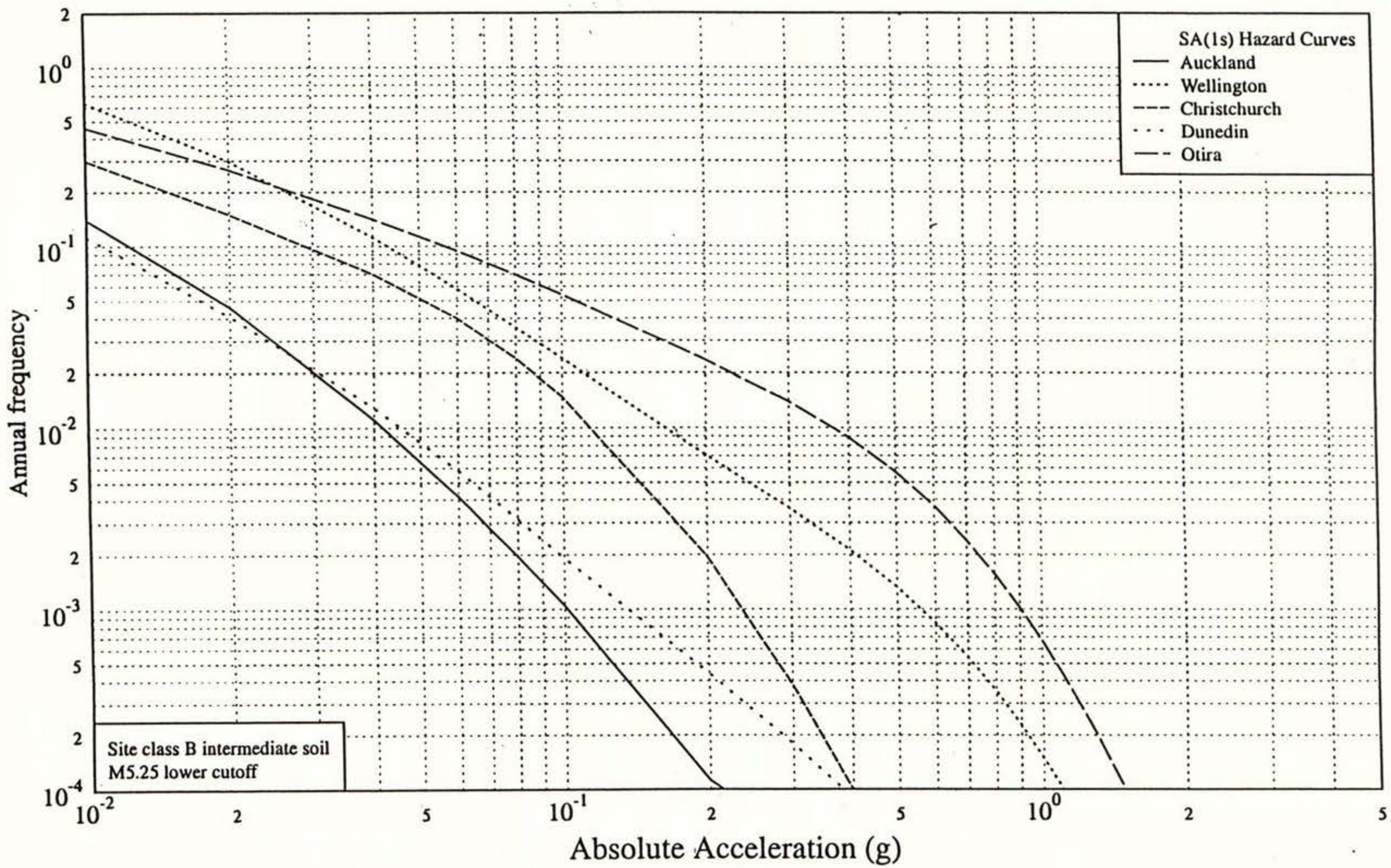

Figure 7a

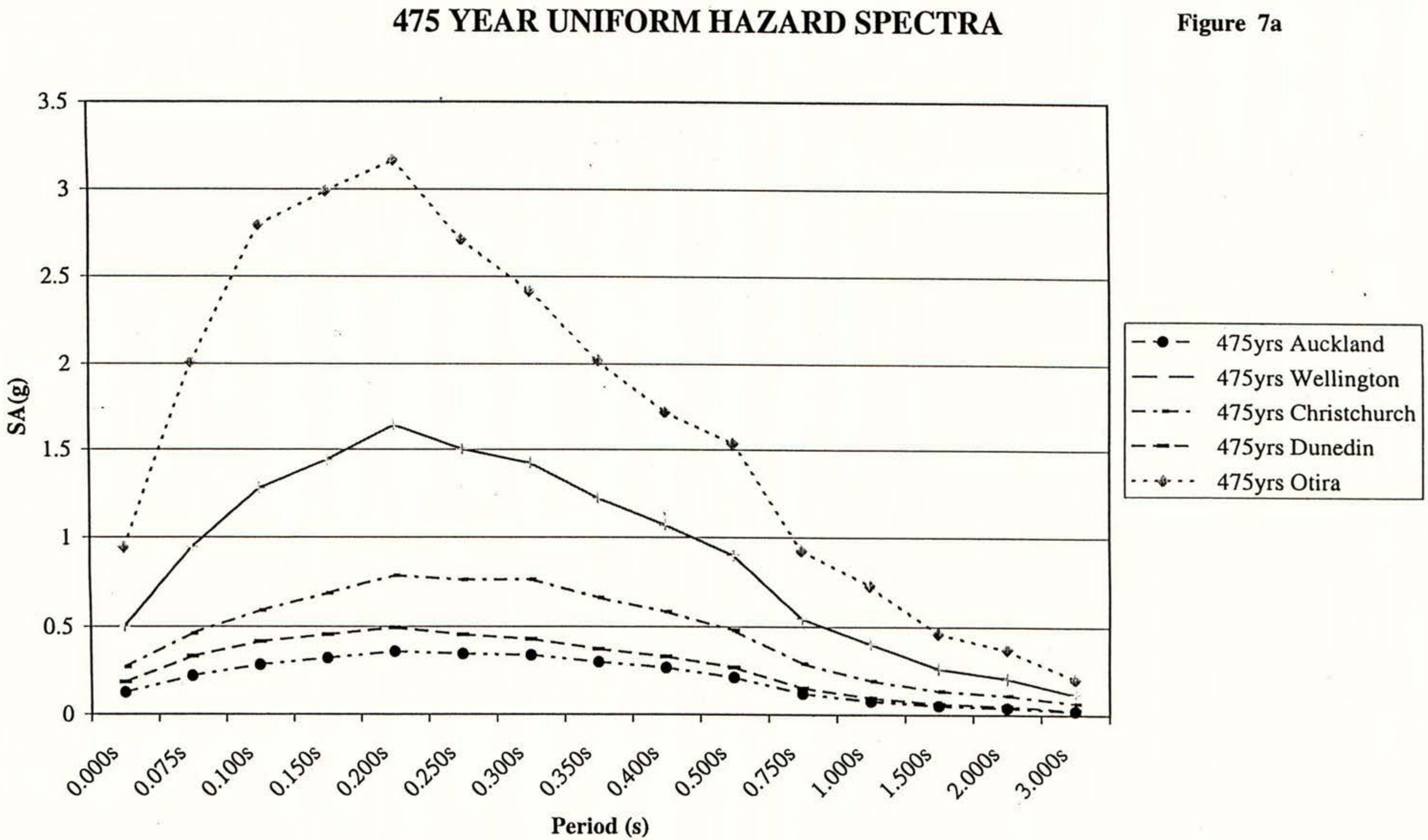
475 YEAR UNIFORM HAZARD SPECTRA
SA(g)
3.5
3
2.5
2
1.5
1
0.5
0
0.000s
0.075s
0.100s
0.150s
0.200s
0.250s
0.300s
0.350s
0.400s
0.500s
0.750s
1.000s
1.500s
2.000s
3.000s
Period (s)
475yrs Auckland
475yrs Wellington
475yrs Christchurch
475yrs Dunedin
475yrs Otira

1000 YEAR UNIFORM HAZARD SPECTRA

Figure 7b

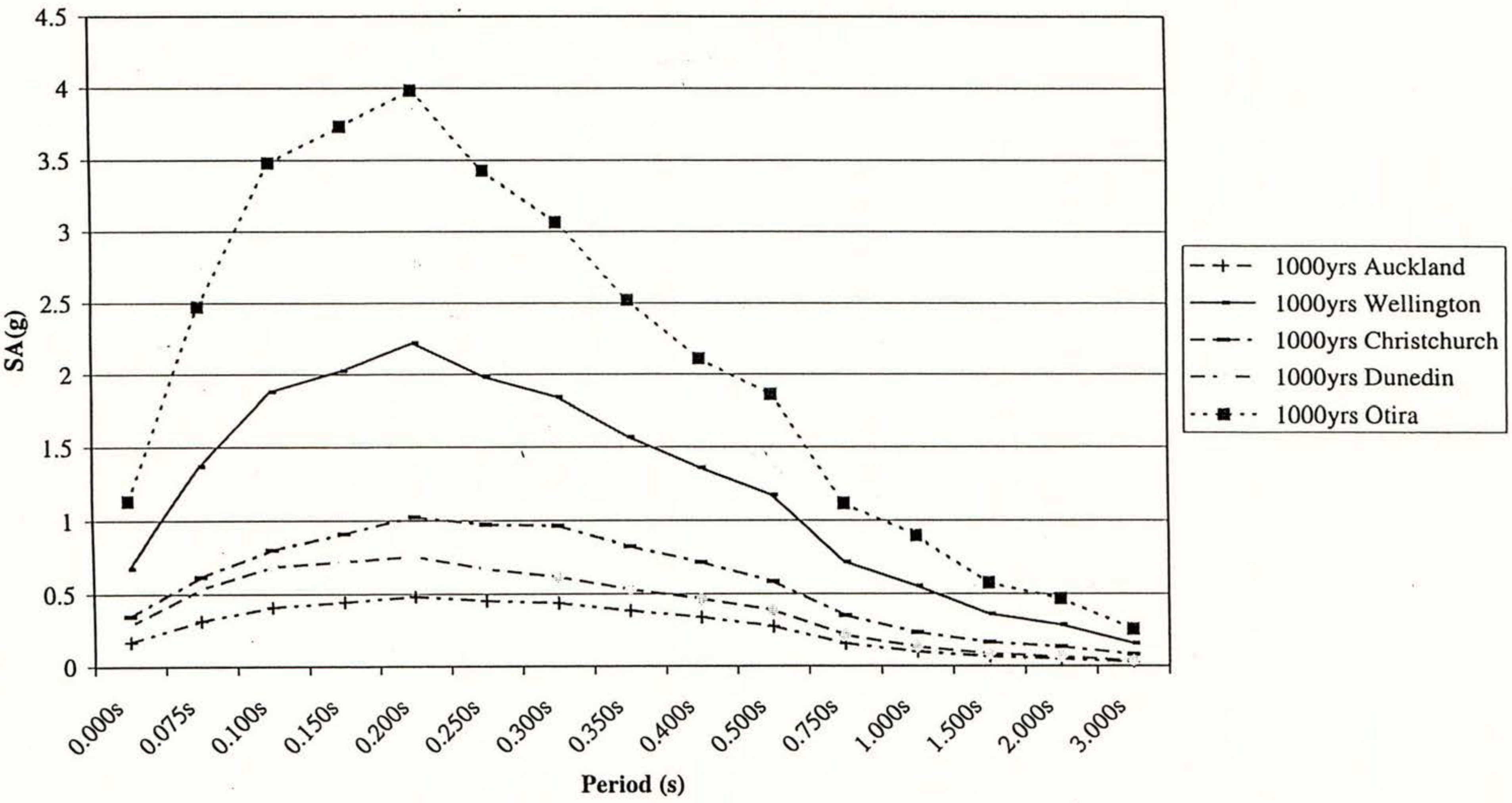

Figure 8a

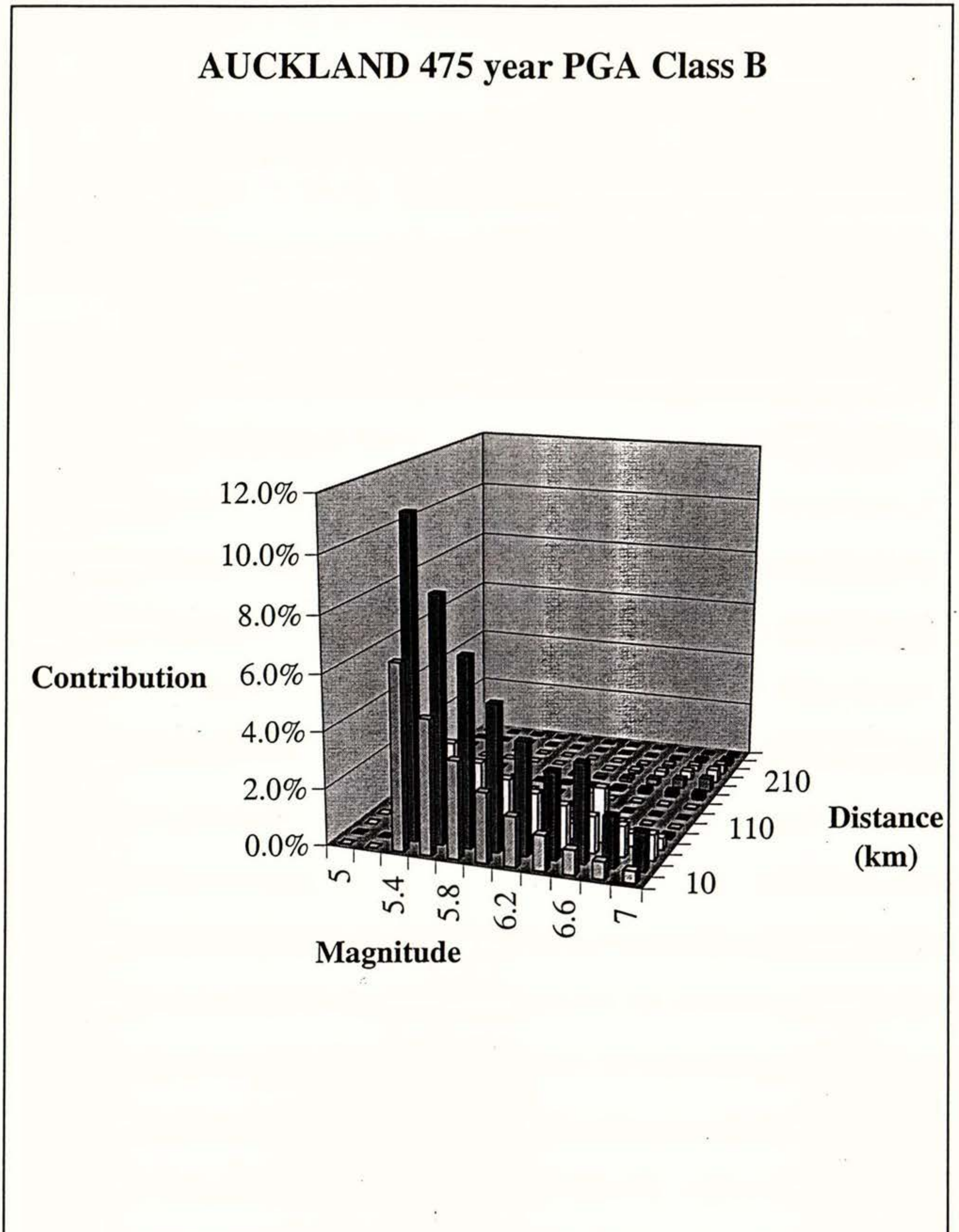

AUCKLAND 475 year PGA Class B
Contribution
12.0%
10.0%
8.0%
6.0%
4.0%
2.0%
0.0%
5
5.4
5.8
6.2
6.6
7
Magnitude
210
110
10
Distance (km)

Figure 8b

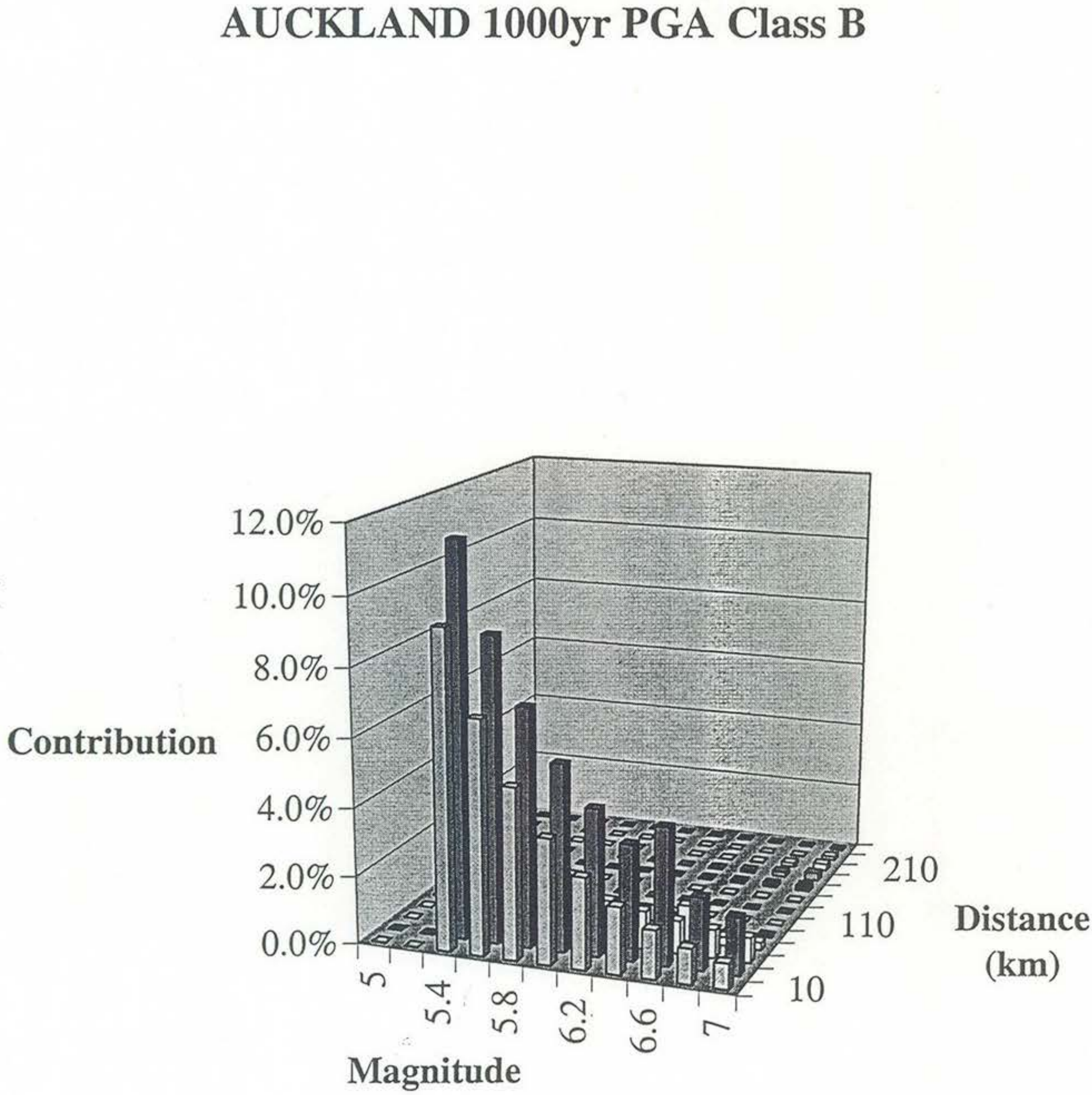
AUCKLAND 1000yr PGA Class B
12.0%
10.0%
8.0%
6.0%
4.0%
2.0%
0.0%
Contribution
5
5.4
5.8
6.2
6.6
7
Magnitude
210
110
10
Distance
(km)

Figure 8c

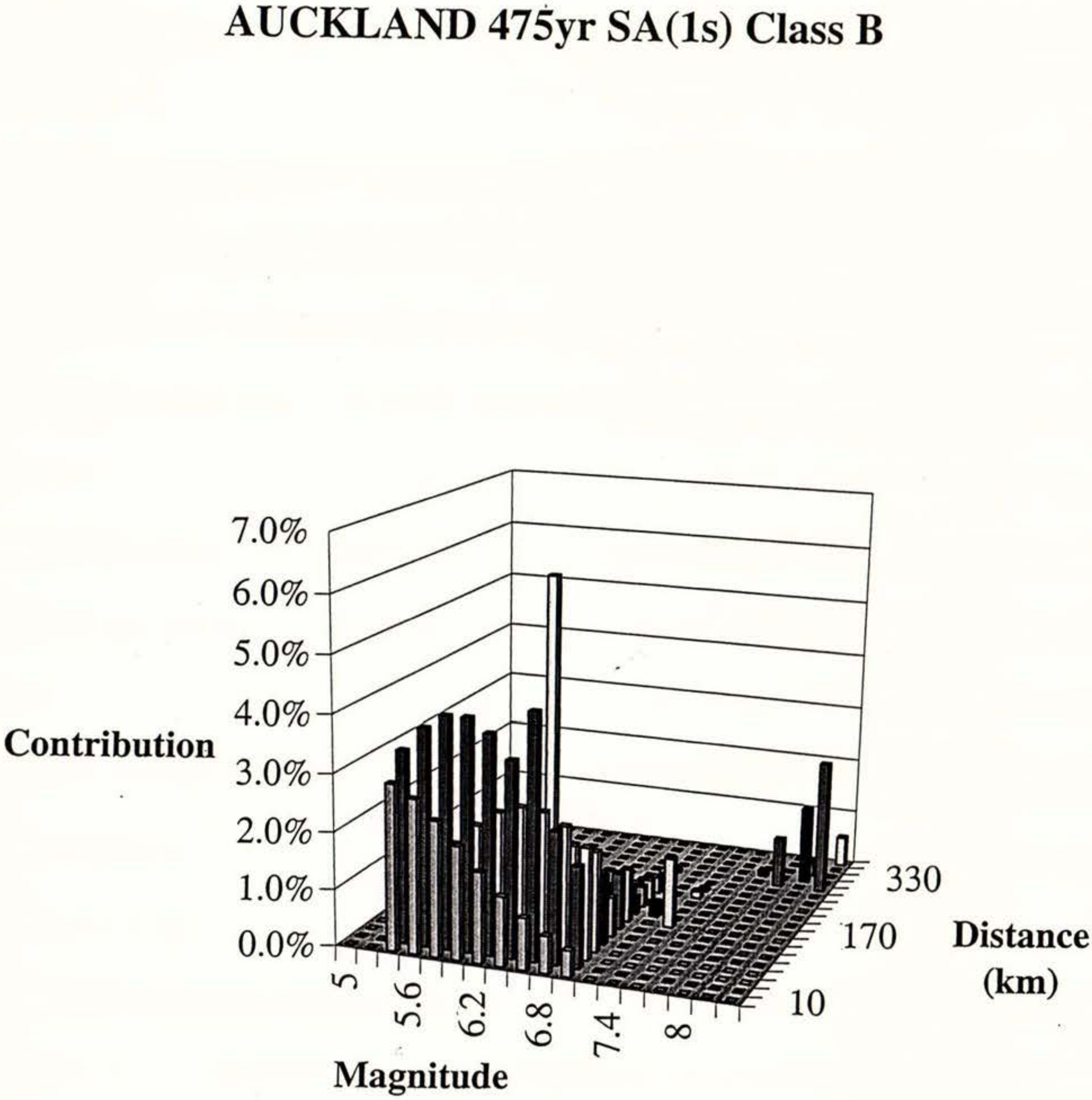

AUCKLAND 475yr SA(1s) Class B
7.0%
6.0%
5.0%
4.0%
3.0%
2.0%
1.0%
0.0%
Contribution
5
5.6
6.2
6.8
7.4
8
Magnitude
330
170
10
Distance (km)

Figure 8d

AUCKLAND 1000yr SA(1s) Class B

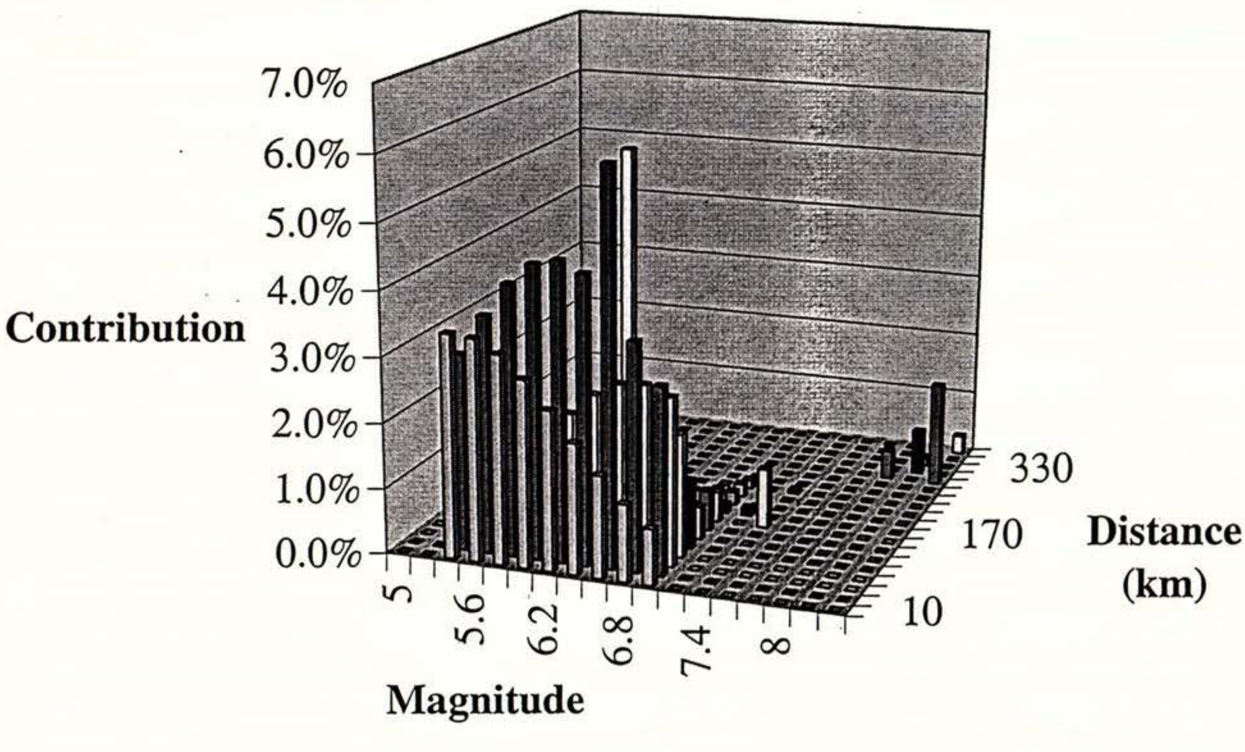

Figure 8e

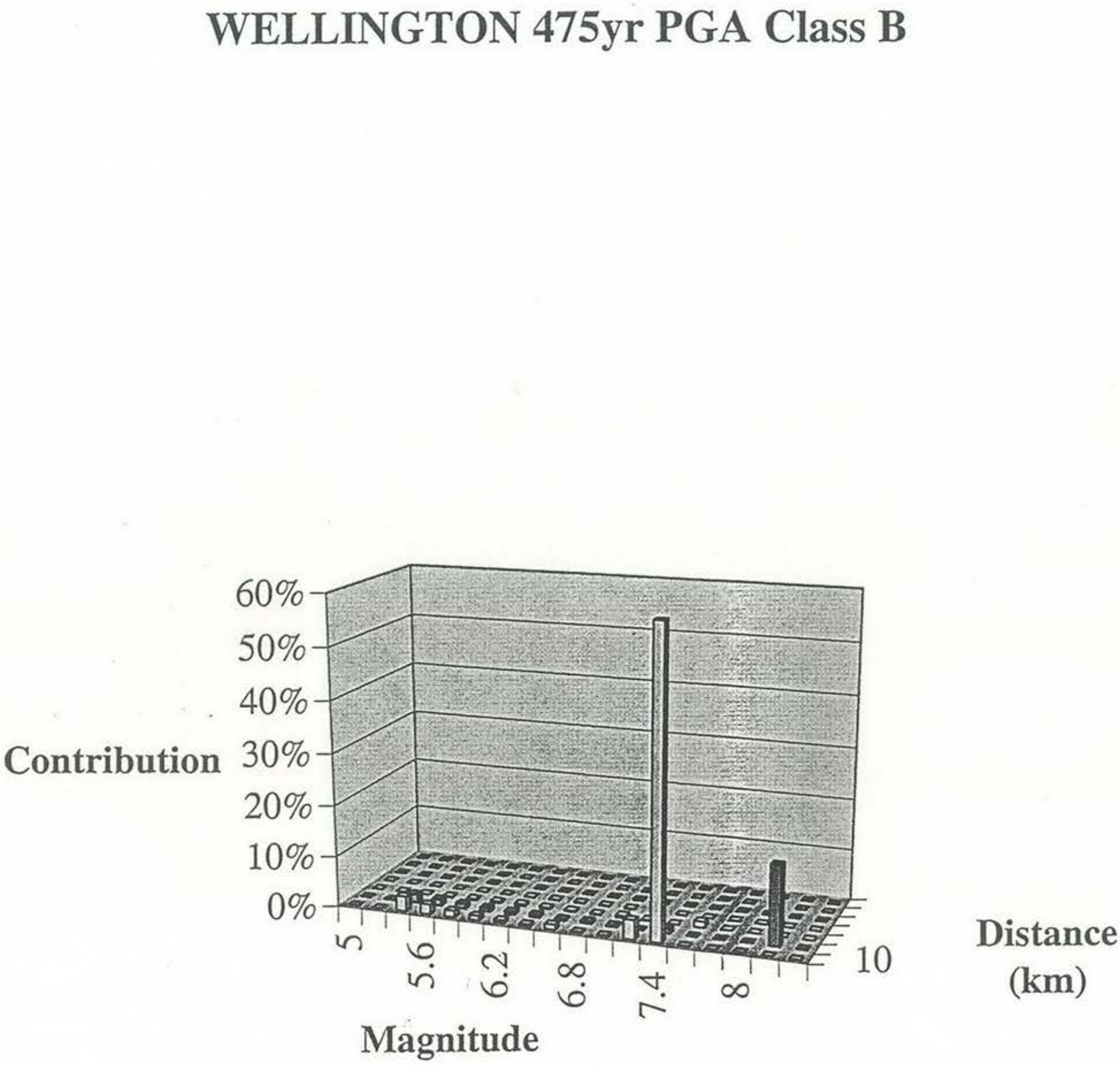
WELLINGTON 475yr PGA Class B
60%
50%
40%
Contribution
30%
20%
10%
0%
5
5.6
6.2
6.8
7.4
8
10
Distance (km)
Magnitude

Figure 8f

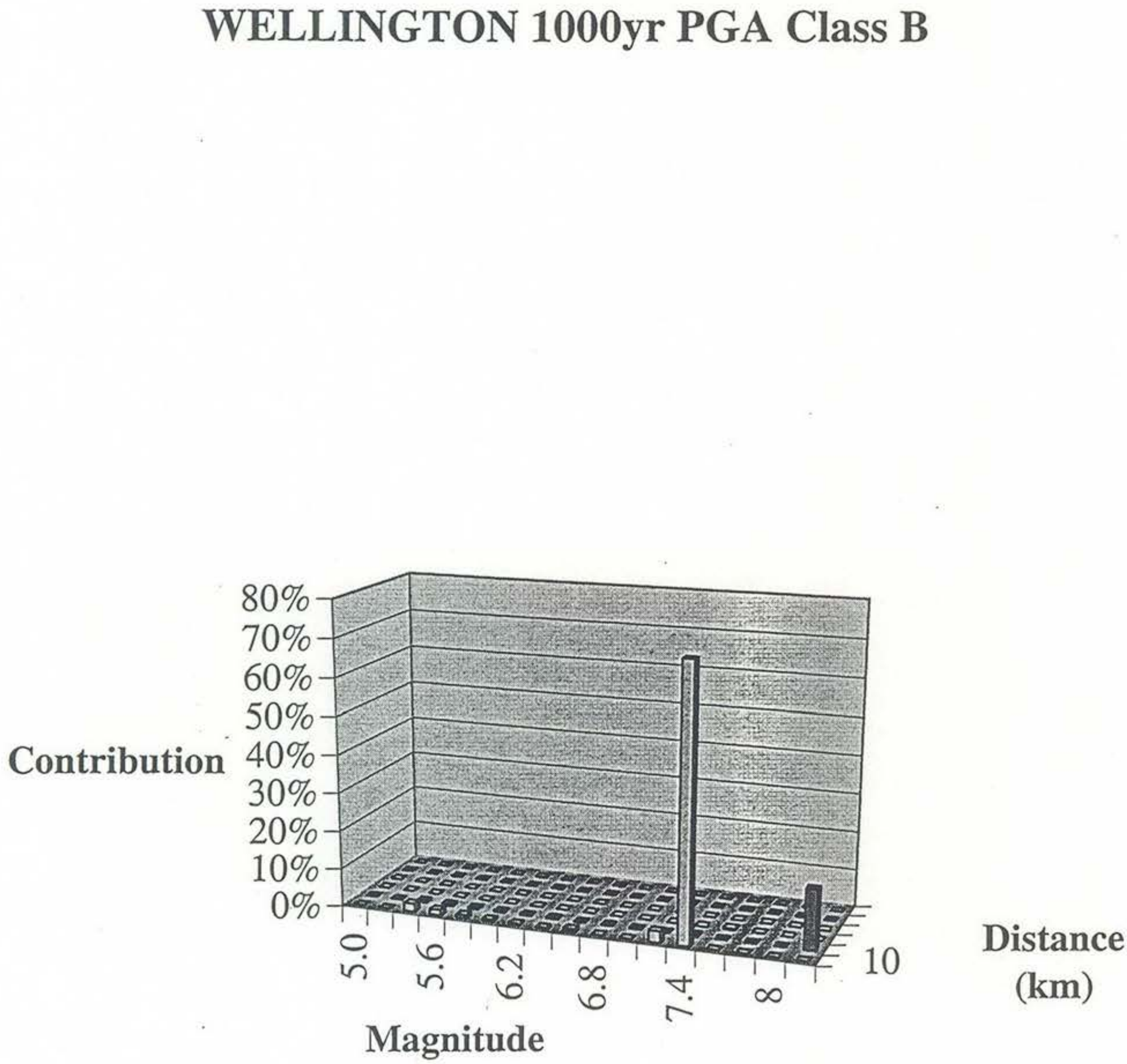
WELLINGTON 1000yr PGA Class B
80%
70%
60%
50%
40%
30%
20%
10%
0%
Contribution
5.0
5.6
6.2
6.8
7.4
8
Magnitude
10
Distance (km)

Figure 8g

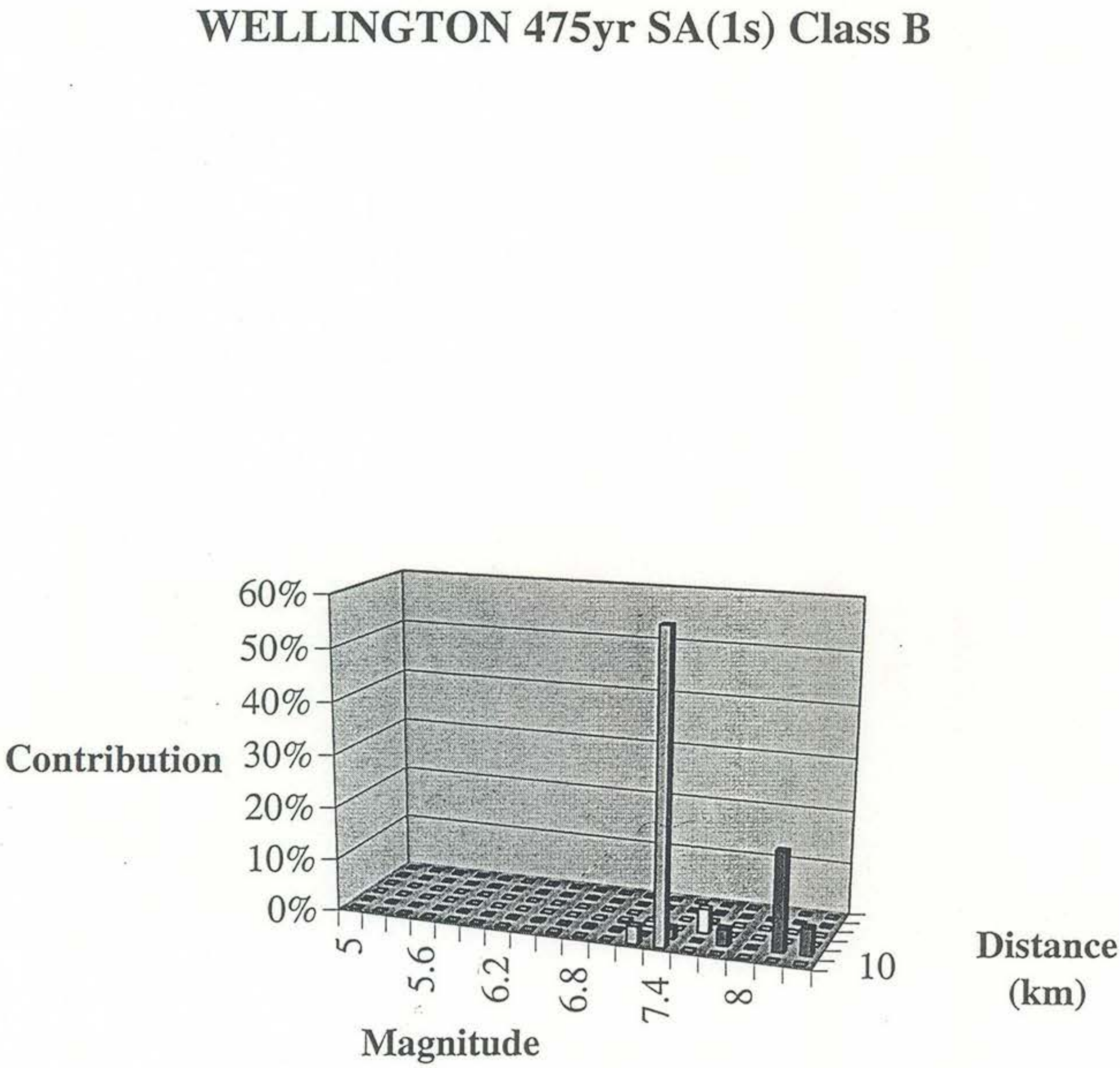
WELLINGTON 475yr SA(1s) Class B
60%
50%
40%
Contribution
30%
20%
10%
0%
5
5.6
6.2
6.8
7.4
8
10
Distance (km)
Magnitude

Figure 8h

WELLINGTON 1000yr SA(1s) Class B

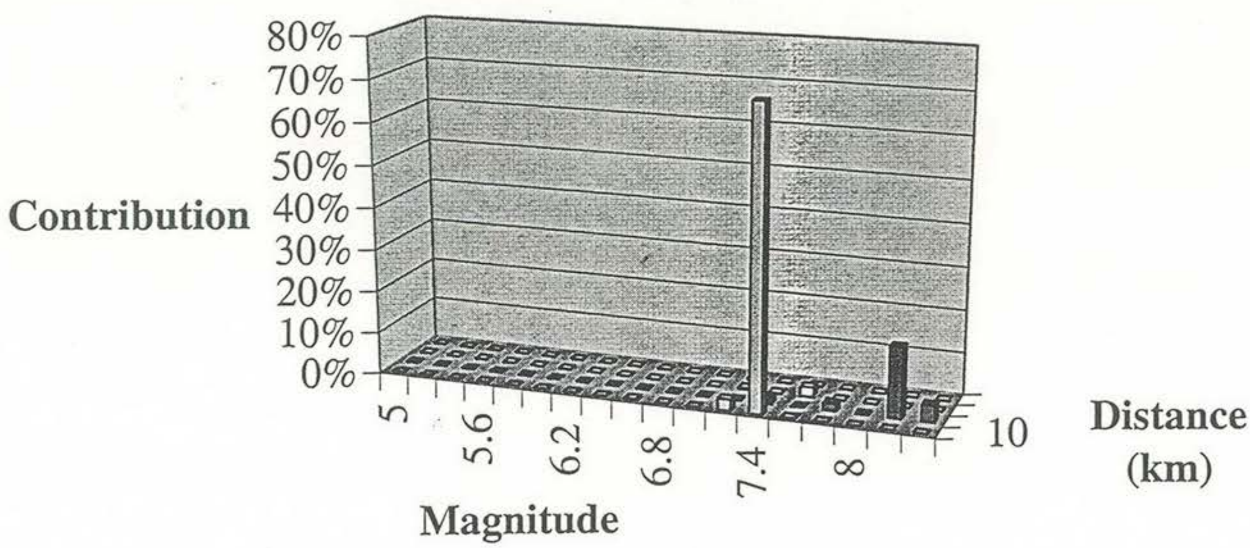

Figure 8i

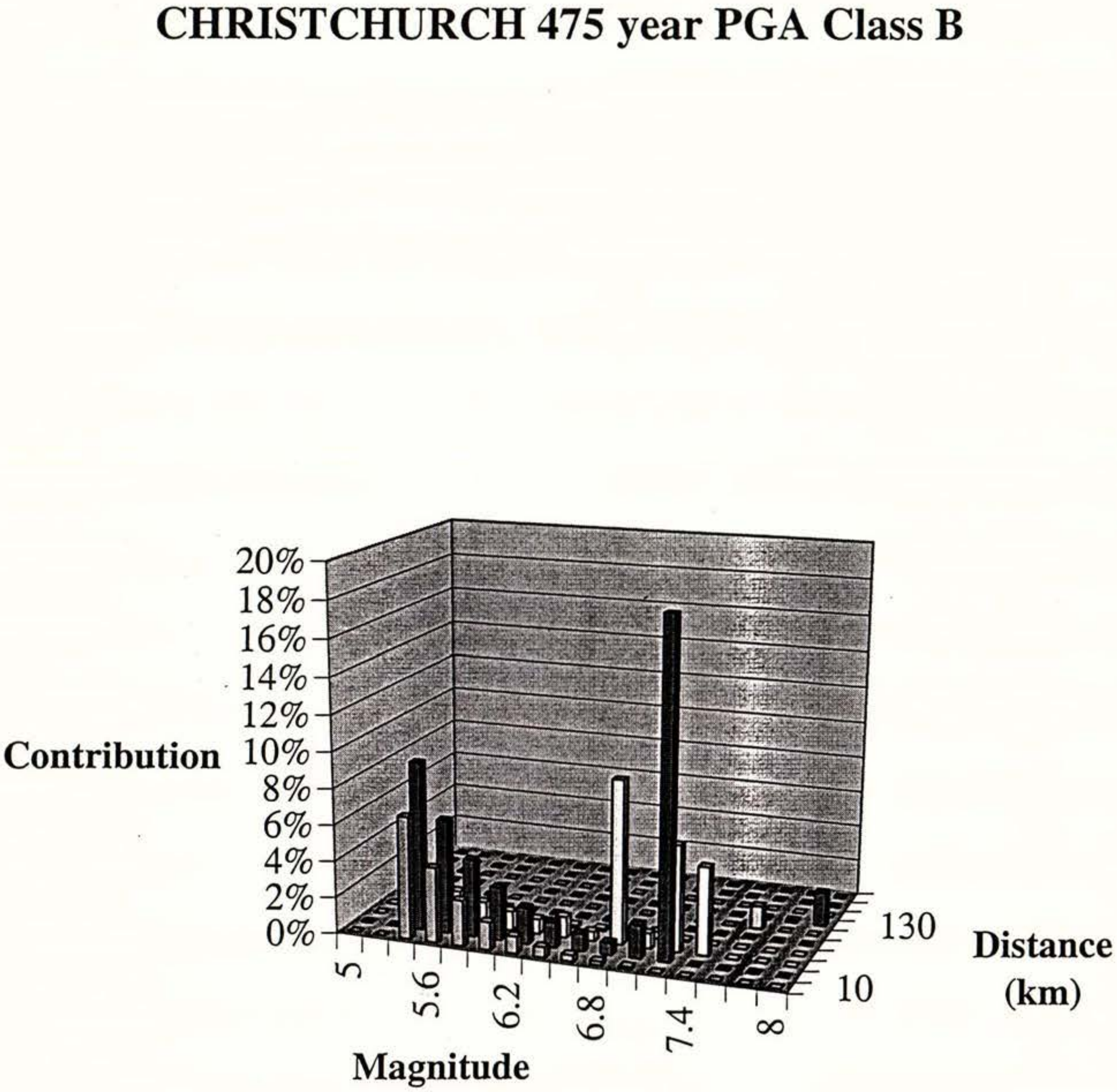
CHRISTCHURCH 475 year PGA Class B
20%
18%
16%
14%
12%
Contribution 10%
8%
6%
4%
2%
0%
5
5.6
6.2
6.8
7.4
8
Magnitude
130
10
Distance (km)

Figure 8j

CHRISTCHURCH 1000yr PGA Class B

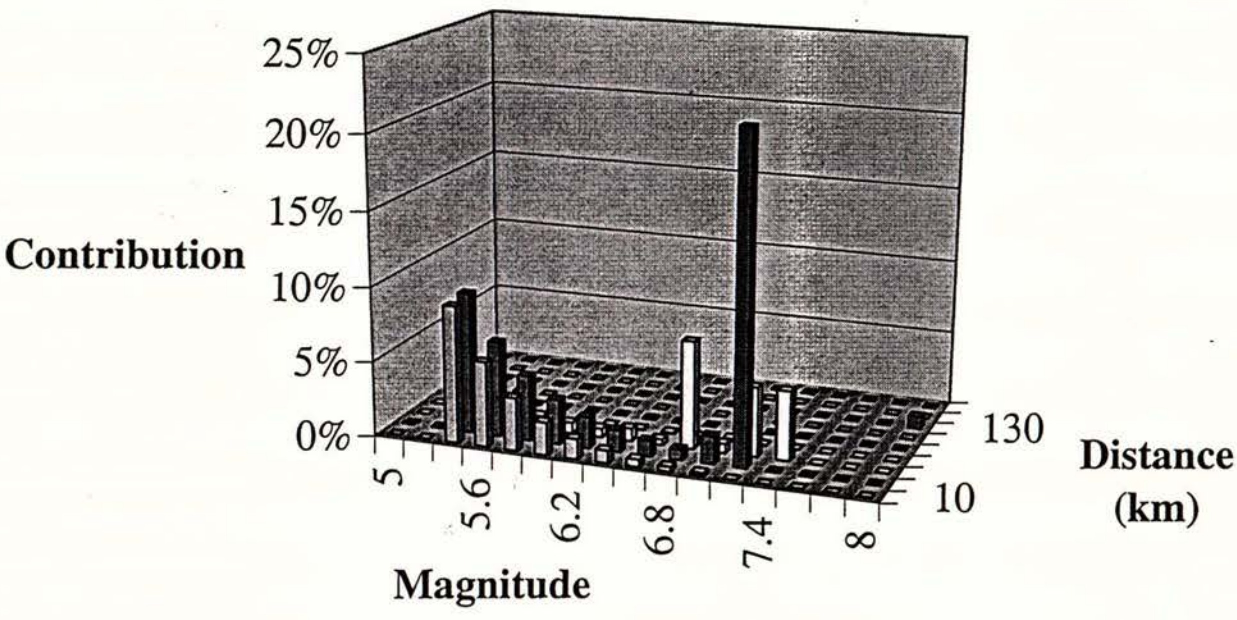

Figure 8k

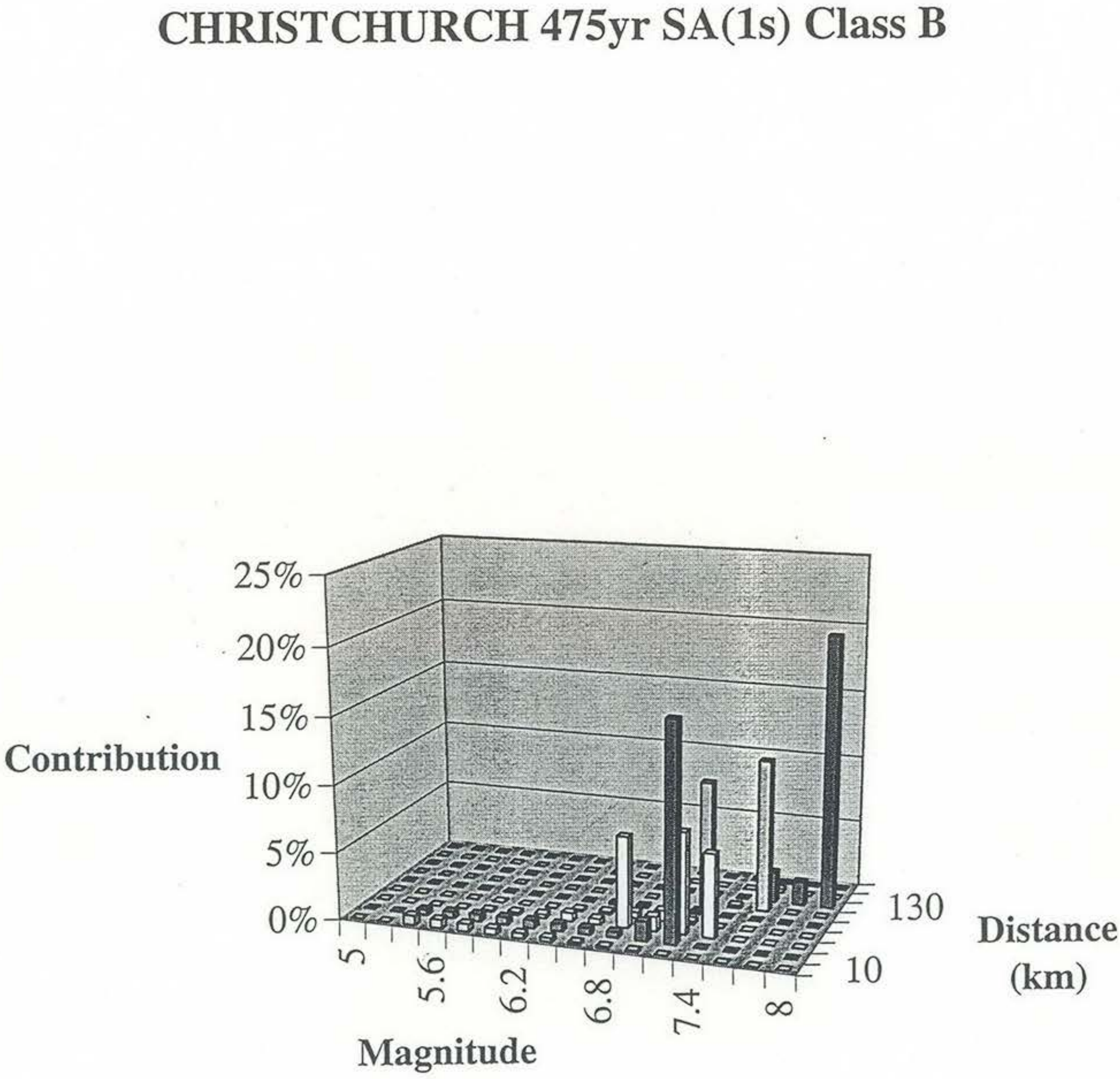
CHRISTCHURCH 475yr SA(1s) Class B
25%
20%
15%
10%
5%
0%
Contribution
5
5.6
6.2
6.8
7.4
8
Magnitude
130
10
Distance
(km)

Figure 8l

CHRISTCHURCH 1000yr SA(1s) Class B

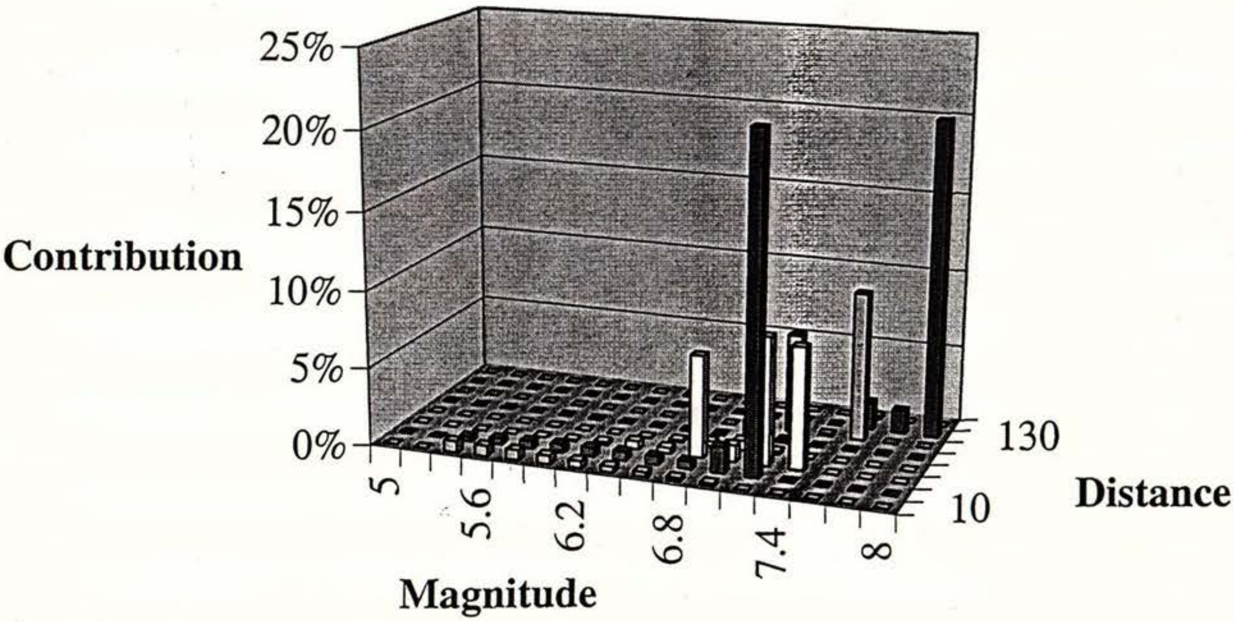

Figure 8m

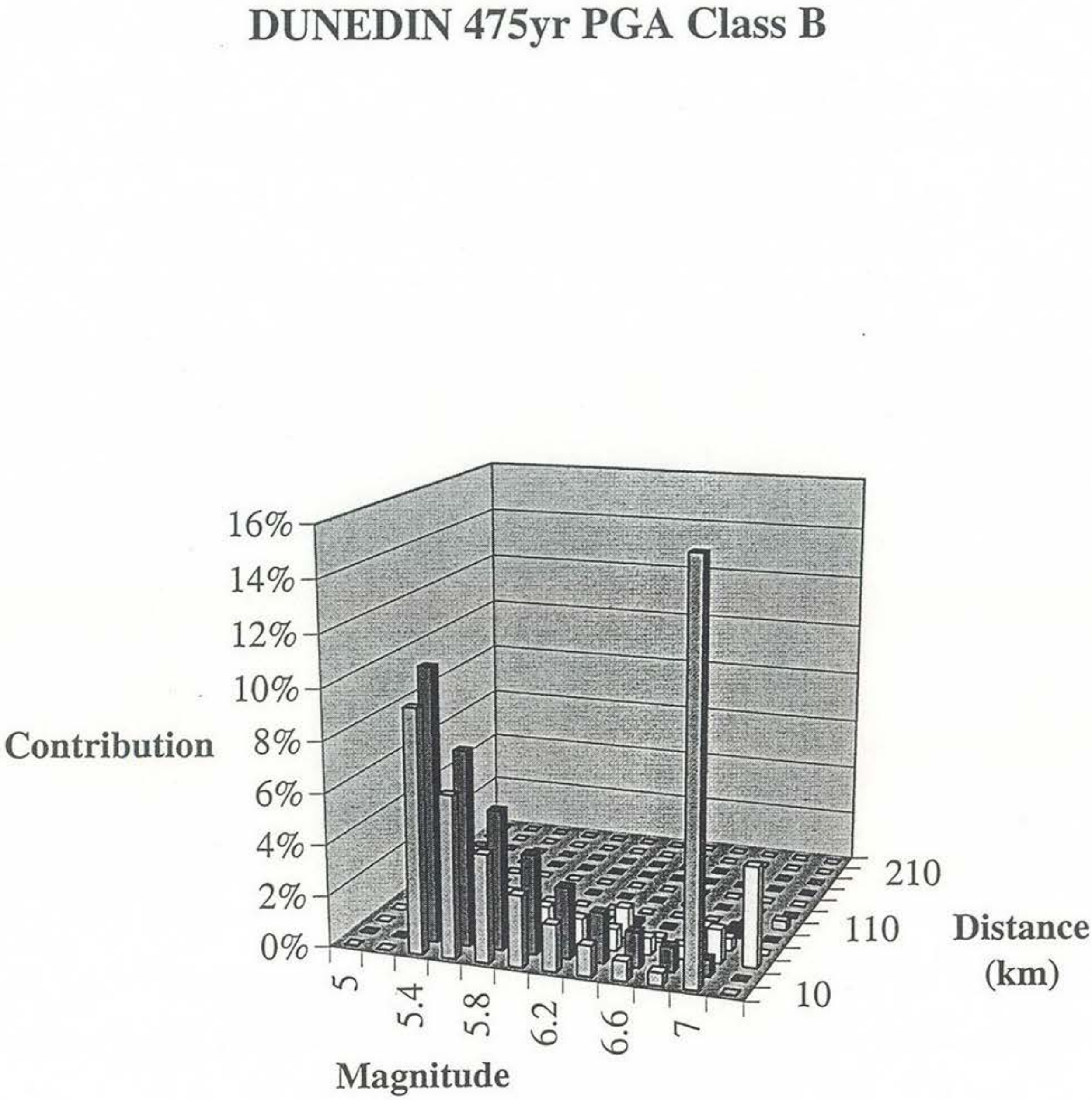
DUNEDIN 475yr PGA Class B
16%
14%
12%
10%
8%
6%
4%
2%
0%
Contribution
5
5.4
5.8
6.2
6.6
7
Magnitude
210
110
10
Distance
(km)

Figure 8n

DUNEDIN 1000yr PGA Class B

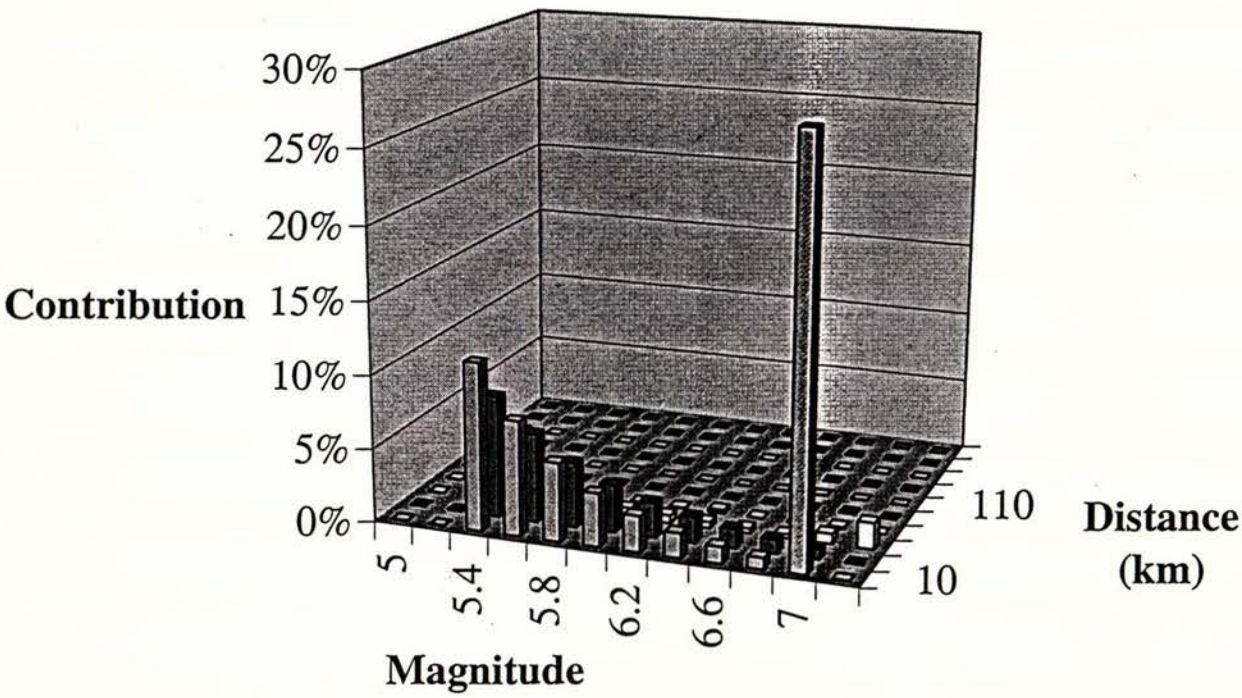

Figure 8o

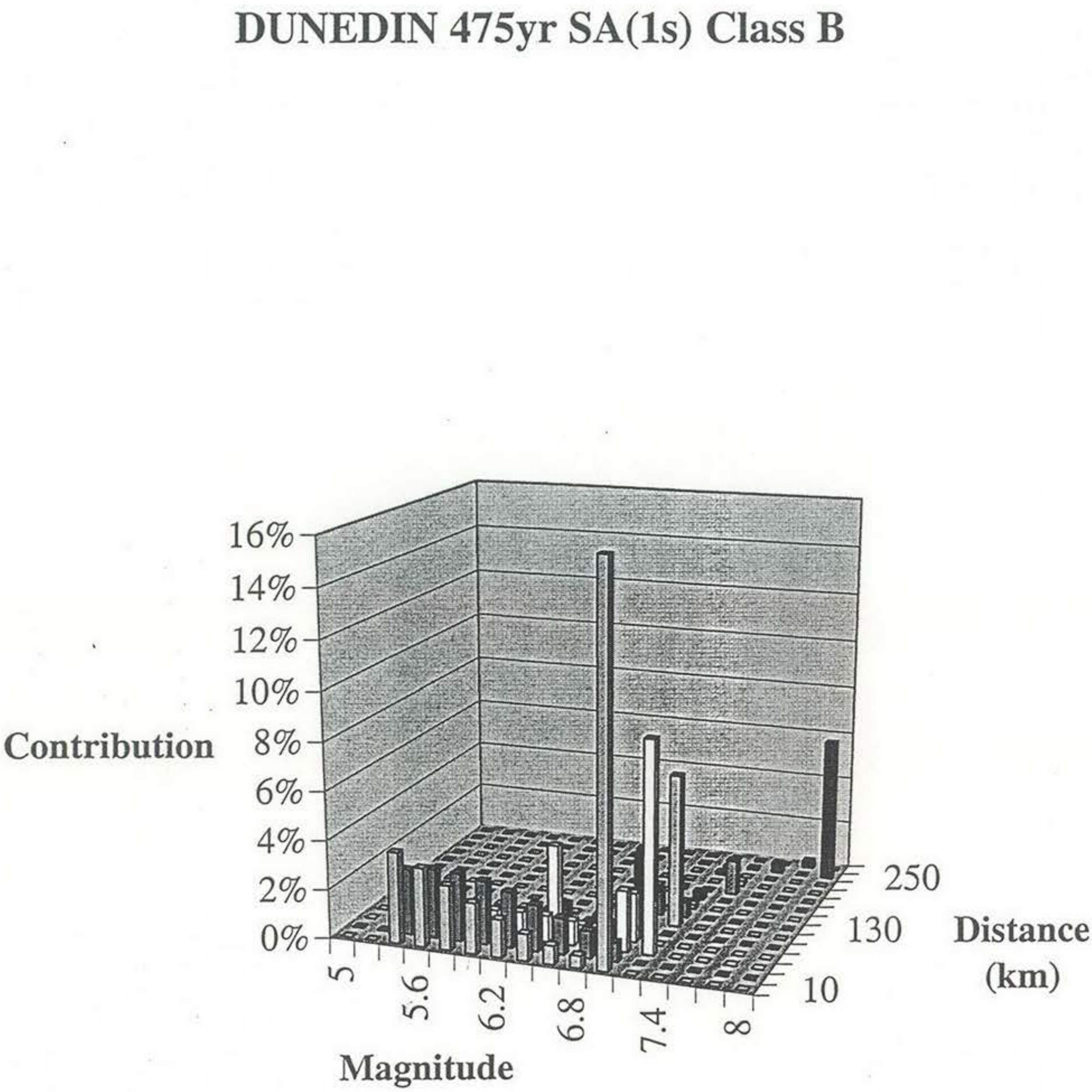
DUNEDIN 475yr SA(1s) Class B
16%
14%
12%
10%
8%
6%
4%
2%
0%
Contribution
5
5.6
6.2
6.8
7.4
8
Magnitude
250
130
10
Distance (km)

Figure 8p

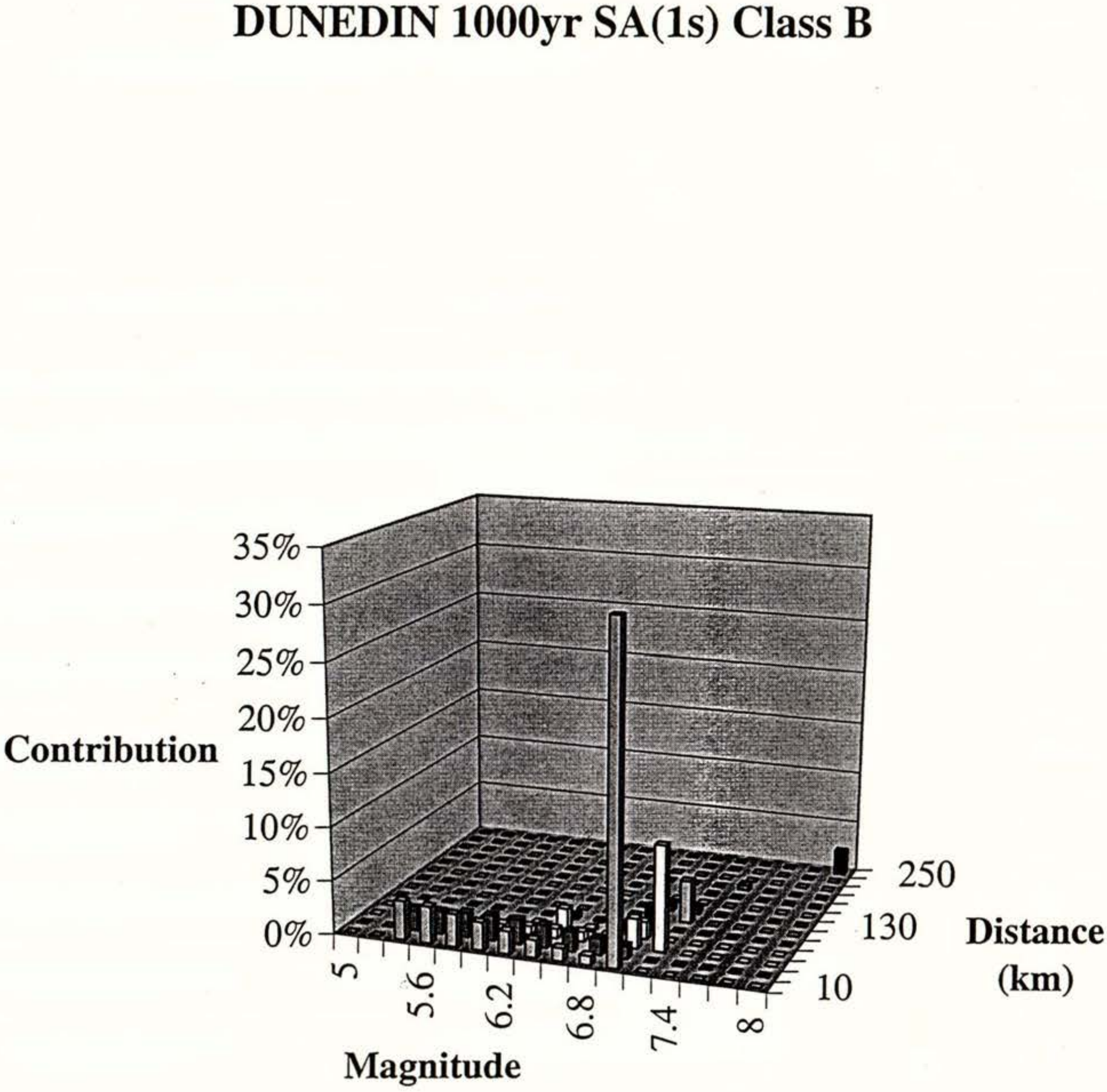
DUNEDIN 1000yr SA(1s) Class B
35%
30%
25%
20%
15%
10%
5%
0%
Contribution
5
5.6
6.2
6.8
7.4
8
Magnitude
250
130
10
Distance
(km)

Figure 8q

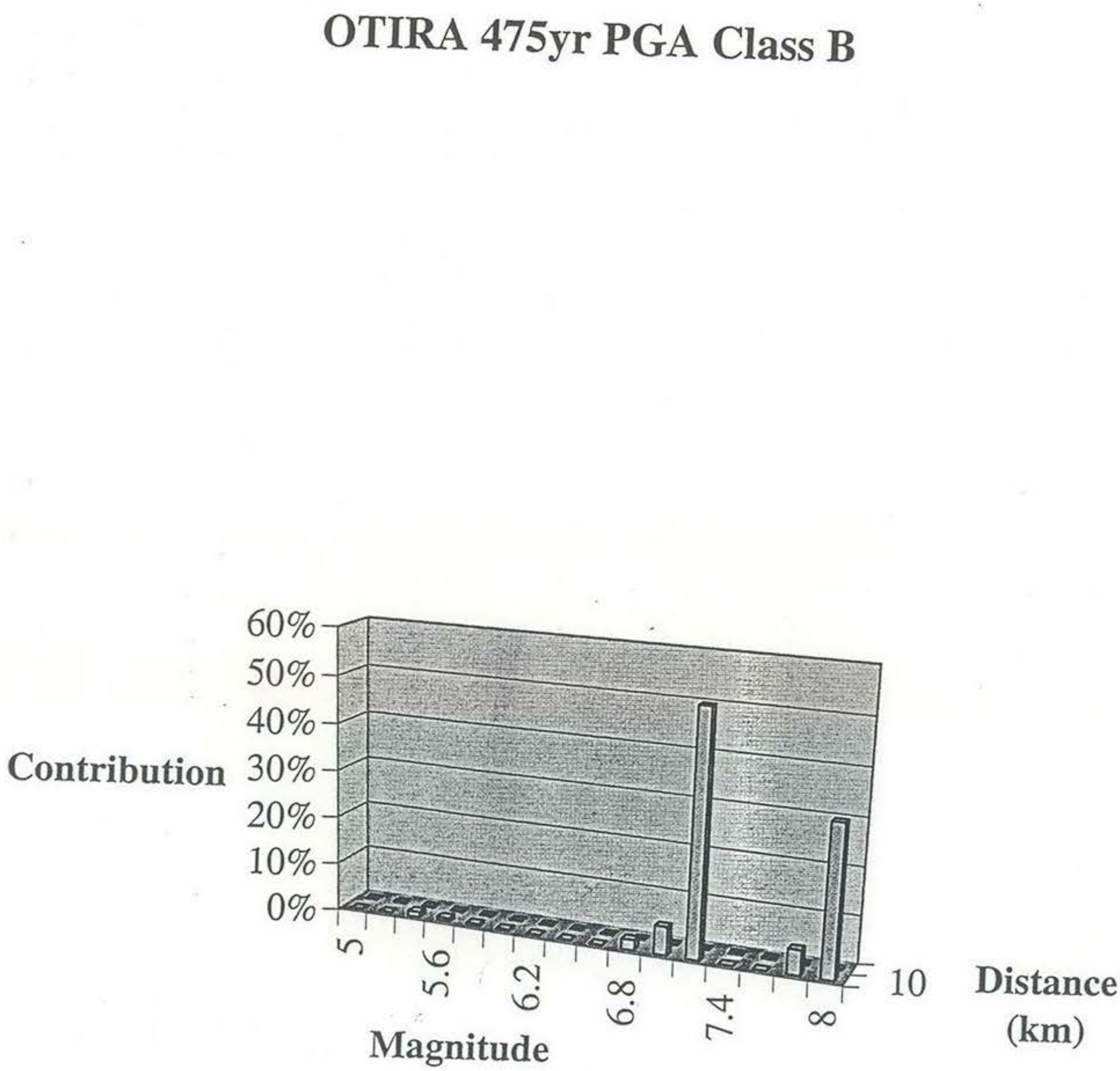

OTIRA 475yr PGA Class B
60%
50%
40%
Contribution
30%
20%
10%
0%
5
5.6
6.2
6.8
7.4
8
Magnitude
10
Distance
(km)

Figure 8r

OTIRA 1000yr PGA Class B

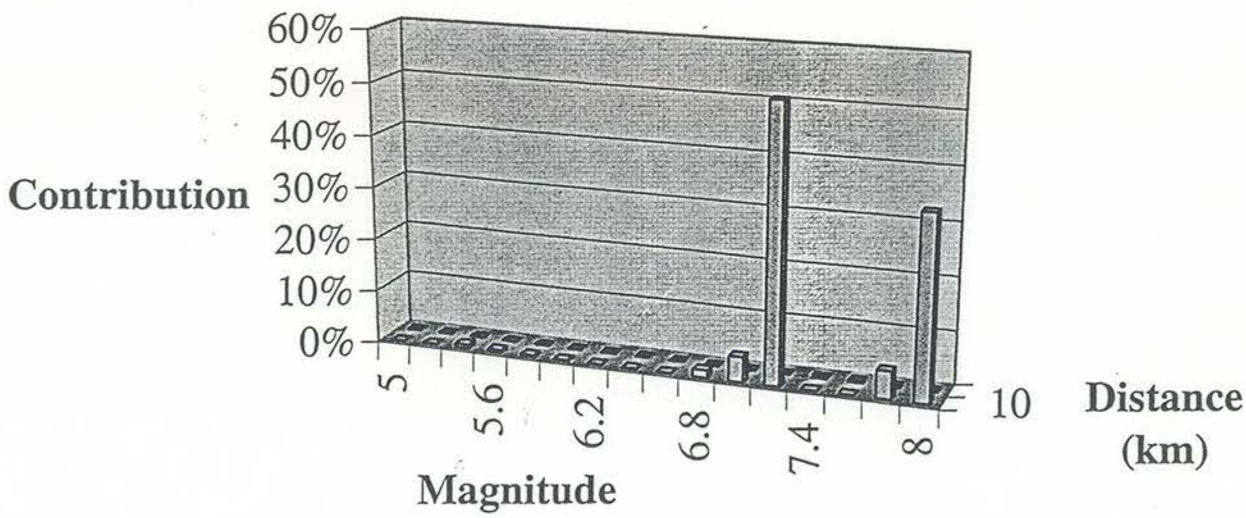

Figure 8s

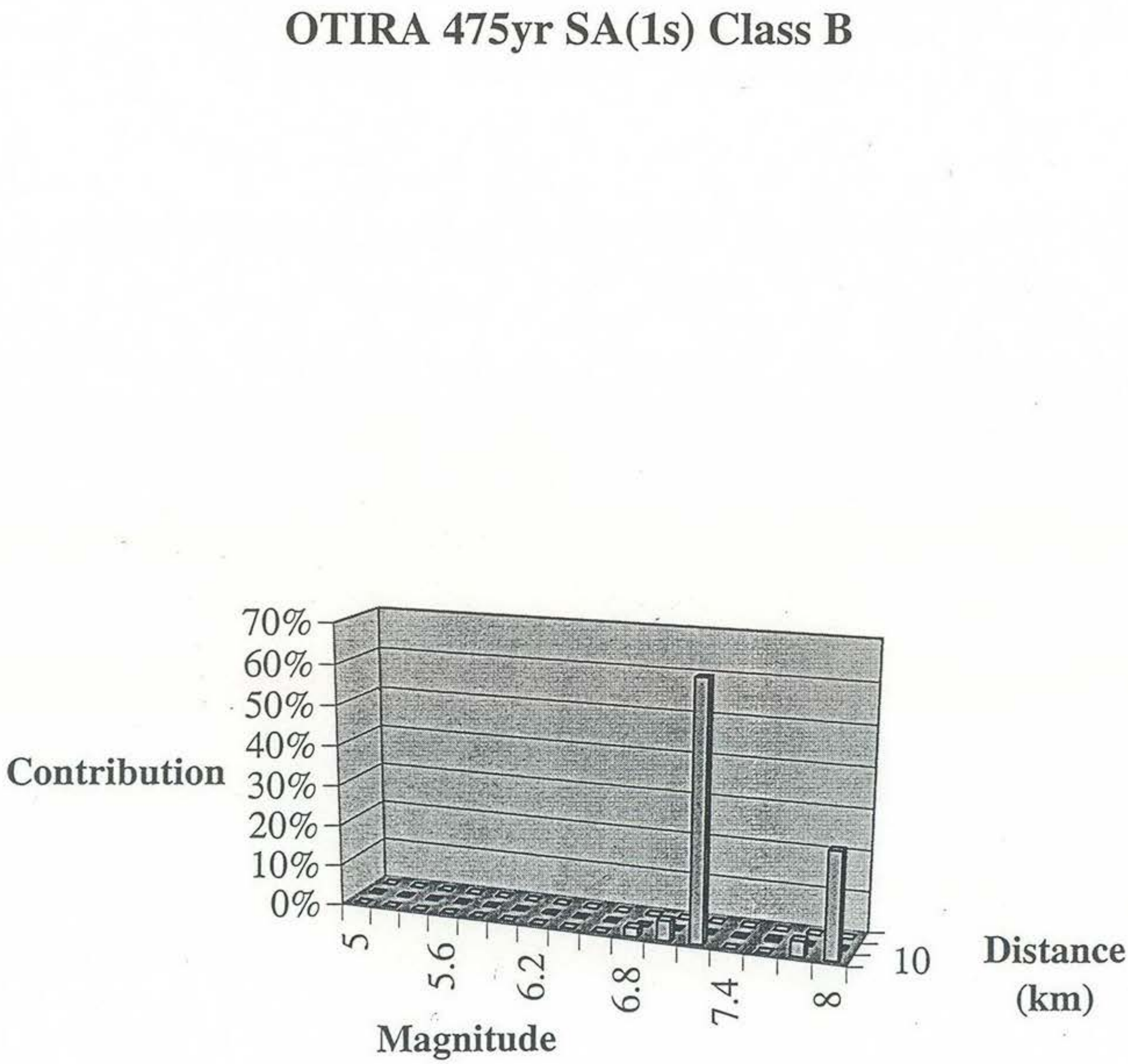
OTIRA 475yr SA(1s) Class B
70%
60%
50%
40%
30%
20%
10%
0%
Contribution
5
5.6
6.2
6.8
7.4
8
Magnitude
10
Distance
(km)

Figure 8t

OTIRA 1000yr SA(1s) Class B

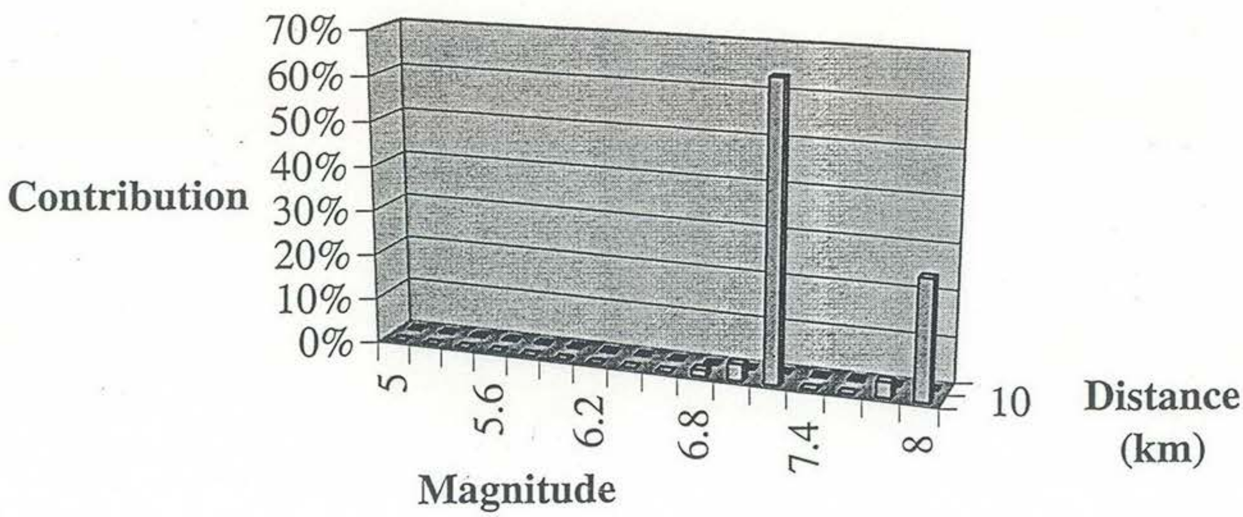

Figure 9a

AUCKLAND 475 yr Class B Comparison of models

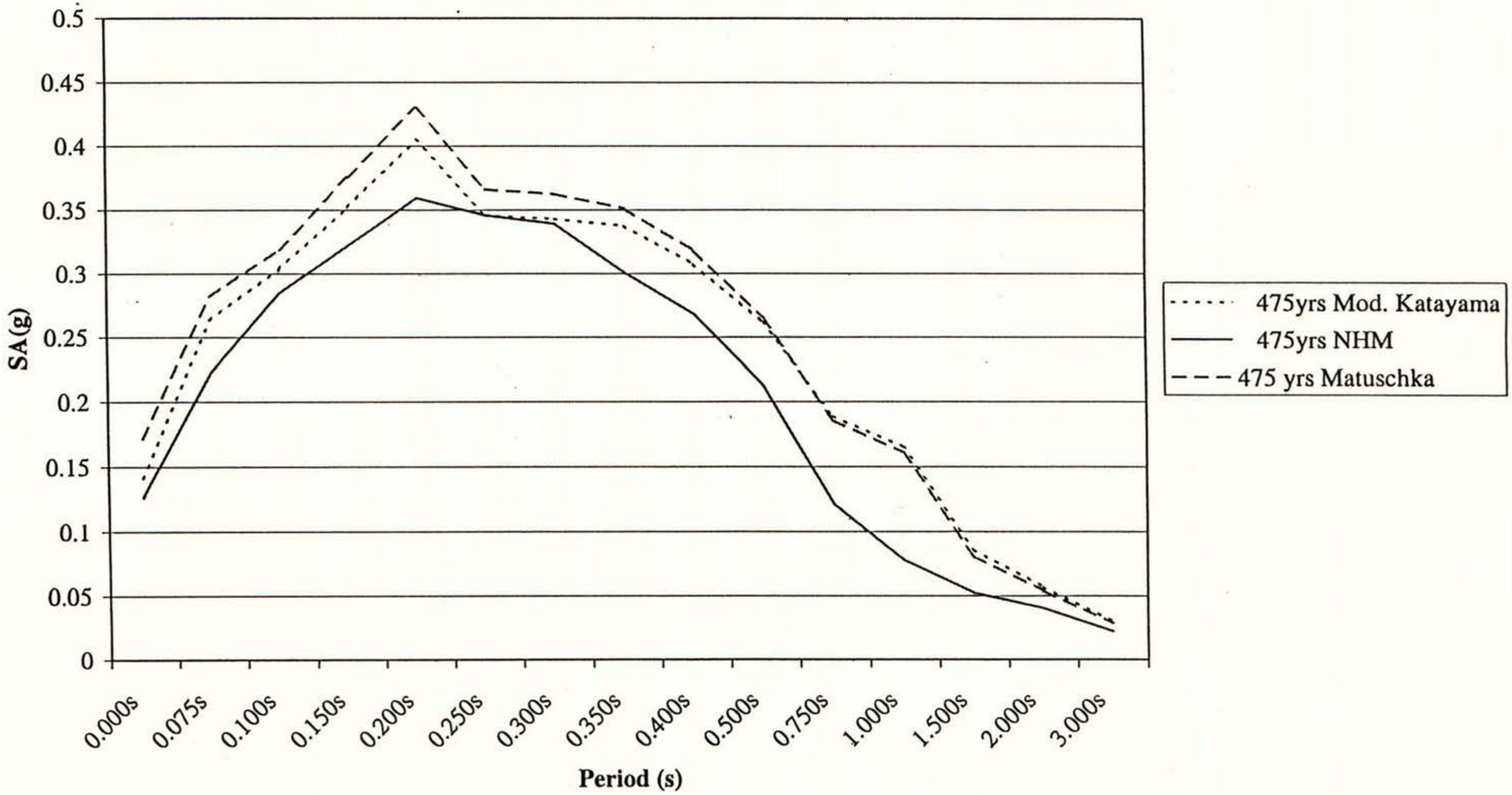

WELLINGTON 475 yr Class B Comparison of models

Figure 9b

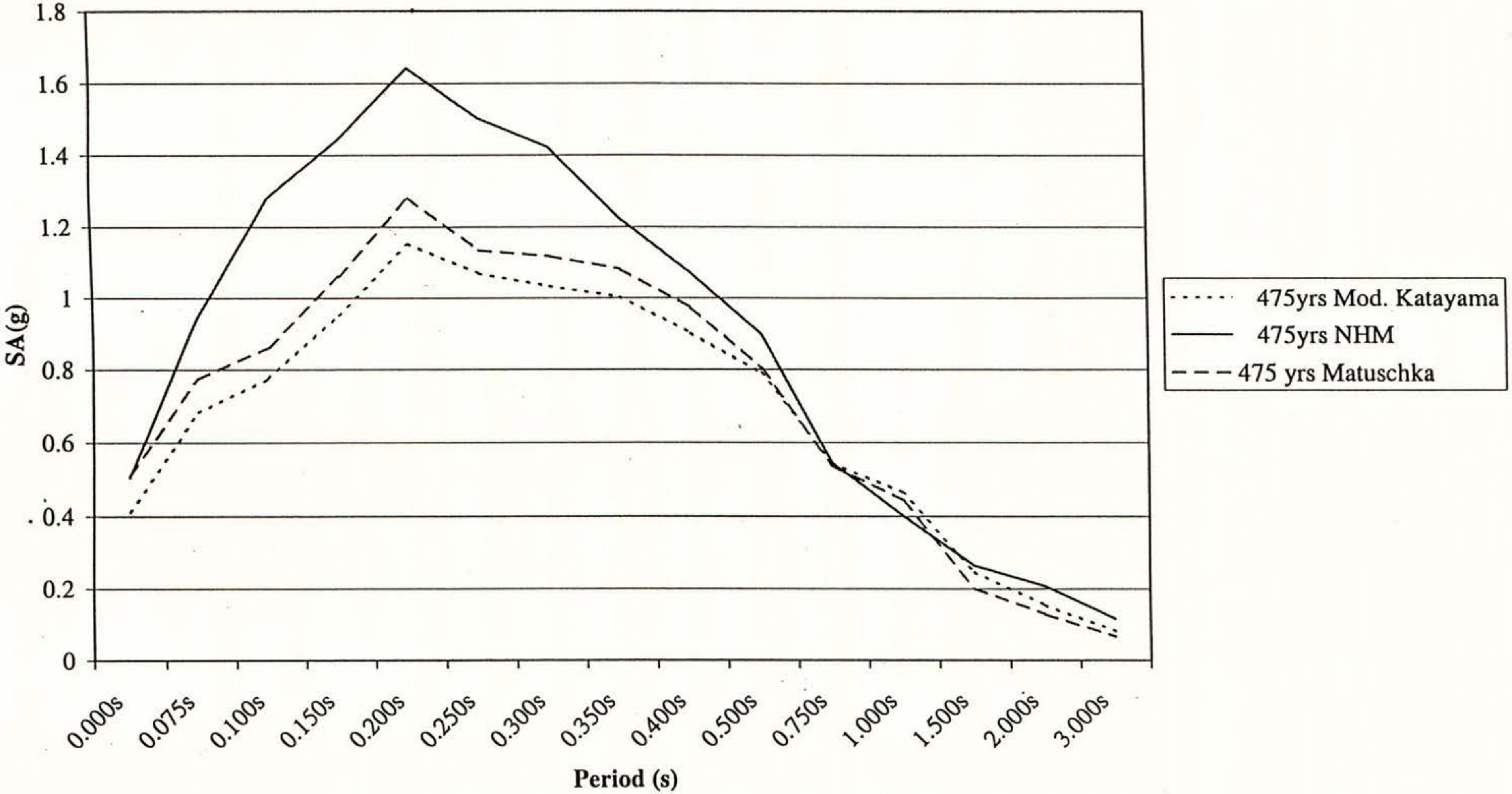

CHRISTCHURCH 475yr Class B Comparison of models

Figure 9c

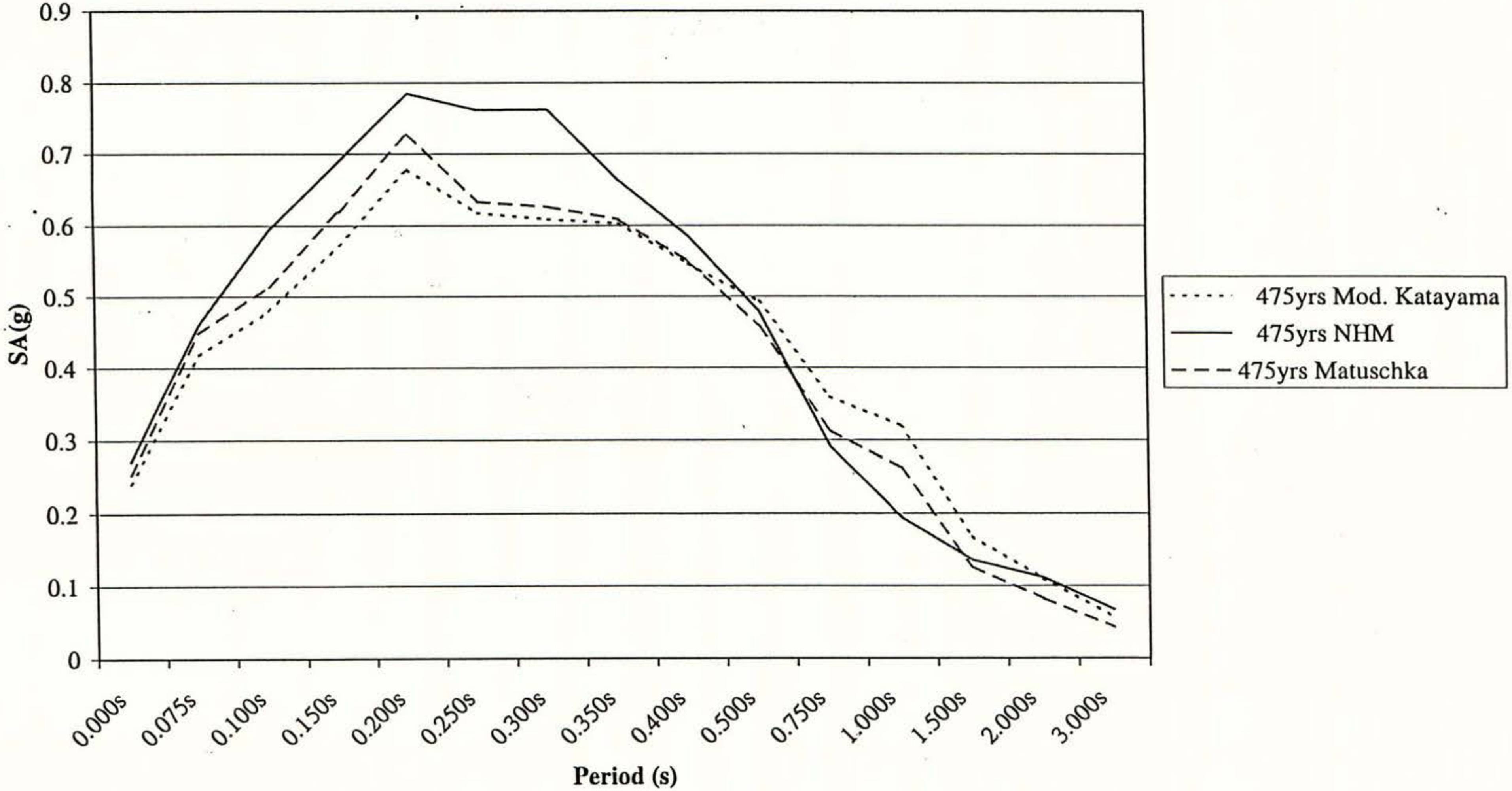

Figure 9d

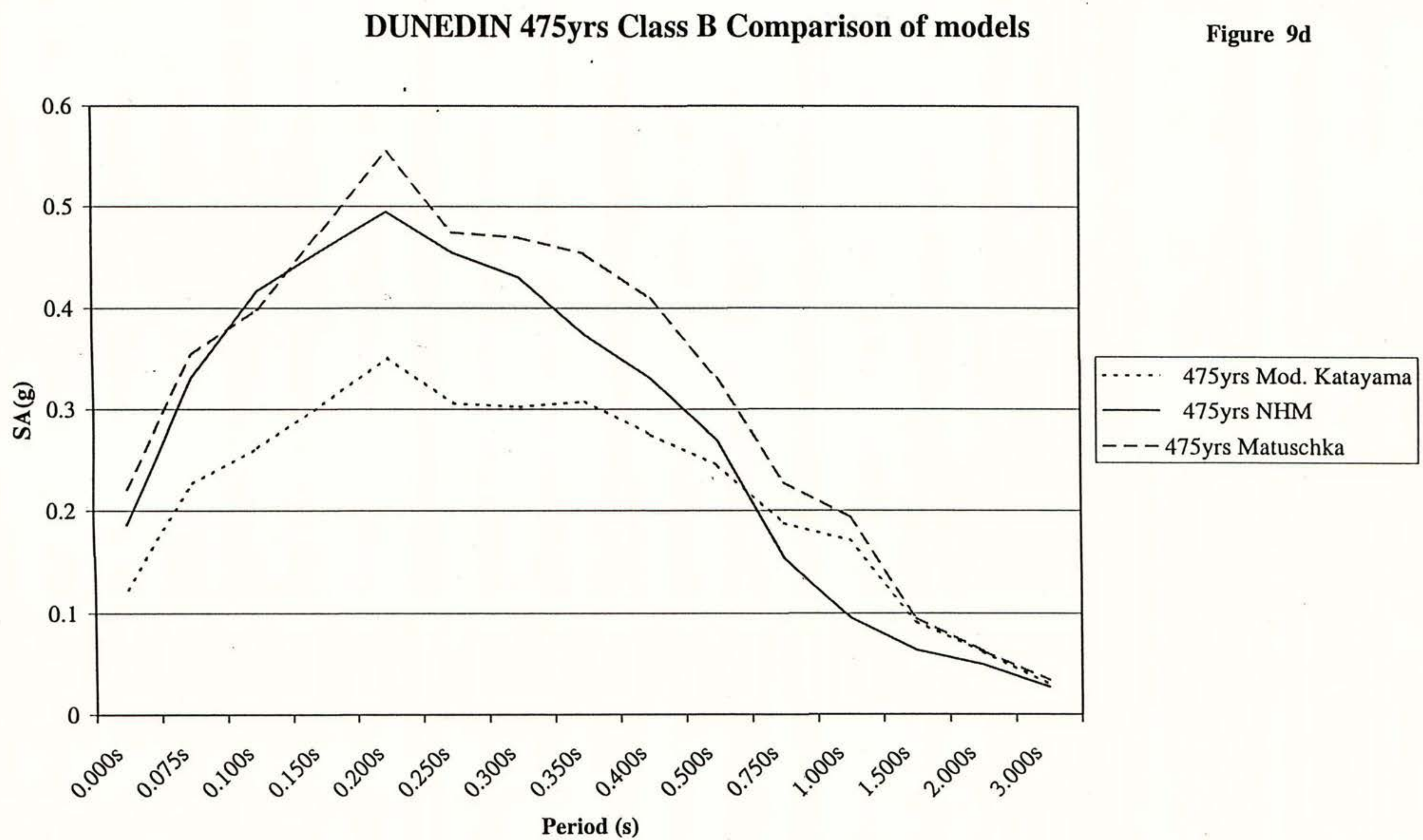

DUNEDIN 475yrs Class B Comparison of models
0.6
0.5
0.4
0.3
0.2
0.1
0
SA(g)
0.000s
0.075s
0.100s
0.150s
0.200s
0.250s
0.300s
0.350s
0.400s
0.500s
0.750s
1.000s
1.500s
2.000s
3.000s
Period (s)
475yrs Mod. Katayama
475yrs NHM
475yrs Matuschka

OTIRA 475yrs Class A Comparison of models

Figure 9e

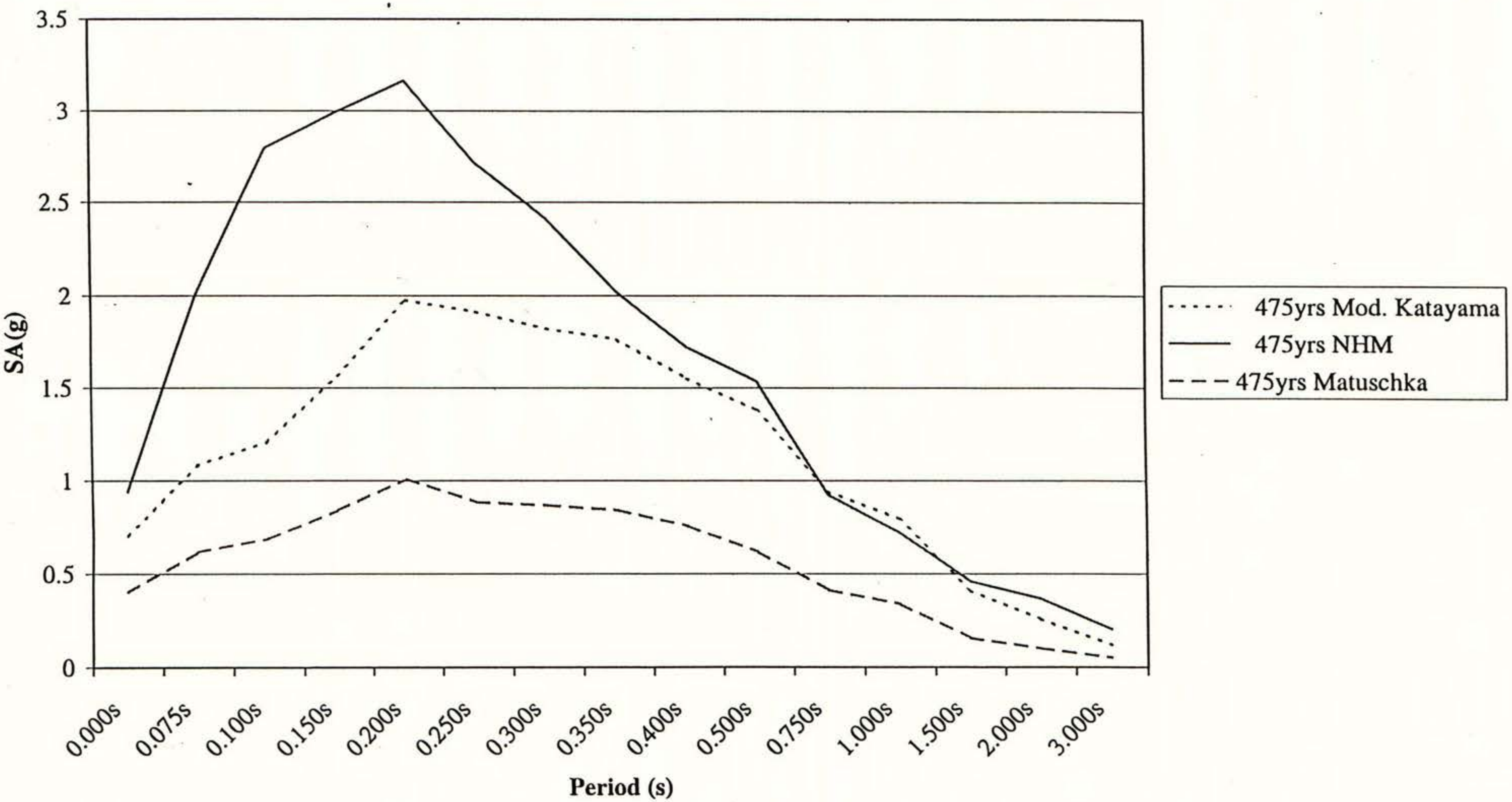

APPENDICES

Appendix 1: Fault Parameters

Index	Fault Name	Slip Type	Dip (°)	Dip Dir (°)	Depth Max (km)	Depth Min (km)	Slip Rate (mm/yr)	Displa-cement (m)	Mmax	Recurrence Interval (yrs)
1	Wairau (Onshore)	ss			15.0	0.0		6.0	(7.6)	1650
2	Wairau (Offshore)	ss			15.0	0.0			(7.3)	1650
3	Awatere SW	ss			15.0	0.0	8.00	6.0	(7.5)	2930
4	Awatere NE	ss			15.0	0.0	6.50	6.5	7.5	1000
5	Alpine (Milford-Haupiri)	sr	60.0	145.0	12.0	0.0	25.00	8.0	(8.1)	300
6	Alpine (Kaniere-Tophouse)	sr	60.0	145.0	12.0	0.0	10.00	6.0	(7.7)	1200
7	Alpine (Kaniere-Haupiri)	sr	60.0	145.0	12.0	0.0	10.00		(6.9)	1200
8	Alpine (Haupiri-Tophouse)	sr	60.0	145.0	12.0	0.0	10.00	6.0	(7.6)	1200
9	Clarence SW	ss			15.0	0.0	6.00		(7.5)	1080
10	Clarence NE	ss			15.0	0.0	4.70	7.0	(7.7)	1500
11	Hope (1888 rupture)	ss			15.0	0.0		2.0	7.2	120
12	Hope (Conway-Offshore)	sr	75.0	345.0	15.0	0.0	23.00	4.5	(7.5)	200
13	Jordan	rv	37.0	290.0	15.0	0.0		3.0	(7.1)	1200
14	Kekerengu	sr	75.0	330.0	15.0	0.0	7.50	5.5	(7.2)	730
15	Paparoa Range Front	rv			15.0	0.0			(7.1)	5000
16	Hundalee	rv	55.0	345.0	15.0	0.0	0.80	1.5	(7.0)	2000
17	Kaiwara	rv	55.0	150.0	15.0	0.0	0.50		(7.1)	3500
18	Omihi	rv	55.0	130.0	15.0	0.0	1.00		(6.7)	(474)
19	Lowry	rv	55.0	150.0	15.0	0.0		2.5	(7.3)	5000
20	Culverden	rv	50.0	290.0	15.0	0.0	1.50	2.0	(6.9)	7500
21	Esk	rs			15.0	0.0			(7.0)	7500

Index	Fault Name	Slip Type	Dip (°)	Dip Dir (°)	Depth Max (km)	Depth Min (km)	Slip Rate (mm/yr)	Displa-cement (m)	Mmax	Recurrence Interval (yrs)
22	MtGrey	rs	55.0	300.0	15.0	0.0	0.95	3.0	(6.9)	3300
23	MtThomas	rs	55.0	290.0	15.0	0.0			(6.5)	7000
24	LeesV	rs	55.0	330.0	15.0	0.0	3.75	2.0	(6.7)	7000
25	Torlesse	rv	65.0	330.0	15.0	0.0			(6.7)	3000
26	Cheesman	rv	45.0	280.0	15.0	0.0	0.50	3.0	(7.0)	3500
27	Harper	rv	35.0	150.0	15.0	0.0			(7.1)	10000
28	Porters Pass (Porters Pass)	sr		160.1	15.0	0.0	3.80	3.5	(7.2)	2900
29	Port2Grey (Porters to Grey)	sr		160.1	15.0	0.0		5.5	(7.5)	2764
30	Ashley	rv	35.0	340.0	15.0	0.0		1.4	(7.2)	2000
31	Springbank	rv	50.0	340.0	15.0	0.0			(7.1)	5000
32	Pegasus 1	rv	55.0	160.0	15.0	0.0		3.0	(7.2)	10000
33	Pegasus 2	rv	55.0	160.0	15.0	0.0		3.0	(6.9)	10000
34	Pegasus 3	rv	55.0	160.0	15.0	0.0		3.0	(7.1)	10000
35	North Mernoo Banks Sth	nn		190.0	15.0	0.0		3.0	(7.4)	1000
36	North Mernoo Banks Nth	nn		190.0	15.0	0.0		3.0	(7.4)	1000
37	Lake Heron	rv	43.0	300.0	15.0	0.0	1.50	4.0	(7.2)	5000
38	Quartz Creek	rs	75.0	240.0	15.0	0.0		2.5	(6.7)	5000
39	Mt Hutt- Mt Peel	rv	55.0	300.0	15.0	0.0	1.00	3.0	(7.3)	7500
40	Fox Peak	rv	55.0	290.0	15.0	0.0	1.00	4.0	(7.2)	7000
41	Hunter Hills Nth	rv	55.0	260.0	15.0	0.0		4.5	(7.1)	(15000)
42	Hunter Hills Sth	rv	55.0	260.0	15.0	0.0		4.5	(7.2)	(15000)
43	Dryburgh SE	rv	60.0	040.0	15.0	0.0	0.05	2.5	(6.9)	22000
44	Dryburgh NW	rv	60.0	040.0	15.0	0.0	0.05	2.5	(6.9)	22000
45	Otamatapaio	rs	89.0	260.0	15.0	0.0	0.01	0.8	(6.4)	(80000)
46	Wharakuri	sr	60.0	230.0	15.0	0.0	0.50	4.0	(7.2)	10000

Index	Fault Name	Slip Type	Dip (°)	Dip Dir (°)	Depth Max (km)	Depth Min (km)	Slip Rate (mm/yr)	Displa-cement (m)	Mmax	Recurrence Interval (yrs)
47	Rostrievor-Big Gully	rv	89.0	260.0	15.0	0.0	0.05	2.5	(6.7)	(50000)
48	Waitangi	nn	89.0	260.0	15.0	0.0	0.02	1.0	(6.5)	(50000)
49	Dalgety	rv	60.0	330.0	15.0	0.0	0.05	3.0	(7.0)	(60000)
50	Kirkliston	rv	60.0	290.0	15.0	0.0	0.05	3.0	(7.1)	(60000)
51	Waimea	rs		135.0	15.0	0.0			(7.0)	(1117)
52	WhiteCk	rv	70.0	100.0	15.0	0.0	0.20	6.0	7.6	34000
53	Lyell	rs		100.0	15.0	0.0	0.20		(6.7)	(14661)
54	BrunAnt	rv			15.0	1.0			(6.9)	15000
55	Inangahua	rv	45.0	100.0	15.0	0.0	0.10	0.4	7.4	4400
56	Pisa	rv	55.0	300.0	15.0	0.0	0.4	3.0	(7.1)	30000
57	Nevis	rv	55.0	300.0	15.0	0.0	0.30		(6.8)	(3677)
58	Wairarapa (1855 rupture)	sr	80.0	315.0	15.0	0.0		11.5	8.1	1500
59	Hikurangi (Nth Rauk-RM)	if	12.0	310.0	22.0	15.0	0.01		7.5	650
60	Hikurangi (Sth Rauk-RM)	if	12.0	310.0	22.0	15.0	0.01		7.5	681
61	Hikurangi (Haw-kes Bay-RM)	if	9.0	310.0	22.0	15.0	0.01		7.8	1053
62	Hikurangi (Sth Hawkes Bay-RM)	if	9.0	310.0	22.0	15.0	0.01		7.4	798
63	Hikurangi (Wellington-RM)	if	9.0	315.0	22.0	15.0	0.01		7.8	1800
64	Hikurangi (Nth Rauk-WM)	if	12.0	310.0	25.0	10.0	0.01		7.7	604
65	Hikurangi (Sth Rauk-WM)	if	12.0	310.0	25.0	10.0	0.01		7.7	633
66	Hikurangi (Haw-kes Bay-WM)	if	9.0	310.0	25.0	10.0	0.01		8.0	979
67	Hikurangi (Sth Hawkes Bay-WM)	if	9.0	310.0	25.0	10.0	0.01		7.7	742

Index	Fault Name	Slip Type	Dip (°)	Dip Dir (°)	Depth Max (km)	Depth Min (km)	Slip Rate (mm/yr)	Displa-cement (m)	Mmax	Recurrence Interval (yrs)
68	Hikurangi (Wellington-WM)	if	9.0	315.0	25.0	10.0	0.01		8.1	1674
69	Hikurangi (Nth Rauk-BM)	if	12.0	310.0	25.0	10.0	0.01		8.1	1236
70	Hikurangi (Sth Rauk-BM)	if	12.0	310.0	25.0	10.0	0.01		8.1	1295
71	Hikurangi (Haw-kes Bay-BM)	if	9.0	310.0	25.0	10.0	0.01		8.3	1490
72	Hikurangi (Sth Hawkes Bay-BM)	if	9.0	310.0	25.0	10.0	0.01		8.1	1629
73	Hikurangi (Wellington-BM)	if	9.0	315.0	25.0	10.0	0.01		8.4	2347
74	Ostler Nth	rv	60.0	280.1	15.0	0.0	1.00	3.0	(7.0)	3000
75	Ostler Central	rv	60.0	280.1	15.0	0.0	1.00	3.0	(7.0)	3000
76	Ostler South	rv	60.0	300.1	15.0	0.0	1.00	3.0	(6.9)	3000
77	Ahuriri River	rv			15.0	0.0		2.5	(6.8)	10000
78	Irishman Creek	rv			15.0	0.0		4.0	(7.0)	15000
79	Lindis Pass	rs			15.0	0.0		3.0	(7.0)	3000
80	Grandview	rv			15.0	0.0		3.0	(7.0)	30000
81	Cardrona South	rv	30.0	300.0	15.0	0.0	0.25	2.0	(7.1)	7500
82	Cardrona North	rs	30.0	300.0	15.0	0.0	0.25	2.0	(7.0)	7500
83	Blue Lake	rv	60.0	060.0	15.0	0.0		3.0	(7.0)	5000
84	Dunstan North	rv	60.0	320.0	15.0	0.0	1.00	4.0	(7.2)	8000
85	Dunstan South	rv	60.0	320.0	15.0	0.0	1.00	4.0	(6.9)	8000
86	Raggedy	rv	60.0	320.0	15.0	0.0		3.0	(7.0)	8000
87	Nth Rough Ridge	rv	60.0	320.0	15.0	0.0		3.0	(7.0)	8000
88	Rough Ridge	rv	60.0	320.0	15.0	0.0		3.0	(7.0)	8000
89	Ranfurly Sth	rv	60.0	320.0	15.0	0.0		3.0	(7.0)	8000
90	Ranfurly Nth	rv	60.0	320.0	15.0	0.0		3.0	(7.0)	8000

Index	Fault Name	Slip Type	Dip (°)	Dip Dir (°)	Depth Max (km)	Depth Min (km)	Slip Rate (mm/yr)	Displa-cement (m)	Mmax	Recurrence Interval (yrs)
91	Hyde	rv	60.0	320.0	15.0	0.0		3.0	(7.0)	15000
92	Hanmer	nn	60.0	170.0	15.0	0.0		2.0	(6.9)	1000
93	Wairoa Nth	nn			15.0	0.0	0.04		(6.6)	(22152)
94	Kerepehi Nth	nn			12.0	0.0	0.40	1.0	(6.7)	(2500)
95	KerepehiNth-Central	nn			12.0	0.0	0.40	1.0	(6.6)	(2500)
96	Kerepehi Central	nn			12.0	0.0	0.40	2.0	(6.7)	(5000)
97	Kerepehi Sth	nn			12.0	0.0	0.40	2.0	(6.7)	(5000)
98	Mayor Island 1	nn	60.0	260.0	12.0	0.0	0.50	2.0	(7.0)	(4000)
99	Mayor Island 2	nn	60.0	080.0	12.0	0.0	0.50	2.0	(7.4)	(4000)
100	Mayor Island 3	nn	60.0	260.0	12.0	0.0	0.50	2.0	(7.1)	(4000)
101	Mayor Island 4	nn	60.0	080.0	12.0	0.0	0.50	2.0	(7.0)	(4000)
102	Tauranga	nn	60.0	140.0	12.0	0.0	1.00	2.0	(7.0)	(2000)
103	Aldeman		nn		12.0	0.0	2.00	2.0	(6.9)	(1000)
104	Matata	nv	60.0	130.0	8.0	0.0	2.00		(6.5)	(374)
105	Braemar	nv	60.0	130.0	8.0	0.0	1.00		(6.5)	(797)
106	Rotoiti	nv	60.0	130.0	8.0	0.0	0.60		(5.7)	(521)
107	Te Teko	nv	60.0	130.0	8.0	0.0	1.00		(5.7)	(339)
108	Onepu	nv	60.0	130.0	8.0	0.0	1.50		(5.8)	(249)
109	Awakere		nv	60.0	300.0	8.0	0.0	1.00	(6.1)	(511)
110	Edgecumbe (1987 rupture)	nv	60.0	300.0	8.0	0.0	2.50		6.5	(1362)
111	Edgecumbe (Coastal)	nv	60.0	300.0	8.0	0.0	2.50		(6.0)	(176)
112	White Island 1	nv	60.0	300.0	8.0	0.0	1.00		(6.0)	(453)
113	White Island 2	nv	60.0	300.0	8.0	0.0	1.00		(6.3)	(627)
114	White Island 3	nv	60.0	300.0	8.0	0.0	1.00		(6.3)	(597)
115	Nukuhou	nv	60.0	300.0	8.0	0.0	2.40		(5.9)	(172)

Index	Fault Name	Slip Type	Dip (°)	Dip Dir (°)	Depth Max (km)	Depth Min (km)	Slip Rate (mm/yr)	Displa- cement (m)	Mmax	Recurrence Interval (yrs)
116	Ohiwa	nv	60.0	300.0	8.0	0.0	0.70		(6.2)	(785)
117	Rangitaiki	nv	60.0	300.0	8.0	0.0	2.30		(6.3)	(261)
118	Rurima A	nv	60.0	120.0	8.0	0.0	0.60		(6.3)	(1076)
119	Rurima B	nv	60.0	120.0	8.0	0.0	0.60		(6.3)	(1079)
120	Ngakuru NE	nv	50.0	120.0	8.0	0.0	0.45		(6.1)	(1100)
121	Ngakuru SW	nv	50.0	120.0	8.0	0.0	0.45		(6.0)	(983)
122	Ohakuri NW	nv	50.0	120.0	8.0	0.0	0.20		(6.0)	(2037)
123	Ohakuri SE	nv	50.0	120.0	8.0	0.0	0.20		(6.1)	(2562)
124	Thorpe SE	nv	50.0	120.0	8.0	0.0	0.10		(6.0)	(4550)
125	Thorpe NW	nv	50.0	120.0	8.0	0.0	0.10		(5.9)	(4031)
126	Puketar NE	nv	50.0	300.0	8.0	0.0	0.80		(6.0)	(553)
127	Puketar SW	nv	50.0	300.0	8.0	0.0	0.80		(6.0)	(535)
128	Orakeik NE	nv	50.0	300.0	8.0	0.0	1.20		(6.0)	(357)
129	Orakeik SW	nv	50.0	300.0	8.0	0.0	1.20		(6.0)	(357)
130	Orakonui NE	nv	50.0	300.0	8.0	0.0	1.20		(6.0)	(384)
131	Orakonui SW	nv	50.0	300.0	8.0	0.0	1.20		(6.0)	(379)
132	Whirinaki Nth	nv	50.0	300.0	8.0	0.0	0.70		(6.0)	(612)
133	Whirinaki Sth	nv	50.0	300.0	8.0	0.0	0.70		(6.1)	(732)
134	Paeroa Nth	nv	50.0	300.0	8.0	0.0	1.50		(6.0)	(303)
135	Paeroa Central	nv	50.0	300.0	8.0	0.0	1.50		(5.9)	(269)
136	Paeroa Sth	nv	50.0	300.0	8.0	0.0	1.50		(6.1)	(322)
137	Whangamoa	nv	50.0	120.0	8.0	0.0	1.30		(5.8)	(293)
138	Ngangiho	nv	50.0	120.0	8.0	0.0	0.80		(6.2)	(698)
139	Whakaipo	nv	50.0	300.0	8.0	0.0	0.60		(6.1)	(860)
140	Kaiapo	nv	50.0	300.0	8.0	0.0	0.80		(6.2)	(731)
141	Aratiatia	nv	50.0	300.0	8.0	0.0	0.80		(6.2)	(678)

Index	Fault Name	Slip Type	Dip (°)	Dip Dir (°)	Depth Max (km)	Depth Min (km)	Slip Rate (mm/yr)	Displa-cement (m)	Mmax	Recurrence Interval (yrs)
142	Waiohau Nth	ns	80.0	270.0	12.0	0.0	1.40		(6.5)	(533)
143	Waiohau Sth	ns	80.0	270.0	12.0	0.0	1.40		(6.9)	(843)
144	Graben Sth	nv			8.0	0.0	3.50		(6.0)	(125)
145	Graben Nth	nv			8.0	0.0	3.50		(5.8)	(100)
146	Kelly	ss			15.0	0.0	20.00	3.0	(7.2)	(150)
147	Hope (Taramakau)	ss			15.0	0.0	5.00	3.0	(7.2)	(600)
148	Hope (Central -west)	ss			15.0	0.0	25.00	3.0	(7.1)	(120)
149	Kakapo	ss			15.0	0.0	6.40	3.0	(7.1)	500
150	Hope (Kokatahi)	ss			15.0	0.0	10.00	3.0	(6.9)	(300)
151	Arthurs Pass (1929 rupture)	ss			15.0	0.0		3.0	7.0	3500
152	Styx	ss			15.0	0.0	10.00	3.0	(6.9)	(300)
153	Ohariu	ss			15.0	0.0		4.0	(7.4)	3250
154	Pohangina Anticline	rv			15.0	1.0	0.30	2.5	(6.9)	8000
155	Levin Anticline	rv			15.0	1.0	0.30	2.5	(6.6)	6500
156	Marton Anticline	rv			15.0	1.0	0.30	2.5	(6.7)	8000
157	Wellington SW	ss			15.0	0.0	7.10	4.2	(7.3)	600
158	Wellington NE	ss			15.0	0.0	7.10	4.2	(7.5)	(592)
159	Wellington Central	ss			15.0	0.0	3.55	4.2	(7.2)	(1183)
160	Wellington W	ss			15.0	0.0	3.55	4.2	(7.2)	(1183)
161	Feilding Anticline	rv			15.0	1.0	0.30	2.5	(6.9)	8000
162	Spylaw	rv	55.0	150.0	15.0	0.0	0.50		(6.3)	(1300)
163	BlueMtn	rv	55.0	125.0	15.0	0.0			(6.4)	800
164	Alfredton	ss			15.0	0.0	3.00	6.0	(7.2)	4500

Index	Fault Name	Slip Type	Dip (°)	Dip Dir (°)	Depth Max (km)	Depth Min (km)	Slip Rate (mm/yr)	Displa-cement (m)	Mmax	Recurrence Interval (yrs)
165	Mohaka Sth	ss			15.0	0.0		2.0	(7.1)	1000
166	Mohaka Nth	ss			15.0	0.0		2.0	(7.1)	1000
167	Ruahine Nth	sr	80.0	315.0	15.0	0.0		3.5	(6.9)	(2800)
168	Ruahine Central	sr	80.0	315.0	15.0	0.0		3.5	(7.4)	(2800)
169	Ruahine Sth	sr	80.0	315.0	15.0	0.0		3.5	(7.2)	(2800)
170	Napier (1931 rupture)	rs	80.0	315.0	30.0	0.0		2.5	7.8	2500
171	Waimana	ss			15.0	0.0		3.5	(7.4)	3500
172	Whakatane	sn			15.0	0.0		3.5	(7.4)	3500
173	Waikaremoana	ss			15.0	0.0		3.5	(7.0)	3500
174	Inglewood	ns		150.0	15.0	0.0	0.20	2.1	(6.8)	4300
175	Ararata	nn	70.0	140.0	5.0	0.0	0.02		(5.7)	(16832)
176	Waverley	nn	70.0	120.0	5.0	0.0	0.03		(6.0)	(14348)
177	Nukumaru	nn	70.0	120.0	15.0	0.0	0.07		(6.2)	12500
178	Mt Stewart Anticline	rv	60.0	270.0	15.0	1.0	0.30	2.5	(6.8)	8000
179	Pukerua-Shephards	ss			15.0	0.0		3.8	3750	
180	Galpin	nn	70.0	100.0	15.0	0.0	0.04		(6.1)	(12983)
181	Leedstown	nn	70.0	120.0	15.0	0.0	0.07		(6.3)	(9164)
182	Upokongaro	nn			15.0	0.0	0.01		(6.6)	(82793)
183	Moumahaki	nn	70.0	120.0	5.0	0.0	0.19		(5.7)	(1730)
184	RidgeR	nn	70.0	300.0	5.0	0.0			(5.5)	(1759)
185	Waitotara	nn	70.0	300.0	5.0	0.0	0.07		(5.6)	(4198)
186	Himatangi Anticline	rv			15.0	1.0	0.30	2.5	(6.7)	8000
187	Aorangi Anticline	rv			15.0	1.0	2.50		(7.0)	(536)
188	PaVally-Makuri	ss			15.0	0.0		6.0	(7.4)	2500
189	EHBSSN-Weber	ss			15.0	0.0		3.0	(6.8)	2000

Index	Fault Name	Slip Type	Dip (°)	Dip Dir (°)	Depth Max (km)	Depth Min (km)	Slip Rate (mm/yr)	Displa-cement (m)	Mmax	Recurrence Interval (yrs)
190	Saunders-Weber	ss			15.0	0.0		3.0	(7.1)	2000
191	Ruataniwha	rs			15.0	0.0		3.0	(6.8)	4000
192	Oruawharo	sr			15.0	0.0		3.0	(6.9)	4000
193	Poukawa Nth	ss			15.0	0.0			(6.4)	9500
194	Waipukurau-Poukawa	rs			15.0	0.0		3.0	(7.1)	5300
195	Kaweka	ss			15.0	0.0		3.5	(7.1)	3500
196	Patoka	ss			15.0	0.0		4.0	(7.0)	2000
197	Rangiora	ss			15.0	0.0		5.0	(7.0)	(962)
198	Kidnappers W	nn			15.0	0.0		2.8	(6.8)	4000
199	Kidnappers E	nn			15.0	0.0		2.8	(6.9)	4000
200	HBNFW-Silver	nn			15.0	0.0		2.8	(6.9)	3500
201	HBNFC-Silver	nn			15.0	0.0		2.8	(6.8)	3500
202	HBNFE-Silver	nn			15.0	0.0		2.8	(6.9)	3500
203	Mangaoranga	sn			15.0	0.0			(6.1)	5000
204	Waitawhiti	sn			15.0	0.0			(6.4)	4000
205	Maunga	sn			15.0	0.0			(6.8)	5000
206	Poroutawhao	rv			15.0	1.0		2.5	(6.8)	20000
207	Ruahine Reverse	rv			15.0	0.0			(6.5)	20000
208	Hihitahi	nn			15.0	0.0			(6.3)	1250
209	Kariori	nv			15.0	0.0			(6.5)	1500
210	Ohakune	nv			15.0	0.0	3.00		(6.5)	(272)
211	Raurimu	nv			15.0	0.0	2.00	1.0	(6.6)	(500)
212	Wanganui Offshore	nn			15.0	0.0			(6.8)	5000
213	CoastalZone	rr			15.0	0.0			(7.0)	2000
214	Hawkes Bay Offshore Reverse 1	rr			15.0	0.0		5.0	(7.3)	1250

Index Fault Name Slip Type Dip (°) Dip Dir (°) Depth Max (km) Depth Min (km) Slip Rate (mm/yr) Displa-cement (m) Mmax Recurrence Interval (yrs)

Index	Fault Name	Slip Type	Dip (°)	Dip Dir (°)	Depth Max (km)	Depth Min (km)	Slip Rate (mm/yr)	Displa-cement (m)	Mmax	Recurrence Interval (yrs)
215	Hawkes Bay Offshore Reverse 2	rr			15.0	0.0		5.0	(7.2)	1250
216	Hawkes Bay Offshore Reverse 3	rr			15.0	0.0		5.0	(7.4)	1250
217	Hawkes Bay Offshore Reverse 4	rr			15.0	0.0		5.0	(7.5)	1250
218	Masterton	sn			15.0	0.0			(6.3)	(1189)
219	Tukituki	rv			15.0	0.0		5.0	(6.8)	5000
221	Raetihi	nv			15.0	0.0			(6.3)	1500
222	ShannonA	rv			15.0	1.0		2.5	(6.6)	20000
223	Avoca	ss			15.0	0.0			6.7	3500
224	Cape Egmont	nn	45.0	120.0	15.0	0.0	0.50		(7.1)	(2915)
225	Mokonui	sr			15.0	0.0	0.20		(6.4)	10000
226	Carterton	sr			15.0	0.0	1.00		(6.9)	(1264)
227	Rangitikei	nv			15.0	0.0			(5.8)	10000
228	Taihape	nv			15.0	0.0			(5.8)	10000
229	Mataroa	nv			15.0	0.0			(5.9)	10000
230	Snowgrass	nv			15.0	0.0	1.00	1.5	(6.7)	1500
231	Rangipo	nv			15.0	0.0	3.00	3.0	(6.4)	1000
232	Shawcroft Rd	nv			15.0	0.0		1.5	(5.4)	1500
233	Raukumara F1	nn			5.0	0.0			(5.4)	10000
234	Raukumara F2	nn			5.0	0.0			(5.9)	10000
235	Raukumara F3	nn			5.0	0.0	0.60		(5.5)	(445)
236	Repongaere F4	nn			5.0	0.0			(5.6)	(1014)
237	Tangihanga F5	nn			5.0	0.0	0.40		(5.7)	(811)
238	Raukumara F6	nn			5.0	0.0	0.50		(5.4)	125000
239	OtokoToto F7	nn			5.0	0.0	0.50		(5.7)	999999
240	Raukumara F8	nn			15.0	0.0	0.50		(6.1)	125000
241	Raukumara F9	nn			15.0	0.0	0.50		(5.9)	125000

242	Raukumara F10	nn	15.0	0.0	0.50		(6.3)	125000
243	Raukumara F11	nn	15.0	0.0	0.50		(6.5)	10000
244	Raukumara F12	nn	15.0	0.0	0.50		(6.5)	10000
245	Raukumara F13	nn	15.0	0.0	0.50		(6.1)	10000
246	Raukumara F15	nn	15.0	0.0	0.50		(6.1)	10000
247	Raukumara F16	nn	15.0	0.0	0.50		(6.1)	10000
248	Raukumara F17	nn	15.0	0.0	0.50		(6.3)	67500
249	Raukumara F18	nn	15.0	0.0	0.50		(6.5)	67500
250	Raukumara F19	nn	15.0	0.0			(6.5)	(22523)
251	Raukumara F20	nn	15.0	0.0			(5.4)	10000
252	Raukumara F21	nn	15.0	0.0			(6.5)	(21445)
253	Raukumara F22	nn	15.0	0.0	0.05		(6.1)	(10170)
254	Raukumara F23	nn	15.0	0.0			(6.4)	125000
255	Raukumara F24	nn	15.0	0.0			(5.8)	125000
256	Raukumara F25	nn	15.0	0.0			(5.5)	(7253)
257	Raukumara F26	nn	15.0	0.0			(5.8)	125000
258	Raukumara F27	nn	5.0	0.0			(5.4)	125000
259	Pangopango F29	nn	5.0	0.0			(5.6)	60000
260	Fernside F28	nn	5.0	0.0			(5.9)	10000
261	Raukumara F30	nn	5.0	0.0			(5.2)	125000
262	Raukumara F31	nn	5.0	0.0			(5.2)	1800
263	Raukumara F32	nn	5.0	0.0			(5.2)	60000
264	Marau F33	rv	5.0	0.0			(5.3)	10000
265	East Cape	nn	5.0	0.0	1.90		(5.6)	(153)
266	Pakarai	nn	5.0	0.0		5.0	(6.3)	2300
267	Dry River-Huangarua	rv	15.0	0.0		2.5	(7.0)	(4545)

Index	Fault Name	Slip Type	Dip (°)	Dip Dir (°)	Depth Max (km)	Depth Min (km)	Slip Rate (mm/yr)	Displa-cement (m)	Mmax	Recurrence Interval (yrs)
268	Otaraia	rv			15.0	0.0			(6.8)	(2068)
269	Bidwill	rv			15.0	0.0			(6.2)	(1032)
270	Moores	rv			15.0	0.0	0.10	2.0	(6.7)	20000
271	Whitemans	rv			15.0	0.0	0.10	2.0	(6.4)	20000
272	Moonhine-Otaki	rv			15.0	0.0			(7.2)	125000
273	Nth Ohariu	ss			15.0	0.0		3.5	(7.2)	2500
274	Waipukaka	ss			15.0	0.0			7.6	1900
275	Oaonui	nn			15.0	0.0	0.50	1.8	(6.5)	2200
276	Norfolk	nn			15.0	0.0		1.6	(6.3)	4500
277	Turi	nn			15.0	0.0			(7.2)	(1612)
278	Fault 6	rs	45.0	55.0	20.0	0.0	0.50		(7.1)	(3176)
279	Fault 7	rs	45.0	67.0	20.0	0.0	0.50		(7.1)	(3089)
280	Akatore	rs	45.0	312.6	20.0	0.0	0.50		(7.1)	(2987)
281	Fault 13	rs	45.0	293.8	20.0	0.0	0.50		(7.3)	(3597)
282	Fault 15	rs	45.0	288.3	20.0	0.0	3.00		(7.4)	(711)
283	Fault 16	rs	45.0	278.8	20.0	0.0	3.00		(7.3)	(633)
284	Fault 18	ss			20.0	0.0	25.00		(7.2)	(66)
285	Fault 19	ss			20.0	0.0	25.00		(7.1)	(63)
286	Fault 20	ss			20.0	0.0	25.00		(7.3)	(76)
287	Fault 21	ss			20.0	0.0	25.00		(7.3)	(76)
288	Fault 22	rs	30.0	153.0	20.0	0.0	1.00		(7.5)	(2379)
289	Fault 23	rs	30.0	145.4	20.0	0.0	2.00		(7.5)	(455)
290	Fault 24	rs	20.0	135.2	20.0	0.0	5.00		(7.7)	(566)
291	Fault 25	rs	20.0	128.2	20.0	0.0	7.00		(7.8)	(467)
292	Fault 26	rs	20.0	116.0	20.0	0.0	15.00		(7.4)	(234)
293	Fault 27 (Hauroko)	rs	45.0	290.4	20.0	0.0	0.01		(7.3)	(187500)

Index	Fault Name	Slip Type	Dip (°)	Dip Dir (°)	Depth Max (km)	Depth Min (km)	Slip Rate (mm/yr)	Displa-cement (m)	Mmax	Recurrence Interval (yrs)
294	Fault 28	rs	45.0	136.5	20.0	0.0	0.50		(7.2)	(3501)
295	Fault 29	rs	45.0	285.0	20.0	0.0	0.50		(7.0)	(2707)
296	Fault 30	rs	45.0	222.9	20.0	0.0	0.30		(7.0)	(4544)
297	Fault 31	rs	45.0	55.4	20.0	0.0	0.50		(7.1)	(3049)
298	Fault 32	rs	45.0	269.0	20.0	0.0	0.50		(7.1)	(2923)
299	Fault 33	ss			20.0	0.0	1.00		(6.8)	(1130)
300	Fault 34	ss			20.0	0.0	0.01		(7.0)	(431)
301	Fault 35	ss			20.0	0.0	0.01		(7.3)	(612)
302	Fault 36	ss			20.0	0.0	3.00		(7.1)	(499)
303	Fault 37	rs	45.0	73.1	20.0	0.0	0.50		(7.2)	(3361)
304	National Park	nv			15.0	0.0	2.00		(6.2)	(289)
305	Poutu	nv			15.0	0.0	2.00		(6.6)	(453)
306	Waihi	nv			15.0	0.0	5.00		(6.8)	(216)

Explanation of Table

Index: Cross reference to the fault sources shown on Figure 3. The index numbers are usually positioned at one end of each fault source.

Fault Name: The first name given is the general name of the fault, and the names inside parentheses indicate the geographic endpoints of modelled fault rupture segments. The abbreviations "RM", "WM" and "BM" identify Hikurangi subduction interface sources developed in consultation with Martin Reyners, Terry Webb and Kelvin Berryman, respectively. See the text for further explanation.

Slip Type: ss=strike-slip; nn=normal; rv=reverse; sr=strike-slip and reverse; sn=strike-slip and normal; rs=reverse and strike-slip; ns=normal and strike-slip, nv=normal in high attenuation Taupo Volcanic Zone; if=subduction interface.

Dip: The preferred or mean value of dip for the fault plane. If no value is given then the dip is either greater than 80° (the case for strike-slip faults), or is uncertain.

Dip Dir: Azimuth of dip.

Depth Max: Depth to the base of the fault.

Depth Min: Depth to the upper edge of the fault.

Slip Rate: The preferred or mean annual rate of slip for the fault.

Displacment: The preferred or mean value of coseismic slip for the fault.

Mmax: Moment magnitude of the earthquake expected to accompany rupture of the fault If a Mmax is given without brackets then it is derived directly from observations of a historical rupture. If the Mmax is given in brackets then it is either calculated with Equations 1 and 2, or estimated from fault area with the regressions of Wells and Coppersmith (1994). See the text for further explanation.

Recurrence Interval: If the value is given in brackets then it is calculated with Equations 3 and 4. See the text for further explanation.

Data Sources: Pettinga et al. (1998), Stirling et al (1998; 1999), Mazengarb et al. (1997), Berryman et al. (1995), Van Dissen et al. (1993), Woodward Clyde and Institute of Geological and Nuclear Sciences (1999), Van Dissen (pers comm.), Villamor (pers comm.), Berryman (pers comm.), Mazengarb (pers comm.), Sutherland (pers comm.), Reyners (pers comm.), Begg and Van Dissen (1998), Grapes et al. (1998), Benson et al. (1998), Little et al. (1998), Van Dissen and Nicol (1998), Kelsey et al. (1998), Reyners et al. (1997), Berryman et al. (1995), Hull and Dellow (1993), Le Cointre et al. (1998), Villamor et al. (1998), Fellows (1996), Beanland et al. (1997), Berryman et al. (1998), Grapes et al. (1997), Nicol and Van Dissen (1997), Grapes and Downes (1997), Heron et al. (1998), Nicol and Van Dissen (1997), Van Dissen et al. (1998), Schermer et al. (1999), Van Dissen and Palmer (1998).

Appendix 2: Graphs of the pgas estimated from the attenuation model as a function of magnitude, distance, tectonic type and focal mechanism, along with spectra for a selection of magnitudes, source-to-site distances, tectonic types and site conditions.

Model P2MRF5AC

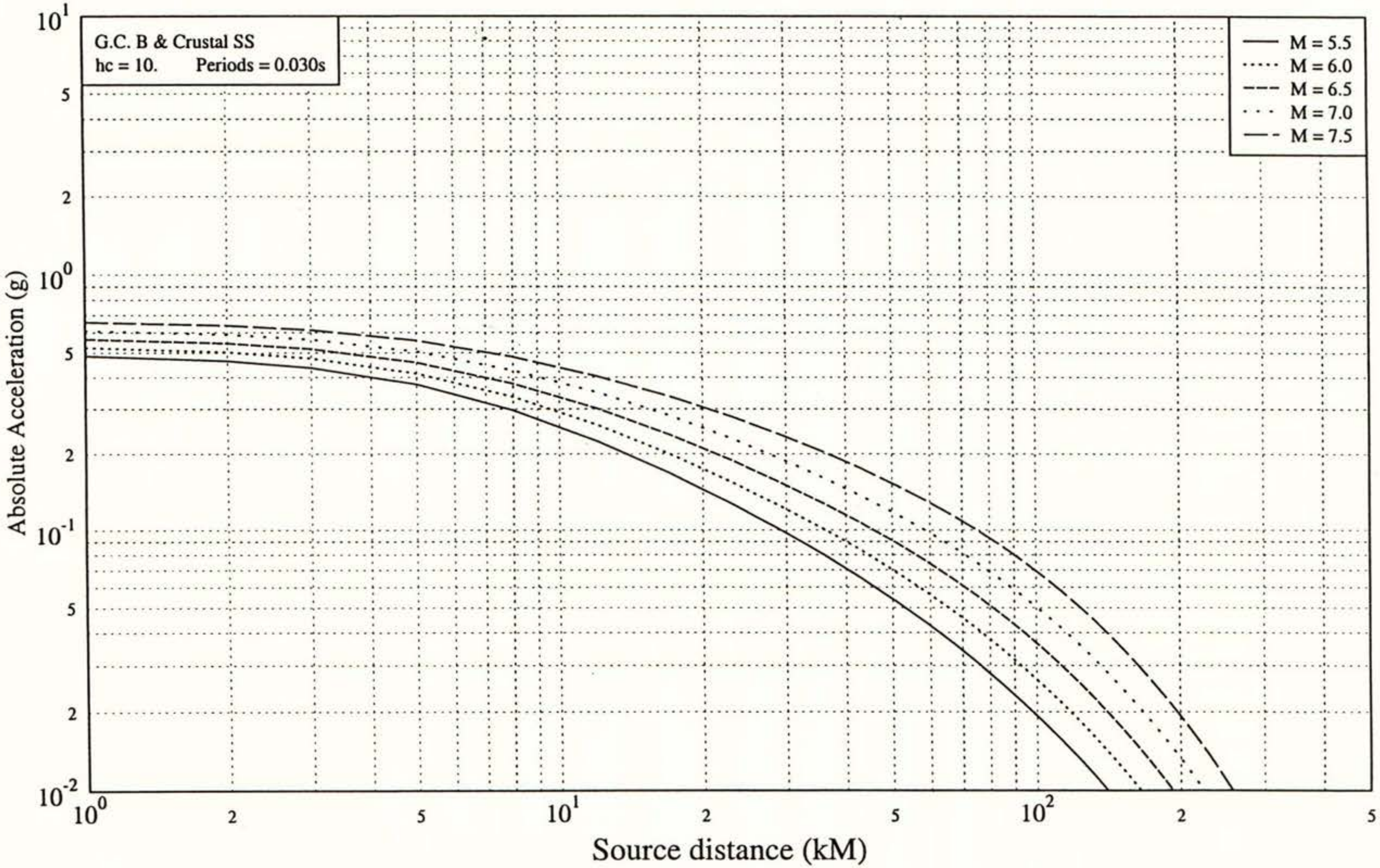

Model P2MRF5AC

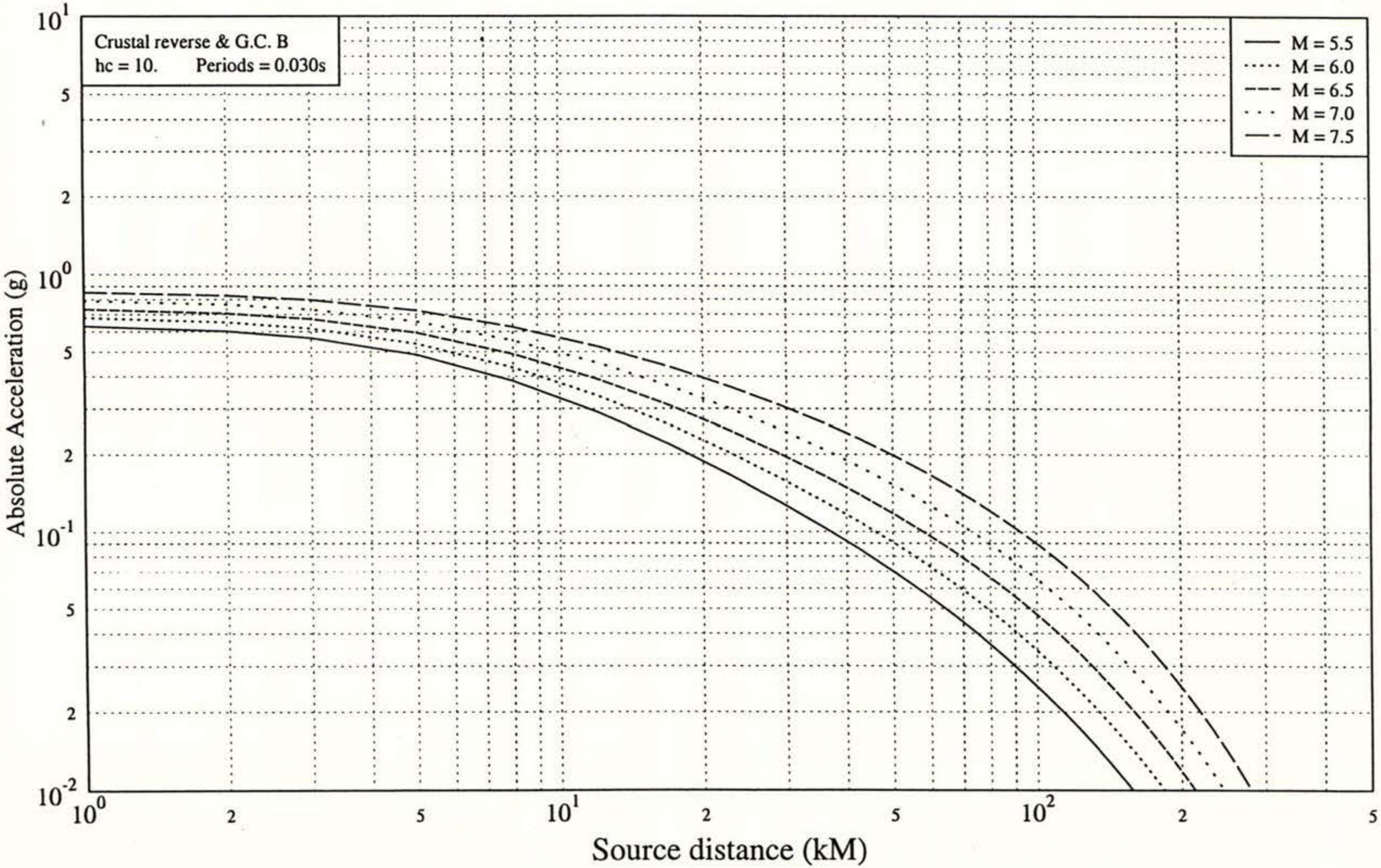

Model P2MRF5AC

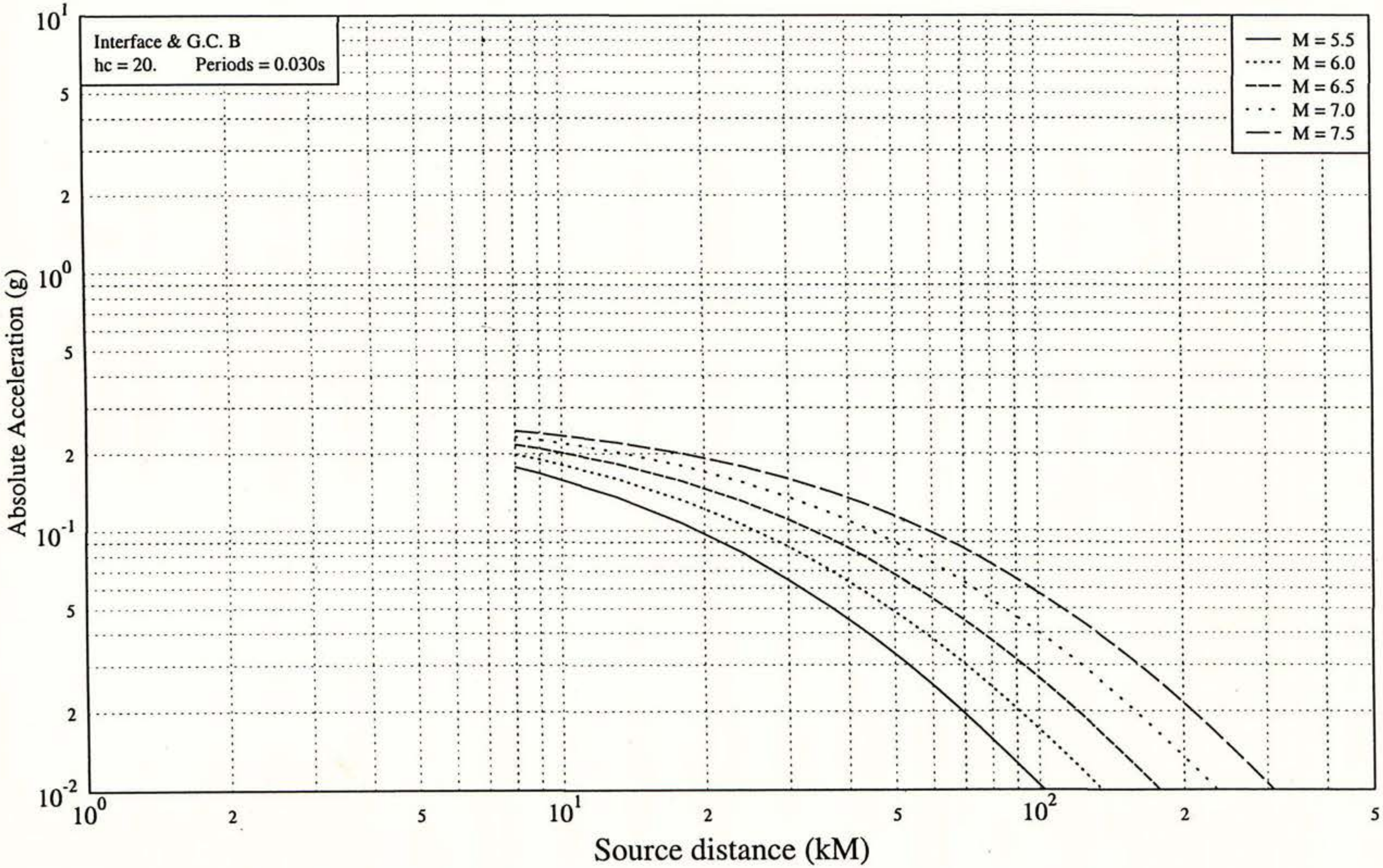

Model P2MRF5AC

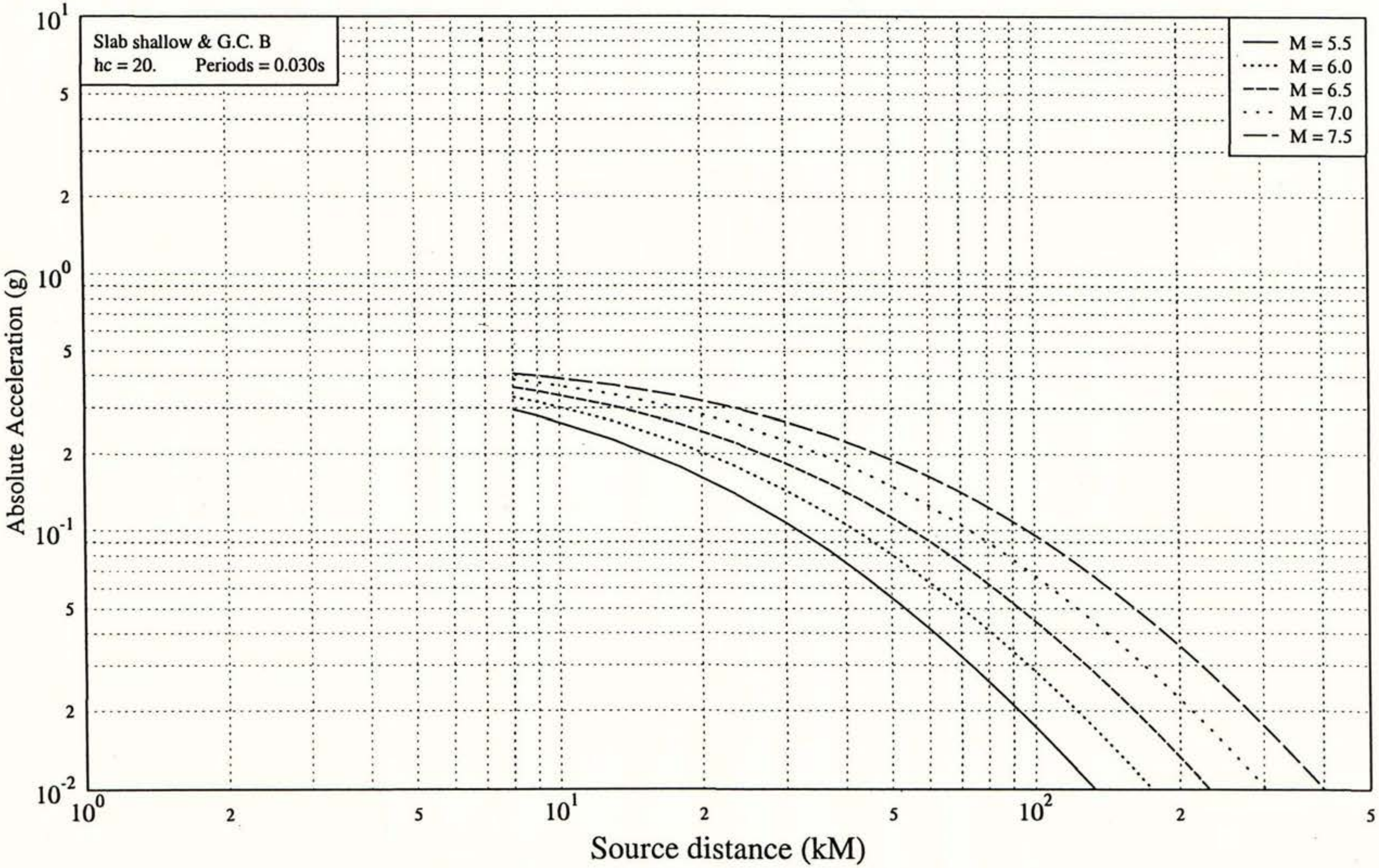

Model P2MRF5AC

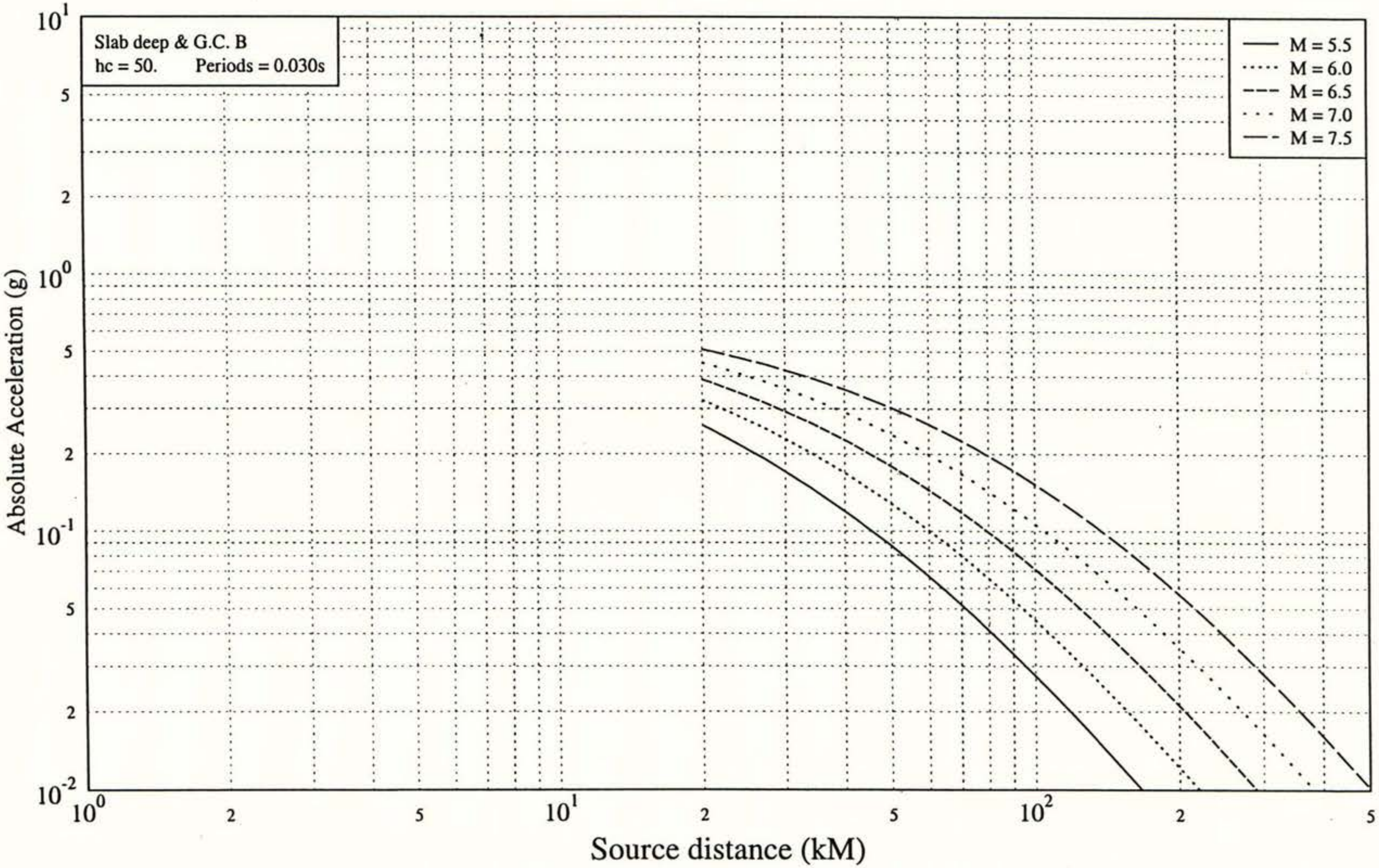

Model P2MRF5AC

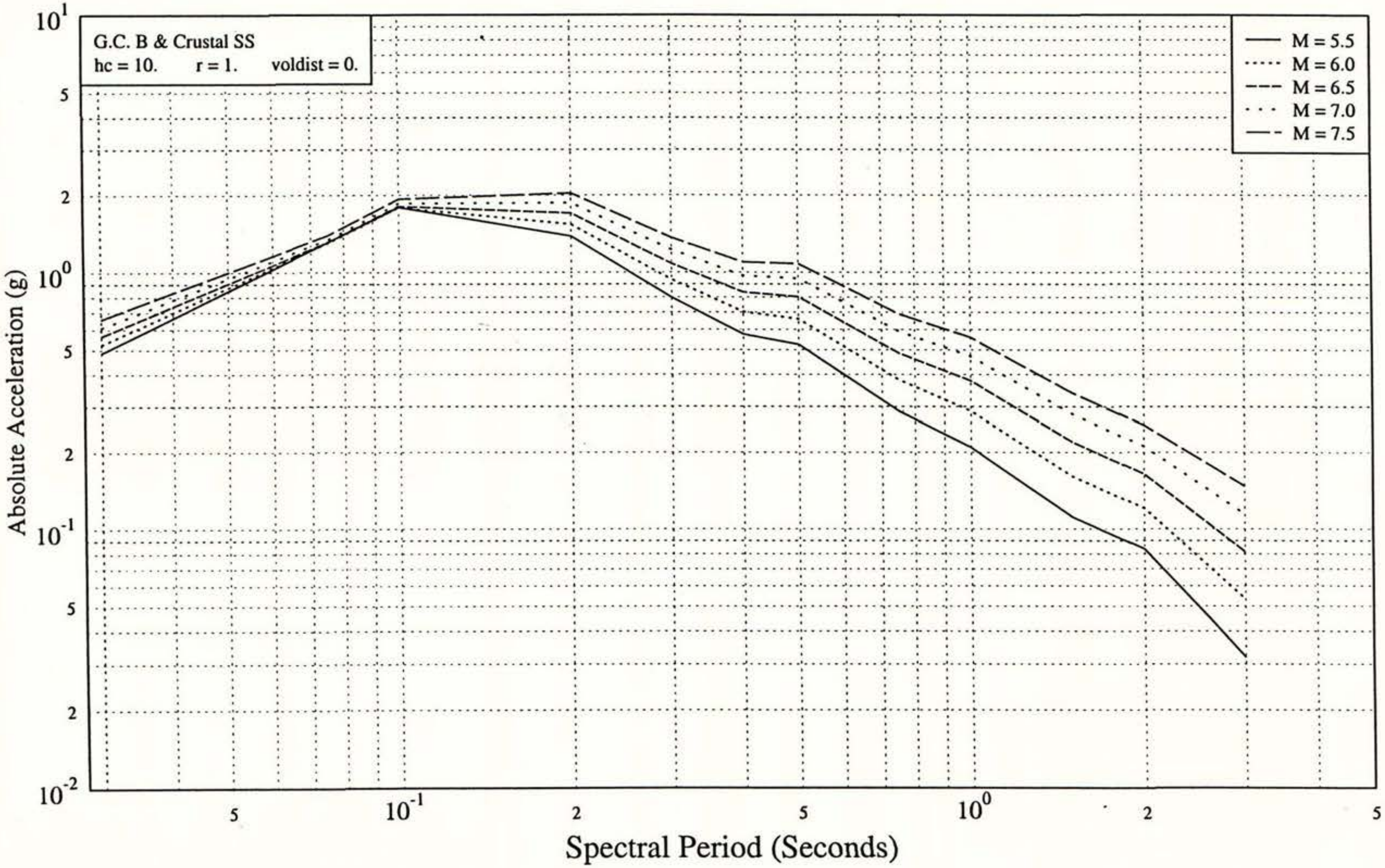

Model P2MRF5AC

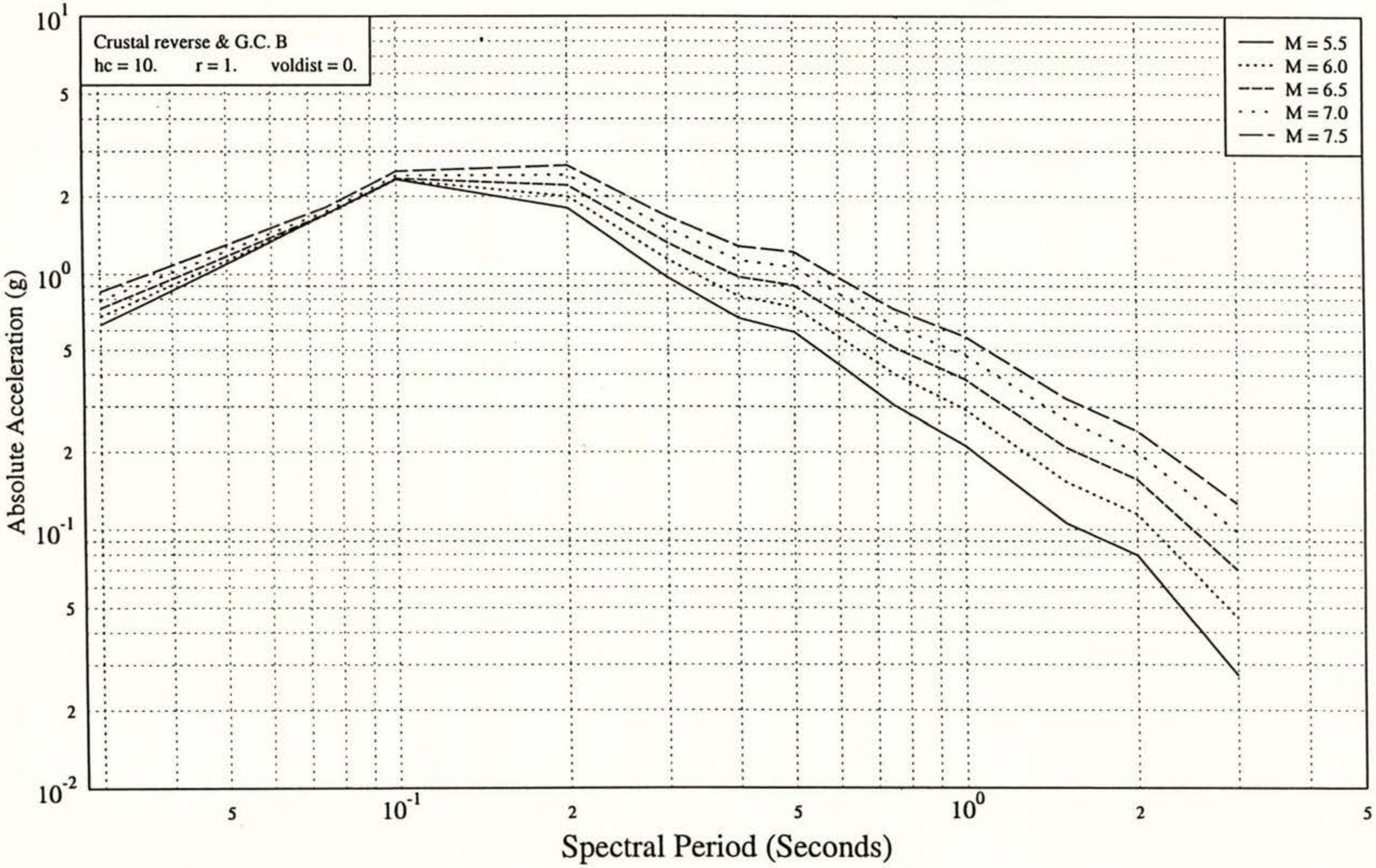

Model P2MRF5AC

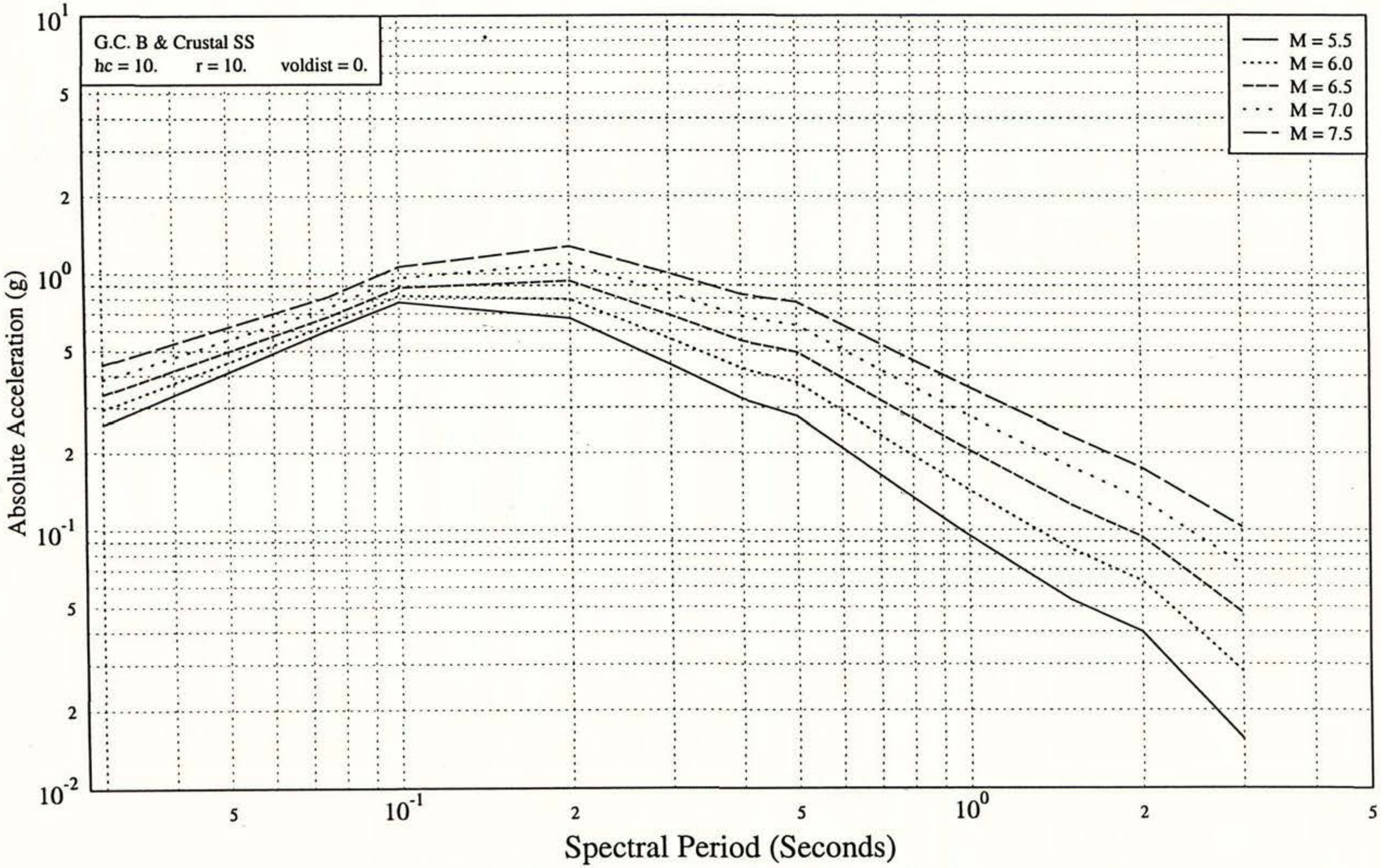

Model P2MRF5AC

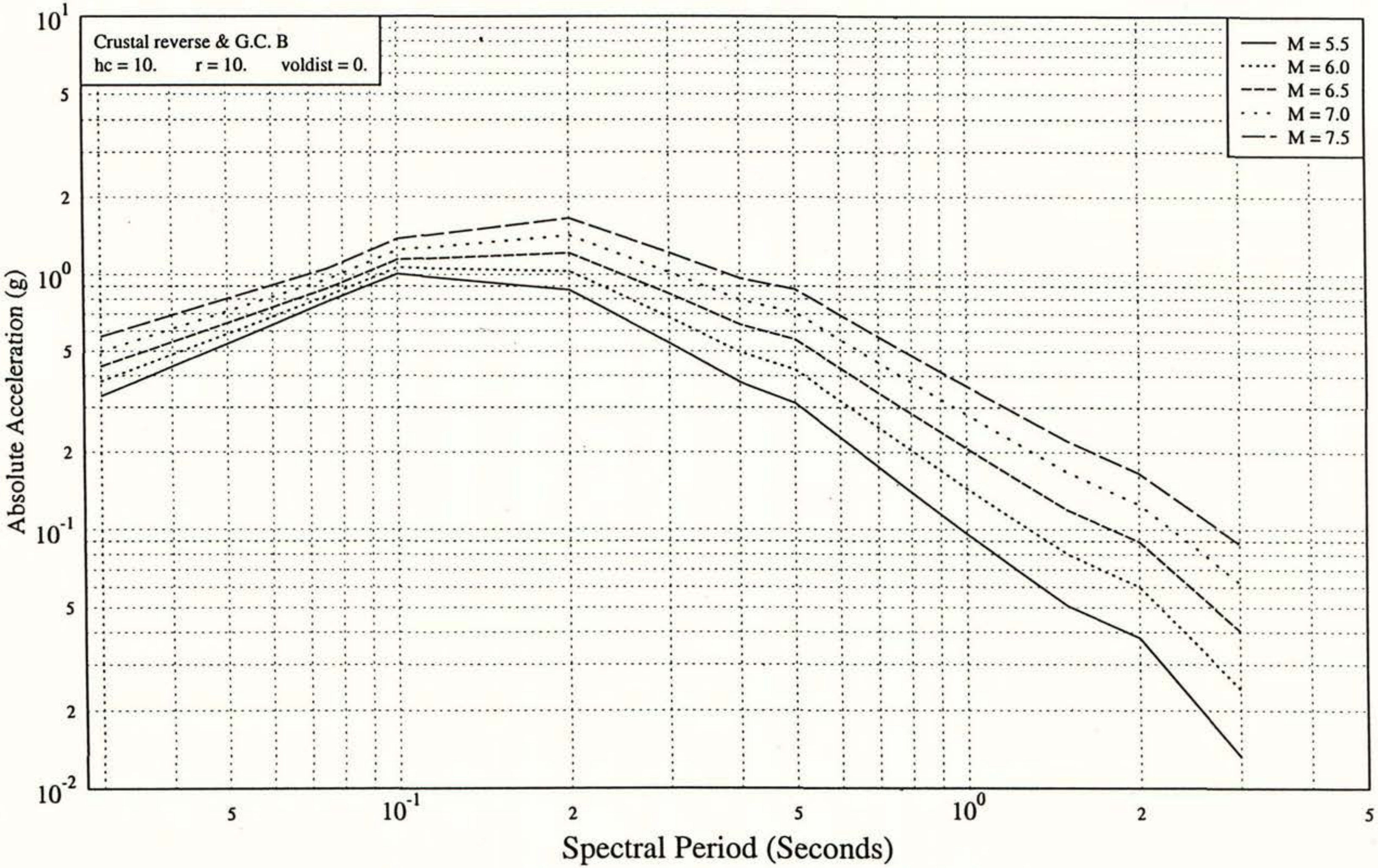

Model P2MRF5AC

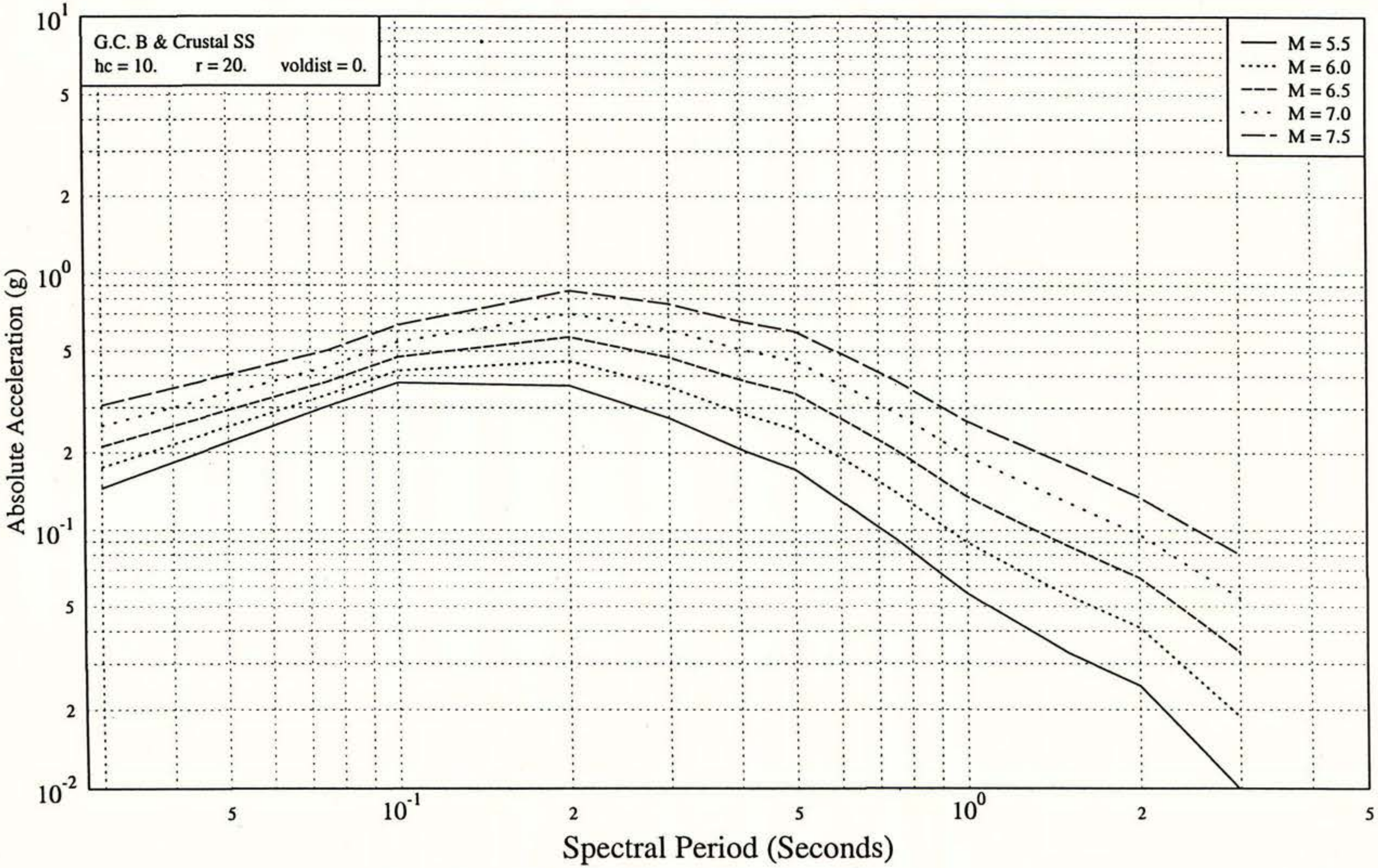

Model P2MRF5AC

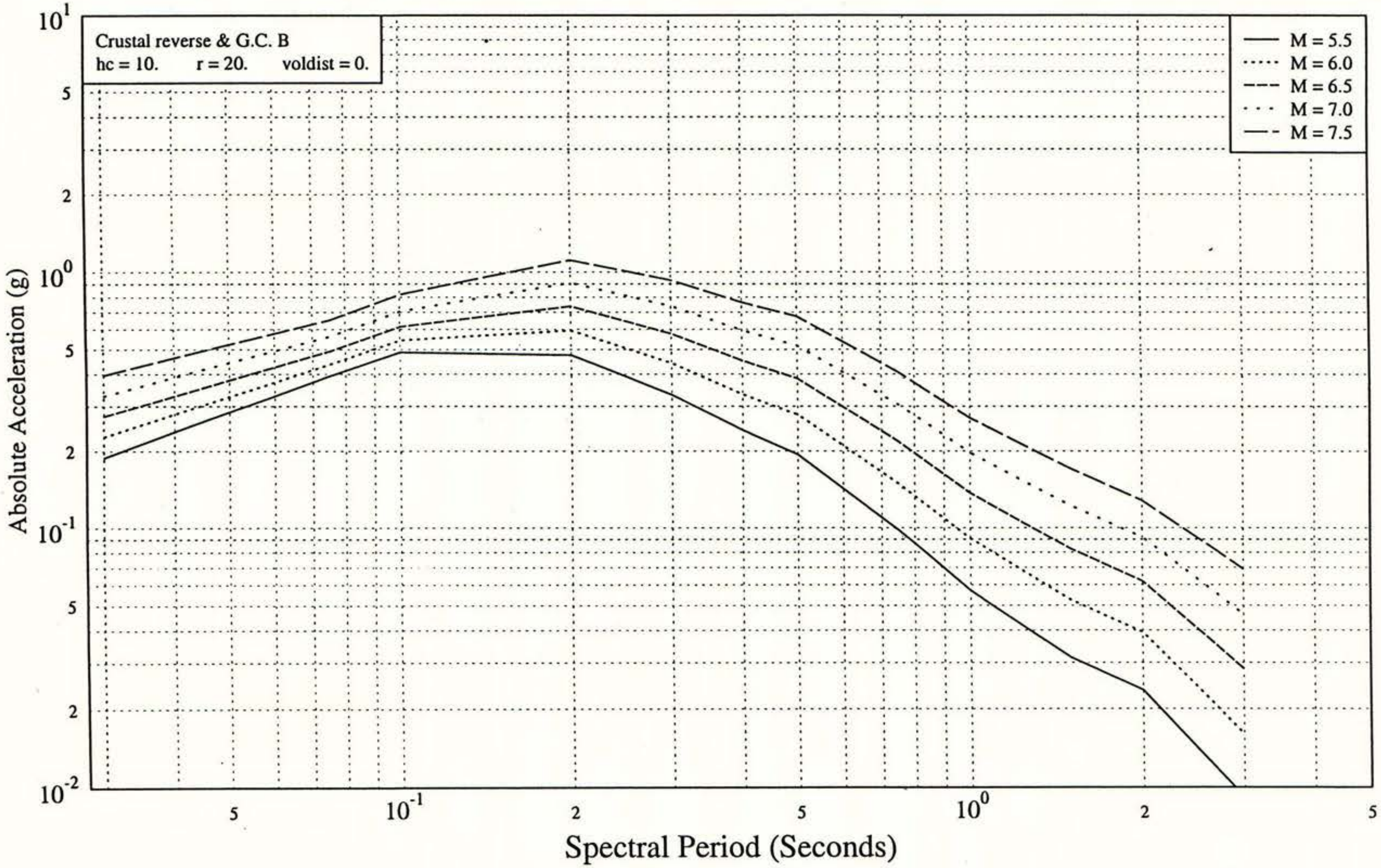

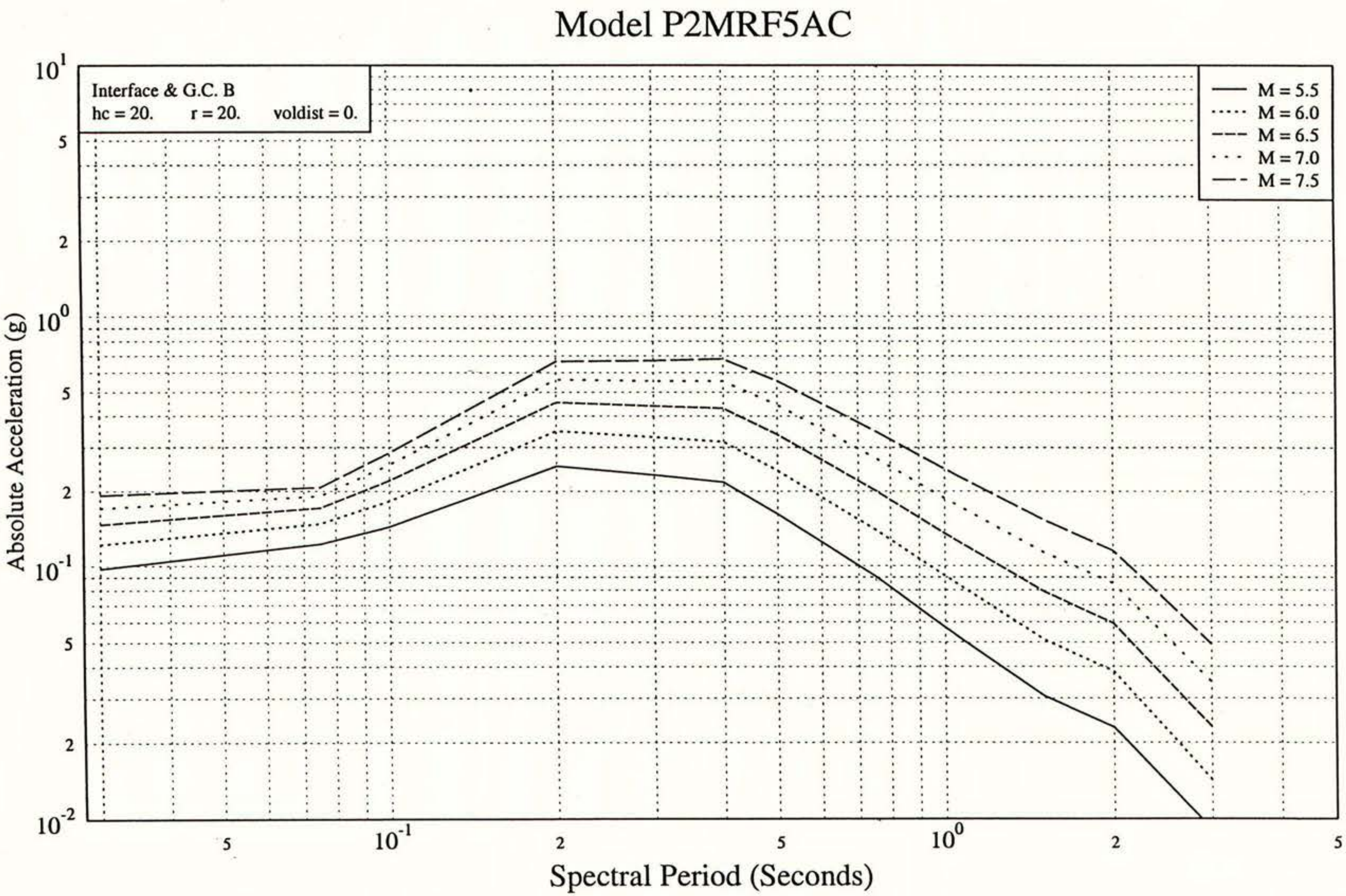

Model P2MRF5AC
Interface & G.C. B
hc = 20. r = 20. voldist = 0.
M = 5.5
M = 6.0
M = 6.5
M = 7.0
M = 7.5
Absolute Acceleration (g)
Spectral Period (Seconds)

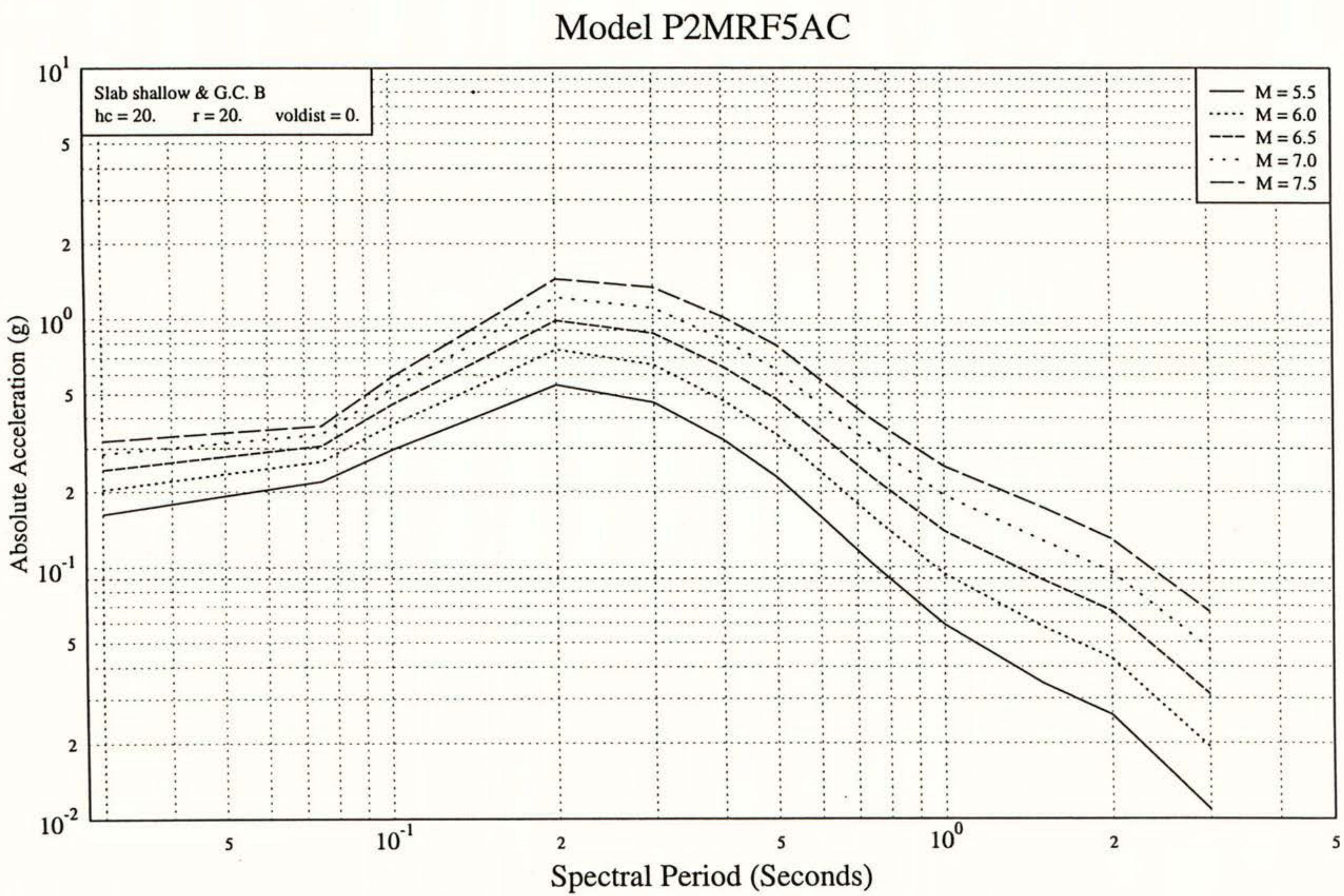
Model P2MRF5AC
Slab shallow & G.C. B
hc = 20. r = 20. voldist = 0.
M = 5.5
M = 6.0
M = 6.5
M = 7.0
M = 7.5
Absolute Acceleration (g)
Spectral Period (Seconds)
10^1
5
2
10^0
5
2
10^{-1}
5
2
10^{-2}
5
10^{-1}
2
5
10^0
2
5

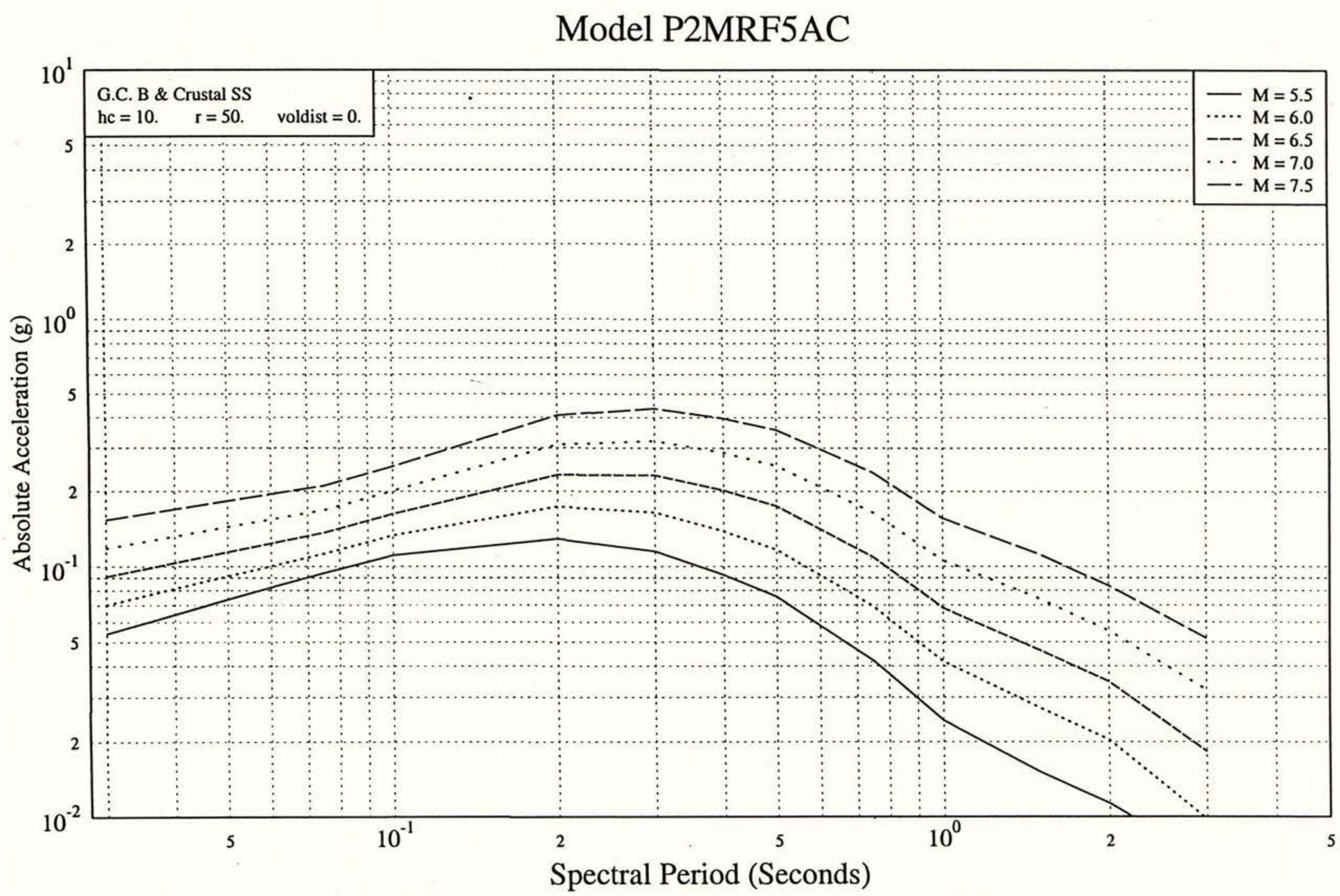

Model P2MRF5AC
G.C. B & Crustal SS
hc = 10. r = 50. voldist = 0.
M = 5.5
M = 6.0
M = 6.5
M = 7.0
M = 7.5
Absolute Acceleration (g)
Spectral Period (Seconds)

Model P2MRF5AC

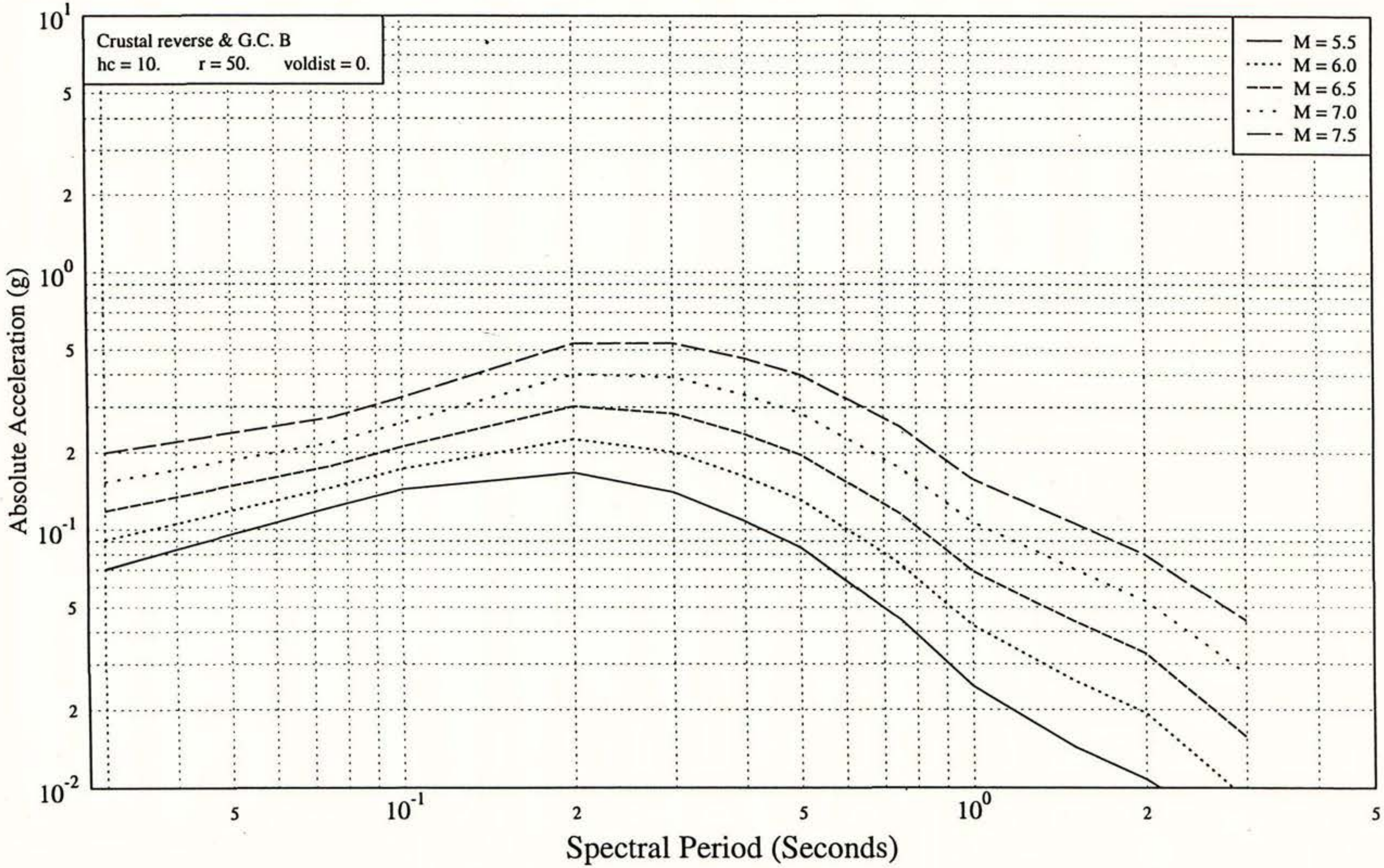

Model P2MRF5AC

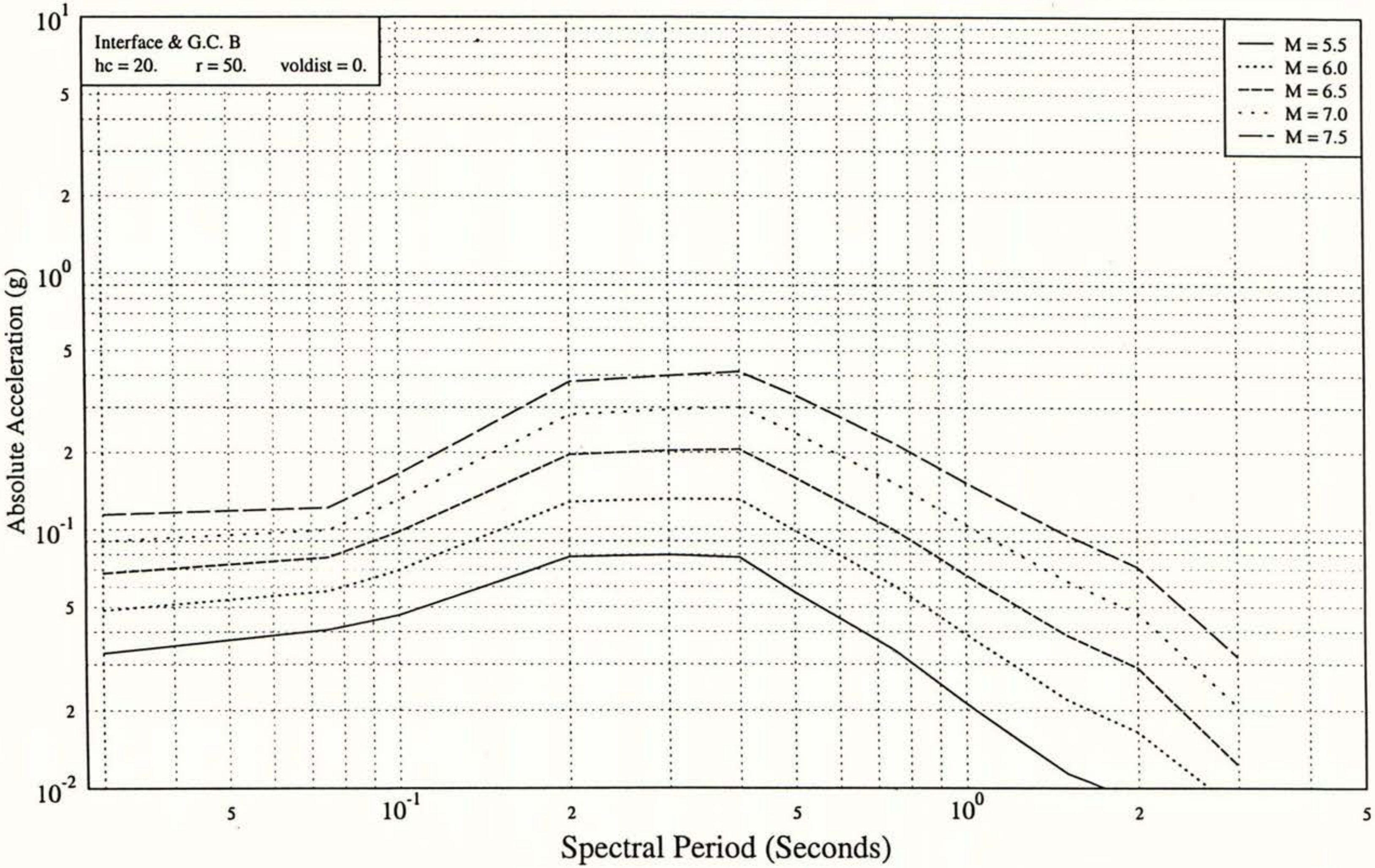

Model P2MRF5AC

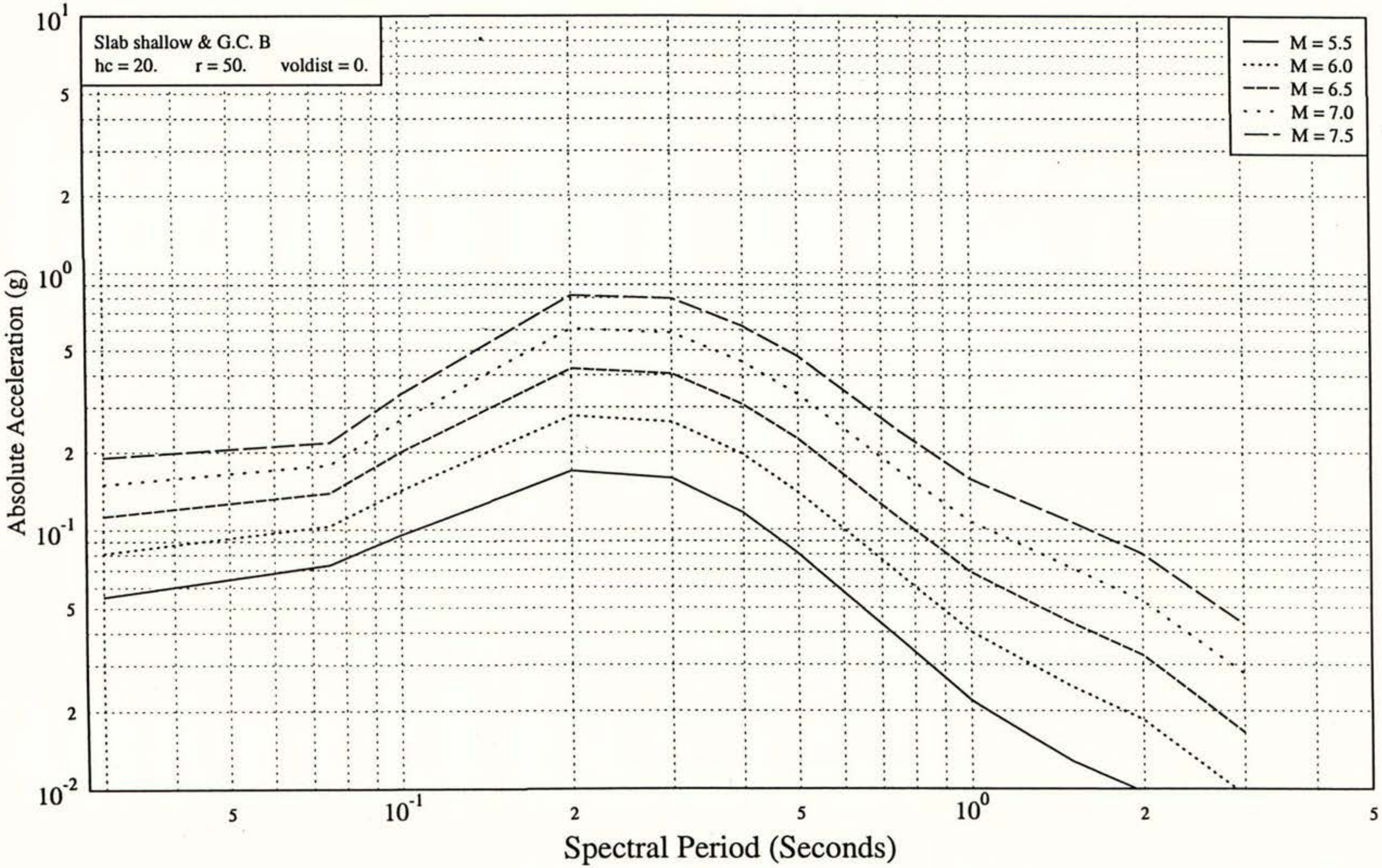

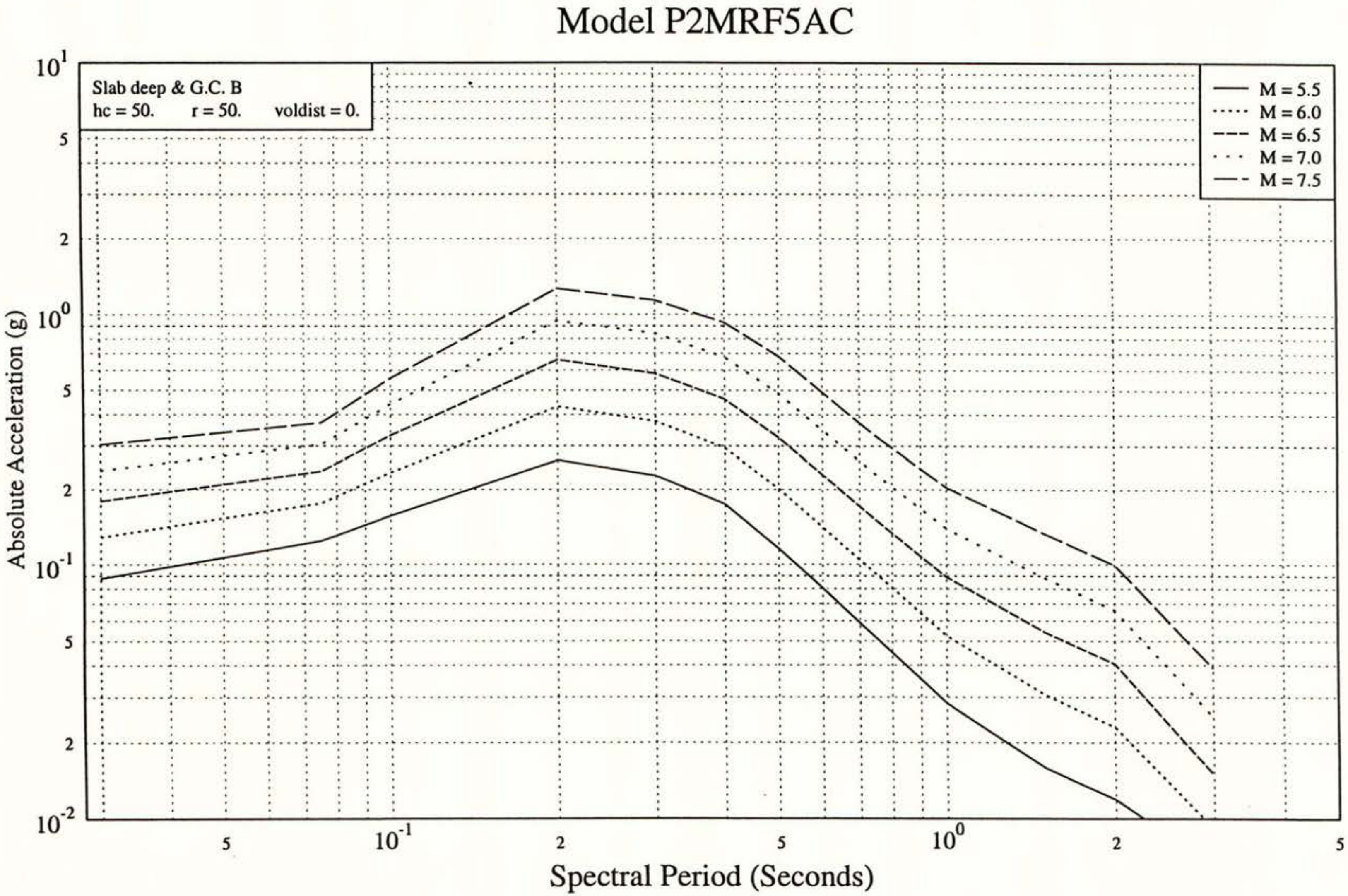
Model P2MRF5AC
Slab deep & G.C. B
hc = 50. r = 50. voldist = 0.
M = 5.5
M = 6.0
M = 6.5
M = 7.0
M = 7.5
Absolute Acceleration (g)
Spectral Period (Seconds)

INSTITUTE OF GEOLOGICAL AND NUCLEAR SCIENCES LIMITED

Gracefield Research Centre
69 Gracefield Road
P0 Box 30368
Lower Hutt
New Zealand
Phone +64-4-570 1444
Fax +64-4-570 4600

Wairakei Research Centre
State Highway 1
Private Bag 2000
Taupo
New Zealand
Phone +64-7-374 8211
Fax +64-7-374 8199

Rafter Research Centre
30 Gracefield Road
P0 Box 31312
Lower Hutt
New Zealand
Phone +64-4-570 4637
Fax +64-4-570 4657

Dunedin Research Centre
764 Cumberland Street
Private Bag 1930
Dunedin
New Zealand
Phone +64-3-477 4050
Fax +64-3-477 5232

A Crown Research Institute

Bulletin of the Seismological Society of America, Vol. 92, No. 5, pp. 1878–1903, June 2002

A New Seismic Hazard Model for New Zealand

by Mark W. Stirling, Graeme H. McVerry, and Kelvin R. Berryman

Abstract We present a new probabilistic seismic hazard analysis (PSHA) for New Zealand. An important feature of the analysis is the application of a new method for the treatment of historical (distributed) seismicity data in PSHA. The PSHA uses the seismicity recorded across and beneath the country to define a three-dimensional grid of *a*-values (i.e., parameter *a* of a Gutenberg–Richter distribution $\log N/\mathrm{yr} = a - bM$, in which *N*/yr is the number of earthquakes per year recorded inside each grid cell equal to or greater than magnitude *M*); parameter *b* and the limiting maximum cutoff magnitude of the Gutenberg–Richter distribution are defined from the surrounding region (14 crustal and 23 subcrustal seismotectonic zones are defined for the country) and then smoothed across the boundaries of the zones. The methodology therefore combines the modern method of defining continuous distributions of seismicity parameters (Frankel, 1995; Frankel *et al.*, 1996) with the traditional method of defining large area sources and the associated seismicity parameters (e.g., Algermissen *et al.*, 1990). The methodology provides a means of including deep (subduction zone) seismicity in a PSHA, preserves the finer-scale spatial variations of seismicity rates across a region, avoids the undesirable edge effects produced in the traditional method when adjacent area sources enclose areas of significantly different seismicity rates, and also enables parameters most reliably defined at a regional scale (parameter *b* and maximum cutoff magnitude of a Gutenberg–Richter distribution, and slip type) to be incorporated into the PSHA. The PSHA combines the modeled seismicity data with geological data describing the location and earthquake recurrence behavior of 305 active faults and new attenuation relationships for peak ground acceleration and spectral acceleration developed specifically for New Zealand. Different attenuation expressions are used for crustal and subduction zone earthquakes. The resulting PSH maps for a 150-year return period show the highest hazard to occur in the center and southwest of the country, in the areas of highest historical crustal and deep subduction zone seismicity. In contrast, the longer return-period maps (475 and 1000 year return period) show the highest hazard to occur from the southwest to northeast ends of the country, along the faults that accommodate the majority of the motion between the Pacific and Australian plates. The maps are currently being used to revise New Zealand's building code, which has previously been based on PSHAs that did not explicitly include individual faults as earthquake sources.

Introduction

In this article we present the results of a probabilistic seismic hazard analysis (PSHA) for New Zealand that include significant advances on the earlier PSHAs for the country. In our PSHA we apply new methods for the treatment of historical seismicity data and combine these data and methods with geologic data describing the geometry and activity (locations, fault lengths, fault type, slip rates, single-event displacements, estimated magnitudes, and average recurrence intervals) of 305 major active earthquake faults to make PSH maps for the country. Our PSH maps show the peak ground accelerations (PGA) and 5% damped response spectral accelerations (SA 0.2- and 1-sec periods, often abbreviated as SA (0.2 sec) and SA (1 sec)) expected for return periods of 150 years (10% probability in 10 years, PGA only), 475 years (10% probability in 50 years) and 1000 years (10% probability in 105 years) at average soil sites (Class B site conditions of Standards New Zealand, 1992).

The prime motivation for our study was that the existing PSH maps for New Zealand are now out of date in terms of the methodology and data used to estimate hazard. The widely used national seismic hazard maps of Matuschka *et al.* (1985) and Smith and Berryman (1986) used the historical record of earthquakes (the historical record dates from 1840, when European settlement began in New Zealand), and did not explicitly incorporate active faults as discrete earthquake sources. The maps of Matuschka *et al.* remain the basis of the current building code (Standards New Zealand, 1992). More recently, national PSH maps have been published that incorporate both geological and historical seismicity data (Stirling *et al.*, 1998), but these maps used an unpublished interim version of the current New Zealand attenuation model and preliminary versions of the fault database and historical earthquake catalog. Our new PSHA is developed from that of Stirling *et al.* (1998), incorporating new developments in the treatment of historical seismicity data, new ground motion attenuation relationships for New Zealand, and a much enlarged and revised active fault database.

Seismotectonic Setting of New Zealand

New Zealand straddles the boundary of the Australian and Pacific plates, where relative plate motion is obliquely convergent across the plate boundary at about 50 mm/yr in the north of the country, 40 mm/yr in the center, and 30 mm/yr in the south (De Mets *et al.*, 1994) (Fig. 1). The relative plate motion is expressed in New Zealand by the presence of numerous active faults, a high rate of small-to-moderate ($M < 7$) earthquakes, and the occurrence of many large earthquakes and one great earthquake in historic time. A southeast-dipping subduction zone lies at the far southwestern end of the country (Fiordland subduction zone, Fig. 1), and this is linked to a major northwest-dipping subduction zone in the eastern North Island (Hikurangi subduction zone, Fig. 1) by a 1000-km-long zone of dextral oblique slip faults (Axial tectonic belt, Fig. 1). Essentially all of the relative plate motion is accommodated by the faults of the axial tectonic belt in the area between the Fiordland and Hikurangi subduction zones.

The Hikurangi subduction interface dips beneath the eastern North Island (Fig. 1), and abrupt changes in the depth distribution of seismicity along the subduction interface have been suggested as marking rupture segment boundaries (Reyners, 1983, 1998, 2000). However, no large to great earthquakes are known to have been produced by the Hikurangi subduction interface in historic time, so little is known about the earthquake potential of this feature. The Fiordland subduction zone (Fig. 1) shows abrupt changes in seismicity patterns along strike. The lateral extent of the aftershock zone of a recent large earthquake (the M_w 7 10 August 1993 Fiordland earthquake; Van Dissen *et al.*, 1994) shows that ruptures can be confined to less than the length of the entire subduction zone. Some of the highest rates of seismicity in the country occur within the dipping slabs of the subduction zones. High rates of moderate earthquakes also occur in the crust above the Fiordland subduction zone, and to a lesser extent in the crust above the Hikurangi subduction zone.

The axial tectonic belt is a zone of dextral transpression,

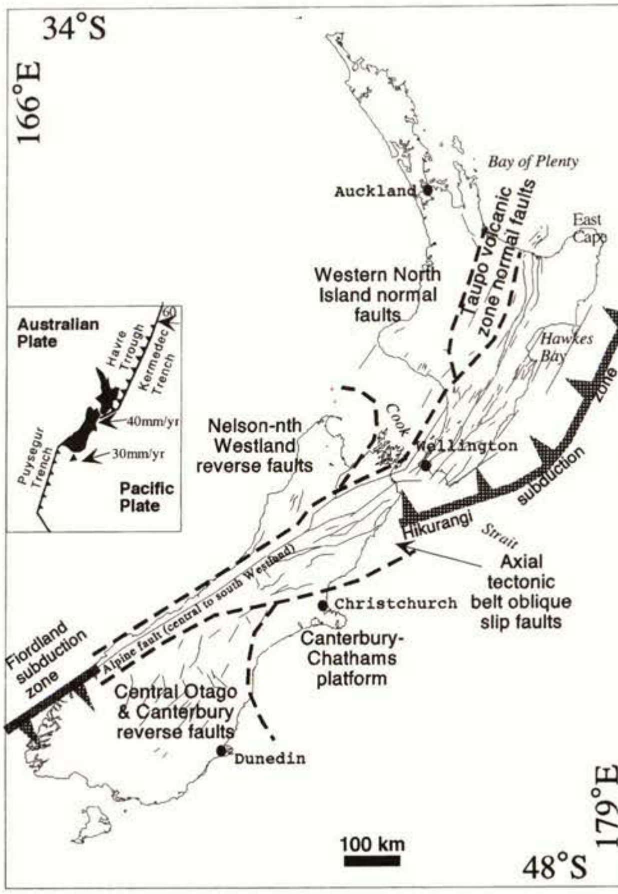

Figure 1. The plate tectonic setting of New Zealand. The country is divided into the tectonic provinces identified by Berryman and Beanland (1988).

most dramatically illustrated by the southern section of the Alpine Fault (Fig. 1), where dextral slip rates of 15–35 mm/yr and dip slip rates of 2–8 mm/yr are observed (Berryman and Beanland, 1988; Berryman *et al.*, 1992; Sutherland and Norris, 1995; Berryman *et al.*, 1998; Norris and Cooper, 2000). The Alpine Fault accommodates virtually all of the relative plate motion in the central South Island, and geologic data provide evidence for the occurrence of large-to-great earthquakes on the Alpine Fault with recurrence intervals of hundreds of years; however, the fault has not produced such earthquakes in historic time and is presently characterized by low rates of seismicity.

Plate motion is distributed across a number of parallel faults with slip rates greater than 1 mm/yr in the axial tectonic belt of the northern South Island and across faults and the Hikurangi subduction zone in the southern and eastern North Island (Fig. 1). Faults in the axial tectonic belt show strike-slip, dip-slip, and oblique-slip motion. Many moderate or larger earthquakes have occurred within the axial tectonic belt in historic time, including the two largest historical earthquakes (the M_w 8.1–8.2 1855 Wairarapa earthquake and the M_w 7.8 1931 Hawkes Bay earthquake).

The Taupo Volcanic Zone (Fig. 1) is a zone of active crustal extension that has developed in response to the southward migration of backarc spreading from the Havre Trough (Fig. 1) into the continental margin of New Zealand in the last million years (Cole and Lewis, 1981). The crustal extension is occurring across the zone at a rate of about 10 mm/yr (e.g., Berryman and Beanland, 1988; Villamor and Berryman, 2001), and normal faults typically have slip rates greater than 1 mm/yr in the zone. Several moderate-sized earthquakes have produced surface ruptures in the Taupo Volcanic Zone (TVZ) in historic time, the most recent being the M_w 6.5 2 March 1987 Edgecumbe earthquake, which was produced by a normal slip rupture along the Edgecumbe Fault. High rates of small earthquakes also characterize the TVZ.

Faults located away from the axial tectonic belt and TVZ tend to have slip rates that are about an order of magnitude less than the faults in those areas. Reverse faults with slip rates of 0.1–1 mm/yr characterize the style of faulting in central Otago and south Canterbury (Fig. 1); similar slip rates characterize the reverse faults in north Westland and Nelson (Fig. 1). The reverse faults have developed in response to oblique compression across the plate boundary. The M_w 7.6 1929 Buller and M_w 7.2 1968 Inangahua earthquakes occurred on reverse faults in the Nelson–north Westland area, and high seismicity rates are observed near the epicenters of these earthquakes. The western North Island is a broad zone of relatively stable crust, disrupted only by normal faults in the northeast and southwest (Fig. 1). Several $M \geq 6.5$ earthquakes have occurred within the western North Island in historic time, all in the southwest. Finally, the Canterbury–Chathams platform is an area of stable continental crust that stretches well east of the map boundary in Fig. 1. Very few earthquakes have occurred on the Canterbury–Chathams platform in historic time.

Methodology and Data

The PSHA methodology of Cornell (1968) forms the basis for our analysis. The steps for our PSHA are: (1) to use geologic data and the historical earthquake record to define the locations of earthquake sources across and beneath the country, as well as the likely magnitudes, tectonic type or mechanism, and frequencies of earthquakes that may be produced by each source; and (2) to estimate the ground motions that the sources will produce at a gridwork of sites that cover the entire country. The computation of ground motions in step 2 is achieved with a seismic hazard code that is an improved version of the code developed by Stirling *et al.* (1998). Improvements to the code come in the treatment of historical seismicity for input to the PSHA and in the use of new ground-motion attenuation relationships for New Zealand (McVerry *et al.*, 2000).

Fault Sources

We show the 305 fault sources used in our PSHA in Figure 2, and list them in the Appendix. The Appendix is the dataset in Stirling *et al.* (2000), which was constructed from Stirling *et al.* (1998) and from unpublished Institute of Geological and Nuclear Sciences (GNS) data held in consulting reports, computer databases, and in recent field notes.

The fault sources shown on Figure 2 are generalizations of mapped fault (or fault segment) traces. These generalized faults are appropriate for regional-scale PSHA. Using the methodology of Stirling *et al.* (1998), we divide a given fault into more than one source if geological data or the rupture length of a historic earthquake provide evidence for a fault having separate rupture segments. Data bearing on the geometry (e.g., fault dip) and activity (slip rates, single-event displacements, and recurrence intervals) of the fault sources are also listed in the Appendix as the average or preferred values. Our method of estimating the likely maximum magnitude (M_{max} in the Appendix) and recurrence interval of M_{max} earthquakes produced by each fault source in Figure 2 varies according to the quantity and quality of available data for each fault. Here, we define M_{max} as the most likely maximum magnitude for a fault source, rather than the maximum possible earthquake for that source. Where possible, the magnitudes of large historical earthquakes (usually constrained from instrumental records or from Modified Mercalli intensity data) and lengths of the associated surface ruptures are used to define the M_{max} and length of particular fault sources. However, in doing this we acknowledge that these historical events may be considerably less than the true M_{max} for a particular fault. Our justification here is that we are maximizing the use of rare historical observations of surface rupturing earthquakes in the PSH model. If historical observations are unavailable for a fault source, then the next preferred method of defining M_{max} is to use published estimates of single-event displacements and fault area in the equations for seismic moment and moment magnitude:

$$M_0 = \mu AD \tag{1}$$

and

$$\log M_0 = 16.05 + 1.5M_{max}, \tag{2}$$

in which M_0 is the seismic moment (in dyne cm) corresponding to M_{max}, μ is the rigidity modulus of the crust of the Earth, A is the fault area, and D is the single-event displacement (equation 1 is from Aki and Richards, 1980; equation 2 is from Hanks and Kanamori, 1979). To calculate fault area, we use the depth to the base of the seismogenic layer (the depth to the base of seismicity recorded in the region surrounding the fault in the GNS earthquake catalog) and dip of the fault to estimate the fault width and we estimate fault length from the length of surface traces. Lastly, if single-event displacement data are unavailable, preventing the calculation of M_{max} with equations (1) and (2), then an empirical regression of Wells and Coppersmith (1994) is used to estimate M_{max} from fault rupture area. The average recurrence interval (T) assigned to M_{max} is the published estimate

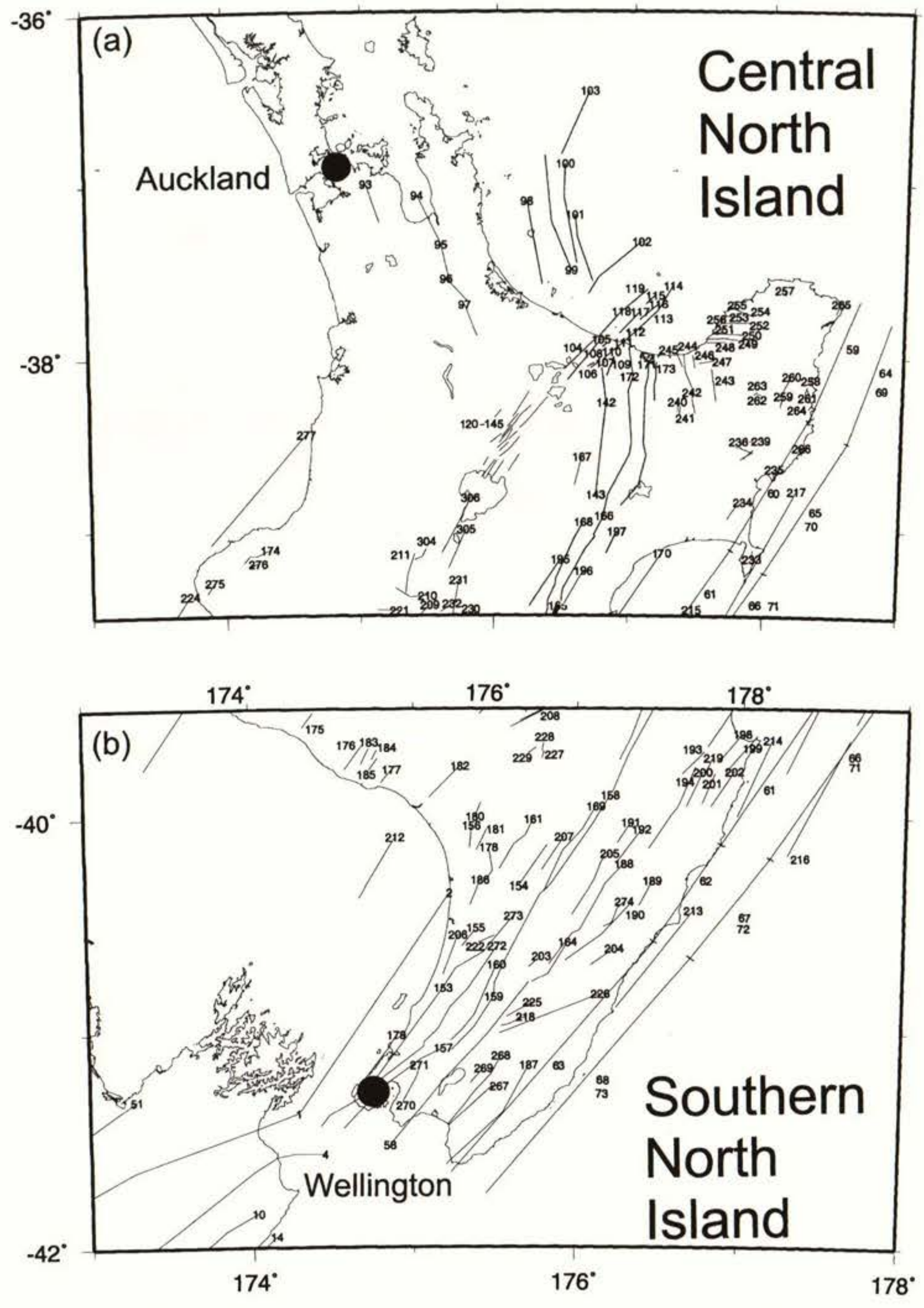

Figure 2. The 305 active fault sources used as input for the probabilistic seismic hazard analysis. The numbers beside each fault correspond to the index numbers given in the fault table (Appendix). We have split the country into four maps to show the different spatial densities of faults at different scales. (*Continues on next page.*)

from geological investigations; or the recurrence interval calculated with the equation

$$T = D/S \tag{3}$$

if a published recurrence interval estimate is unavailable (D is average single-event displacement and S is the fault slip rate); or the recurrence interval calculated with the equation of Wesnousky (1986)

$$T = M_0/M_{0_{\text{rate}}} \tag{4}$$

if single-event displacement data are unavailable ($M_{0_{\text{rate}}}$ is the rate of seismic moment release on the fault, equal to μAS,

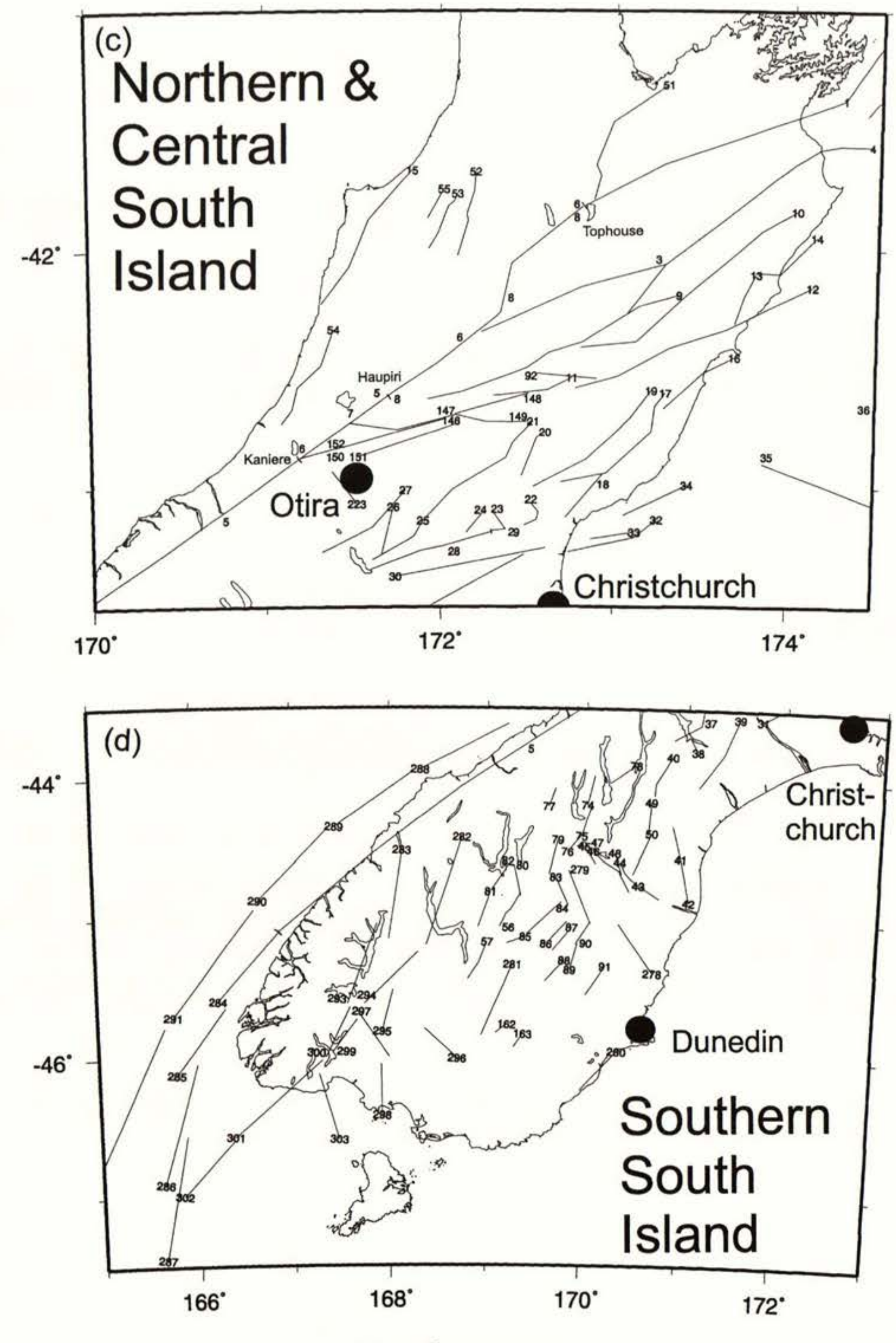

Figure 2. (*Continued*)

in which μ is the rigidity modulus, 3×10^{11} dyne/cm^2, A is the fault area, and S is the fault slip rate in cm/yr). Where possible, we use the preferred values of D, S, and T in equations 1–4; otherwise we use values that are the means of the minimum and maximum values. We also use the mean or preferred values of $M_{\max}$ (Appendix) in the equations.

Our knowledge of the earthquake potential of the Hikurangi and Fiordland subduction zones is considerably less than for the crustal faults, due to the absence of any large-to-great earthquakes on the subduction interfaces in historic time and a lack of paleoseismic data that can be attributed to subduction zone earthquakes. Our approach for the Hikurangi subduction zone is to combine the results of several alternative subduction earthquake models (Appendix). Two of these models (fault names ending with WM and RM in the Appendix) use empirical regressions developed from global subduction zone earthquakes (Abe, 1975; Somerville *et al.*, 1999) to estimate the M_{max} for earthquakes on the Hikurangi subduction interface from estimates of the area of subduction interface segments. The segments are defined from the results of Reyners (1998, 2000) and from changes in the cumulative slip rate of dip slip faults along the upper plate of the subduction zone in central Hawkes Bay (Beanland *et al.*, 1998). The recurrence intervals for the subduction interface earthquakes are then estimated by taking account of the relative plate motion rates orthogonal to the subduction zone at the latitude of each segment, the amount of the plate motion taken up by dip-slip faults in the upper plate, and estimates of the degree of coupling (ratio of seismic slip to total slip) on the plate interface. The global average for the coupling coefficient is about 0.5 (Hyndman *et al.*, 1997). Typical M_{max} values of 7.5–7.9 (associated with single-event displacements of about 3 m) and recurrence intervals of between 140 and 400 years are estimated by way of the two models if it is assumed that these earthquakes accommodate all of the coseismic slip on the interface. We use the global average of the coupling coefficient, because we have no direct constraints on this parameter for the Hikurangi subduction zone. A third model (fault names ending with BM in the Appendix) allows for the possibility that subduction zone earthquakes are great ($M > 8$), and therefore have much longer recurrence intervals (600–1200 years) if these earthquakes are assumed to accommodate all of the coseismic slip on the interface. The justification for this model is that earthquakes in the upper plate have produced large (11 m) displacements (e.g., 1931 M_w 7.8 Hawkes Bay earthquake; McGinty *et al.*, 2000), and these would be consistent with the stress regime of a strongly coupled subduction interface that slips with large single-event displacements. Furthermore, the short recurrence intervals calculated for the first two models (i.e., the WM and RM models) are in conflict with the absence of large subduction interface earthquakes in the historical record. If these first two models are viable, then we would expect there to have been at least one of these earthquakes on the five Hikurangi subduction interface segments in the last 150 years. In the Appendix, we combine the three models to develop a subduction interface earthquake model with a weighting scheme that gives the third model a weight equal to the combined weights of the first two models. The resulting recurrence intervals range from 600 to 2400 years for large to great Hikurangi subduction interface earthquakes.

For the Fiordland subduction zone (Figs. 1 and 2), we use the relative plate motion rates for the latitude of Fiordland along with a plate boundary model (Sutherland *et al.*, 2000; Sutherland, personal commun.) to estimate the locations, magnitudes, and recurrence intervals for Fiordland subduction interface earthquakes. In addition, the model provides estimates of the location and slip rate of other major active structures of the plate boundary, including the offshore continuation of the Alpine Fault and onshore faults east of Fiordland (Fig. 2). These onshore faults are in some cases defined from scattered field observations, but are generally not from detailed field studies. Other than the subduction zones, we define only a limited number of offshore faults sources in our PSH model, because data are largely unavailable for coverage of these faults in our model at the present time.

Distributed Seismicity Sources

We use the historical catalog of earthquakes (Fig. 3) to model the occurrence of moderate-to-large ($M \sim 5$ up to some maximum cutoff magnitude) distributed earthquakes both on and away from the major faults. Our reasons for considering distributed earthquakes in our PSHA are twofold. First, a large percentage of earthquakes in the historical record have not occurred directly on the mapped faults. They are presumably due to interseismic strain accumulation in areas between the major faults or due to displacements on unmapped or blind faults. Second, earthquakes of less than M 6.5 generally do not produce surface ruptures (e.g., Wesnousky, 1986) that contribute to the measureable (geological) displacement of the ground surface across the major faults. This occurs when the rupture widths of these earthquakes are less than the width of the fault plane. A good example of a distributed earthquake is the M_w 6.8 1994 Arthur's Pass earthquake, which occurred on a previously unknown fault and did not rupture to the surface.

We apply a methodology developed from that of Frankel (1995) to characterize the PSH from distributed earthquakes. We use the spatial distribution of seismicity recorded or documented by GNS and the Department of Scientific and Industrial Research (DSIR) since 1840 to estimate the likely locations and recurrence rates of distributed earthquakes at a gridwork of point sources across and beneath the country. Our minimum magnitude for distributed earthquakes (M 5.25) is slightly larger than the M 5.0 typically used in PSHA (the lower-bound magnitude for damaging ground motions); it is chosen to eliminate the erroneously high short-period accelerations predicted for $M <$ 5.25 earthquakes with the new attenuation model for New Zealand (McVerry *et al.*, 2000) M 5.25 was also used as the minimum magnitude for New Zealand by Matuschka *et al.* (1985).

We first divide the country into 37 seismotectonic zones (14 crustal and 23 deep zones enclosing the subsurface seismicity to a depth of 100 km; Fig. 3d,e). The maximum cutoff magnitude (M_{cutoff}) is estimated separately for the 37 seismotectonic zones, based on criteria such as the approximate magnitude of the largest historical earthquakes that cannot or have not been assigned to specific faults (e.g., the M_w 6.8 1994 Arthur's Pass earthquake), how comprehensively the zone has been studied to identify active faults (i.e., the completeness of the fault database in that zone), and the tectonic regime of the zone (e.g., a zone likely to enclose blind thrusts). The M_{cutoff} ranges from 7 to 7.8 for the seismotec-

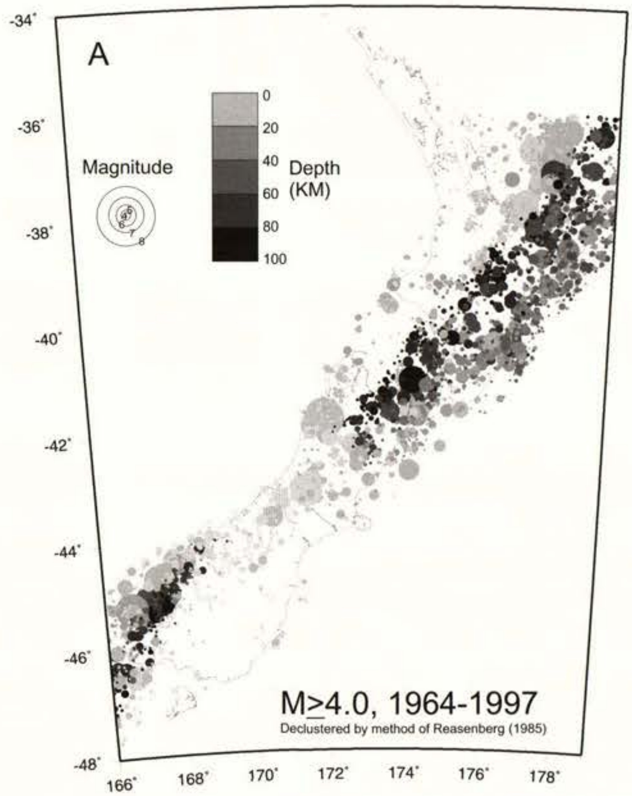

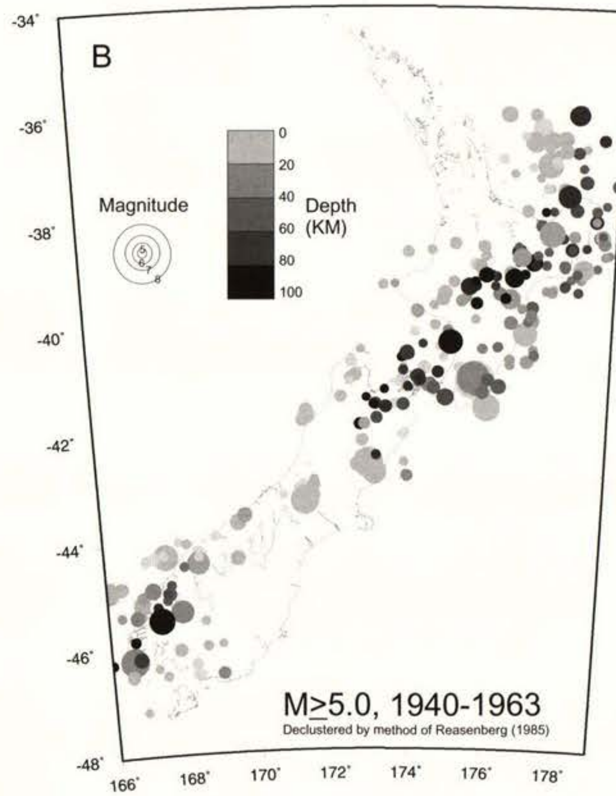

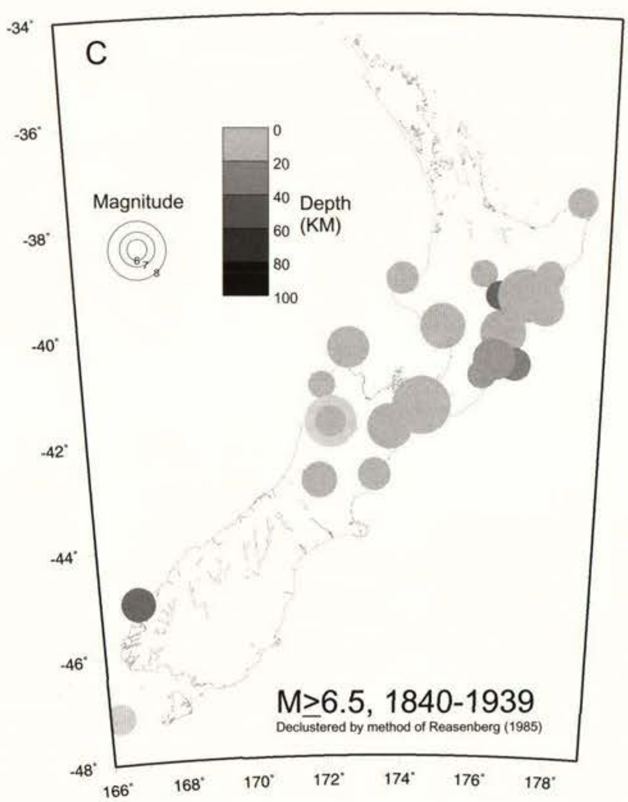

Figure 3. The three-dimensional distribution of historical seismicity in New Zealand, divided into the three completeness magnitudes and timespans used in the probabilistic seismic hazard model (a–c). We also show the surface projection of the 14 crustal and 23 deep (subduction) seismotectonic zones used to sort the catalog (d–e), assign initial regional maximum cutoff magnitudes (M_{cutoff}), and calculate parameter b of the Gutenberg–Richter relationship for seismicity. In the case of (e), many of the deep zones overlap in plan view, so we simply show a single outline that encompasses the surface projections of all North Island zones, and do the same for the South Island zones. *(continued)*

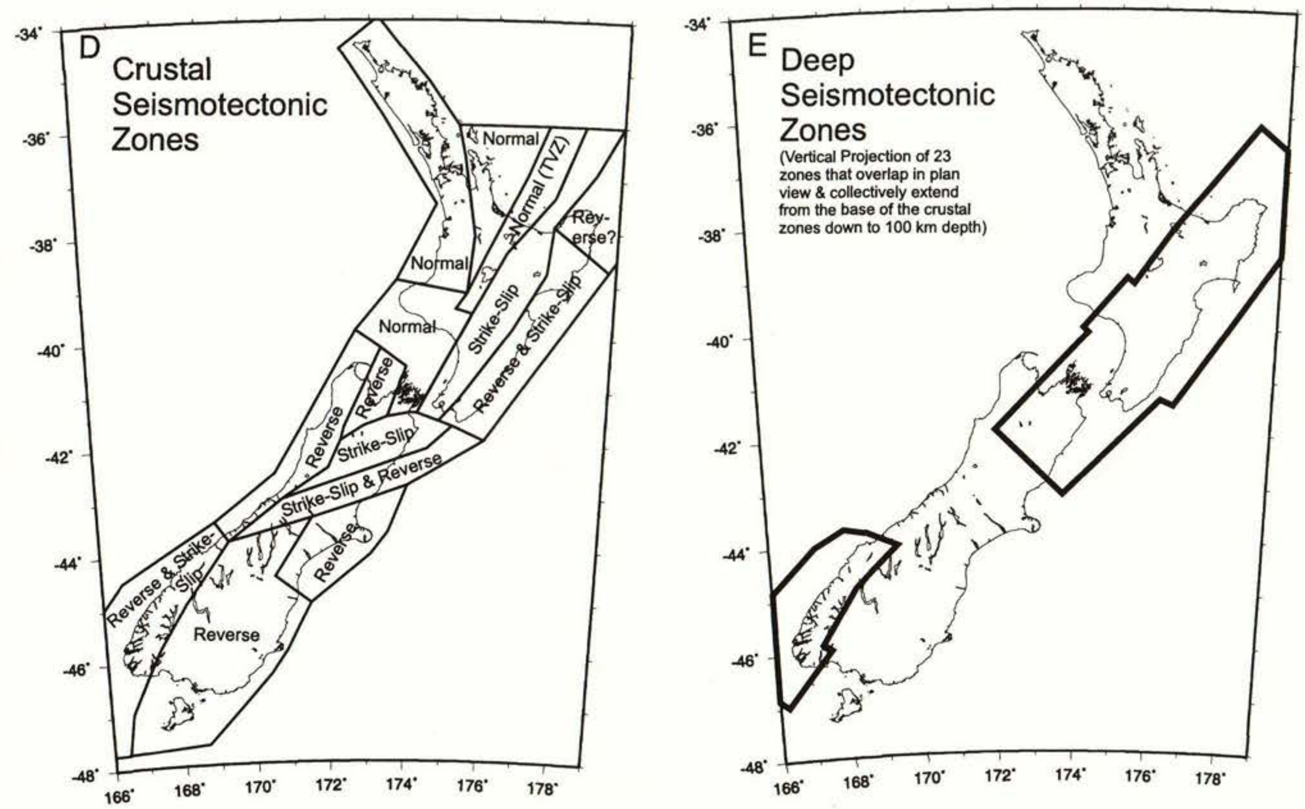

Figure 3. *(Continued)*

tonic zones (Fig. 3). The M_{cutoff} for all of the deep seismotectonic zones is set at 7, which is the approximate maximum magnitude observed for intraslab seismicity in New Zealand. The next step is to decluster the catalog by the method of Reasenberg (1985), and then use the method of McGinty (2001) to assign new depths to the restricted-depth earthquakes. Restricted-depth events are the large number of events in the catalog that were randomly assigned depths of 5, 12, and 33 km because of poor depth control.

The next step in our procedure is to subdivide the catalog according to the 14 crustal and 23 deep seismotectonic zones (Fig. 3), define five layers of point sources over the map area (at depths of 10, 30, 50, 70, and 90 km) with a spacing of 0.1° in latitude and longitude, and then use a Gutenberg–Richter distribution log N/yr $= a - bM$ (N/yr is the number of events per year greater than or equal to magnitude M, and a and b are empirical constants; Gutenberg and Richter, 1944) to estimate the recurrence rates of distributed earthquakes at each point source. Gutenberg and Richter found that this type of distribution of seismicity applied to large areas, and it has also been shown to describe the earthquakes that occur along a given fault zone that are smaller than the M_{max} of the fault (e.g., Stirling *et al.*, 1996). We use the SEISRISK program CALCRATE (Bender and Perkins, 1987; Hanson *et al.*, 1992) to calculate parameter b of the Gutenberg–Richter relationship for each seismotectonic zone, and that value of b is then assigned initially to each point source within the zone. CALCRATE, which is based on the methodology of Weichert (1980), allows the use of different magnitude completeness levels for various time periods to calculate parameter b. Because the New Zealand historical earthquake catalog is generally thought to be complete for $M \geq 4$ since 1964, $M \geq 5$ since about 1940, and $M \geq 6.5$ since 1840, we use these three completeness levels and time periods to calculate b for the zones. As with the b-values, the M_{cutoff} assigned initially to each point source is simply the M_{cutoff} of the enclosing seismotectonic zone.

After calculating the b-values, we count the earthquake epicenters found inside each grid cell (i.e., within ±10 km depth of the grid layer) to give N-values for the grid cell. Three N-values are calculated for each grid cell based on the three catalog completeness levels and time periods in the earthquake catalog; $N_1 = N(M \geq 4$ for 1964–1997), $N_2 = N(M \geq 5$ for 1940–1963), and $N_3 = N(M \geq 6.5$ for 1840–1939). Within each grid layer, the three sets of gridded N, b, and M_{cutoff} values are then spatially smoothed with a Gaussian smoothing function, following the methodology of Frankel (1995). For each grid cell, the smoothing involves multiplying the N, b, and M_{cutoff} values for the grid cell and all of the neighboring values within the particular grid layer (i.e., the values that are within a specified horizontal distance from the grid cell) by the Gaussian function, summing all of the products, and then dividing by the sum of all of the Gaussian functions. The equation is

$$N \text{ or } b \text{ or } M_{\text{cutoff}}(\text{smoothed}) = \frac{\sum[(N \text{ or } b \text{ or } M_{\text{cutoff}}(\text{each site}))\exp(-d^2/c^2)]}{\sum[\exp(-d^2/c^2)]}, \quad (5)$$

in which c is the correlation distance (50 km) and d is the distance from the center of the grid cell to the center of each neighboring grid cell (neighboring grid cells further than three times the correlation distance from the grid cell are not used in equation 5). The Gaussian smoothing preserves the total number of earthquakes in the catalog after every N-value in the gridwork has been smoothed with equation 5. The 50-km correlation distance is used, because it has been found to produce a spatial distribution of N-values that correlates well with the general seismicity patterns across the country (Stirling *et al.*, 1998). No smoothing is done in the vertical axis (i.e., between the various grid layers). The recurrence rates of M 5.25–M_{cutoff} events at each point source are then calculated from the three sets of smoothed N-values by way of the following maximum likelihood method to give a Gutenberg–Richter a-value based on the entire catalog:

$$a = \log [(N_1 + N_2 + N_3)/(\text{tb1} + \text{tb2} + \text{tb3})], \quad (6)$$

in which tb1 = ctime1 $\times 10^{(-\text{magmin1} \times b)}$, tb2 = ctime2 $\times 10^{(-\text{magmin2} \times b)}$, tb3 = ctime3 $\times 10^{(-\text{magmin3} \times b)}$, and ctime1 = 1997 − 1964, ctime2 = 1964 − 1940, and ctime3 = 1940 − 1840.

The a-value is then used in the Gutenberg–Richter relationship (this time equal to $\log N/\text{yr} = a - bM$) to solve for $N/\text{yr}(M \geq 4)$, and then the incremental rates ($n/\text{yr} = M$) are calculated for each 0.1 increment of magnitude from M 5.25 to M_{cutoff}. We show plots of the $N/\text{yr}(M \geq 4)$ and b-value for the five depth layers and M_{cutoff} for the 10-km (crustal) layer in Figure 4. Because M_{cutoff} is set to 7 for all of the deeper zones, we do not show the M_{cutoff} for these zones.

Our methodology for the treatment of distributed seismicity is an improvement over the commonly used approach in PSHA of defining large area source zones over a region and uniformly distributing the seismicity recorded inside each source across the source. This is because our methodology preserves the smooth transitions in seismicity rates within and across the boundaries of the seismotectonic zones and avoids the edge effects that often appear on hazard maps when adjacent area sources enclose areas of significantly different seismicity rates. Our methodology builds on the Frankel methodology (Frankel, 1995; Frankel *et al.* 1996), which was limited to one crustal and one subcrustal layer of point sources, combined the different completeness levels of seismicity catalogs by way of a subjective weighting scheme (compare our use of a maximum-likelihood method to combine the different completeness levels), and assumed a single b-value and M_{cutoff} across large regions (e.g., the entire eastern USA in the example shown in Frankel, 1995). The Stirling *et al.* (1998) adaptation of the Frankel (1995) methodology to New Zealand considered only one (crustal) layer of point sources (i.e., only one depth layer of point sources), a single catalog completeness level ($M \geq 4$ for the period 1964–1996), single M_{cutoff} (7.5), and single b-value (1.1) for the entire country.

A final adjustment to our distributed seismicity model is to assign a minimum floor rate of 8×10^{-4} events per year of $M \geq 4$ to each $0.1^\circ \times 0.1^\circ$ grid cell that has rates less than this value. This is chosen as the lowest seismicity rate that can be detected with 90% certainty in the 33-year completeness period for $M \geq 4$ from a 50-km radius circle (i.e., radius equal to the 50-km correlation distance c in equation 5 above).

Attenuation Model

The attenuation relationships used in this study have been developed recently by McVerry *et al.* (2000) for 5% damped acceleration response spectra (SA(T)) from a data set of New Zealand earthquake records, supplemented by PGA values from overseas records (1995 Kobe and 1994 Northridge earthquake data in particular) in the near-source range (less than 10 km source-to-site distance) that are lacking in the New Zealand data. The attenuation model takes account of the different tectonic types of earthquakes in New Zealand (i.e., crustal, subduction interface, and dipping slab) and their range of centroid depths. The attenuation expressions for crustal earthquakes have further subdivisions, through mechanism terms, for different types of fault rupture (strike-slip, normal, oblique–reverse, and reverse). The model was developed for site classifications based on those of the current New Zealand Loadings Standard NZS4203:1992 (Standards New Zealand, 1992), with one modification of the site classifications to give better matching of the New Zealand spectra and a subdivision of the rock classification for specialist applications. A term was also included in the attenuation expression to model the rapid attenuation of high-frequency motions through the Taupo Volcanic Zone (McVerry *et al.*, 2000).

The McVerry *et al.* attenuation model is used in this study because it has specific relevance to New Zealand conditions, in contrast to most other available attenuation relationships, which were developed using data from other regions of the world. The functional form of the McVerry *et al.* model for crustal earthquakes is based on the Abrahamson and Silva (1997) model; the Youngs *et al.* (1997) model was the base model used to develop the McVerry *et al.* model for subduction zone earthquakes. All PSH maps in this paper are for McVerry *et al.*'s site class B, a class best described as stiff-soil sites, or rock sites mantled by more than 3 m of soil.

For comparison, we show in Figure 5 response spectra for a M 7.5 crustal earthquake at a distance of 10 km from

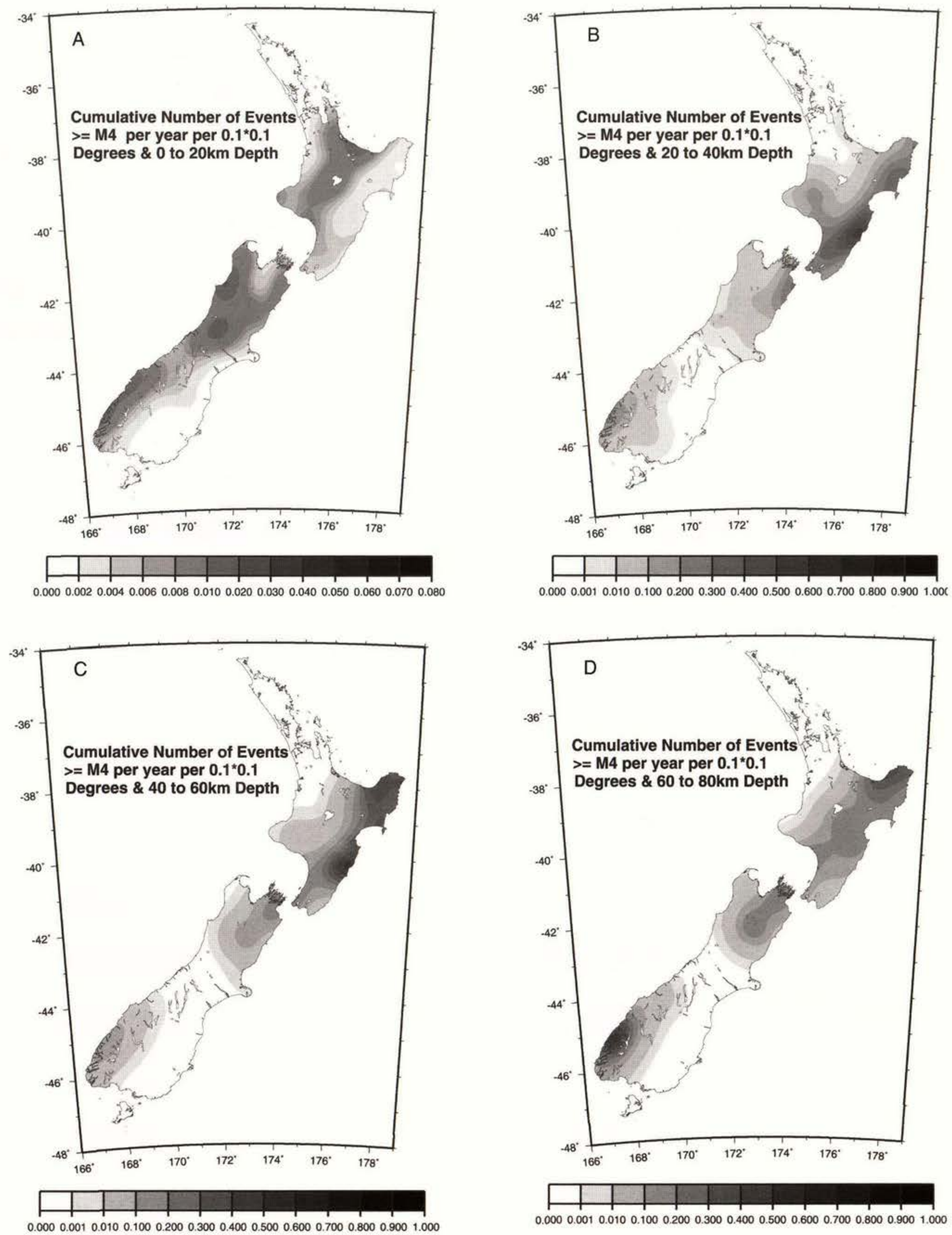

Figure 4. (*Caption on page 1889.*)

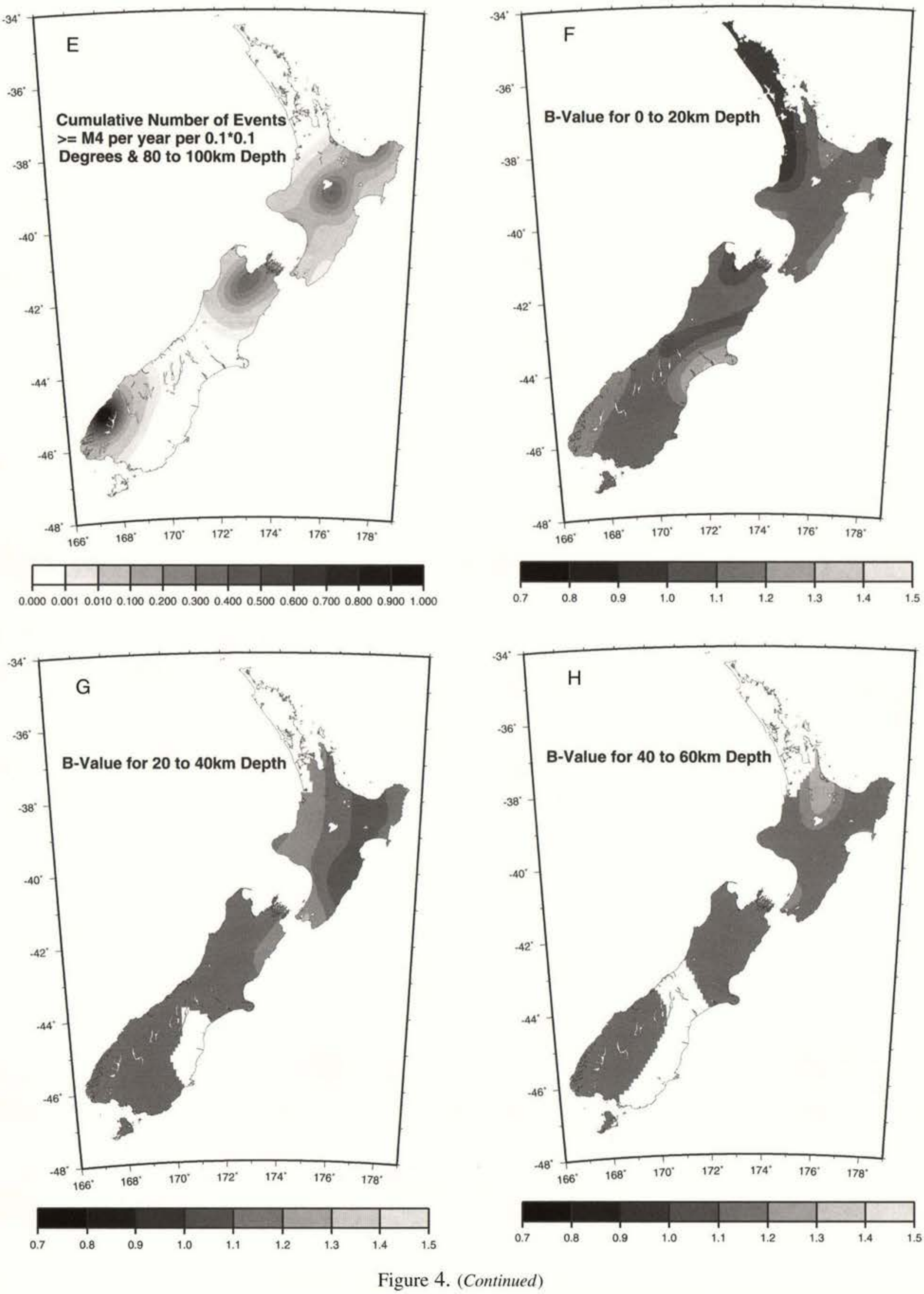

Figure 4. *(Continued)*

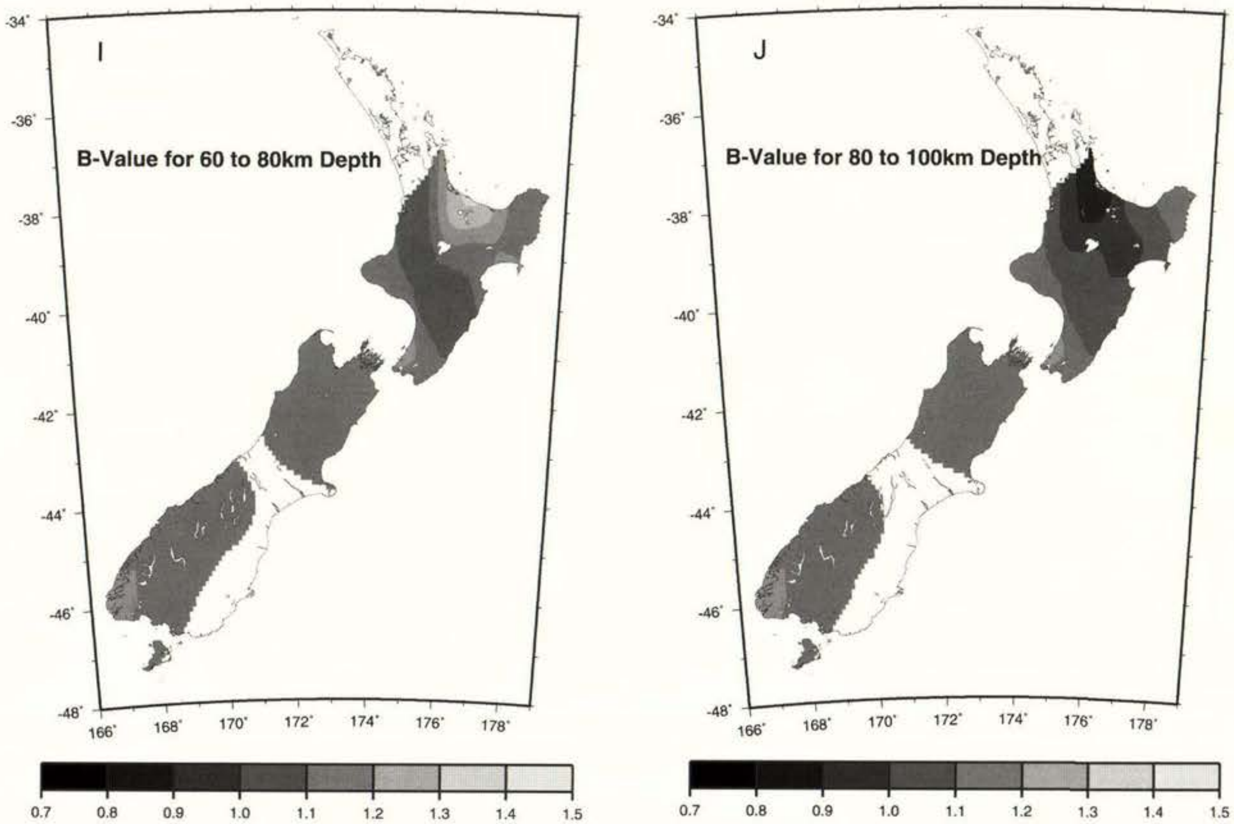

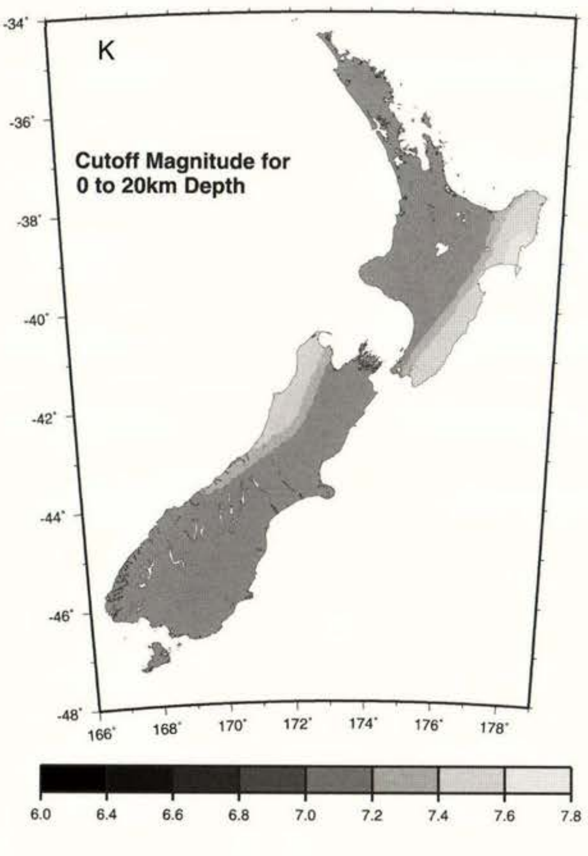

Figure 4. (a–e) Contours of the maximum-likelihood cumulative number of events per year for $M \geq 4$, calculated from three catalog completeness levels and magnitudes ($M \geq 4$ since 1964, $M \geq 5$ since 1940, and $M \geq 6.5$ since 1840); (f–j) parameter b of the Gutenberg–Richter relationship $\log N = A - bM$; and (k) the maximum cutoff magnitude (M_{cutoff}) assumed for distributed earthquakes, for various depth layers beneath the country. The contours have been made over a gridwork of N, b, and M_{cutoff} that have been smoothed with a Gaussian smoothing function, in which the correlation distance (standard deviation) is set to 50 km. Because M_{cutoff} for all of the deep seismotectonic zones is set to 7, we show a contour plot of M_{cutoff} only for the crustal (20 km) depth layer.

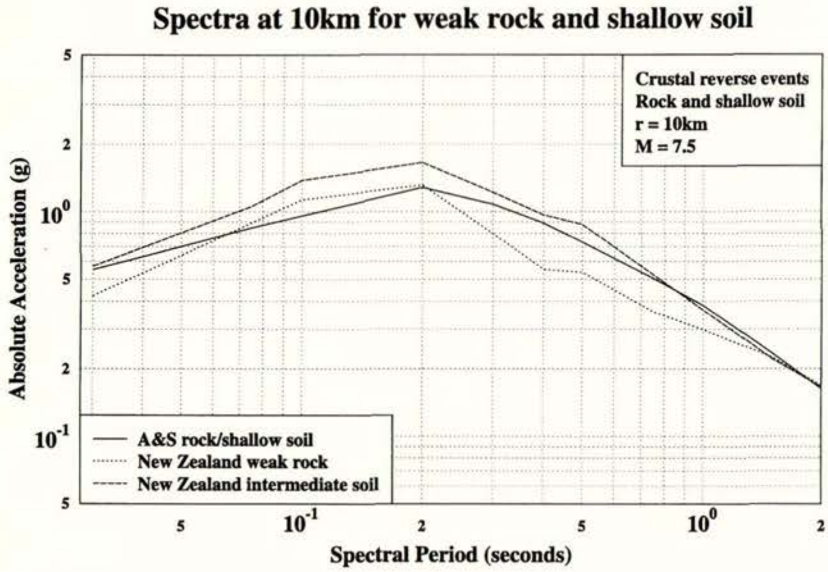

Figure 5. Response spectra for the New Zealand attenuation model (McVerry *et al.*, 2000) and the equivalent spectrum from Abrahamson and Silva (1997).

the McVerry *et al.* model and from the Abrahamson and Silva (1997) model. We show spectra for weak rock and intermediate soil (the latter being the site conditions assumed in this paper) from the McVerry model and the rock–shallow soil spectrum from Abrahamson and Silva (1997), because the latter spectrum is effectively intermediate between the two former spectra.

Hazard Calculation

We use the locations, sizes, tectonic type or crustal mechanism, and recurrence rates of earthquakes defined in our source model to estimate the PSH for a gridwork of sites with a grid spacing of 0.1 degrees in latitude and longitude. Our measures of PSH are the acceleration levels (PGA; 5% damped response spectral acceleration at 0.2 and 1s period) with 475-year and 1000-year return periods at class B (intermediate soil) sites. We use the standard methodology of PSHA (Cornell, 1968) to construct PSH maps. For a given site, we (1) calculate the annual frequencies of exceedance for a suite of ground motion levels (i.e., develop a hazard curve) from the magnitude, recurrence rate, earthquake type, and source-to-site distance of earthquakes predicted from the source model; and (2) estimate the maximum acceleration level that is expected to be exceeded in 10, 50, and 105 years, each with a 10% chance of happening. These time periods and probabilities are chosen to show the accelerations that have return periods of 150, 475, and 1000 years, respectively. For each site, step 1 is repeated for all sources in the source model, and the step 2 estimate is calculated by summing the results of step 1 to give the annual frequencies of exceedance for a suite of acceleration levels at the site due to all sources and finding the ground motion levels that correspond to annual frequencies of 1/150, 1/475, and 1/1000.

We assume a Poisson model of earthquake occurrence for the ground motions expected in a certain time period. These estimates are based on the average time-independent rate of earthquake occurrence on each fault. Our calculation of ground motions follows the standard practice of modern PSHA and accounts for the uncertainty in estimates of ground motion from the McVerry *et al.* (2000) attenuation model in the calculation of PSH (up to 3 standard deviations below and above the median). Only magnitudes 5.25 and greater are included in the hazard analysis.

Because the McVerry *et al.* attenuation model has separate expressions for crustal earthquakes of different slip type (i.e., strike slip, normal and reverse, and slip types intermediate between these extremes) and for subduction interface, shallow subduction slab and deep slab earthquakes, we estimate accelerations applicable to the slip type and tectonic environment of each earthquake source. Each fault is assigned a particular slip type, and the attenuation expression for that slip type is used for the fault in the hazard calculations. In the case of the dipping subduction interface sources, we use the interface attenuation expression. For the distributed seismicity (point) sources, the slip type assigned to the point source is the slip type of the enclosing seismotectonic zone (Fig. 3d,e). For the deep zones we simply use the shallow and deep slab expressions of the model, based on the observation that essentially all of the deep seismicity in the country is attributed to the dipping Hikurangi and Fiordland slabs. Application of the volcanic-path attenuation expression for the TVZ, which strongly reduces accelerations with distance, is approximately limited to faults and point sources located within the TVZ, taken as corresponding to the zone labeled Normal (TVZ) in Figure 3d. We apply this to the whole path length for earthquakes in this zones, rather than just the part of the path contained within the TVZ.

Results

In Figure 6a–g we show maps of the levels of PGA and 5% damped response spectral acceleration (0.2- and 1-sec

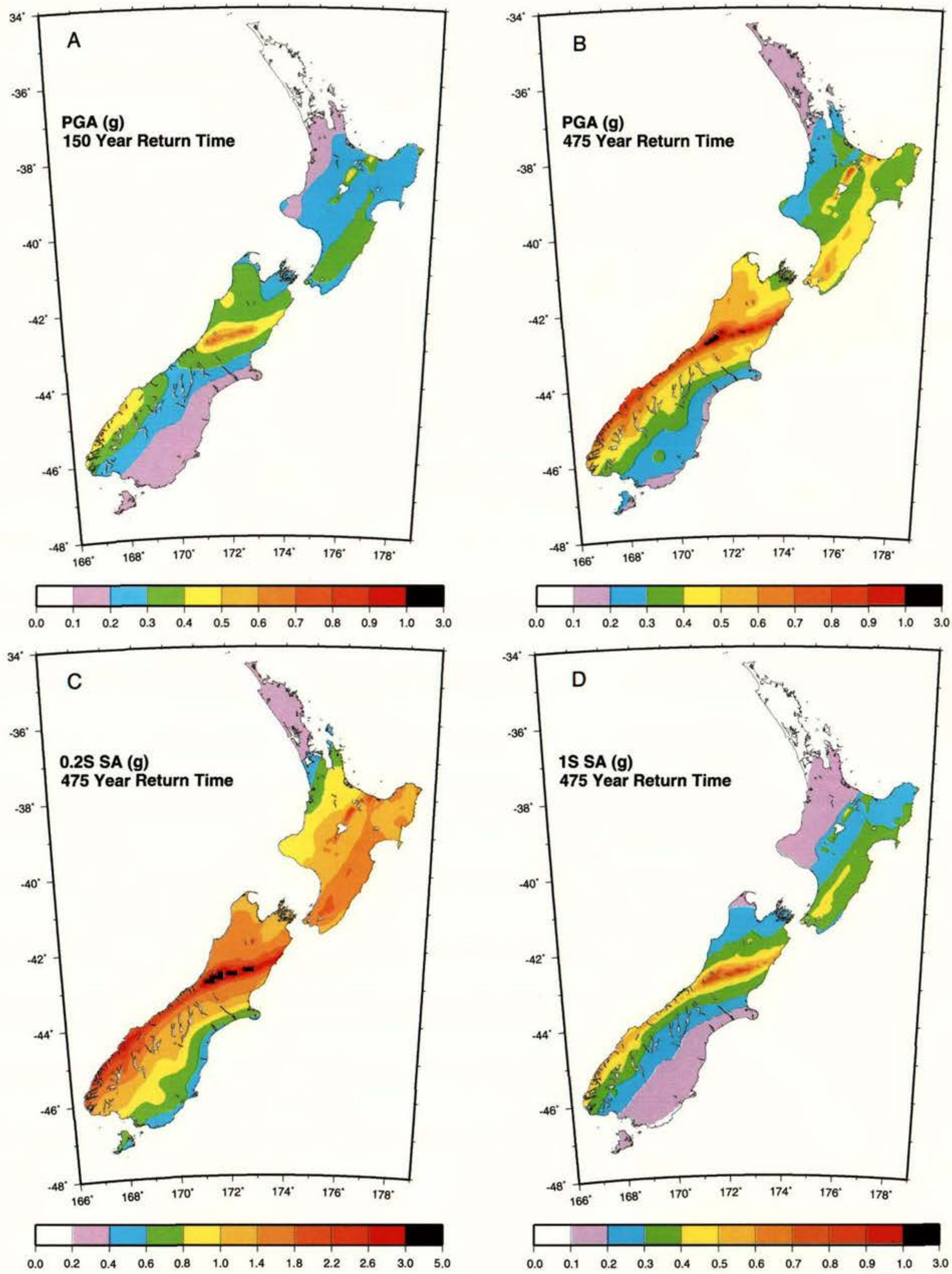

Figure 6. (a–g). Probabilistic seismic hazard maps for New Zealand for site class B (intermediate soil). The maps show the levels of peak ground acceleration (PGA) and 5% damped response spectral acceleration (0.2 and 1 sec period) with return periods of 150 years (10% probability in about 10 years; PGA only), 475 years (i.e., 10% probability in 50 years), and 1000 years (10% probability in 105 years). Also shown are the 475-year levels of PGA that are estimated after including conditional probabilities for great earthquakes on the Alpine Fault (map h only). See the text for further explanation.

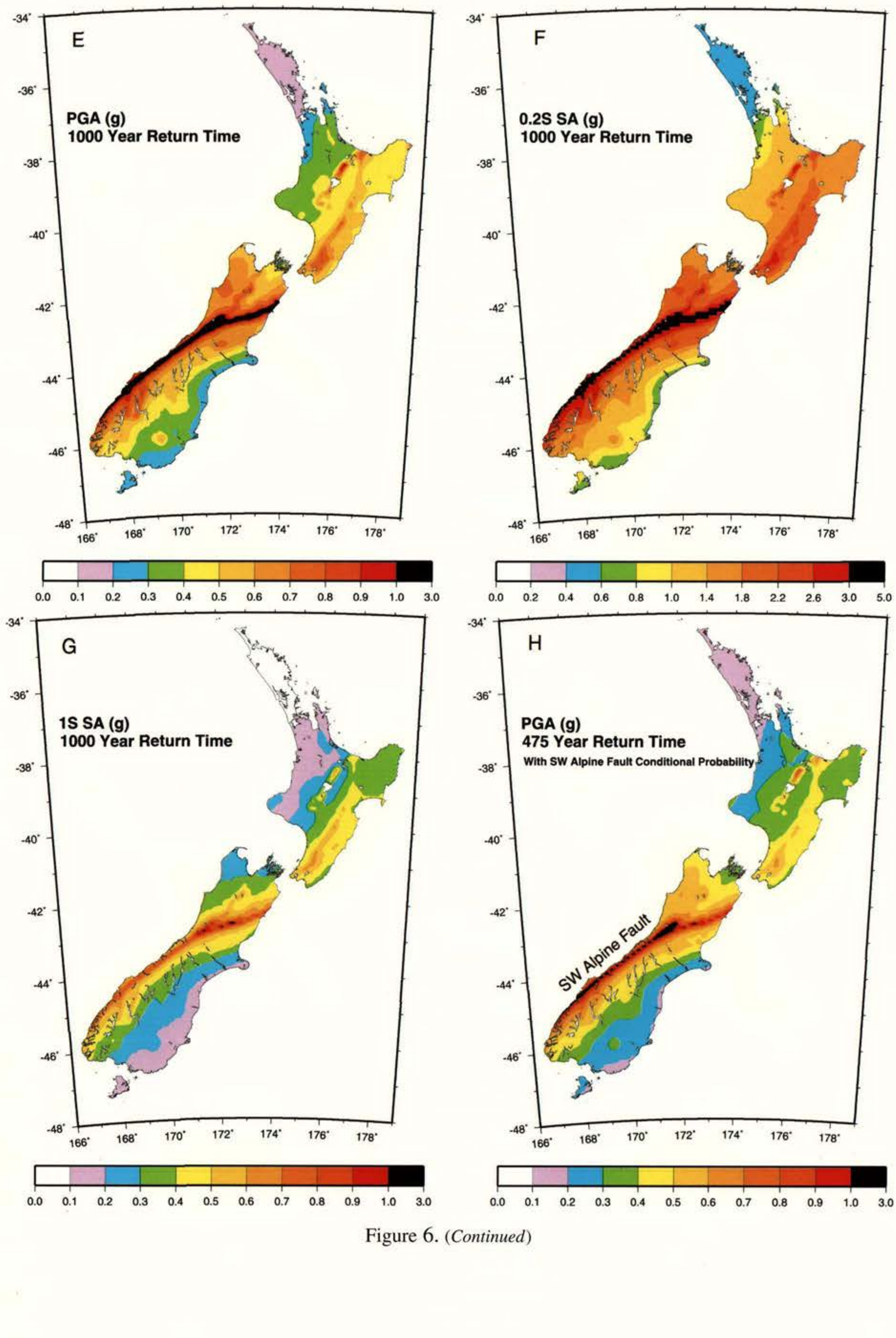

Figure 6. (*Continued*)

period) with return periods of 150 years (PGA only), 475, and 1000 years (10% probability of exceedance in 10, 50, and 105 years, respectively). The 150-year return period map (Fig. 6a) generally shows the highest levels of hazard where the heaviest concentrations of crustal seismicity are located (central and southwestern New Zealand) and also where the heaviest concentrations of deeper subduction zone seismicity are located (primarily in the southern North Island). Figures 4b and 6a illustrate the correlation between seismicity rates at the 20 to 40 km depth and the levels of PGA. The latter observation demonstrates that including deeper intraslab seismicity in the PSH can have a significant influence on hazard in areas above the Hikurangi subduction zone. The only area where active fault sources significantly influence the 150-year return time hazard is in the central west of the South Island, where a number of major faults (e.g., Hope and Alpine Faults) have short recurrence intervals and lie in close proximity to one another.

In contrast to the 150-year return period maps (Fig. 6b–g), the 475- and 1000-year return period maps allow sources of longer recurrence interval to contribute to the hazard. The result is a suite of maps that show an overwhelming dominance of active fault sources over distributed seismicity sources in controlling the hazard. In the South Island, the highest accelerations occur in the west along the Alpine Fault and again in the central west of the South Island (Fig. 2). The highest accelerations in the North Island occur along the northeast striking faults of the Axial Tectonic Belt and TVZ, again where the greatest concentrations of active faults are located. The contribution to the hazard from the Hikurangi subduction zone is to produce a broad zone of relatively high hazard from the TVZ to the east coast. The 475- and 1000-year return period maps generally show a smooth distribution of hazard that is highest along the major plate boundary faults of the axial tectonic belt and the subduction zones and progressively decreasing away from these areas. This is a broadly similar pattern of hazard to the PSH maps of Stirling *et al.* (1998) (Fig. 7). Notable differences in our new maps occur in the easternmost North Island, and are due to differences in modeling of the Hikurangi subduction interface in the two studies. The other large difference is that the hazard in the TVZ is lower than in Stirling *et al.* (1998). This is due to major differences in modeling of the TVZ faults between the two studies and to implementation of the volcanic path attenuation relationship in this study. The new maps show significantly different patterns compared with the much older maps of Matuschka *et al.* (1985) and Smith and Berryman (1986) (Fig. 8).

Several areas of anomalously high hazard on the 475- and 1000-year return time maps interrupt the otherwise smooth distribution of hazard across the country. Some of these are attributed to very short recurrence intervals calculated for active faults with equations (1) to (4). The area of highest hazard in the central west of the South Island (the blackest areas in Fig. 6a–g) is attributed to the combined effects of intersecting and overlapping rupture segments of the Alpine Fault, and other faults that intersect the Alpine Fault in this area (Fig. 2 and Appendix). The small area of anomalously high hazard in the southeast of the South Island is due to the short recurrence intervals calculated with equation (4) for the Blue Mountain and Spylaw Faults (fault sources 162 and 163 in the Appendix and Fig. 2). These short recurrence intervals may not be realistic, given that the surrounding Otago region is one of low tectonic activity and these faults are not considered to be the most active in the region. Short recurrence intervals could theoretically arise from underestimation of the fault lengths, which in turn results in underestimation of seismic moment (M_o) from M_{max} with the regression of magnitude on fault area from Wells and Coppersmith (1994). Potential issues such as these will focus some of our efforts for future versions of the New Zealand national seismic hazard model.

For comparison, we also show in Figure 6h a map of the 475-year PGAs estimated after incorporating conditional probabilities for great earthquakes on the Alpine Fault (Milford–Haupiri segment; see Fig. 2 and the Appendix) from Rhoades and Van Dissen (2000). The recurrence interval for rupture of this section of the Alpine Fault is estimated to be about 300 years, and just over 280 years have elapsed since the last event (Rhoades and Van Dissen, 2000). Comparison of Figures 6h and 6b indicates an increase in the 475-year PGA from about 0.8 g to greater than 1 g when the conditional probabilities are incorporated.

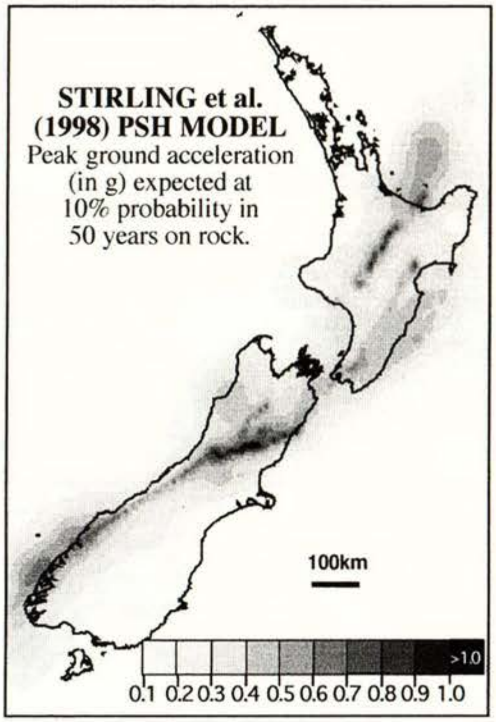

Figure 7. Probabilistic seismic hazard map from the Stirling *et al.* (1998) analysis. The map shows the peak ground acceleration expected with a return period of 475 years (10% probability in 50 years).

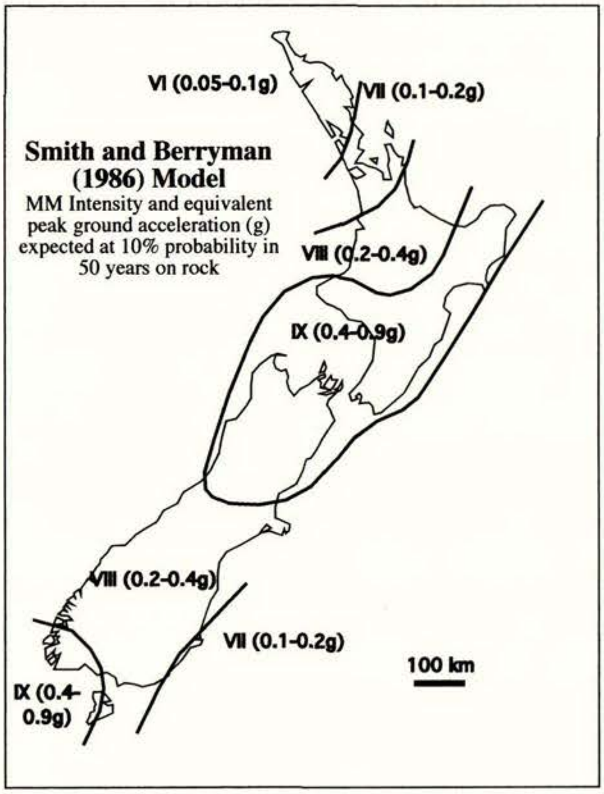

Figure 8. Probabilistic seismic hazard map from the Smith and Berryman (1986) analysis. The map shows the peak ground acceleration (converted from Modified Mercalli Intensity) expected with a return period of 475 years (10% probability in 50 years).

In addition to defining maps of the expected levels of PGA and spectral accelerations for New Zealand, we also compare the PSH model at five sites from diverse seismotectonic environments around the country (Fig. 9). The sites are the four major centers (Auckland, Wellington, Christchurch, and Dunedin; Figs. 1 and 2), which respectively come from areas of low, high, low, and low concentrations of active faults and historical seismicity. For comparison, we also examine the hazard of Otira township, not because it is a major center, but because it is located in the area of highest hazard in the country (compare Figs. 1 and 6b–g). In Figure 9 we show PGA hazard curves (graphs of the annual rate of exceedance for a suite of PGA levels) for the five centers. The graphs show more than a factor-of-10 to factor-of-100 range in annual rate for a given acceleration between the five centers, and about a factor-of-10 range in acceleration for a given annual rate. Clearly, the township of Otira shows the highest hazard, consistent with a location close to several major active faults (e.g., Alpine Fault; Figs. 1 and 2) and within an area of relatively high historical seismicity (Fig. 3). In decreasing order of hazard are the centers of Wellington (close to five major faults, above the Hikurangi subduction interface, and in an area of high historical seismicity), Christchurch (at a distance of about 50 km from a number of active faults in the foothills of the Southern Alps), and Dunedin and Auckland (both far from areas of active faults and in areas of relatively low seismicity rates). The presence of the Akatore Fault close to Dunedin (fault source 280 in Fig. 2 and Appendix), modeled as producing *M* 7.1 earthquakes with an average recurrence interval of 3000 years, causes Dunedin's estimated PGA hazard at low frequencies of exceedance to be similar to that of Christchurch.

Lastly, we illustrate the significant effect that including active fault sources in our PSH model will have on the building code, by comparing our response spectrum for Wellington (475-year return period) with the equivalent spectrum derived from the older Matuschka *et al.* (1985) model. In Figure 10 we show that our accelerations for SA(0.1 sec) to SA(0.3 sec) are about 1.3 times greater than the older Matuschka *et al.* model. These differences tend to be largest in

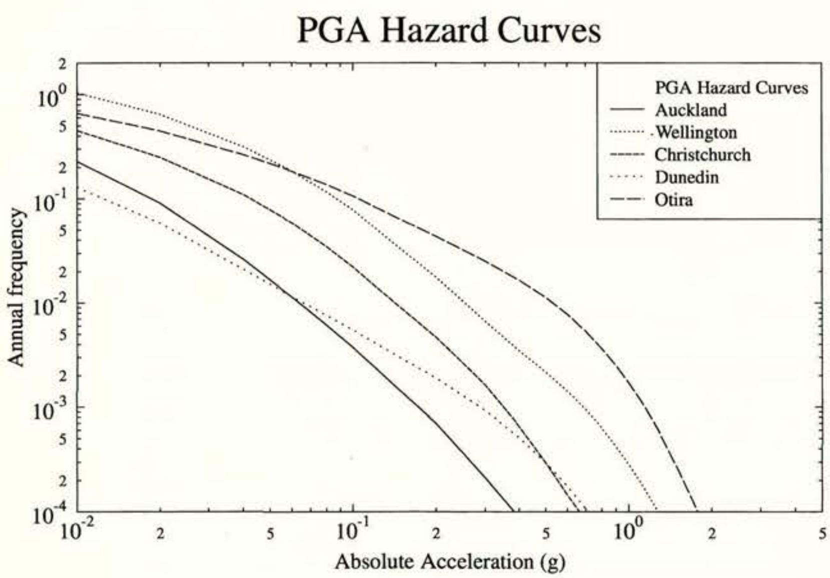

Figure 9. Seismic hazard curves for site class B of the annual rate of exceedance for various levels of PGA for the centers of Auckland, Wellington, Christchurch, Dunedin, and Otira (see Fig. 1 for the locations of these centers). Otira is included in the plots as a useful comparison to the main centers, since it is located in the area of highest hazard in the country (compare Figs. 1 and 6a–g). The plots are constructed according to the Poissonian hazard calculations (i.e., Figs. 6a, b, and e) and so do not include the conditional probabilities for Alpine Fault earthquakes shown in Fig. 6h.

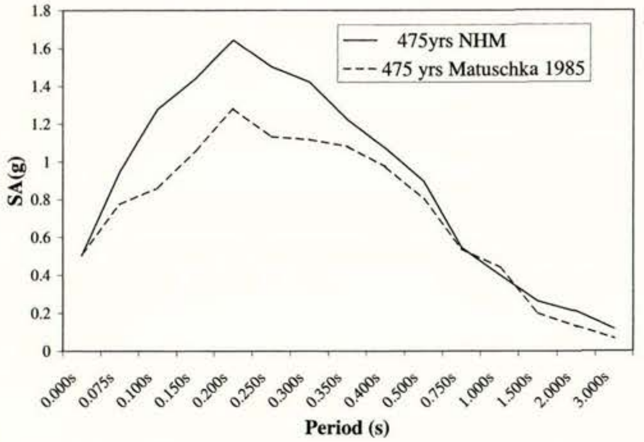

Figure 10. Comparison of our new hazard model's (NHM) 475-year return period spectrum for Wellington city, the capital city of New Zealand, with the equivalent Matuschka *et al.* (1985) spectrum. Acceleration estimates for our spectrum range up to a factor of 1.3 greater than the Matuschka *et al.* spectrum.

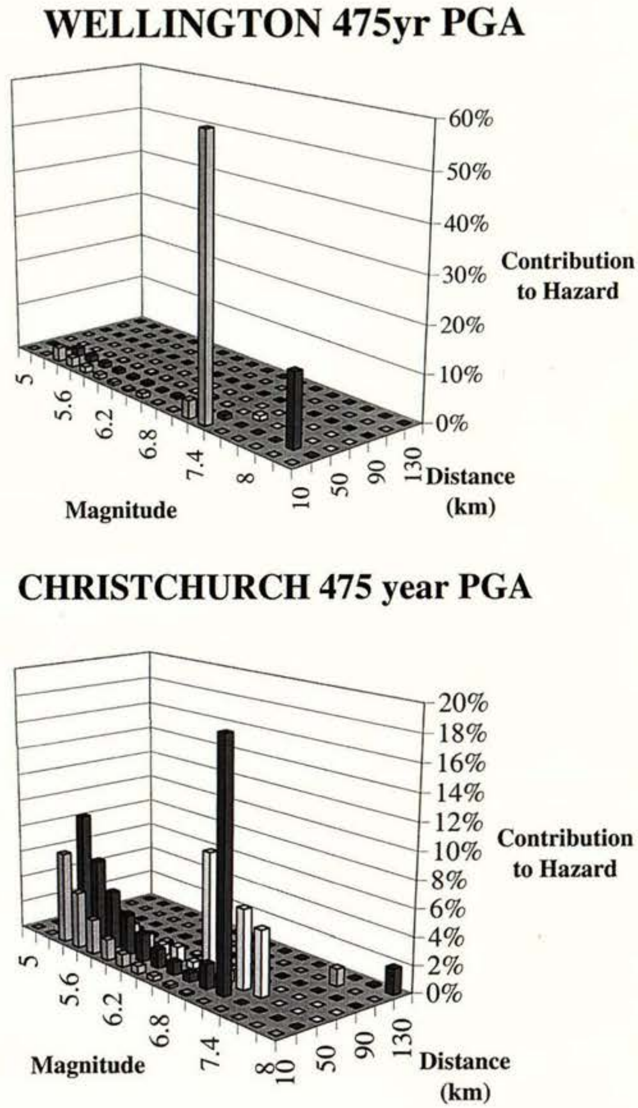

Figure 11. Disaggregation plots for Wellington and Christchurch. The plots show the contribution to hazard (in this case the 475-year PGA; Figs. 6b and 9) from the different magnitude and distance categories of earthquake sources in the probabilistic seismic hazard model. The plots are constructed according to the Poissonian hazard calculations (i.e., Fig. 6b) and so do not include the conditional probabilities for Alpine Fault earthquakes shown in Fig. 6h.

the areas close to the major active faults of the plate boundary (especially in the western South Island) and smallest in the areas away from the plate boundary (the far north and south of the country). We also illustrate the significance of including fault sources in our PSH model with disaggregation graphs for Wellington and Christchurch (Fig. 11). The graphs show that about 60% of the 475-year PGA in Wellington is produced by the Wellington Fault (the highest peak on the graph for Wellington), and that 20% is produced by the Hikurangi subduction interface (the second highest peak at $M > 8$). The distributed seismicity sources contribute most of the remaining 20%. In Christchurch, fault sources contribute a total of about 40% to the 475-year PGA (the peaks at $M > 6.8$), and distributed seismicity contributes the remaining 60%. These disaggregation plots provide important information on the design or scenario earthquakes most likely to affect the two cities at the 475-year level of hazard.

Summary and Conclusions

We have developed a new probabilistic seismic hazard model for New Zealand. An important feature of the new model is the application of new methods for the treatment of historical (distributed) seismicity data. The methodology combines the modern method of defining continuous distributions of seismicity parameters (e.g., Frankel, 1995) with the traditional method of defining seismicity parameters for large area sources (e.g., Smith and Berryman, 1986; Algermissen *et al.*, 1990). It provides a means of including deep (subduction zone) seismicity in a PSHA, preserves the finer-scale spatial variations of seismicity rates, avoids the undesirable edge effects produced in the traditional method when adjacent area sources enclose areas of significantly different seismicity rates, and also enables parameters most reliably defined at a regional scale (parameter *b* and maximum cutoff magnitude of Gutenberg–Richter distribution, and slip type) to be incorporated into the PSHA. The PSHA combines the modeled seismicity data with geological data describing the location and earthquake recurrence behaviour of 305 active faults and incorporates new attenuation relationships for peak ground acceleration and spectral acceleration developed specifically for New Zealand. The resulting PSH maps show the highest hazard to occur from the southwest to northeast ends of the country, along the axis of the plate boundary. The maps are currently being used to revise the building code for the country, which has long been based on PSHAs that did not explicitly include individual faults as earthquake sources.

Acknowledgments

The financial support of the Foundation for Research, Science and Technology and the Earthquake Commission Research Foundation in developing this PSH model is gratefully acknowledged. We thank the journal reviewers Chris Cramer and Donald Wells for their helpful comments on the manuscript, and GNS scientists Hugh Cowan and Judith Zachariasen for their internal reviews. Numerous people deserve acknowledgement for their technical input to this study. GNS colleagues, in particular Peter McGinty, Pilar Villamor, Russ Van Dissen, Rupert Sutherland, Martin Reyners, Terry Webb, Julian Garcia (visiting researcher) and John Zhao, deserve special thanks. Jarg Pettinga and Mark Yetton of the University of Canterbury and Peter Kingsbury (Environment Canterbury) are also thanked for their contributions to the fault database in the central South Island. Philip Barnes (National Institute of Water and Atmospheric Research, New Zealand) is thanked for contributing some offshore fault data to the model. Our U.S. collaborators Norm Abrahamson, Paul Somerville, and Nancy Smith contributed to the development of the New Zealand response spectrum attenuation relation. We also thank the participants of the workshops held in Wellington, Auckland, and Christchurch in mid 2000. Their positive feedback gave us the confidence to publish our model as 'the' New Zealand seismic hazard model, and their constructive criticism will form the basis for significant future developments of the model. Finally, I (M.W.S.) wish to dedicate this paper to my dearest mother Joyce, who finally lost a long battle with her ailing heart in October 2001. She was my mentor, motivator, and inspiration throughout my formative years, and I would not be in the absorbing and fulfilling world of scientific research if things were different. She is gone, greatly missed, and will never be forgotten.

References

Abe, K. (1975). Reliable estimation of the seismic moment of large earthquakes, *J. Phys. Earth* **23,** 381–390.

Abrahamson, N. A., and W. J. Silva (1997). Empirical response spectral relations for shallow crustal earthquakes, *Seism. Res. Lett.* **68,** 94–127.

Aki, K., and P. G. Richards (1980). *Quantitative Seismology: Theory and Methods*, W.H. Freeman, San Francisco.

Algermissen, S. T., D. M. Perkins, P. C. Thenhaus, S. L. Hanson, and B. L. Bender (1990). Probabilistic earthquake acceleration and velocity maps for the United States and Puerto Rico, U.S. Geol. Surv. Misc. Field Studies Map MF-2120.

Beanland, S., A. Melhuish, A. Nicol, and J. Ravens (1998). Structure and deformational history of the inner forearc region, Hikurangi subduction margin, New Zealand, *N. Z. J. Geol. Geophys.* **41,** 325–342.

Bender, B., and D. M. Perkins (1987). Seisrisk II: A computer program for seismic hazard estimation, U.S. Geol. Surv. Bull. 1772.

Berryman, K. R., and S. Beanland (1988). The rate of tectonic movement in New Zealand from geological evidence, *Trans. Inst. Profess. Eng. N. Z.* **15,** 25–35.

Berryman, K. R., S. Beanland, A. F. Cooper, H. N. Cutten, R. J. Norris, and P. R. Wood (1992). The Alpine Fault, New Zealand: variation in Quaternary structural style and geomorphic expression, *Ann. Tectonicae* **6** (suppl.), 126–163.

Berryman, K. R., R. F. Cooper, R. J. Norris, R. Sutherland, and P. Villamor (1998). Paleoseismic investigation of the Alpine Fault at Haast and Okuru, Geological Society of New Zealand and New Zealand Geophysical Society Joint Annual Conference, Programme and Abstracts, Geological Society of New Zealand Misc. Publ. **101A,** 44.

Cole, J. W., and K. B. Lewis (1981). Evolution of the Taupo–Hikurangi subduction system, *Tectonophysics* **72,** 1–21.

Cornell, C. A. (1968). Engineering seismic risk analysis, *Bull. Seism. Soc. Am.* **58,** 1583–1606.

DeMets, C., R. G. Gordon, D. F. Argus, and S. Stein (1994). Effect of recent revisions to the geomagnetic time scale on estimates of current plate motion, *Geophys. Res. Lett.* **21,** 2191–2194.

Frankel, A. (1995). Mapping seismic hazard in the central and eastern United States, *Seism. Res. Lett.* **66,** 8–21.

Frankel, A., C. Mueller, T. Barnhard, D. Perkins, E. V. Leyendecker, N. Dickman, S. Hanson, and M. Hopper (1996). *National Seismic Hazard Maps, June 1996 Documentation. U.S. Geol. Surv. Open-File Rept 96–532.*

Gutenberg, B., and C. F. Richter (1944). Frequency of earthquakes in California, *Bull. Seism. Soc. Am.* **34,** 185–188.

Hanks, T. C., and H. Kanamori (1979). A moment magnitude scale, *J. Geophys. Res.* **84,** 2348–2350.

Hanson, S. L., Thenhaus, P. C., Chapman-Wilbert, M. and Perkins, D. M. (1992). *Analyst's Manual for USGS Seismic Hazard Programs Adapted to the Macintosh Computer System, U.S. Geol. Surv. Open-File Rept. 92–529.*

Hyndman, R. D., M. Yamano, and D. A. Oleskevich (1997). The seismogenic zone of subduction thrust faults, *Island Arc* **6,** 244–260.

Matuschka, T., K. R. Berryman, A. J. O'Leary, G. H. McVerry, W. M. Mulholland, and R. I. Skinner (1985). New Zealand seismic hazard analysis, *Bull. N.Z. Soc. Earthq. Eng.* **18,** no. 4, 313–322.

McGinty, P., D. Darby, and J. Haines, (2001). Earthquake triggering in the Hawkes Bay, New Zealand, region from 1931 to 1934 as inferred from elastic dislocation and static stress modelling. *J. Geophys. Res.* **106,** no. B11, 26,593–26,604.

McGinty, P. (2001). Preparation of the New Zealand Seismicity Catalog for a probabilistic seismic hazard analysis of New Zealand, *Bull. N. Z. Soc. Earthq. Eng.* **34,** no. 1, 60–67.

McVerry, G. H., J. X. Zhao, N. A. Abrahamson, and P. G. Somerville (2000). Crustal and subduction zones attenuation relations for New Zealand earthquakes, Proceedings of the 12th World Conference of Earthquake Engineering 2000, Auckland, New Zealand.

Norris, R. J., and A. F. Cooper (2000). Late Quaternary slip rates and slip partitioning on the Alpine Fault, New Zealand, *J. Struct. Geol.* **23,** 507–520.

Reasenberg, P. (1985). Second-order moment of central California seismicity, 1969–1982, J. Geophys. Res. **90,** 5479–5496.

Reyners, M. (1983). Lateral segmentation of the subducted plate at the Hikurangi margin, New Zealand: seismological evidence, *Tectonophysics* **96,** 203–223.

Reyners, M. (1998). Plate coupling and the hazard of large subduction thrust earthquakes at the Hikurangi subduction zone, New Zealand, *N. Z. J. Geol. Geophys.* **41,** 343–354.

Reyners, M. (2000). Quantifying the hazard of large subduction thrust earthquakes in Hawkes Bay, *Bull. N. Z. Soc. Earthq. Eng.* **33,** no. 4, 477–483.

Rhoades, D. A., and R. J. Van Dissen (2000). Probability of rupture of the Alpine Fault allowing for uncertainties, Institute of Geological and Nuclear Sciences Client Report 2000/118, IGNS, Lower Hutt, New Zealand.

Smith, W. D., and K. R. Berryman (1986). Earthquake hazard in New Zealand: inferences from seismology and geology, *Bull. R. Soc. N. Z.* **24,** 223–243.

Somerville, P. G., T. Sato, and T. Ishii (1999). Characterising subduction earthquake slip models for the prediction of strong ground motion. *EOS Trans. Am. Geophys. Union* (1998 Fall Meet.) **79,** no. 46, F658.

Standards New Zealand (1992). Code for Practice for General Structural Design and Design Loadings for Buildings, Vol. 1, Code of practice, NZS 4203:1992, Private Bay, Wellington, New Zealand.

Stirling, M. W., S. G. Wesnousky, and K. Shimazaki (1996). Fault trace complexity, cumulative slip, and the shape of the magnitude–frequency distribution for strike-slip faults: a global survey, *Geophys. J. Int.* **124,** 833–868.

Stirling, M. W., S. G. Wesnousky, and K. R. Berryman (1998). Probabilistic seismic hazard analysis of New Zealand, *N. Z. J. Geol. Geophys.* **41,** 355–375.

Stirling, M. W., G. H. McVerry, K. R. Berryman, P. McGinty, P. Villamor, R. J. Van Dissen, D. Dowrick, J. Cousins, and R. Sutherland (2000). Probabilistic seismic hazard assessment of New Zealand: new active fault data, seismicity data, attenuation relationships and methods, Institute of Geological and Nuclear Sciences Client Report 2000/53, IGNS, Lower Hutt, New Zealand.

Sutherland, R., and R. J. Norris (1995). Late Quaternary displacement rate, paleoseismicity, and geomorphic evolution of the Alpine Fault: evidence from Hokuri Creek, South Westland, New Zealand, *N. Z. J. Geol. Geophys.* **38,** 419–430.

Sutherland, R., F. Davey, and J. Beavan, (2000). Plate boundary deformation in South Island, New Zealand, is related to inherited lithospheric structure, *Earth Planet. Sci. Lett.* **177,** 141–151.

Van Dissen, R. J., J. Cousins, R. Robinson, and M. Reyners (1994). The Fiordland earthquake of 10 August 1993: a reconnaissance report covering tectonic setting, peak ground acceleration, and landslide damage, *Bull. N. Z. Soc. Earthq. Eng.* **27,** no. 2, 147–154.

Villamor, P., and K. R. Berryman (2001). A late Quaternary extension rate in the Taupo Volcanic Zone, New Zealand, derived from fault slip data, *N. Z. J. Geol. Geophys.* **44,** no. 2, 243–269.

Weichert, D. H. (1980). Estimation of the earthquake recurrence parameters for unequal observation periods for different magnitudes, *Bull. Seism. Soc. Am.* **70,** 1337–1346.

Wells, D. L., and K. J. Coppersmith (1994). New empirical relationships among magnitude, rupture length, rupture width, rupture area, and surface displacement, *Bull. Seism. Soc. Am.* **84,** 974–1002.

Wesnousky, S. G. (1986). Earthquakes, Quaternary faults and seismic hazard in California, *J. Geophys. Res.* **91,** 12,587–12,631.

Youngs, R. R., S.-J. Chiou, W. J. Silva, and J. R. Humphrey (1997). Strong ground motion attenuation relationships for subduction zone earthquakes, *Seism. Res. Lett.* **68,** no. 1, 58–73.

Appendix

Index. In the table of fault source parameters that follows, the index column gives cross references to the fault sources shown on Figure 3. Index numbers are usually positioned at one end of each fault source.

Fault Name. The first name given is the general name of the fault, and the names in parentheses indicate the geographic endpoints of modeled fault rupture segments. The abbreviations RM, WM, and BM identify Hikurangi subduction interface sources developed m consultation with Martin Reyners, Terry Webb, and Kelvin Berryman, respectively. Anticlines are marked with the letter 'A'; four-digit numbers in parentheses indicate the year of the historical earthquake rupture used to define the length of the source. See the text for further explanation. Faults 13 to 37 represent modeled fault sources (R. Sutherland, personal commun.) for southwestern New Zealand, where detailed neotectonic studies have not yet been conducted. Sutherland's fault model conserves the rate of plate motion across the plate boundary, which is assumed to extend both onshore and offshore (as shown by the distribution fault sources in southwest New Zealand in Figure 2).

Slip Type. The abbreviations for slip type are: ss, strike-slip; nn, normal; rv, reverse; sr, strike-slip and reverse; sn, strike-slip and normal; rs, reverse and strike-slip; ns, normal and strike-slip; nv, normal in the high-attenuation Taupo Volcanic Zone; if, subduction interface.

Dip. Values shown are the preferred or mean value of dip for the fault plane. If no value is given, the dip is either greater than 80° (the case for strike-slip faults) or is unknown.

Dip Dir. Azimuth of dip.

Depth Max. Depth to the base of the fault.

Depth Min. Depth to the upper edge of the fault.

Slip Rate. The preferred or mean annual rate of slip for the fault.

Displacement. The preferred or mean value of coseismic slip for the fault.

M_{max}. Moment magnitude of the earthquake expected to accompany rupture of the fault. If a M_{max} is given without parentheses, it is derived directly from observations of a historical rupture. If the M_{max} is given in parentheses, it is either calculated with equations (1) and (2), or estimated from fault area with the regressions of Wells and Coppersmith (1994). See the text for further explanation.

Recurrence Interval. If the value is given in parentheses, it is calculated with equations (3) and (4). See the text for further explanation.

Institute of Geological and Nuclear Sciences
P.O. Box 30-368
Lower Hutt
New Zealand

Manuscript received 10 April 2001.

Table A1
Fault Source Parameters

Index	Fault Name	Slip Type	Dip (°)	Dip Dir (°)	Depth Max (km)	Depth Min (km)	Slip Rate (mm/yr)	Displacement (m)	Mmax	Recurrence Interval (yrs)
1	Wairau (Onshore)	ss			15	0		6	(7.6)	1 650
2	Wairau (Offshore)	ss			15	0			(7.3)	1 650
3	Awatere SW	ss			15	0	8	6	(7.5)	2 930
4	Awatere NE	ss			15	0	6.5	6.5	7.5	1 000
5	Alpine (Milford–Haupiri)	sr	60	145	12	0	25	8	(8.1)	300
6	Alpine (Kaniere–Tophouse)	sr	60	145	12	0	10	6	(7.7)	1 200
7	Alpine (Kaniere–Haupiri)	sr	60	145	12	0	10		(6.9)	1 200
8	Alpine (Haupiri–Tophouse)	sr	60	145	12	0	10	6	(7.6)	1 200
9	Clarence SW	ss			15	0	6		(7.5)	1 080
10	Clarence NE	ss			15	0	4.7	7	(7.7)	1 500
11	Hope (1888)	ss			15	0		2	7.2	120
12	Hope (Conway–Offshore)	sr	75	345	15	0	23	4.5	(7.5)	200
13	Jordan	rv	37	290	15	0		3	(7.1)	1 200
14	Kekerengu	sr	75	330	15	0	7.5	5.5	(7.2)	730
15	Paparoa Range	rv			15	0			(7.1)	5 000
16	Hundalee	rv	55	345	15	0	0.8	1.5	(7.0)	2 000
17	Kaiwara	rv	55	150	15	0	0.5		(7.1)	3 500
18	Omihi	rv	55	130	15	0	1		(6.7)	(474)
19	Lowry	rv	55	150	15	0		2.5	(7.3)	5 000
20	Culverden	rv	50	290	15	0	1.5	2	(6.9)	7 500
21	Esk	rs			15	0			(7.0)	7 500
22	Mt Grey	rs	55	300	15	0	0.95	3	(6.9)	3 300
23	Mt Thomas	rs	55	290	15	0			(6.5)	7 000
24	Lees Valley	rs	55	330	15	0	3.75	2	(6.7)	7 000
25	Torlesse	rv	65	330	15	0			(6.7)	3 000
26	Cheesman	rv	45	280	15	0	0.5	3	(7.0)	3 500
27	Harper	rv	35	150	15	0			(7.1)	10 000
28	Porters Pass	sr		160	15	0	3.8	3.5	(7.2)	2 900
29	Porters to Grey	sr		160	15	0		5.5	(7.5)	2 764
30	Ashley	rv	35	340	15	0		1.4	(7.2)	2 000
31	Springbank	rv	50	340	15	0			(7.1)	5 000
32	Pegasus 1	rv	55	160	15	0		3	(7.2)	10 000
33	Pegasus 2	rv	55	160	15	0		3	(6.9)	10 000
34	Pegasus 3	rv	55	160	15	0		3	(7.1)	10 000
35	North Mernoo Sth	nn		190	15	0		3	(7.4)	1 000
36	North Mernoo Nth	nn		190	15	0		3	(7.4)	1 000
37	Lake Heron	rv	43	300	15	0	1.5	4	(7.2)	5 000
38	Quartz Creek	rs	75	240	15	0		2.5	(6.7)	5 000
39	Mt Hutt–Mt Peel	rv	55	300	15	0	1	3	(7.3)	7 500
40	Fox Peak	rv	55	290	15	0	1	4	(7.2)	7 000
41	Hunter Hills Nth	rv	55	260	15	0		4.5	(7.1)	(15 000)
42	Hunter Hills Sth	rv	55	260	15	0		4.5	(7.2)	(15 000)
43	Dryburgh SE	rv	60	040	15	0	0.05	2.5	(6.9)	22 000
44	Dryburgh NW	rv	60	040	15	0	0.05	2.5	(6.9)	22 000
45	Otamatapaio	rs	89	260	15	0	0.01	0.8	(6.4)	(80 000)
46	Wharakuri	sr	60	230	15	0	0.5	4	(7.2)	10 000
47	Rostrievor–Big Gu	rv	89	260	15	0	0.05	2.5	(6.7)	(50 000)
48	Waitangi	nn	89	260	15	0	0.02	1	(6.5)	50 000
49	Dalgety	rv	60	330	15	0	0.05	3	(7.0)	(60 000)
50	Kirkliston	rv	60	290	15	0	0.05	3	(7.1)	(60 000)
51	Waimea	rs		135	15	0			(7.0)	(1 117)
52	WhiteCreek	rv	70	100	15	0	0.2	6	7.6	34 000
53	Lyell	rs		100	15	0	0.2		(6.7)	(14 661)
54	BrunAnt	rv			15	1			(6.9)	15 000
55	Inangahua	rv	45	100	15	0	0.1	0.4	7.4	4 400
56	Pisa	rv	55	300	15	0	0.4	3	(7.1)	30 000
57	Nevis	rv	55	300	15	0	0.3		(6.8)	(3 677)
58	Wairarapa (1855)	sr	80	315	15	0		11.5	8.1	1 500
59	Hikurangi (Nth Rauk: RM)	if	12	310	22	15			7.5	650
60	Hikurangi (Sth Rauk: RM)	if	12	310	22	15			7.5	681

(*continued; footnotes on page 1903*)

Table A1
(*Continued*)

Index	Fault Name	Slip Type	Dip (°)	Dip Dir (°)	Depth Max (km)	Depth Min (km)	Slip Rate (mm/yr)	Displacement (m)	Mmax	Recurrence Interval (yrs)
61	Hikurangi (Hawkes Bay: RM)	if	9	310	22	15			7.8	1 053
62	Hikurangi (Sth Hawkes Bay: RM)	if	9	310	22	15			7.4	798
63	Hikurangi (Wellington: RM)	if	9	315	22	15			7.8	1 800
64	Hikurangi (Nth Rauk: WM)	if	12	310	25	10			7.7	604
65	Hikurangi (Sth Rauk: WM)	if	12	310	25	10			7.7	633
66	Hikurangi (Hawkes Bay: WM)	if	9	310	25	10			8	979
67	Hikurangi (Sth Hawkes Bay: WM)	if	9	310	25	10			7.7	742
68	Hikurangi (Wellington: WM)	if	9	315	25	10			8.1	1 674
69	Hikurangi (Nth Rauk: BM)	if	12	310	25	10			8.1	1 236
70	Hikurangi (Sth Rauk: BM)	if	12	310	25	10			8.1	1 295
71	Hikurangi (Hawkes Bay: BM)	if	9	310	25	10			8.3	1 490
72	Hikurangi (Sth Hawkes Bay: BM)	if	9	310	25	10			8.1	1 629
73	Hikurangi (Wellington: BM)	if	9	315	25	10			8.4	2 347
74	Ostler Nth	rv	60	280	15	0	1	3	(7.0)	3 000
75	Ostler Central	rv	60	280	15	0	1	3	(7.0)	3 000
76	Ostler South	rv	60	300	15	0	1	3	(6.9)	3 000
77	Ahuriri River	rv			15	0		2.5	(6.8)	10 000
78	Irishman Creek	rv			15	0		4	(7.0)	15 000
79	Lindis Pass	rs			15	0		3	(7.0)	3 000
80	Grandview	rv			15	0		3	(7.0)	30 000
81	Cardrona Sth	rv	30	300	15	0	0.25	2	(7.1)	7 500
82	Cardrona Nth	rs	30	300	15	0	0.25	2	(7.0)	7 500
83	Blue Lake	rv	60	060	15	0		3	(7.0)	5 000
84	Dunstan North	rv	60	320	15	0	1	4	(7.2)	8 000
85	Dunstan South	rv	60	320	15	0	1	4	(6.9)	8 000
86	Raggedy	rv	60	320	15	0		3	(7.0)	8 000
87	Nth Rough Ridge	rv	60	320	15	0		3	(7.0)	8 000
88	Rough Ridge	rv	60	320	15	0		3	(7.0)	8 000
89	Ranfurly Sth	rv	60	320	15	0		3	(7.0)	8 000
90	Ranfurly Nth	rv	60	320	15	0		3	(7.0)	8 000
91	Hyde	rv	60	320	15	0		3	(7.0)	15 000
92	Hanmer	nn	60	170	15	0		2	(6.9)	1 000
93	Wairoa Nth	nn			15	0	0.04		(6.6)	(22 152)
94	Kerepehi Nth	nn			12	0	0.4	1	(6.7)	(2 500)
95	Kerepehi Nth-Cent	nn			12	0	0.4	1	(6.6)	(2 500)
96	Kerepehi Central	nn			12	0	0.4	2	(6.7)	(5 000)
97	Kerepehi Sth	nn			12	0	0.4	2	(6.7)	(5 000)
98	Mayor Island 1	nn	60	260	12	0	0.5	2	(7.0)	(4 000)
99	Mayor Island 2	nn	60	080	12	0	0.5	2	(7.4)	(4 000)
100	Mayor Island 3	nn	60	260	12	0	0.5	2	(7.1)	(4 000)
101	Mayor Island 4	nn	60	080	12	0	0.5	2	(7.0)	(4 000)
102	Tauranga	nn	60	140	12	0	1	2	(7.0)	(2 000)
103	Aldeman	nn			12	0	2	2	(6.9)	(1 000)
104	Matata	nv	60	130	8	0	2		(6.5)	(374)
105	Braemar	nv	60	130	8	0	1		(6.5)	(797)
106	Rotoiti	nv	60	130	8	0	0.6		(5.7)	(521)
107	Te Teko	nv	60	130	8	0	1		(5.7)	(339)
108	Onepu	nv	60	130	8	0	1.5		(5.8)	(249)
109	Awakere	nv	60	300	8	0	1		(6.1)	(511)
110	Edgecumbe (1987)	nv	60	300	8	0	2.5		6.5	(1 362)
111	Edgecumbe (Coastal)	nv	60	300	8	0	2.5		(6.0)	(176)
112	White Island 1	nv	60	300	8	0	1		(6.0)	(453)
113	White Island 2	nv	60	300	8	0	1		(6.3)	(627)
114	White Island 3	nv	60	300	8	0	1		(6.3)	(597)
115	Nukuhou	nv	60	300	8	0	2.4		(5.9)	(172)
116	Ohiwa	nv	60	300	8	0	0.7		(6.2)	(785)
117	Rangitaiki	nv	60	300	8	0	2.3		(6.3)	(261)
118	Rurima A	nv	60	120	8	0	0.6		(6.3)	(1 076)
119	Rurima B	nv	60	120	8	0	0.6		(6.3)	(1 079)
120	Ngakuru NE	nv	50	120	8	0	0.45		(6.1)	(1 100)

(*continued; footnotes on page 1903*)

Table A1
(*Continued*)

Index	Fault Name	Slip Type	Dip (°)	Dip Dir (°)	Depth Max (km)	Depth Min (km)	Slip Rate (mm/yr)	Displacement (m)	Mmax	Recurrence Interval (yrs)
121	Ngakuru SW	nv	50	120	8	0	0.45		(6.0)	(983)
122	Ohakuri NW	nv	50	120	8	0	0.2		(6.0)	(2 037)
123	Ohakuri SE	nv	50	120	8	0	0.2		(6.1)	(2 562)
124	Thorpe SE	nv	50	120	8	0	0.1		(6.0)	(4 550)
125	Thorpe NW	nv	50	120	8	0	0.1		(5.9)	(4 031)
126	Puketar NE	nv	50	300	8	0	0.8		(6.0)	(553)
127	Puketar SW	nv	50	300	8	0	0.8		(6.0)	(535)
128	Orakeik NE	nv	50	300	8	0	1.2		(6.0)	(357)
129	Orakeik SW	nv	50	300	8	0	1.2		(6.0)	(357)
130	Orakonui NE	nv	50	300	8	0	1.2		(6.0)	(384)
131	Orakonui SW	nv	50	300	8	0	1.2		(6.0)	(379)
132	Whirinaki Nth	nv	50	300	8	0	0.7		(6.0)	(612)
133	Whirinaki Sth	nv	50	300	8	0	0.7		(6.1)	(732)
134	Paeroa Nth	nv	50	300	8	0	1.5		(6.0)	(303)
135	Paeroa Central	nv	50	300	8	0	1.5		(5.9)	(269)
136	Paeroa Sth	nv	50	300	8	0	1.5		(6.1)	(322)
137	Whangamoa	nv	50	120	8	0	1.3		(5.8)	(293)
138	Ngangiho	nv	50	120	8	0	0.8		(6.2)	(698)
139	Whakaipo	nv	50	300	8	0	0.6		(6.1)	(860)
140	Kaiapo	nv	50	300	8	0	0.8		(6.2)	(731)
141	Aratiatia	nv	50	300	8	0	0.8		(6.2)	(678)
142	Waiohau Nth	ns	80	270	12	0	1.4		(6.5)	(533)
143	Waiohau Sth	ns	80	270	12	0	1.4		(6.9)	(843)
144	Graben Sth	nv			8	0	3.5		(6.0)	(125)
145	Graben Nth	nv			8	0	3.5		(5.8)	(100)
146	Kelly	ss			15	0	20	3	(7.2)	(150)
147	Hope (West)	ss			15	0	5	3	(7.2)	(600)
148	Hope (Central)	ss			15	0	25	3	(7.1)	(120)
149	Kakapo	ss			15	0	6.4	3	(7.1)	500
150	Hope (Kokatahi)	ss			15	0	10	3	(6.9)	(300)
151	Arthurs Pass (1929)	ss			15	0		3	7	3 500
152	Styx	ss			15	0	10	3	(6.9)	(300)
153	Ohariu	ss			15	0		4	(7.4)	3 250
154	Pohangina	rv			15	1	0.3	2.5	(6.9)	8 000
155	Levin A	rv			15	1	0.3	2.5	(6.6)	6 500
156	Marton A	rv			15	1	0.3	2.5	(6.7)	8 000
157	Wellington SW	ss			15	0	7.1	4.2	(7.3)	600
158	Wellington NE	ss			15	0	7.1	4.2	(7.5)	(592)
159	Wellington Cent	ss			15	0	3.6	4.2	(7.2)	(1 183)
160	Wellington W	ss			15	0	3.6	4.2	(7.2)	(1 183)
161	Feilding A	rv			15	1	0.3	2.5	(6.9)	8 000
162	Spylaw	rv	55	150	15	0	0.5		(6.3)	(1 300)
163	BlueMtn	rv	55	125	15	0			(6.4)	800
164	Alfredton	ss			15	0	3	6	(7.2)	4 500
165	Mohaka Sth	ss			15	0		2	(7.1)	1 000
166	Mohaka Nth	ss			15	0		2	(7.1)	1 000
167	Ruahine Nth	sr	80	315	15	0		3.5	(6.9)	(2 800)
168	Ruahine Central	sr	80	315	15	0		3.5	(7.4)	(2 800)
169	Ruahine Sth	sr	80	315	15	0		3.5	(7.2)	(2 800)
170	Napier (1931)	rs	80	315	30	0		2.5	7.8	2 500
171	Waimana	ss			15	0		3.5	(7.4)	3 500
172	Whakatane	sn			15	0		3.5	(7.4)	3 500
173	Waikaremoana	ss			15	0		3.5	(7.0)	3 500
174	Inglewood	ns		150	15	0	0.2	2.1	(6.8)	4 300
175	Ararata	nn	70	140	5	0	0.02		(5.7)	(16 832)
176	Waverley	nn	70	120	5	0	0.03		(6.0)	(14 348)
177	Nukumaru	nn	70	120	15	0	0.07		(6.2)	12 500
178	Mt Stewart A	rv	60	270	15	1	0.3	2.5	(6.8)	8 000
179	Pukerua-Sheph	ss			15	0			3.8	3 750
180	Galpin	nn	70	100	15	0	0.04		(6.1)	(12 983)

(*continued; footnotes on page 1903*)

Table A1
(*Continued*)

Index	Fault Name	Slip Type	Dip (°)	Dip Dir (°)	Depth Max (km)	Depth Min (km)	Slip Rate (mm/yr)	Displacement (m)	Mmax	Recurrence Interval (yrs)
181	Leedstown	nn	70	120	15	0	0.07		(6.3)	(9 164)
182	Upokongaro	nn			15	0	0.01		(6.6)	(82 793)
183	Moumahaki	nn	70	120	5	0	0.2		(5.7)	(1 730)
184	RidgeR	nn	70	300	5	0			(5.5)	(1 759)
185	Waitotara	nn	70	300	5	0	0.07		(5.6)	(4 198)
186	Himatangi A	rv			15	1	0.3	2.5	(6.7)	8 000
187	Aorangi A	rv			15	1	2.5		(7.0)	(536)
188	PaValley–Makuri	ss			15	0		6	(7.4)	2 500
189	EHBSSN–Weber	ss			15	0		3	(6.8)	2 000
190	Saunders–Weber	ss			15	0		3	(7.1)	2 000
191	Ruataniwha	rs			15	0		3	(6.8)	4 000
192	Oruawharo	sr			15	0		3	(6.9)	4 000
193	Poukawa Nth	ss			15	0			(6.4)	9 500
194	Waipuk–Pouk	rs			15	0		3	(7.1)	5 300
195	Kaweka	ss			15	0		3.5	(7.1)	3 500
196	Patoka	ss			15	0		4	(7.0)	2 000
197	Rangiora	ss			15	0		5	(7.0)	(962)
198	Kidnappers W	nn			15	0		2.8	(6.8)	4 000
199	Kidnappers E	nn			15	0		2.8	(6.9)	4 000
200	HBNFW–Silver	nn			15	0		2.8	(6.9)	3 500
201	HBNFC–Silver	nn			15	0		2.8	(6.8)	3 500
202	HBNFE–Silver	nn			15	0		2.8	(6.9)	3 500
203	Mangaoranga	sn			15	0			(6.1)	5 000
204	Waitawhiti	sn			15	0			(6.4)	4 000
205	Maunga	sn			15	0			(6.8)	5 000
206	Poroutawhao	rv			15	1		2.5	(6.8)	20 000
207	Ruahine Reverse	rv			15	0			(6.5)	20 000
208	Hihitahi	nn			15	0			(6.3)	1 250
209	Kariori	nv			15	0			(6.5)	1 500
210	Ohakune	nv			15	0		30	(6.5)	(272)
211	Raurimu	nv			15	0	2	1	(6.6)	(500)
212	Wanganui Offsh.	nn			15	0			(6.8)	5 000
213	Coastal Zone	rr			15	0			(7.0)	2 000
214	HB Offshore 1	rr			15	0		5	(7.3)	1 250
215	HB Offshore 2	rr			15	0		5	(7.2)	1 250
216	HB Offshore 3	rr			15	0		5	(7.4)	1 250
217	HB Offshore 4	rr			15	0		5	(7.5)	1 250
218	Masterton	sn			15	0			(6.3)	(1 189)
219	Tukituki	rv			15	0		5	(6.8)	5 000
221	Raetihi	nv			15	0			(6.3)	1 500
222	Shannon A	rv			15	1		2.5	(6.6)	20 000
223	Avoca	ss			15	0			6.7	3 500
224	Cape Egmont	nn	45	120	15	0	0.5		(7.1)	(2 915)
225	Mokonui	sr			15	0	0.2		(6.4)	10 000
226	Carterton	nv			15	0			(5.8)	10 000
228	Taihape	nv			15	0			(5.8)	10 000
229	Mataroa	nv			15	0			(5.9)	10 000
230	Snowgrass	nv			15	0	1	1.5	(6.7)	1 500
231	Rangipo	nv			15	0	3	3	(6.4)	1 000
232	Shawcroft Rd	nv			15	0		1.5	(5.4)	1 500
233	Raukumara F1	nn			5	0			(5.4)	10 000
234	Raukumara F2	nn			5	0			(5.9)	10 000
235	Raukumara F3	nn			5	0	0.6		(5.5)	(445)
236	Repongaere F4	nn			5	0			(5.6)	(1 014)
237	Tangihanga F5	nn			5	0	0.4		(5.7)	(811)
238	Raukumara F6	nn			5	0	0.5		(5.4)	125 000
239	OtokoToto F7	nn			5	0	0.5		(5.7)	999 999
240	Raukumara F8	nn			15	0	0.5		(6.1)	125 000
241	Raukumara F9	nn			15	0	0.5		(5.9)	125 000
242	Raukumara F10	nn			15	0	0.5		(6.3)	125 000

(*continued; footnotes on page 1903*)

Table A1
(*Continued*)

Index	Fault Name	Slip Type	Dip (°)	Dip Dir (°)	Depth Max (km)	Depth Min (km)	Slip Rate (mm/yr)	Displacement (m)	Mmax	Recurrence Interval (yrs)
243	Raukumara F11	nn			15	0	0.5		(6.5)	10 000
244	Raukumara F12	nn			15	0	0.5		(6.5)	10 000
245	Raukumara F13	nn			15	0	0.5		(6.1)	10 000
246	Raukumara F15	nn			15	0	0.5		(6.1)	10 000
247	Raukumara F16	nn			15	0	0.5		(6.1)	10 000
248	Raukumara F17	nn			15	0	0.5		(6.3)	67 500
249	Raukumara F18	nn			15	0	0.5		(6.5)	67 500
250	Raukumara F19	nn			15	0			(6.5)	(22 523)
251	Raukumara F20	nn			15	0			(5.4)	10 000
252	Raukumara F21	nn			15	0			(6.5)	(21 445)
253	Raukumara F22	nn			15	0	0.05		(6.1)	(10 170)
254	Raukumara F23	nn			15	0			(6.4)	125 000
255	Raukumara F24	nn			15	0			(5.8)	125 000
256	Raukumara F25	nn			15	0			(5.5)	(7 253)
257	Raukumara F26	nn			15	0			(5.8)	125 000
258	Raukumara F27	nn			5	0			(5.4)	125 000
259	Pangopango F29	nn			5	0			(5.6)	60 000
260	Fernside F28	nn			5	0			(5.9)	10 000
261	Raukumara F30	nn			5	0			(5.2)	125 000
262	Raukumara F31	nn			5	0			(5.2)	1 800
263	Raukumara F32	nn			5	0			(5.2)	60 000
264	Marau F33	rv			5	0			(5.3)	10 000
265	East Cape	nn			5	0	1.9		(5.6)	(153)
266	Pakarai	nn			5	0		5	(6.3)	2 300
267	Dry–Huangarua	rv			15	0		2.5	(7.0)	(4 545)
268	Otaraia	rv			15	0			(6.8)	(2 068)
269	Bidwill	rv			15	0			(6.2)	(1 032)
270	Moores	rv			15	0	0.1	2	(6.7)	20 000
271	Whitemans	rv			15	0	0.1	2	(6.4)	20 000
272	Moonshine–Otaki	rv			15	0			(7.2)	125 000
273	Nth Ohariu	ss			15	0		3.5	(7.2)	2 500
274	Waipukaka	ss			15	0			7.6	1 900
275	Oaonui	nn			15	0	0.5	1.8	(6.5)	2 200
276	Norfolk	nn			15	0		1.6	(6.3)	4 500
277	Turi	nn			15	0			(7.2)	(1 612)
278	Fault 6	rs	45	55	20	0	0.5		(7.1)	(3 176)
279	Fault 7	rs	45	67	20	0	0.5		(7.1)	(3 089)
280	Akatore	rs	45	312.6	20	0	0.5		(7.1)	(2 987)
281	Fault 13	rs	45	293.8	20	0	0.5		(7.3)	(3 597)
282	Fault 15	rs	45	288.3	20	0	3		(7.4)	(711)
283	Fault 16	rs	45	278.8	20	0	3		(7.3)	(633)
284	Fault 18	ss			20	0	25		(7.2)	(66)
285	Fault 19	ss			20	0	25		(7.1)	(63)
286	Fault 20	ss			20	0	25		(7.3)	(76)
287	Fault 21	ss			20	0	25		(7.3)	(76)
288	Fault 22	rs	30	153	20	0	1		(7.5)	(2 379)
289	Fault 23	rs	30	145.4	20	0	2		(7.5)	(455)
290	Fault 24	rs	20	135.2	20	0	5		(7.7)	(566)
291	Fault 25	rs	20	128.2	20	0	7		(7.8)	(467)
292	Fault 26	rs	20	116	20	0	15		(7.4)	(234)
293	Hauroko (Fault 27)	rs	45	290.4	20	0	0.01		(7.3)	(187 500)
294	Fault 28	rs	45	136.5	20	0	0.5		(7.2)	(3 501)
295	Fault 29	rs	45	285	20	0	0.5		(7.0)	(2 707)
296	Fault 30	rs	45	222.9	20	0	0.3		(7.0)	(4 544)
297	Fault 31	rs	45	55.4	20	0	0.5		(7.1)	(3 049)
298	Fault 32	rs	45	269	20	0	0.5		(7.1)	(2 923)
299	Fault 33	ss			20	0	1		(6.8)	(1 130)
300	Fault 34	ss			20	0	0.01		(7.0)	(431)
301	Fault 35	ss			20	0	0.01		(7.3)	(612)
302	Fault 36	ss			20	0	3		(7.1)	(499)

(*continued; footnotes on page 1903*)

Table A1
(*Continued*)

Index	Fault Name	Slip Type	Dip (°)	Dip Dir (°)	Depth Max (km)	Depth Min (km)	Slip Rate (mm/yr)	Displacement (m)	Mmax	Recurrence Interval (yrs)
303	Fault 37	rs	45	73.1	20	0	0.5		(7.2)	(3 361)
304	National Park	nv			15	0	2		(6.2)	289
305	Poutu	nv			15	0	2		(6.6)	(453)
306	Waihi	nv			15	0	5		(6.8)	(216)

Data Sources: (Full references for the following citations are found in Stirling *et al.* (2000)). Pettinga *et al.* (1998); Stirling *et al.* (1998, 1999); Mazengarb *et al.* (1997); Berryman and Hull (1994); Van Dissen *et al.* (1993); Institute of Geological and Nuclear Sciences (1999); Van Dissen (personal commun.); Villamor (personal commun.); Berryman (personal commun.); Mazengarb (personal commun.); Sutherland (personal commun.); Reyners (personal commun.); Begg and Van Dissen (1998); Grapes *et al.* (1998); Benson *et al.* (1998); Little *et al.* (1998); Van Dissen and Nicol (1998); Kelsey *et al.* (1998); Reyners *et al.* (1997); Berryman *et al.* (1995); Hull and Dellow (1993); Le Cointre *et al.* (1998); Villamor *et al.* (1998); Fellows (1996); Beanland *et al.* (1997); Berryman *et al.* (1998); Grapes *et al.* (1997); Nicol *et al.* (1997); Grapes and Downes (1997); Heron *et al.* (1998); Nicol and Van Dissen (1997); Van Dissen *et al.* (1998); Schermer *et al.* (1999); Van Dissen and Palmer (1998).

Institute of
GEOLOGICAL
& NUCLEAR
SCIENCES
Limited

NEW PROBABILISTIC SEISMIC HAZARD MAPS FOR NEW ZEALAND

Mark Stirling, Graeme McVerry and Kelvin Berryman Institute of Geological & Nuclear Sciences Ltd, PO Box 30 368 Lower Hutt, New Zealand m.stirling@gns.cri.nz

SUMMARY

We present the results of a new probabilistic seismic hazard analysis (PSHA) for New Zealand, a country that straddles the active boundary of the Pacific and Australian plates (Fig. 1). The PSHA incorporates geological data describing the location and earthquake recurrence behaviour of 305 active faults (Fig. 2), a seismicity catalogue with greatly improved locations for many events, a new seismotectonic (area source) zonation scheme (Figs. 3 and 4), new attenuation relationships for peak ground acceleration and spectral acceleration developed specifically for New Zealand, and state-of-the-art PSH methodology developed in New Zealand and the USA. In particular, the treatment of distributed (historical) seismicity in the new model is a significant departure from the traditional method of assuming that the seismicity of an area source zone is uniformly distributed across the zone. Instead, the new methodology preserves the spatial variations of seismicity rates within each zone (Figs. 5 & 6), while still using the seismicity parameters of the zone as a whole (b-value and maximum cutoff magnitude "Mcutoff" of the Gutenberg-Richter relationship) in the PSHA. The new PSHA is based on a recent "experimental" PSHA of New Zealand (Stirling et al. 1998), and supercedes the PSHAs of Matuschka et al. (1985) and Smith and Berryman (1986). These older PSHAs were largely based on the 150 year historical record of earthquakes, and used as the basis for the New Zealand Loadings Code for well over a decade. PSH maps produced from the new model for uniform ("Class B"average soil) ground conditions (Figs. 7-9) show the highest hazard to occur in the southwest of the country (vicinity of the Fiordland subduction zone and the offshore extent of the Alpine Fault; Fig. 1), along the axial tectonic belt (Fig. 1), the Taupo Volcanic Zone (a zone of active crustal extension and volcanism running from the central North Island volcanoes to the Bay of Plenty; Fig. 1), and in the seismically active northwestern South Island (Fig. 1). The maps show generally similar patterns of hazard to the maps of Stirling et al (1998), but very different patterns to those shown on the maps of Smith and Berryman (1986). The largest differences exist in the vicinity of the major active faults, which are generally absent of large earthquakes in historic time, but have produced them abundantly in prehistoric time. Examination of the PSHA at the major population centres of New Zealand (Fig. 1) by way of hazard curves (Fig. 10) and response spectra (Fig. 11) reveals that the centres have the following rank in decreasing order of hazard; Wellington, Christchurch, Dunedin and Auckland. The hazard is highest in Wellington since it is close to a number of major active faults, and in an area of high seismicity in historical time. In comparison, the other centres are generally located in areas away from the major active faults, and in areas of relatively low seismicity rates. Disaggregation of the hazard at these centres shows that in general the centres will most likely be shaken by large earthquakes on the closest major active faults, and by moderate-to-large earthquakes occurring on or away from these faults (Figs. 12 & 13).
Ongoing work on the New Zealand PSH model is focused on addressing the uncertainty in the estimates of PSH (Figs. 7-9), incorporating variable site geology and offshore faults into the model, improving earthquake occurrence models for the Hikurangi subduction zone (Fig. 1), and developing tests for the estimates of PSH from historical data (including geodetic data) not already included in the existing model.

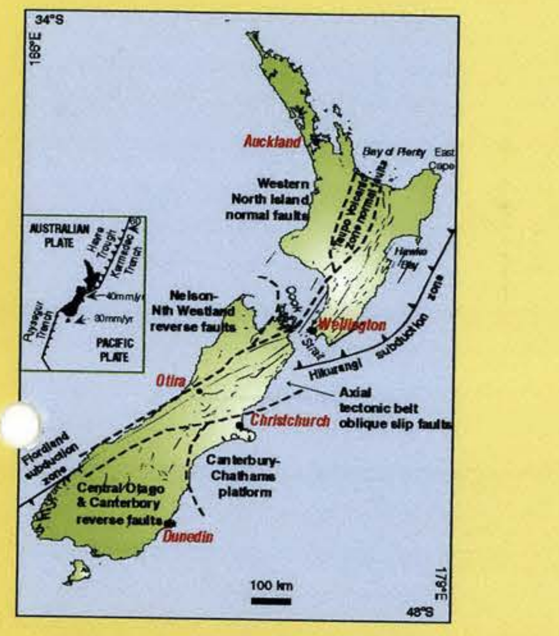

Figure 1. The plate tectonic setting of New Zealand, and neotectonic provinces of Berryman & Beanland (1988).

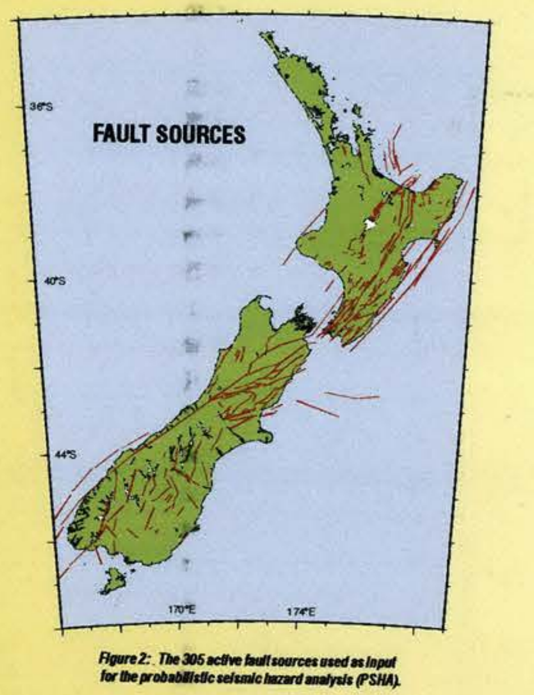

Figure 2: The 305 active fault sources used as input for the probabilistic seismic hazard analysis (PSHA).

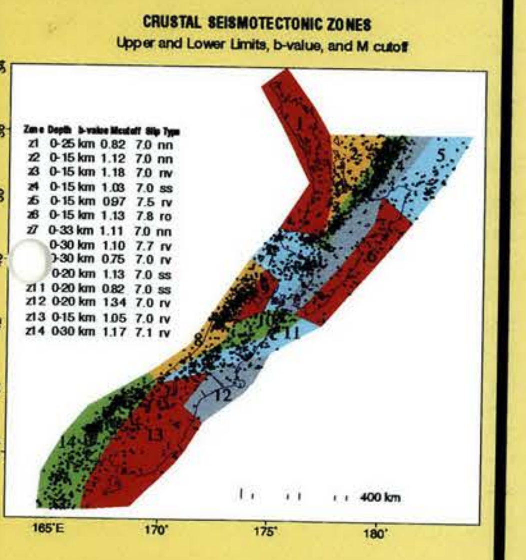

Figure 3: . The distribution of shallow crustal seismicity in New Zealand, and crustal seismotectonic zones defined to sort the catalogue and calculate parameter b of the Gutenberg-Richter relationship for estimating distributed seismicity rates for the PSHA. The minimum and maximum depths of the zones, and the associated seismicity parameters are listed on the figure.

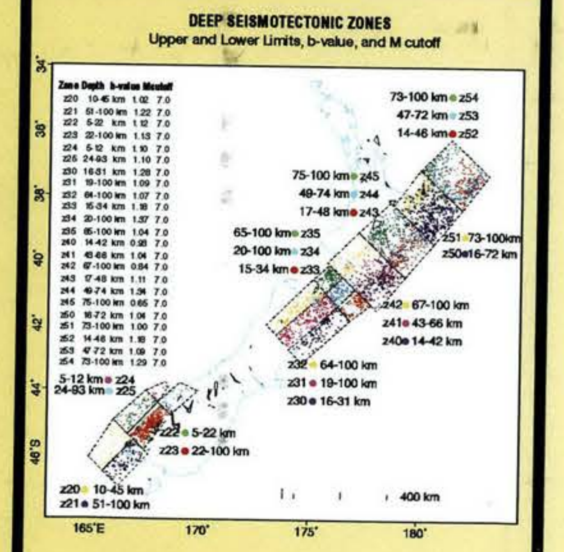

Figure 4: The distribution of deeper seismicity of the Fiordland and Hikurangi subduction zones. Since many of the deep zones overlap in plan view, we show the seismicity of each zone as a particular colour, rather than trying to colour code the actual zones. The general location and size of the zones are shown by dashed or solid lines The minimum and maximum depths of the zones, and the associated seismicity parameters are listed on the figure.

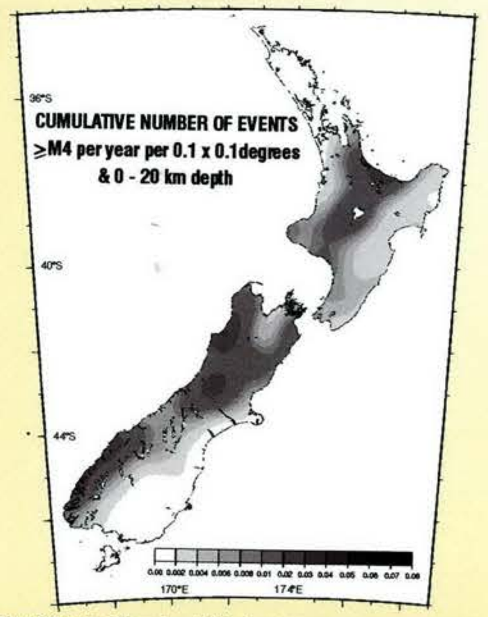

Figure 5. Contours of the maximum-likelihood cumulative number of events per year for M>4, calculated from three catalogue completeness levels and magnitudes (M>4 since 1964, M>5 since 1940, and M>6.5 since 1840), and parameter b of the Gutenberg-Richter relationship LogN=A-bM for seismicity recorded at 0-20 depth beneath the country (the complete depth range considered in the PSHA is down to 100km). The contours have been made over a gridwork of N and b that have been smoothed with a Gaussian smoothing function, in which the correlation distance (standard deviation) is set to 50 km. The methodology is largely based on that of Frankel (1995).

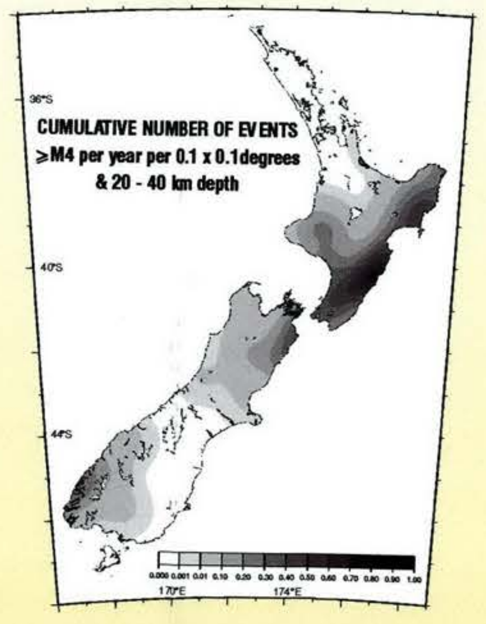

Figure 6. As for Figure 5, except the seismicity rates shown are for seismicity recorded at 20-40km depth beneath the country.

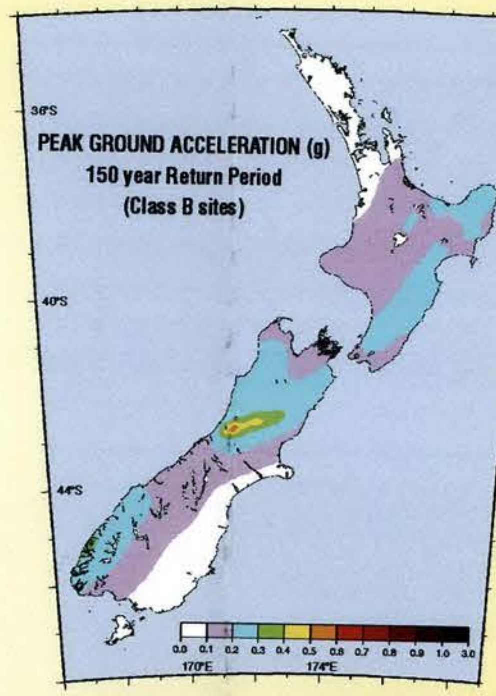

Figure 7. PSH map for New Zealand. This map shows the levels of peak ground acceleration expected with a return time of 150 years. The 150 year map is mainly controlled by the distribution of historical seismicity, and in areas where there is a high density of active faults.

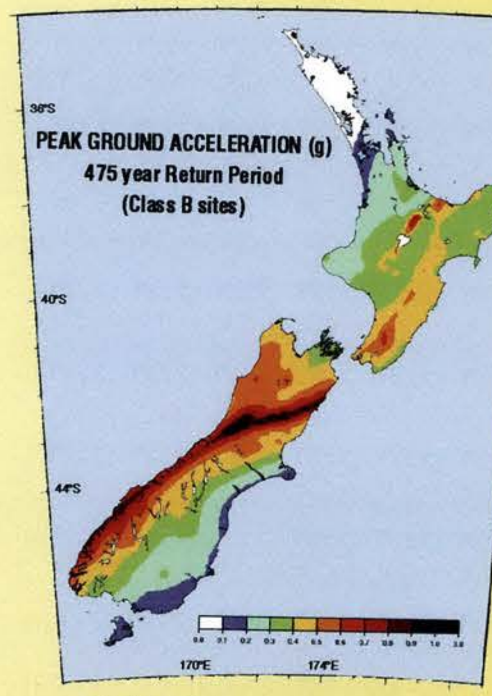

Figure 8. As for Figure 7 but showing the levels of peak ground acceleration expected with a return period of 475 years (i.e. 10% probability in 50 years). The maps assume uniform ("Class B") site conditions.

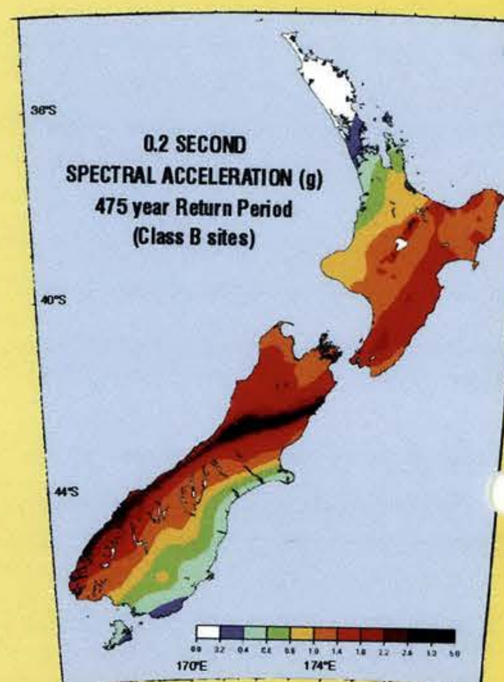

Figure 9. As for Figure 7, but showing the levels of 0.2 second spectral acceleration expected with a return period of 475 years (10% probability in 50 years).

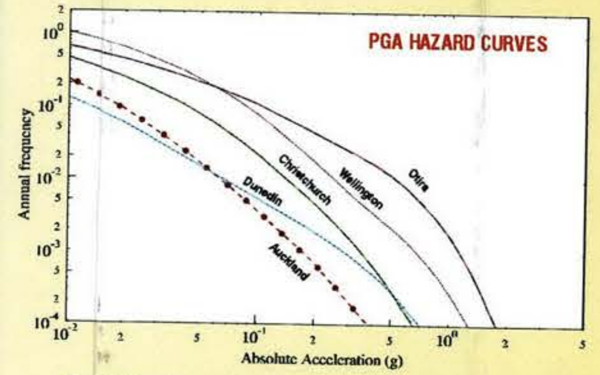

Figure 10. Hazard curves of the annual rate of exceedance of various levels of peak ground acceleration at the centres of Auckland, Wellington, Christchurch, Dunedin and Otira. See Figure 1 for the location of these centres. The curves assume uniform ("Class B") site conditions.

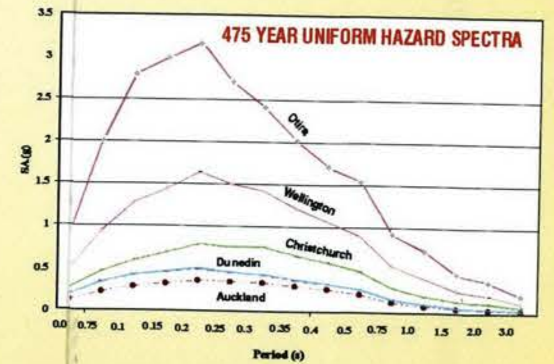

Figure 11. 475 year response spectra for the centres of Auckland, Wellington, Chritchurch, Dunedin and Otira. See Figure 1 for the location of these centres. The spectra assume uniform ("Class B") site conditions.

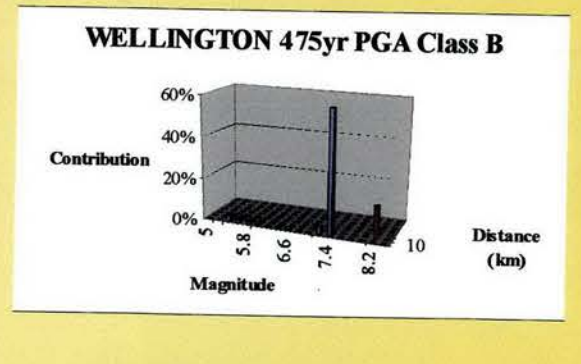

Figure 12. Disaggregation plots showing the contribution to hazard (475 year peak ground acceleration from Fig. 10) from the various classes of magnitude and source-to-site distances in the PSH model for the city of Wellington.

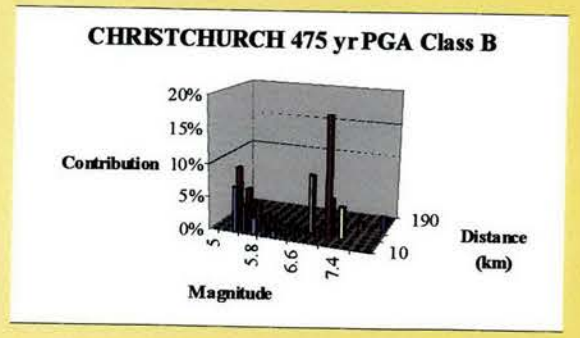

Figure 13. As for Figure 12, but focused on the city of Christchurch.

REFERENCES
Berryman & Beanland (1988), Frankel (1995),
McVerry (2000), Matuschka et al. (1985),
Smith & Berryman (1986), Stirling et al (1998)
Stirling et al (2000)

NEW PROBABILISTIC SEISMIC HAZARD MAPS FOR NEW ZEALAND

Institute of Geological & Nuclear Sciences Limited

Mark Stirling, Graeme McVerry and Kelvin Berryman Institute of Geological & Nuclear Sciences Ltd, PO Box 30 368 Lower Hutt, New Zealand m.stirling@gns.cri.nz

SUMMARY

We present the results of a new probabilistic seismic hazard analysis (PSHA) for New Zealand, a country that straddles the active boundary of the Pacific and Australian plates (Fig. 1). The PSHA incorporates geological data describing the location and earthquake recurrence behaviour of 305 active faults (Fig. 2), a seismicity catalogue with greatly improved locations for many events, a new seismotectonic (area source) zonation scheme (Figs. 3 and 4), new attenuation relationships for peak ground acceleration and spectral acceleration developed specifically for New Zealand, and state-of-the-art PSH methodology developed in New Zealand and the USA. In particular, the treatment of distributed (historical) seismicity in the new model is a significant departure from the traditional method of assuming that the seismicity of an area source zone is uniformly distributed across the zone. Instead, the new methodology preserves the spatial variations of seismicity rates within each zone (Figs. 5 & 6), while still using the seismicity parameters of the zone as a whole (b-value and maximum cutoff magnitude "Mcutoff" of the Gutenberg-Richter relationship) in the PSHA. The new PSHA is based on a recent "experimental" PSHA of New Zealand (Stirling et al. 1998), and supercedes the PSHAs of Matuschka et al. (1985) and Smith and Berryman (1986). These older PSHAs were largely based on the 150 year historical record of earthquakes, and used as the basis for the New Zealand Loadings Code for well over a decade. PSH maps produced from the new model for uniform ("Class B"average soil) ground conditions (Figs. 7-9) show the highest hazard to occur in the southwest of the country (vicinity of the Fiordland subduction zone and the offshore extent of the Alpine Fault; Fig. 1), along the axial tectonic belt (Fig. 1), the Taupo Volcanic Zone (a zone of active crustal extension and volcanism running from the central North Island volcanoes to the Bay of Plenty; Fig. 1), and in the seismically active northwestern South Island (Fig. 1). The maps show generally similar patterns of hazard to the maps of Stirling et al (1998), but very different patterns to those shown on the maps of Smith and Berryman (1986). The largest differences exist in the vicinity of the major active faults, which are generally absent of large earthquakes in historic time, but have produced them abundantly in prehistoric time. Examination of the PSHA at the major population centres of New Zealand (Fig. 1) by way of hazard curves (Fig. 10) and response spectra (Fig. 11) reveals that the centres have the following rank in decreasing order of hazard; Wellington, Christchurch, Dunedin and Auckland. The hazard is highest in Wellington since it is close to a number of major active faults, and in an area of high seismicity in historical time. In comparison, the other centres are generally located in areas away from the major active faults, and in areas of relatively low seismicity rates. Disaggregation of the hazard at these centres shows that in general the centres will most likely be shaken by large earthquakes on the closest major active faults, and by moderate-to-large earthquakes occurring on or away from these faults (Figs. 12 & 13).

Ongoing work on the New Zealand PSH model is focused on addressing the uncertainty in the estimates of PSH (Figs. 7-9), incorporating variable site geology and offshore faults into the model, improving earthquake occurrence models for the Hikurangi subduction zone (Fig. 1), and developing tests for the estimates of PSH from historical data (including geodetic data) not already included in the existing model.

Figure 1. The plate tectonic setting of New Zealand, and neotectonic provinces of Berryman & Beanland (1988).

Figure 2: The 305 active fault sources used as input for the probabilistic seismic hazard analysis (PSHA).

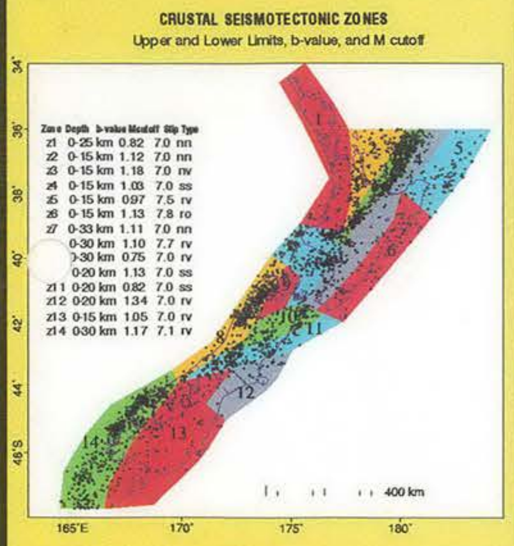

Figure 3: . The distribution of shallow crustal seismicity in New Zealand, and crustal seismotectonic zones defined to sort the catalogue and calculate parameter b of the Gutenberg-Richter relationship for estimating distributed seismicity rates for the PSHA. The minimum and maximum depths of the zones, and the associated seismicity parameters are listed on the figure.

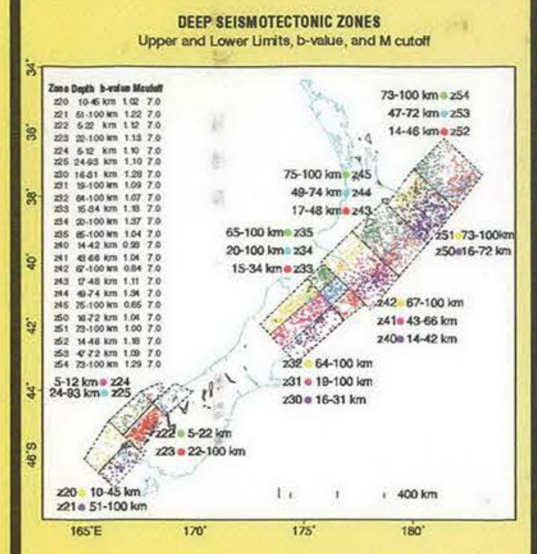

Figure 4: The distribution of deeper seismicity of the Fiordland and Hikurangi subduction zones. Since many of the deep zones overlap in plan view, we show the seismicity of each zone as a particular colour, rather than trying to colour code the actual zones. The general location and size of the zones are shown by dashed or solid lines The minimum and maximum depths of the zones, and the associated seismicity parameters are listed on the figure.

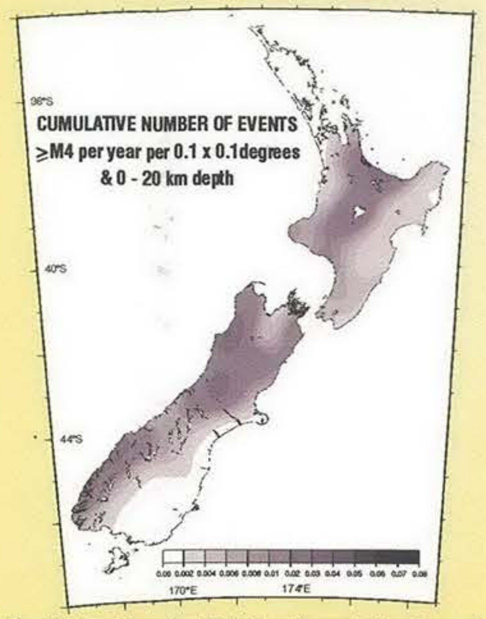

Figure 5. Contours of the maximum-likelihood cumulative number of events per year for M>4, calculated from three catalogue completeness levels and magnitudes (M>4 since 1964, M>5 since 1940, and M>6.5 since 1840), and parameter b of the Gutenberg-Richter relationship LogN=A-bM for seismicity recorded at 0-20 depth beneath the country (the complete depth range considered in the PSHA is down to 100km). The contours have been made over a gridwork of N and b that have been smoothed with a Gaussian smoothing function, in which the correlation distance (standard deviation) is set to 50 km. The methodology is largely based on that of Frankel (1995).

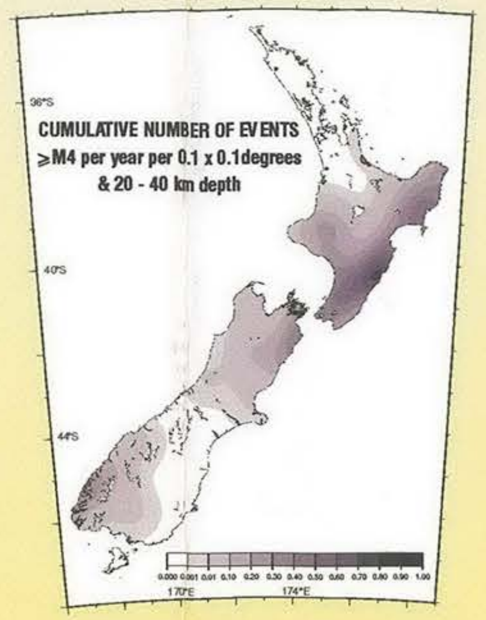

Figure 6. As for Figure 5, except the seismicity rates shown are for seismicity recorded at 20-40km depth beneath the country.

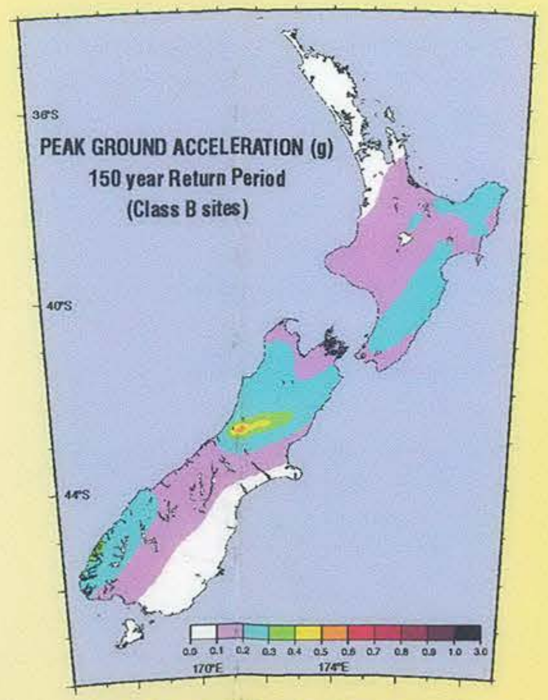

Figure 7. PSH map for New Zealand. This map shows the levels of peak ground acceleration expected with a return time of 150 years. The 150 year map is mainly controlled by the distribution of historical seismicity, and in areas where there is a high density of active faults.

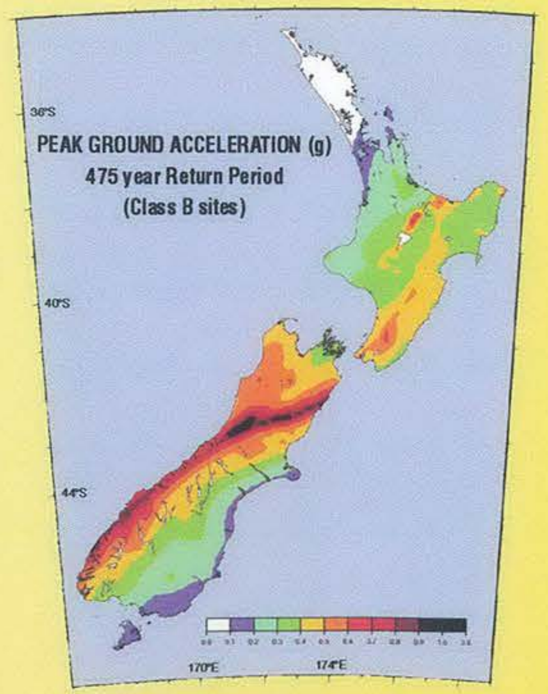

Figure 8. As for Figure 7 but showing the levels of peak ground acceleration expected with a return period of 475 years (i.e. 10% probability in 50 years). The maps assume uniform ("Class B") site conditions.

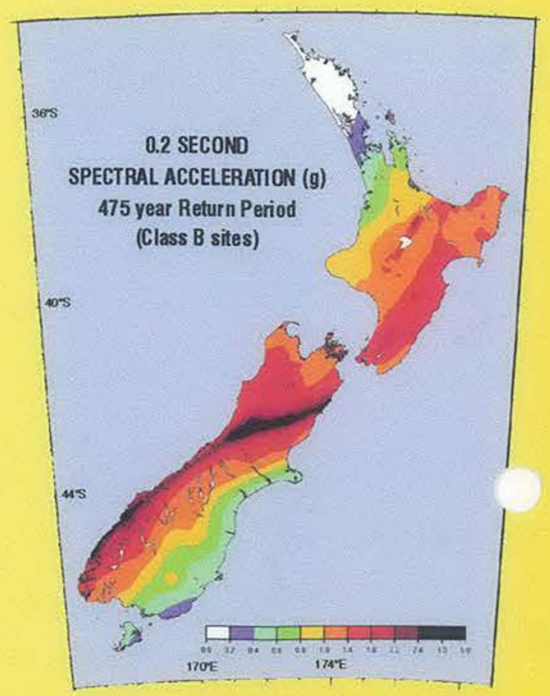

Figure 9. As for Figure 7, but showing the levels of 0.2 second spectral acceleration expected with a return period of 475 years (10% probability in 50 years).

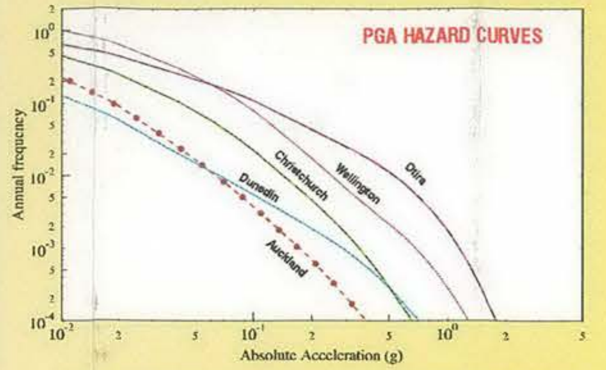

Figure 10. Hazard curves of the annual rate of exceedance of various levels of peak ground acceleration at the centres of Auckland, Wellington, Christchurch, Dunedin and Otira. See Figure 1 for the location of these centres. The curves assume uniform ("Class B") site conditions.

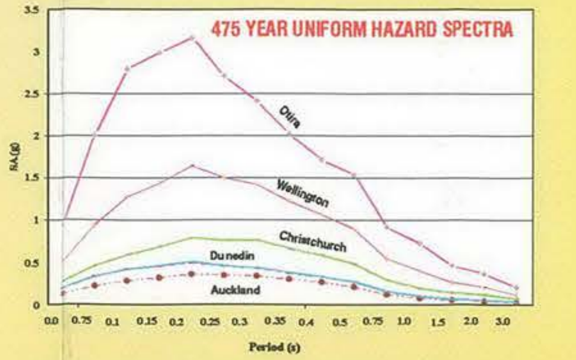

Figure 11. 475 year response spectra for the centres of Auckland, Wellington, Christchurch, Dunedin and Otira. See Figure 1 for the location of these centres. The spectra assume uniform ("Class B") site conditions.

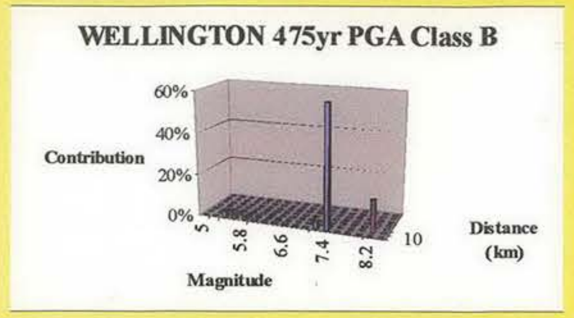

Figure 12. Disaggregation plots showing the contribution to hazard (475 year peak ground acceleration from Fig. 10) from the various classes of magnitude and source-to-site distances in the PSH model for the city of Wellington.

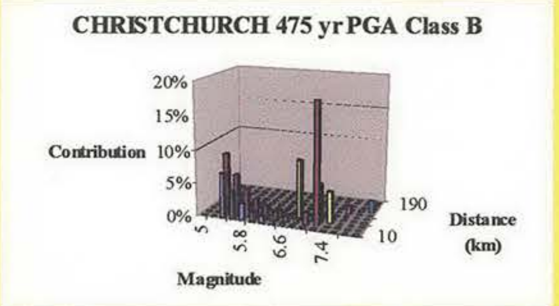

Figure 13. As for Figure 12, but focused on the city of Christchurch.

REFERENCES

Berryman & Beanland (1988), Frankel (1995), McVerry (2000), Matuschka et al. (1985), Smith & Berryman (1986), Stirling et al (1998) Stirling et al (2000)